



HAL
open science

Bio-based additives from fatty acid derivatives for PLA : enhancing its thermomechanical and gas barrier properties

Jamie Rubinstein

► To cite this version:

Jamie Rubinstein. Bio-based additives from fatty acid derivatives for PLA : enhancing its thermomechanical and gas barrier properties. Polymers. Université de Bordeaux, 2022. English. NNT : 2022BORD0279 . tel-03909225

HAL Id: tel-03909225

<https://theses.hal.science/tel-03909225>

Submitted on 21 Dec 2022

HAL is a multi-disciplinary open access archive for the deposit and dissemination of scientific research documents, whether they are published or not. The documents may come from teaching and research institutions in France or abroad, or from public or private research centers.

L'archive ouverte pluridisciplinaire **HAL**, est destinée au dépôt et à la diffusion de documents scientifiques de niveau recherche, publiés ou non, émanant des établissements d'enseignement et de recherche français ou étrangers, des laboratoires publics ou privés.

THÈSE PRÉSENTÉE
POUR OBTENIR LE GRADE DE
DOCTEUR DE
L'UNIVERSITÉ DE BORDEAUX

ÉCOLE DOCTORALE DES SCIENCES CHIMIQUES

SPÉCIALITÉ POLYMÈRES

Par Jamie RUBINSTEIN

**Additifs biosourcés dérivés d'acides gras pour
l'amélioration des propriétés thermomécaniques et barrière
du PLA**

**Bio-based additives from fatty acid derivatives for PLA: enhancing its
thermomechanical and gas barrier properties**

Sous la co-direction de : Pr. Henri CRAMAIL et Dr. Véronique COMA

Co-encadrant : Dr. Etienne GRAU

Thèse soutenue le 27 Octobre 2022

Membres du jury :

M. AVEROUS, Luc
M. RAQUEZ, Jean-Marie
Mme. DUCHET-RUMEAU, Jannick
M. GRAU, Etienne
M. CRAMAIL, Henri
Mme. COMA, Véronique
M. CHOLLET, Guillaume
M. DOLE, Patrice

Professeur, Université de Strasbourg
Professeur, Université de Mons
Professeur, Université de Lyon
Maître de conférences, Université de Bordeaux
Professeur, Université de Bordeaux
Maître de conférences - HDR, Université de Bordeaux
Responsable d'unité R&D, ITERG
Directeur scientifique, CTCPA

Rapporteur
Rapporteur
Examinateur
Examinateur
Directeur de thèse
Directrice de thèse
Invité
Invité

« Indulge your passion for science...but let your science be human, and such as may have a direct reference to action and society. Be a philosopher; but amidst all your philosophy, be still a man. » - David Hume, An Enquiry Concerning Human Understanding

« The important thing is not to stop questioning. Curiosity has its own reason for existing. One cannot help but be in awe when one contemplates the mysteries of eternity, of life, of the marvellous structure of reality. It is enough if one tries to comprehend only a little of this mystery every day. » - Albert Einstein

Remerciements

C'est avec beaucoup d'émotions que j'écris ces quelques lignes de remerciements à la suite de ces très riches trois années de thèse. En tout premier lieu, je tiens à remercier très chaleureusement le Professeur Henri Cramail pour son écoute, sa patience, ses conseils toujours judicieux ainsi que sa disponibilité lorsque j'ai eu besoin de lui. Il ne serait pas juste de ne pas autant remercier mon autre directeur de thèse, le Dr Véronique Coma, qui a toujours été présente et motivante par son dynamisme, sa bonne humeur et sa bienveillance. De même, je tiens particulièrement à remercier le Dr Etienne Grau avec qui j'ai eu de nombreuses discussions, partagé de nombreuses interrogations durant ma thèse mais qui a toujours su prendre du temps pour y réfléchir et être force de proposition pour me permettre d'avancer. J'ai bien évidemment une pensée pour mes autres encadrants de thèse. Tout d'abord, le Dr Patrice Dole qui m'a accueilli au CTCPA de Bourg-en-Bresse et qui m'a permis de découvrir le monde de la plasturgie, l'environnement d'un laboratoire agro-alimentaire et qui s'est montré particulièrement présent malgré son emploi du temps chargé. Je remercie aussi le Dr Guillaume Chollet et le Dr Marie Reulier de l'ITERG pour leurs conseils et les moyens mis en œuvre pour me permettre de réaliser ce projet de thèse.

De façon plus formelle, je remercie bien évidemment le Professeur Sébastien Lecommandoux, directeur du LCPO, de m'avoir accueilli au sein de ces locaux, permis d'y travailler et de jouir des nombreux équipements et moyens disponibles. Je remercie la région Nouvelle-Aquitaine ainsi que l'ITERG et le CTCPA d'avoir financé ces travaux de thèse ainsi que le LCPO pour les moyens mis-en-œuvre en termes de matériel, équipements et financements. Je remercie de nouveau l'ITERG pour m'avoir généreusement fourni divers produits pour la réalisation de mes travaux de thèse. À ce titre, je remercie aussi le CTCPA de m'avoir accueilli et permis d'utiliser des équipements auxquels je n'aurais pas eu accès au LCPO. Je remercie bien évidemment toutes les personnes m'ayant aidé à réaliser mes travaux. Au CTCPA, Florian Catinot pour son accueil et son temps, Sophie Thivind pour les mesures de perméabilité, Marine Démares pour les tests mécaniques et David Allain pour son aide avec l'exploitation des données. Au BIC, Isabelle Svahn pour son aide et son expertise avec le MEB. Au CRPP, Ahmed Bentaleb pour avoir effectué les analyses DRX. Merci aussi à Matthieu Pedros de l'IUT de Bordeaux pour son aide avec les essais de choc même si ceux-ci n'ont pas été concluants.

Et bien sûr, au LCPO, un très grand merci à Cédric Le Coz pour son assistance avec la DSC et la DMA, les nombreuses discussions et l'aide qu'il a pu m'apporter ainsi que son partage de connaissance sur ces appareils. Merci aussi à Amélie Vax-Weber et Sylvain Bourasseau pour leur aide avec la chromatographie d'exclusion stérique à l'ENSCBP et à Mélanie Bousquet au B8, à Anne-Laure Wirotius-Lambert pour l'utilisation de la RMN, à Paul Marque pour la spectroscopie infra-rouge et l'informatique, à Emmanuel Ibarboure pour la microscopie optique et nos discussions, à Loïc Pétrault et Nina Lavenette pour les services techniques. Bien évidemment, merci aux personnels administratifs, Claude Le Pierres, Corinne Goncalves de Carvalho, Olivier Fihey, Dominique Richard et Séverine Saint-Drenant. Plus généralement, merci à toutes les personnes que j'ai pu croiser que j'ai pu croiser à mes divers endroits de travail et avec qui j'ai pu échanger avec plaisir. Je pense ici au reste des personnels du CTCPA de Bourg-en-Bresse, Manon, Géraldine, Stacy, Claudine, Philippe, Samuel, Fred et Frédérique. Je pense aussi aux autres personnels permanents du LCPO non-cités précédemment que j'ai pu côtoyer, le Dr Frédérique Ham-Pichavant, le Pr Stéphane Grelier, le Pr Stéphane Carlotti, le Dr Thomas Vidil, le Dr Audrey Llevot, le Dr Elisabeth Garanger, le Dr Colin Bonduelle, the other Aussie the Dr Simon Harrisson, le Dr Guillaume Fleury, le Dr Joan Vignolle et tant d'autres.

Enfin... Que serait le LCPO sans tous les thésards, post-docs, stagiaires et autres membres permanents qui contribuent à la vie de ce laboratoire et auprès de qui j'ai tant appris. Pour certains, vous resterez des amis très chers pendant de nombreuses années je l'espère. Je pense à mon jumeau de labo et de bureau Anderson qui m'aura suivi pendant la totalité de ma thèse, à toutes les personnes de mon bureau, Quentin, Virgile, Manon, Nichollas, Ariella, Florent (Vive la Belgique !), Martin, Christopher, Stéphanie. Bien sûr, les autres membres de la Fatty Team (le gras c'est la vie) et de la Team 2, Victor qui m'aura suivi toute la thèse aussi, au N0 Solène, Gaël, Erwan, Cabral, Tiffaine, Yelin, Yunhui, Azmil,, Lou, Maëva, Romain, Pitou, Chloé, Gilles, Frédérique, Stéphane, Christian, Véronique ; au N1 Simon (encore Joyeux 30 ans !!!!), Zakir, Thaissa, Wafa, Nicolas, Péroline, Logan, Charles, Clément, Cédric, Thomas, Etienne et Henri. Évidemment, merci aussi aux autres membres des autres équipes du LCPO qui m'ont fait passer un très agréable moment : Quentin S., Anouk, Florian l'Alpha., Margaux, Ségolène (#Team San Diego), Diana, Julien, Paul, Manon L., Élise, Corentin, David, Guillaume P., Mostafa, Rosanna, Nadia, Assia, Samir (#Team PLA), Thomas L., Alban, Barbara, Hannah, Eloïse, Johanna, Leslie et Pablo.

La thèse est aussi faite de nombreuses rencontres et j'ai eu la chance particulière de rencontrer énormément de gens formidables par les conférences ou autre. Alors merci aux autres Bordelais, Léa, Magda, Catherine, Vaïana, Romane, Vaclav, Carmelo ; aux Toulousains, Clémence, Camille, Maxime ; aux Strasbourgeois, Thibault, Ian et Capucine ; aux Lyonnaises Marie (félicitations Docteure !!!) et Ariane, et aux Parisiennes Louise et Capucine (Joyeux anniversaire encore une fois aussi !). Merci aussi aux membres de la Team 8 au JEPO Porquerolles ainsi qu'à la Team Soirées qui a permis de créer un lien incroyable entre ses membres et qui a largement contribué à ce que cette conférence reste gravée dans beaucoup de mémoires.

Bien sûr, une très grosse pensée aux Plus Motivés pas encore cités, aussi bien pour les murs que le sauna, Lamia, Alexandre (félicitations Docteur !!), Margot, Cédric, Guillaume, Romane et la team INRAE. Je pense aussi très fort au Bruges 33 Handball qui m'a accueilli avec gentillesse et m'a permis de beaucoup m'amuser/me faire allumer au goal pendant 2 ans (sauté de Covid !!) et particulièrement Alexandre Go pour ses qualités humaines et sa faculté à prendre du recul rapidement sur les situations.

Durant 3 ans (et demi), il a bien fallu habiter quelque part, et donc ceux qui ont eu le malheur de devoir me ~~côtoyer~~ supporter tous les jours, weekends inclus, les résidents de la cour de l'impasse de la Rue Neuve : Augui (for ever the first) & Guigui, Titi la mémoire ambulante, Thomas et Zoë, Lucie (courage pour la vaisselle), Bobby, Vincent, Marine et la star, Rafale !

Et bien sûr, les meilleurs pour la fin, celles et ceux sans qui ces dernières années auraient été bien ternes et moroses... C'est sans aucun doute vous qui m'avez permis de traverser ses trois années, qui avez été là pour moi, et qui comptez beaucoup pour moi. Alors, merci aux meilleurs, Anouk... Margaux... Manon C. ... Florian l'Alpha... Sylvain... Jessie... Jérém... Anne... Et bien évidemment, Boris/Bobby, toi qui m'as tant apporté et soutenu lorsque j'en avais besoin alors que de ton côté tout n'était pas rose.

Il me reste encore quelques personnes à mentionner très importantes pour moi. En premier, mes amis de longue date d'avant la thèse, Simon, toujours là pour moi malgré les années, je te souhaite tout le meilleur et encore beaucoup de contacts pour toutes les années à venir; Thomas, merci de m'avoir donné le goût de la chimie et des polymères qui a fait que j'en suis là aujourd'hui, j'espère que tu voleras bientôt de tes propres ailes de métal à travers

le monde (vive l'A380), le reste de la 432/434 de Fermat, Sélim (Monsieur le français) et Pierre (#Gyver), my mates from Melbourne who are expecting me any moment in NYC now, Daniel, Michelle and Bob.

Un immense merci à Joëlle, ma spé, on n'a vraiment pas assuré de s'être lâchés pendant 3 ans, je ne réalise que maintenant à quel point tu m'as manqué ; mais ça y est, on compense ! Tu m'as guidé pendant mes 2 années à Fermat, maintenant à mon tour d'être là pour ta thèse. Courage ! Je ne t'échangerai pour rien au monde. Bien évidemment, Vincent, M.Tabouret, qui m'a fait découvrir ce qu'était une soutenance de thèse et m'a toujours fait découvrir de nouvelles choses par la suite (#Motocultor _88/o & Dark Souls <3) et Antoine, fidèle depuis la passation de la JE (#Team Trésoriers), vous êtes des personnes formidables et j'ai de la chance de vous compter parmi mes amis.

And of course, what would be life without a family, first and foremost my family from Australia, Donna, Aunt Mary, Peter and the kids, I really hope to see you all very soon; ma famille en France, les couz de Ch'Nord et du Midi , on va pouvoir se voir beaucoup plus souvent à present; and Gordon, I'll make sure to meet you soon and have another wonderful night out in the streets of Dublin.

Enfin, Jean-Luc, merci pour ta bonne humeur et ces chouettes moments toujours passés en ta compagnie ; Siodhbhra, thank you for your support, especially during lockdown. David, grand frère, ça faisait beaucoup trop longtemps, merci de t'être levé à 3h du matin pour suivre la soutenance, on se refait une virée à Berlin en été très bientôt !! Maman, merci pour ton aide et ce soutien inconditionnel au fil des années, depuis la prépa jusqu'à la réalisation de cette thèse. Merci pour ton aide au fil de ces années qui m'a rendu la vie bien plus aisée.

And last but not least... Dad, Mate... I cannot tell you how grateful I am for all the love, patience, support and help throughout all these years. You have always been there for me. Every day I realise even more how lucky I am to have you and cannot emphasise enough how dear you are to me. I would not have made it up to this point if you had not been here. Thank you so much for everything.

Table of Contents

Resume

List of abbreviations

General introduction 1

Chapter I: Poly(lactide): from a bio-based monomer to a potentially industrial polymer. Assets, drawbacks and industrial challenges

1. Poly(lactic acid), from a bio-based monomer to an economically viable polymer	10
1.1. From a green synthesis to an industrially available polymer.....	10
a. Lactic acid production and industrial stakes	10
b. PLA synthesis and production	12
1.2. PLA properties	17
a. Chemical structure and thermal transitions	17
b. Crystallographic properties and crystallisation behaviour	18
c. Processability.....	20
d. Mechanical properties	22
e. Gas permeation properties	23
f. End of life.....	26
2. PLA materials as food packaging: original drawbacks and requirements	31
2.1. Mechanical properties	31
2.2. Thermal properties.....	32
2.3. Gas barrier properties	32
2.4. End of life – Degradation and collection	33
3. Improving the properties of PLA through additives	34
3.1. Limiting the brittleness of PLA	34
a. Plasticisers: lowering the Tg below service temperature	36

b.	Synthetic copolymers	37
c.	Blending with soft low Tg polymers	44
d.	Global summary and perspectives	60
3.2.	Improving the heat deflection temperature of PLA.....	60
a.	Enhancing the crystallisation kinetics (NAs, plasticisers...)	61
b.	Stereocomplexation	67
3.3.	Tuning the O ₂ gas barrier properties.....	70
a.	Improving the crystallisation rate	70
b.	Specific additives	72
c.	Multi-layer films	76
3.4.	Improving the biodegradation of PLA materials	78
4.	Summary and strategy presentation for the research project	79
5.	References	82

Chapter II: Use of nucleating agents for PLA. Enhancing its heat deflection temperature and its gas barrier properties

1.	Introduction	101
2.	Fatty bis-amides from fatty acids as nucleating agents	103
2.1.	Synthesis.....	103
a.	Selection of long chain precursors and amines	103
b.	Synthetic procedures	105
2.2.	Chemical structure and thermal properties.....	108
3.	Use with PLA to enhance its crystallisation kinetics	117
3.1.	DSC preliminary analysis	117
3.2.	Blending to make DMA samples in isothermal conditions	121
a.	Melt-blending.....	121

b.	Preliminary study: mould temperature screening.....	122
c.	Optimisation: effect of time and loading.....	128
d.	Crystallographic structure.....	135
4.	Conclusion and perspectives	139
5.	Experimental & SI	141
	References	145

Chapter III: Use of poly(methyl ricinoleate) (PRic) and its derivatives as additives for PLA. Toughening effect and modification of gas barrier properties

	Global Introduction	150
	Part A: Synthesis of a well-controlled and defined PRic from a 99% pure monomer...	155
1.	PRIC-LCPO and its derivatives as additives for PLA	155
1.1.	Synthesis and characterisation	155
a.	Synthesis.....	155
b.	Characterisation	156
1.2.	Chemical modification: epoxidation of the alkene function.....	159
a.	Synthesis.....	159
b.	Characterisation	160
2.	Melt-blending with PLA: towards improved mechanical and gas barrier properties...166	
2.1.	Melt-blending and injection moulding process	166
2.2.	Structural characterisation.....	167
2.3.	Thermal characterisation	169
2.4.	Morphology through SEM.....	170
2.5.	Vertical compression testing.....	173
2.6.	Oxygen barrier properties	180
3.	Discussion and conclusion	183

4. Experimental & SI	184
4.1. Synthesis of PRic-LCPO	184
4.2. Synthesis and purification of PRic-LCPO-EXX	184
4.3. SEM analysis	184
4.4. Vertical compression testing.....	185
4.5. Oxygen permeability measurement.....	185
Part B: Use of the industrial PRic grade	187
1. PRIC-100 and its derivatives as additives for PLA	187
1.1. Characterisation of PRic-100	187
a. Structure.....	187
b. Thermal analysis	190
1.2. Epoxidation of PRic-100	190
a. Synthesis.....	190
b. Characterisation	190
1.3. Carbonatation of epoxidized PRic-100.....	194
a. Synthesis.....	194
b. Characterisation	195
2. Melt-blending with PLA: study of the mechanical and gas barrier properties	200
2.1. Structural characterisation.....	200
2.2. Thermal characterisation	202
2.3. Morphology through SEM.....	203
2.4. Vertical compression testing.....	207
a. PLA + PRic-100.....	208
b. PLA + PRic-100-EXX.....	209
c. PLA + PRic-100-Carbonate.....	212

2.5. Oxygen barrier properties	215
3. Discussion and conclusions	219
4. Experimental & SI	221
Comparison between both PRic grades	223
General conclusion and perspectives	225
References	227
Conclusion and perspectives	229
Materials and methods	233

Résumé général

Ce travail de thèse se construit dans un contexte mondial de développement durable. Nos modes de consommation évoluent actuellement vers des pratiques plus durables en particulier au regard d'une pollution grandissante et du changement climatique. Dans le cas des matériaux polymères, dits « plastiques » lors de leur usage commun, les enjeux concernent leur origine ainsi que leur fin de vie car ceux-ci sont majoritairement pétrosourcés et non-biodégradables ou compostables¹. Ce dernier point est particulièrement important dans la mesure où le domaine d'application des matériaux plastiques est principalement celui de l'emballage et d'autres applications mono-usages². En ce sens, les récentes réglementations européennes et françaises contraignent les matériaux plastiques mono-usages à être soit compostables, biodégradables ou inscrits dans une filière de collecte et de recyclage³. De telles mesures incitent donc les industriels à envisager des alternatives plus vertueuses aux polymères traditionnels issus de la pétrochimie. Actuellement, la production de nouveaux polymères, biosourcés, dont certains qualifiés de « bioplastiques », est en plein essor. Un polymère tel le poly(acide lactique), ou poly(lactide), connu sous le nom de PLA, atteint ainsi un coût d'achat au kilo avoisinant 1,5€ à 2€⁴, le rendant ainsi viable d'un point de vue économique et lui permettant de concurrencer des polymères traditionnels comme le poly(téréphtalate d'éthylène) ou le poly(styrène) possédant certaines propriétés comparables⁵.

Le PLA est obtenu par voie de bio-raffinage, à partir de ressources sucrières tels que le maïs, la canne à sucre ou la betterave permettant d'obtenir son monomère chiral par fermentation, l'acide lactique puis le dimère associé servant à la polymérisation, le lactide⁶ (Figure R 1). Selon son degré de pureté optique, le PLA peut être amorphe ou semi-cristallin ; un PLA synthétisé à partir de plus de 93%mol de L-lactide (le plus abondant naturellement) ou de D-lactide sera semi-cristallin⁷.

Résumé général

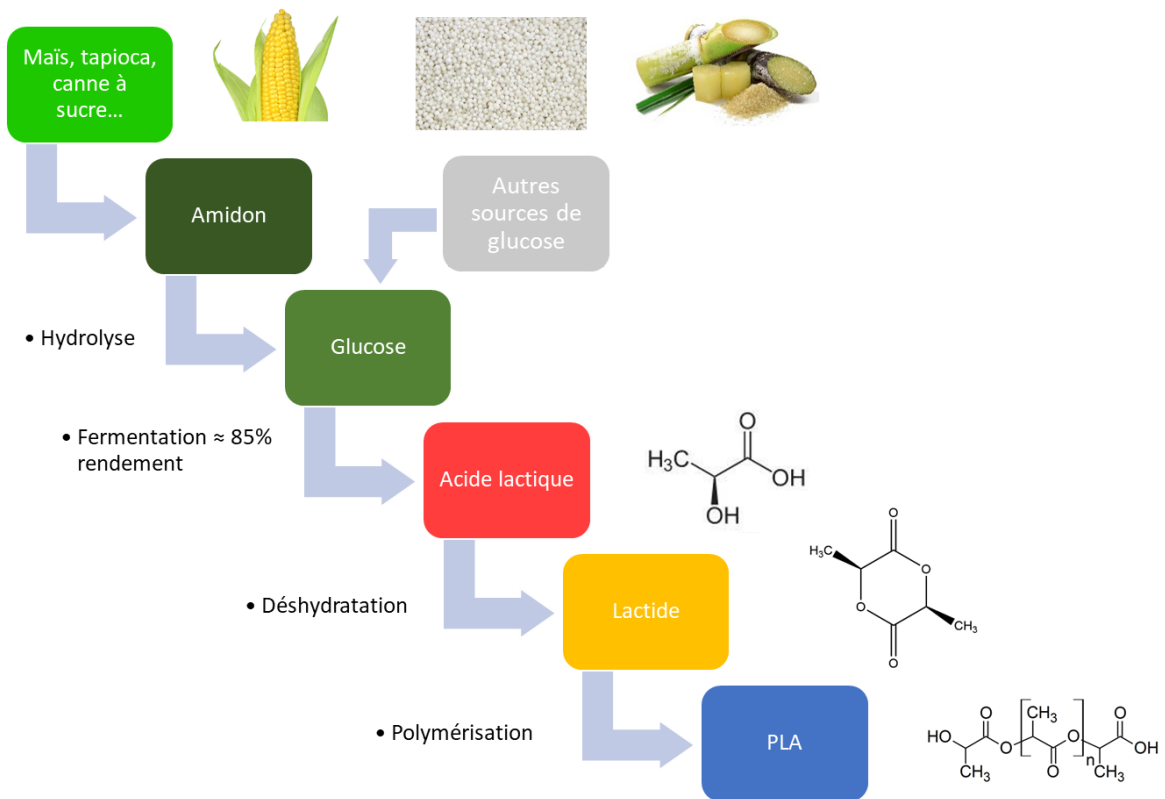


Figure R 1: Étapes d'obtention du PLA à partir de ressources végétales

Ce polymère biosourcé est compostable en milieu industriel et est approuvé pour le contact alimentaire, permettant son utilisation comme emballage pour des denrées alimentaires. Cependant, son utilisation à grande échelle est limitée par certaines de ses propriétés intrinsèques : un comportement mécanique fragile à température ambiante, une température de transition vitreuse comprise entre 55°C et 60°C couplée à une cinétique de cristallisation lente et des propriétés barrière aux gaz intermédiaires⁸ (Tableau R 1). Les deux derniers points soulevés induisent deux problèmes majeurs ; le premier étant une impossibilité d'utiliser le PLA comme matériau à des températures au-delà de 55°C car, du fait de la cinétique de cristallisation lente, des objets en PLA produits à des cadences industrielles n'auront pas le temps de cristalliser et ne présenteront que de très faibles taux de cristallinité. Le second problème soulevé concerne les propriétés barrière du PLA qui ne sont considérées ni barrière ni perméables et qui ne permettent donc pas une préservation optimale des aliments contenus dans des emballages en PLA⁹ (Figure R 2).

Tableau R 1: Propriétés thermomécaniques d'un PLA semi-cristallin

Température de transition vitreuse (°C)	55 - 60
Point de fusion (°C)	130 - 180
Modulus d'Young (GPa)	3.8
Allongement à rupture (%)	4-7
Résilience (J.m⁻¹)	26
Température de fléchissement sous charge (°C)	55

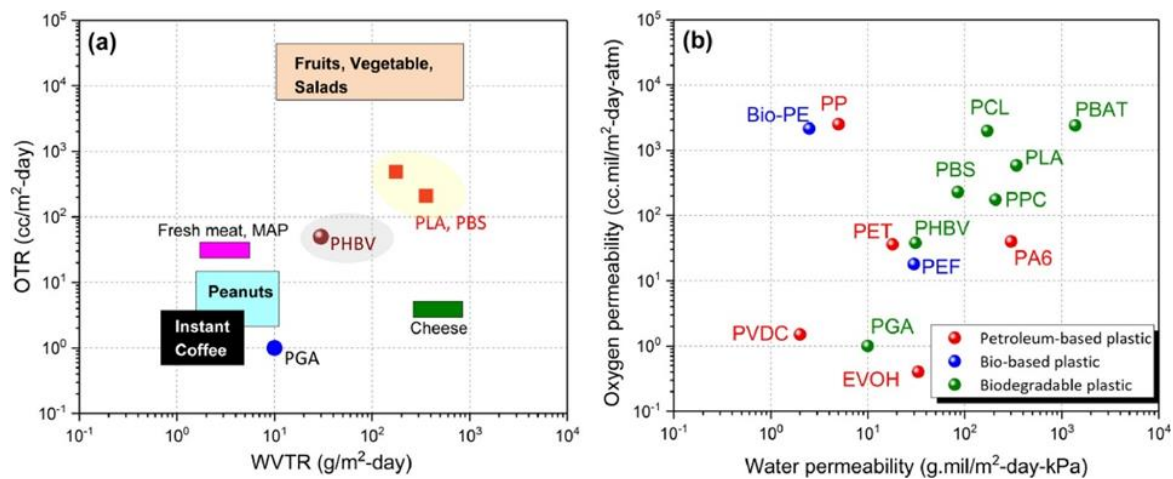


Figure R 2: (a) Gamme de perméabilité requise pour différentes applications en emballage alimentaire et comparaison des taux de transmission de dioxygène et de vapeur d'eau de films de 25 µm de polymères biodégradables. (b) Perméabilité au dioxygène et à la vapeur d'eau de différents polymères. (Copyright 2022, Adapted from Wu et al.⁹ with permission from Elsevier)

Des objets en PLA avec de hauts taux de cristallinité, au-delà de 40%, vont présenter des domaines d'utilisation jusqu'à 110°C voire 120°C dans les meilleurs des cas. Conjointement, cette impossibilité d'obtenir des objets en PLA à hauts taux de cristallinité par les procédés de fabrication actuels joue un rôle sur les propriétés barrière du PLA. En effet, diverses études ont rapporté une amélioration des propriétés barrière lorsque que le taux de cristallinité du PLA est élevé, au-delà de 40%. Typiquement, la perméabilité au dioxygène peut être divisée par un facteur deux entre un matériau PLA amorphe et un matériau PLA à 40% de taux de cristallinité¹⁰. Ces problématiques sont centrales dans un contexte de matériaux pour l'emballage alimentaire, préoccupation principale de cette thèse. En effet, un matériau destiné à la préservation alimentaire se doit de respecter certaines propriétés mécanique, thermique et barrière (perméabilité gaz, arômes, contaminants extérieurs) pour optimiser la conservation alimentaire. L'amélioration de ces propriétés permet d'élargir le champ

Résumé général

d'application du PLA en emballage alimentaire. Par ailleurs, un matériau résistant à des températures supérieures à 100°C permet d'envisager des procédés de pasteurisation et de stérilisation.

Ainsi, ce travail a pour objectif la synthèse de nouveaux additifs pour le PLA, en choisissant spécifiquement de travailler avec un grade de poly(L-Lactide) optiquement très pur, et ce pour deux objectifs. Le premier concerne la tenue thermique du PLA et, dans ce cas, de l'amélioration de sa cinétique de cristallisation par le biais d'agents nucléants de forme bis-amide symétriques synthétisés à partir de ressources oléagineuses. Le second fait référence au renfort mécanique du PLA par l'utilisation d'additifs polymères issus de l'huile de ricin, le poly(ricinoléate de méthyle) (PRic) et ses dérivés.

La première partie de ce travail est donc centrée sur la synthèse et l'utilisation d'agents nucléants pour le PLA avec pour objectif d'améliorer la cinétique de cristallisation de ce dernier. De la littérature, très riche sur ce sujet, deux agents nucléants issus d'acides gras ont été rapportés, le N,N'-éthylène-bis-stéaramide et le N,N'-12-hydroxy-éthylène-bis-stéaramide. Utilisés à des taux de 1% massique, ceux-ci abaissent le temps caractéristique de cristallisation de plusieurs dizaines de minutes à 1,5min à 110°C¹¹⁻¹³. Ces deux composés de type amide étant issus d'acides gras à 18 atomes de carbone, le choix s'est donc porté sur l'utilisation de cette famille d'acides gras pour synthétiser les agents nucléants de cette étude. Typiquement, les acides gras sélectionnés ont été l'acide stéarique, l'acide 12-hydroxystéarique, l'acide oléique et l'acide ricinoléique. De même, uniquement des diamines linéaires aliphatiques ont été utilisées au cours des synthèses effectuées, l'intérêt de cette étude résidant dans l'étude de l'influence de la longueur de la chaîne carbonée entre les fonctions amide (effet de la diamine) et de la présence de fonctions chimiques, ou non, sur l'acide gras considéré sur les propriétés de l'agent nucléant (Figure R 3). Selon le dérivé d'acide gras utilisé (acide carboxylique, ester méthylique ou chlorure d'acyle), trois voies de synthèses appropriées ont été développées pour synthétiser les bis-amides.

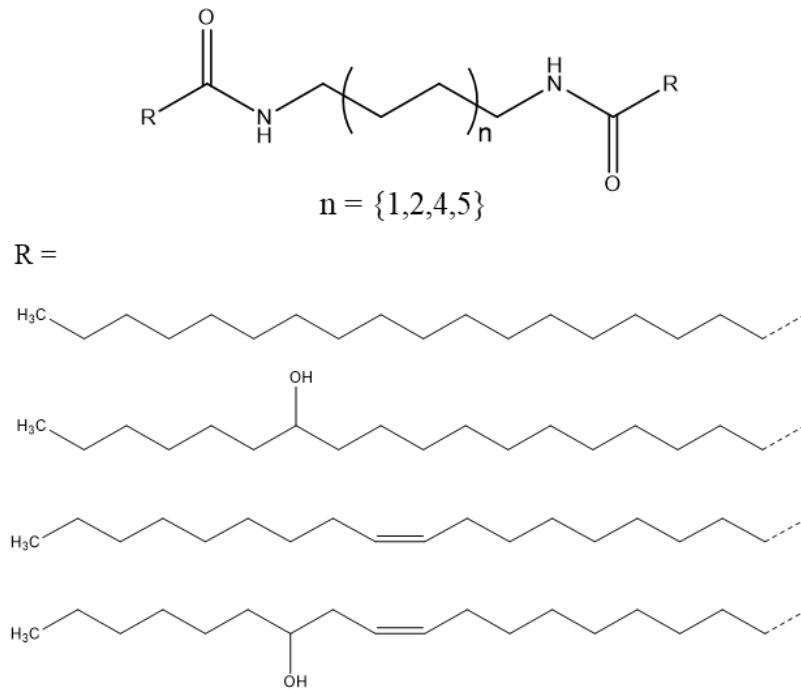


Figure R 3: Structure des bisamides synthétisés pour être utilisés comme agents nucléants

Les agents nucléants obtenus à partir d'acide stéarique ont été ceux ayant les points de fusion les plus élevés. Suivent ceux provenant de l'acide 12-hydroxystéarique, de l'acide oléique et de l'acide ricinoléique, montrant ainsi un clair effet de la fonctionnalisation de la chaîne grasse. De façon similaire, plus la diamine utilisée comprend une chaîne longue (respectivement à 4, 6, 10 ou 12 unités méthylènes), plus le point de fusion obtenu s'abaisse, à l'exception de la combinaison acide 12-hydroxystéarique/diamine C12 pour cause d'espacement propice à la création de liaisons hydrogène supplémentaires. Ces 16 agents nucléants potentiels ont été mélangés à hauteur de 1% massique dans du PLA « pur » pour rapidement évaluer leur efficacité par analyse DSC. Au travers de cette analyse, les composés issus de l'acide stéarique et de l'acide 12-hydroxystéarique ont été ceux présentant la plus grande amélioration de la cinétique de cristallisation du PLA avec des taux de cristallinité atteignant 50% dans des conditions de refroidissement contrôlées (-10°C/min) depuis l'état fondu, contre 3% pour du PLA pur.

À la suite de ces résultats prometteurs en conditions dynamiques, divers mélanges ont été effectués en utilisant une mini-extrudeuse bi-vis couplée à un système d'injection-moulage, permettant ainsi de fabriquer des éprouvettes rectangulaires en conditions isothermes pour des tests en analyse mécanique différentielle (DMA). Plusieurs paramètres ont été étudiés tels que le ratio massique agent nucléant/PLA, la température du moule d'injection à un temps

Résumé général

fixé et le temps de séjour dans ce moule à une température fixée. Des taux de cristallinité supérieurs à 50% ont été obtenus pour des temps de séjour de 25s, le plus court temps reproductible, à une température de 110°C pour un échantillon contenant 0,5% massique d'agent nucléant. De surcroît, le comportement observé en DMA évoluait en fonction du taux de cristallinité de l'échantillon. Un critère de tenue thermique a été établi comme suit : la température validant ce critère fut relevée lorsque la valeur du module de conservation atteignait 10% de celle à 25°C, à savoir au début du test. Pour le PLA non-additivé, la valeur relevée est de 67°C, dans le meilleur des cas, cette valeur a atteint 119°C en utilisant l'agent nucléant synthétisé à partir d'acide stéarique et de la putrescine (1,4-diaminobutane). Des essais de scale-up ont été menés grâce à une mini-injecteuse industrielle Babyplast. Malheureusement, le matériel disponible n'a pas permis de contrôler correctement la température du moule d'injection, menant à l'obtention d'échantillons hétérogènes en termes de taux de cristallinité. Les propriétés de perméabilité au dioxygène n'ont donc pas été mesurées.

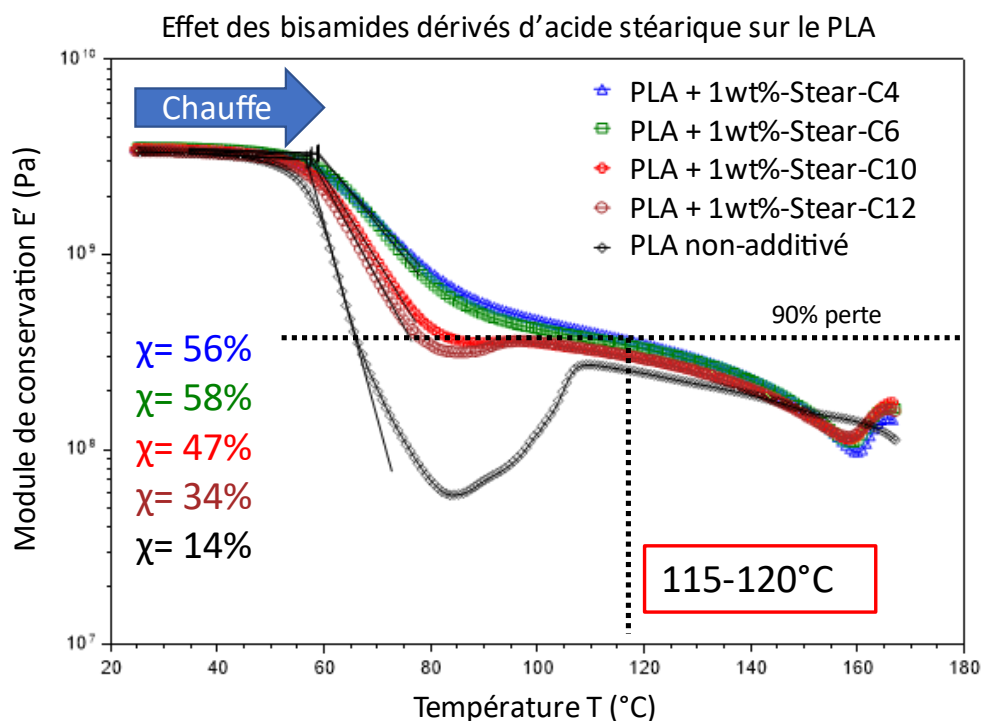


Figure R 4: Courbes DMA d'échantillons de PLA contenant des agents nucléants dérivés d'acide stéarique, rampe 3°C/min, 1Hz, 0,1% de déformation

La seconde partie de ce travail s'est attachée à l'utilisation du poly(ricinoléate de méthyle), ou PRic, et de ses dérivés comme agents de renforts aux chocs du PLA et à l'évaluation des

propriétés barrière de ces matériaux. Grâce à de précédents travaux effectués au LCPO en collaboration avec l'ITERG, le poly(ricinoléate de méthyle) avait déjà montré son efficacité pour améliorer le comportement mécanique du PLA^{14,15}. Ce polymère a l'avantage de comporter une insaturation sur sa chaîne principale pour chaque motif de répétition. Ainsi, il est donc envisageable d'utiliser ce site réactif pour post-fonctionnaliser ce polymère et étudier l'évolution de ses propriétés ainsi que l'effet de ces modifications sur un mélange PLA/poly(ricinoléate de méthyle) modifié. En parallèle, deux grades de poly(ricinoléate de méthyle) ont été sélectionnés, un grade industriel synthétisé par l'ITERG à partir de monomère pur à 85% et utilisé lors des précédentes études menées au LCPO (PRic-100), et un grade synthétisé au LCPO à partir d'un monomère pur à plus de 99% (PRic-LCPO). Outre les impuretés présentes lors de la polymérisation, la différence entre ces deux grades se caractérise par une différence de masses molaires, un $M_w = 5200\text{g/mol}$, $\bar{D} = 2,1$ pour le PRic de l'ITERG et $M_w = 24000\text{g/mol}$, $\bar{D} = 4,1$ pour le PRic synthétisé au LCPO. Cette différence de masses molaires est expliquée par une quantité supérieure de fonctions ester par rapport aux fonctions hydroxyle dans le cas du PRic de l'ITERG. Les esters méthyliques d'acides gras présents en plus du ricinoléate de méthyle, et ne comportant pas de fonction alcool permettant la polycondensation, vont agir comme des stoppeurs de chaînes et donc limiter les masses obtenues ainsi que présenter des bouts de chaînes différents.

Deux réactions de post-fonctionnalisation ont été effectuées, une époxydation pour les deux grades de PRic en utilisant de l'acide 3-métachloroperbenzoïque (*m*-CPBA) et, dans le cas du PRic de l'ITERG, ces fonctions époxyde ont été converties en carbonates cycliques en utilisant un autoclave chargé avec une pression de 40 bars de CO_2 avant chauffage. Des taux de fonctionnalisation de 25%, 50% et 85% ont été atteints en époxydes et en carbonates cycliques. Au cours de ces réactions, les masses molaires des additifs ont augmenté, notamment lors de l'étape d'époxydation. En effet, le polymère fonctionnalisé a été purifié par précipitation dans du méthanol froid pour éliminer le *m*-CPBA en excès ainsi que l'acide 3-chlorobenzoïque produit. Lors de cette précipitation, les plus petites chaînes restent solubilisées dans le méthanol et sont donc éliminées, conduisant à des masses molaires moyennes mesurées plus élevées. Conjointement à cette augmentation de masses molaires, la fonctionnalisation des PRic eut pour conséquence d'augmenter la valeur de la température de transition vitreuse avec le même constat, plus le taux de fonctionnalisation est élevé, plus

Résumé général

l'augmentation de la Tg est importante. Pour le PRic du LCPO, la Tg est passée de -72°C à -53°C pour un PRic fonctionnalisé à 85% et dans le cas du PRic de l'ITERG, l'augmentation a été de -81°C à -52°C. L'ajout d'une fonction carbonate cyclique a eu un effet encore plus prononcé, l'évolution de Tg évoluant de -81°C à -30°C pour 85% de taux de fonctionnalisation.

Les neuf additifs synthétisés ont été mélangés à du PLA à raison de 2%, 4% et 6% massiques pour chaque additif en utilisant une extrudeuse industrielle bi-vis. Les granulés obtenus ont été utilisés dans une mini-injecteuse industrielle Babyplast pour produire des mini barquettes par injection moulage, ces barquettes permettant de caractériser les matériaux en effectuant des tests de résistance à la compression verticale ainsi que des tests de perméabilité à l'O₂. Le meilleur comportement mécanique fut observé en utilisant le PRic de l'ITERG non modifié ; à partir de seulement 2% de taux d'additivation, le comportement mesuré n'est plus fragile et permet une très haute déformation en compression, supérieure à 50%, alors que le PLA non additivé casse à environ 6% de déformation (Figure R 5 et Figure R 6).

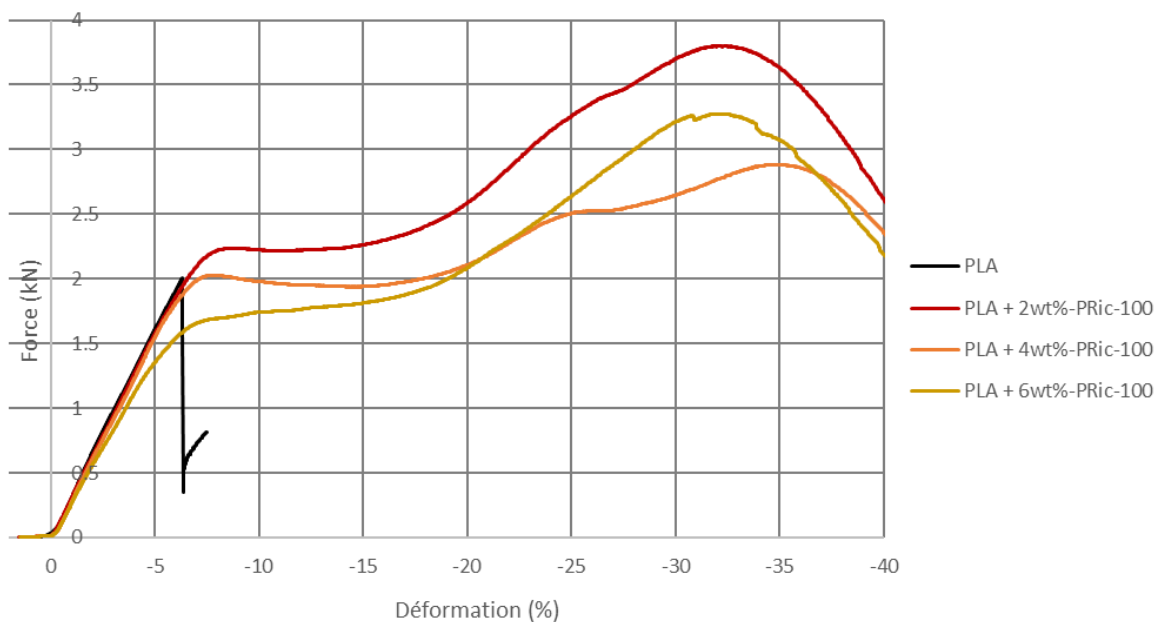


Figure R 5: Test de résistance à la compression verticale pour des échantillons de PLA et PLA additivés avec du PRic-100, -10mm/min

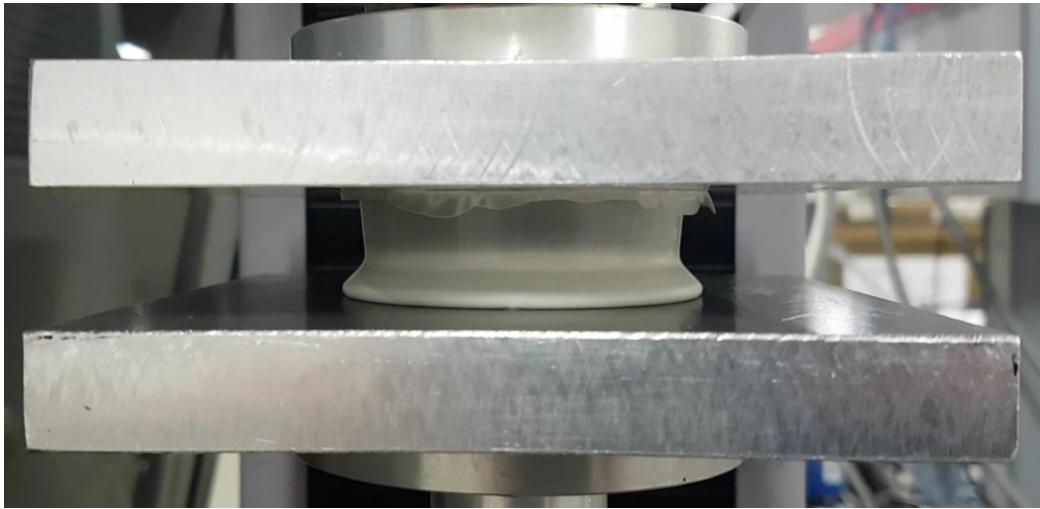


Figure R 6: Échantillon de PLA additivé avec du PRic-100 durant un test de résistance à la compression verticale

L'époxydation de ce grade de PRic eut pour effet de diminuer l'amélioration de la résistance à la compression verticale. A 25% de taux de fonctionnalisation, il fallait au minimum 4% d'additif pour obtenir un PLA non-cassant. A 50% et 85%, ce comportement n'était observé plus qu'à 6% de taux d'additivation. Cela fut expliqué par le fait que les plus petites chaînes de PRic, éliminées lors de l'étape de purification par précipitation, ne jouent plus le rôle de plastifiant/compatibilisant dans la matrice PLA et à l'interface entre le PRic et le PLA ; deuxièmement, la Tg des additifs époxydés ayant augmenté par rapport au PRic initial, les nodules formés ont une capacité moindre à absorber une déformation et donc plus d'additif est nécessaire. Dans le cas des additifs carbonatés, peu de conclusions purent être formulées du fait d'un biais causé par une forte diminution de la masse molaire des échantillons lors de leur élaboration. Ce phénomène entraîna une réponse mécanique très mauvaise lors des essais effectués, non représentative de l'effet des additifs utilisés. Ceci fut le cas pour les PRics fonctionnalisés à 25% et 50% en carbonates cycliques. Dans le cas du PRic carbonaté à 85%, la masse molaire fut conservée. Les propriétés mécaniques mesurées ont été meilleures en termes de déformations à rupture, plus élevées que celle du PLA vierge, cependant bien inférieures à celles mesurées avec des PRics purs ou époxydés. Les déformations à ruptures atteignirent 15% et 17% dans le cas de 4% et 6% d'additivation, cependant, la réponse en force mesurée fut plus faible qu'avec les autres additifs permettant d'obtenir ces taux de déformation.

En comparaison, le PRic synthétisé au LCPO ne présenta pas la même efficacité d'amélioration du comportement mécanique que le PRic de l'ITERG. Typiquement, 6%

Résumé général

d'additif ont été nécessaires pour obtenir un matériau ne cassant pas tandis que pour le PRic de l'ITERG, uniquement 2% ont été nécessaires. Cependant, l'apport de fonctions époxydes eut un effet différent qu'avec le PRic de l'ITERG. Contrairement à ce dernier, l'ajout d'époxydes améliore le comportement mécanique, augmentant la déformation à rupture à partir de 50% de fonctionnalisation. Cependant, cette tendance ne put être confirmée car les échantillons contenant le PRic du LCPO époxydé à 85% présentèrent une forte diminution de leur masse molaire, résultant en un comportement mécanique non représentatif du matériau obtenu.

En ce qui concerne la perméabilité à l'O₂, l'ajout de PRic non modifié eut pour effet d'augmenter la perméabilité, quel que soit le grade utilisé. Cela peut s'expliquer par une augmentation du volume libre dans la matrice PLA par ajout d'un additif non miscible. La fonctionnalisation avec des époxydes du PRic du LCPO sembla limiter ce phénomène en stabilisant les valeurs de perméabilité autour de celle du PLA non-additivé, et ce malgré 6% d'additif. En revanche, cet effet fut moins prononcé dans le cas du PRic de l'ITERG époxydé. Les échantillons présentant les meilleures propriétés barrière ont été ceux contenant du PRic carbonaté à hauteur de 25% et 50%. En effet, les matériaux correspondants ont présenté une réduction graduelle de la perméabilité, allant jusqu'à 50%, avec des taux d'additivation croissants, indiquant un réel effet de la fonction carbonate (Figure R 7). Cependant, ce phénomène ne fut pas observé pour le PRic carbonaté à 85% où les perméabilités mesurées ont été proches de celle du PLA non-additivé. Des tests complémentaires restent donc à effectuer avec ces additifs, notamment reproduire les tests mécaniques et de perméabilité avec des formulations dont la masse molaire n'a pas été dégradée lors du procédé de fabrication.

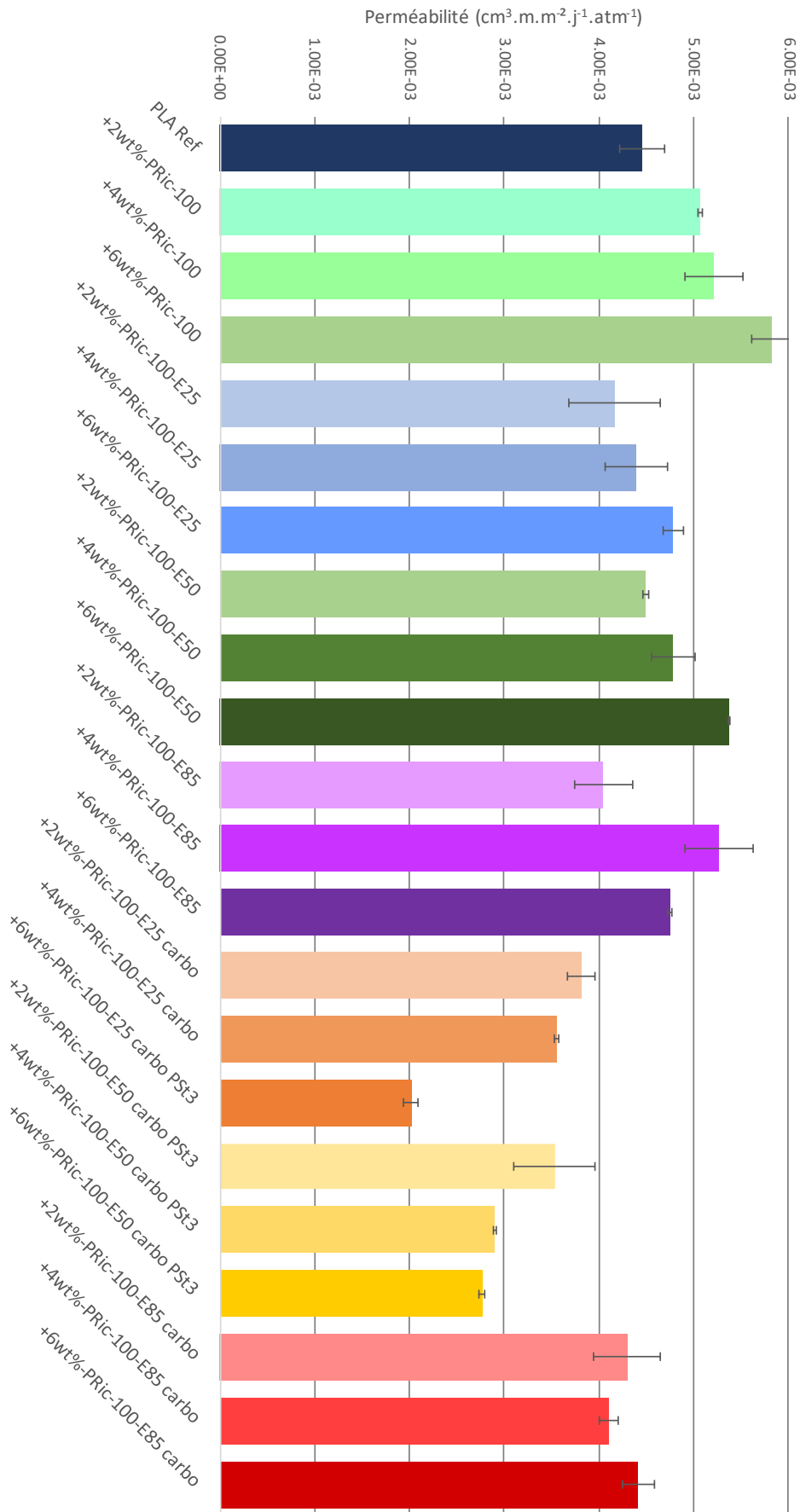


Figure R 7: Perméabilités mesurées pour différents matériaux à base de PLA

Résumé général

En définitive, ces travaux de thèse ont permis de synthétiser et d'étudier de nouveaux additifs pour le PLA issus de matières biosourcées. L'utilisation de ces additifs avait pour objectif de résoudre certaines limitations majeures du PLA pour envisager son utilisation à grande échelle. Des agents nucléants permettant d'obtenir des taux de cristallinité supérieurs à 50% ont été synthétisés mais malheureusement, l'appareillage de mise en forme disponible n'a pas permis de procéder à des essais de montée en échelle satisfaisants. Concernant les additifs dérivés du poly(ricinoléate de méthyle), ceux-ci ont démontré une capacité d'amélioration des propriétés mécaniques du PLA, les meilleurs résultats étant obtenus avec le grade industriel non-modifié, directement commercialisé par l'ITERG. Au regard des propriétés de perméabilité au dioxygène, les additifs carbonatés à 25% et 50% ont présenté la plus forte réduction. Malheureusement, ces matériaux ont été aussi ceux présentant les plus mauvaises propriétés mécaniques à cause d'un biais de fabrication. Ainsi, il n'est pas possible de conclure quant à leur réel effet sur les propriétés mécaniques du PLA.

Les enjeux restants sur ce travail sont donc multiples. Les formulations contenant les agents nucléants devraient être testées sur une autre machine d'injection moulage, permettant un meilleur contrôle de la température au sein du moule, pour tenter de produire des objets en PLA ayant un taux de cristallinité élevé. La détermination de leur propriété barrière à l'O₂ et mécanique permettrait de conclure plus finement quant à l'intérêt de l'utilisation de ces agents nucléants. De plus, les essais avec certains dérivés fonctionnalisés du poly(ricinoléate de méthyle) devraient eux aussi être répétés pour conclure quant à leur effet sur les propriétés mécaniques du PLA. Au regard des résultats obtenus, il serait souhaitable de combiner les différents types d'additifs utilisés dans ces travaux. Un agent nucléant utilisé avec un additif polymère de renforcement du comportement mécanique pourrait permettre d'obtenir un matériau en PLA avec une cinétique de cristallisation rapide et des propriétés mécaniques grandement améliorées. De plus, dans un contexte de développement durable, il pourrait être judicieux d'évaluer la biodégradabilité et la toxicité de ces nouveaux matériaux pour appréhender leur fin de vie potentielle dans l'environnement. Cette toxicité est aussi nécessaire pour conclure quant à l'alimentarité des additifs et des matériaux.

Références bibliographiques

1. European Bioplastics. <https://www.european-bioplastics.org/>.
2. Plastics - the Facts 2021 • Plastics Europe. *Plastics Europe* <https://plasticseurope.org/knowledge-hub/plastics-the-facts-2021/>.
3. Décret n° 2021-517 du 29 avril 2021 relatif aux objectifs de réduction, de réutilisation et de réemploi, et de recyclage des emballages en plastique à usage unique pour la période 2021-2025. 2021-517 (2021).
4. Polylactic Acid (PLA) Market | 2022 - 2026 | MarketsandMarkets. <https://www.marketsandmarkets.com/Market-Reports/polylactic-acid-pla-market-29418964.html>.
5. *Polymer handbook*. (Wiley, 1999).
6. Avérous, L. Chapter 21 - Polylactic Acid: Synthesis, Properties and Applications. in *Monomers, Polymers and Composites from Renewable Resources* (eds. Belgacem, M. N. & Gandini, A.) 433–450 (Elsevier, 2008). doi:10.1016/B978-0-08-045316-3.00021-1.
7. Tsuji, H. Poly(Lactic Acid). in *Bio-Based Plastics* 171–239 (John Wiley & Sons, Ltd, 2013). doi:10.1002/9781118676646.ch8.
8. Södergård, A. & Stolt, M. Properties of lactic acid based polymers and their correlation with composition. *Prog. Polym. Sci.* **27**, 1123–1163 (2002).
9. Wu, F., Misra, M. & Mohanty, A. K. Challenges and new opportunities on barrier performance of biodegradable polymers for sustainable packaging. *Prog. Polym. Sci.* **117**, 101395 (2021).
10. Fernandes Nassar, S. *et al.* Multi-scale analysis of the impact of polylactide morphology on gas barrier properties. *Polymer* **108**, 163–172 (2017).
11. Nam, J. Y. *et al.* Morphology and crystallization kinetics in a mixture of low-molecular weight aliphatic amide and polylactide. *Polymer* **47**, 1340–1347 (2006).
12. Xing, Q. *et al.* Tailoring crystallization behavior of poly(l-lactide) with a low molecular weight aliphatic amide. *Colloid Polym. Sci.* **293**, 3573–3583 (2015).
13. Saitou, K. & Yamaguchi, M. Transparent poly(lactic acid) film crystallized by annealing beyond glass transition temperature. *J. Polym. Res.* **27**, 104 (2020).
14. Lebarbé, T., Ibarboure, E., Gadenne, B., Alfos, C. & Cramail, H. Fully bio-based poly(l-lactide)-b-poly(ricinoleic acid)-b-poly(l-lactide) triblock copolyesters: investigation of solid-state morphology and thermo-mechanical properties. *Polym. Chem.* **4**, 3357 (2013).
15. Cramail, H., Lebarbe, T., Gadenne, B. & Alfos, C. Use of polymers as additives in a polymer matrix. (2017).

List of abbreviations

12-HSA : 12-hydroxystearic acid	PLLA: poly(L-lactide)
ABS : acrylonitrile-butadiene-styrene copolymer	PM: polymenthide
\bar{D} : dispersity	PMCL: poly(6-methyl- ϵ -caprolactone)
DCM: dichloromethane	POM: polarized optical microscopy
DCP: dicumyl peroxide	PP: polypropylene
DMA: dynamic mechanical analysis	PPDL: poly(pentadecalactone)
DSC: differential scanning calorimetry	PRic: poly(methyl ricinoleate)
E' : storage modulus	PRic-EXX: XX% epoxidized poly(methyl ricinoleate)
E'' : loss modulus	PRic-EXX-Carbo: XX% carbonated poly(methyl ricinoleate)
EBHS: N,N'-ethylenebis(12-hydroxystearamide)	PS: polystyrene
EBS: N,N'-ethylenebisstearamide	PTMC: poly(trimethylene carbonate)
EVA: ethylene-co-vinyl acetate copolymer	PU: polyurethane
FTIR-ATR: Fourier transformed infra-red-attenuated total reflection	Ric: ricinoleic acid
FWHM: Full width at height maximum	ROP: ring opening polymerisation
HDPE: high density polyethylene	SBS: styrene-butadiene-styrene copolymer
HDT: heat deflection temperature	SEBS: styrene-ethylene-butadiene-styrene copolymer
LDPE: low density polyethylene	SEC: size exclusion chromatography
LLDPE: linear low density polyethylene	SEM: scanning electronic microscopy
LTI: lysine triisocyanate	Sn(Oct) ₂ : stannous octoate
<i>m</i> -CPBA: 3-chloroperbenzoic acid	Stear: stearic acid
MDI: 4,4'-methylenebis(phenylisocyanate)	T: temperature
MeOH: methanol	$t_{1/2}$: crystallisation half-time
Me-Ric: methyl ricinoleate	TBD: 1,5,7-Triazabicyclododecene
Mn: number average molar mass	Tc: crystallization temperature
Mw: mass average molar mass	Tcc: cold-crystallization temperature
NMR: nuclear magnetic resonance	Tg: glass transition temperature
PA-11: polyamide 11	THF: tetrahydrofuran
PA-12: polyamide 12	Ti(iOPr) ₄ : titanium (IV) isopropoxide
PBAT: poly(butylene adipate-co-terephthalate)	T _m : melting temperature
PBS: poly(butylene succinate)	TMC: trimethylene carbonate
PBSA: poly(butylene succinate-co-adipate)	TPE: thermoplastic elastomer
PCL: poly(ϵ -caprolactone)	T _{α} : α -relaxation temperature
PDLA: poly(D-lactide)	T _{β} : β -relaxation temperature
PDLLA: poly(D,L-lactide)	V: volume fraction
PE: polyethylene	VLDPE: very low-density polyethylene
PEA: poly(ester-amide)	WAXD (WAXS): wide-angle X-ray scattering
PEG: polyethylene glycol	ΔH_c : crystallization enthalpy
PEO: polyethylene oxide	ΔH_{cc} : cold-crystallization enthalpy
PET: poly(ethylene terephthalate)	ΔH_m : melting enthalpy
PHAs: poly(hydroxyalkanoate)s	$\Delta H_{m,0}$: melting enthalpy of the completely crystalline state
PHB: poly([R,S]-3-hydroxybutyrate)	χ_c : crystallinity degree
PI: polyisoprene	ω : weight fraction
PIB: polyisobutylene	
PLA: polylactide or poly(lactic acid)	

Unless mentioned otherwise, PLA will refer to PLLA in the experimental chapters of this work

General introduction

Since their discovery, polymers have been used in a very wide range of different applications thanks to the multiple properties they can offer. The first use of synthetic polymers is known through the famous Bakelite materials, first synthesised in 1907 by Leo Baekeland, and stockings made from Nylon 6,6 developed by DuPont. One common feature of polymers is their light weight. Indeed, compared to many other materials, polymers have the particularity of being very light. For instance, the density of polyethylene (PE) is measured around 0.93 and the one of atactic polypropylene (PP) is around 0.87 and 0.90 for an isotactic PP¹. In comparison, the density of glass is 2.5 meaning, for the same volume of material, glass materials will be 2.8 times heavier than the ones made from PE or PP. Also, thanks to their inherent properties, polymers offer mechanical properties that allow manufacturers to use much less material, leading to much lighter objects, in the case of packaging materials, which tend to be more convenient for the consumers. However, our plastic (a material consisting of a polymer to which additives or other substances may have been added, and which can function as a main structural component of final products, with the exception of natural polymers that have not been chemically modified²) production has skyrocketed during the past years of the 21st century. Growing from 2 million tons in 1950, 245 million metric tons of plastics have been globally produced in 2006³. Reports for 2019, published in 2020, showed this number went up to approximately 370 million metric tons⁴, which represents a 3.2% increase per year on average over 13 years. Since most plastics are single use plastics such as packaging, which account for 40% of produced plastics⁴, there is, therefore, more and more waste to manage. Unfortunately, huge amounts of these materials are not properly collected and treated leading to increasing levels of pollution. It is hard to precisely estimate proper amounts of lost waste, for instance, an article from 2014 by Eriksen *et al.*⁵ estimated that 250 thousand tons of plastic were afloat on the oceans. A report published in Science in 2015 established that around 8 million metric tons of plastic ended up in the ocean annually⁶ mainly originating from coastal areas where mismanaged plastic waste was estimated to 31.9 million metric tons. An article in Nature published in 2017 however brought the amount of new annual plastic waste ending in the ocean down to about 5 million metric tons⁷. In any case, this constitutes a major issue since most plastics are made from non-biodegradable polymers

General introduction

such as predominantly PE, PP, PVC and PET⁴ which are the most produced plastics per year (around 75%). Moreover, these polymers are often mixed with multiple additives in order to enhance their properties, spanning from thermal or mechanical properties to their resistance to wear and degradation⁸. These materials will therefore accumulate in the environment instead of disappearing. Degradation studies have shown these polymeric materials will break-up into small fragments, so-called microplastics^{6,9,10}. These microplastics are a source of poisoning for marine fauna as they can be eaten or release toxic chemical compounds, which are used as additives, directly in the ocean water. To limit such a pollution, more sustainable alternatives have to be embraced, notably using more sustainable plastic materials. For instance, regarding the use of such materials, 46% of plastic waste is due to packaging, which itself represents 40% of the plastic demand every year¹¹.

Along this, most of the produced plastics are oil-based and their production accounts for 10% of the global oil demand per year¹². The growing demand for oil along with the scarcity of such resource constitutes another challenge with soaring prices and the contribution to global warming. Such concerns push researchers to look for more sustainable alternatives in regard to replacing fossil-based resources by renewable ones. In this context, renewable resources from the Biomass constitute a very promising solution in terms of renewable carbon. Contrary to fossil fuels, which take millions of years to regenerate, resources from the biomass can be regenerated within a few decades and are highly available. Therefore, biorefineries were developed in order to transform the biomass and use it as a low-cost feedstock for the chemical industries¹³⁻¹⁵. As such, novel building blocks could be accessed through direct extraction from the biomass such as starch, chitin, lignin, fatty derivatives, or could be obtained through chemical or bacterial transformation of the biomass such as lactic acid for instance. In the particular case of polymers, monomers could be obtained and used to develop novel bio-based polymers with interesting properties and with a high biodegradable potential.

Global production capacities of bioplastics 2021 (by material type)

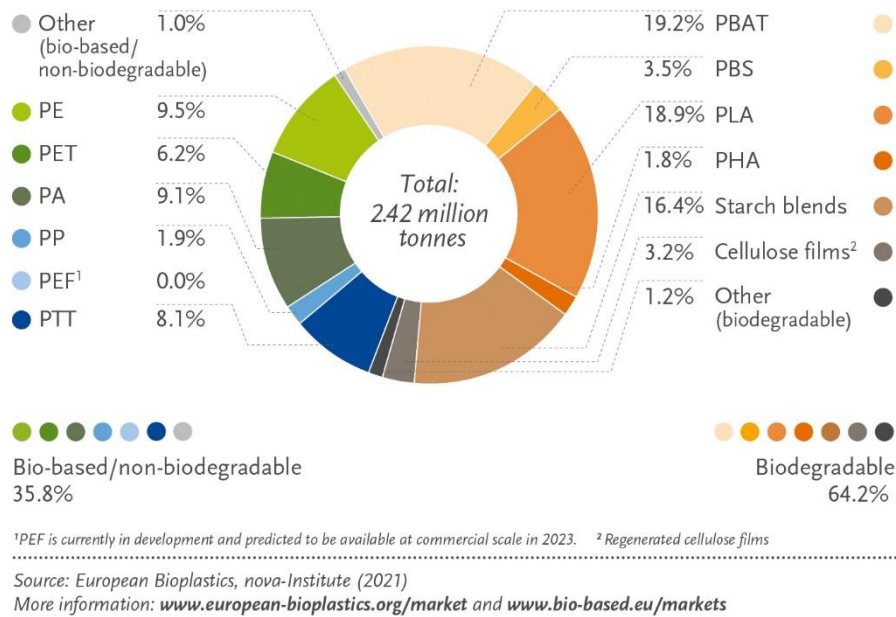


Figure 1: Bio-based plastics' global production capacity in 2021, reproduced from European bioplastics¹⁶

As such, poly(lactic acid) or poly(lactide) (PLA) is one of the most produced bio-based plastics with about 460 thousand tons produced in 2021¹⁷ which represents about 19% of the total bio-based plastics' market (Figure 1). Moreover, its production is expected to reach 760 thousand tons by 2026 due to a surge in demand for such material, along with major manufacturers such as NatureWorks and Total Corbion announcing the opening of new production plants¹⁸. PLA is an industrially compostable material obtained from lactide (the cyclic dimer of lactic acid) which is itself obtained from the fermentation of starch. Since it is biocompatible and has been approved for food contact by the FDA, multiple applications are suitable for it such as bioresorbable materials, drug delivery systems or food packaging. Thanks to such high production volumes and improved processes, its price now nears \$2/kg which makes it economically competitive compared to other commodity polymers such as poly(styrene) or poly(ethylene terephthalate)¹⁹, in particular regarding packaging applications. However, the inherent brittleness of PLA at room temperature along with its low heat deflection temperature and medium O₂ barrier properties are very important drawbacks to its widespread use. Therefore, additives are required to improve the properties of PLA, many of them which are oil-based and non-biodegradable. As such, recent works have been

General introduction

dedicated to the design of more environmentally friendly solutions but much more is required to be done.

This thesis work was financially supported by the Nouvelle-Aquitaine Region, the ITERG and the CTCPA. The two later are recognised French technical centres which are respectively involved in the development and promotion of biorefineries and fatty resources in France, and the development of better food preservation means through novel techniques or packaging. This manuscript will therefore describe two strategies to render PLA suitable as a food packaging material using bio-based and potentially biodegradable additives.

In the first chapter of this manuscript, the state-of-the-art reviewing the toughening of PLA, the enhancement of its heat deflection temperature, the improvement of its barrier properties regarding O₂ and more recent works regarding its biodegradability will be discussed. First, the synthesis and production of PLA from lactic acid will be reported along with an extensive description of its properties to clearly identify the assets and weaknesses of such polymer. Then, the state-of-the-art on the rubber-toughening of PLA will be exposed, notably discussing the performances of the developed solutions up to this date and identifying low T_g polyesters as the most sustainable impact enhancers. Next, the strategies to enhance the heat deflection temperature of PLA will be described and will reveal the potential of bio-based nucleating agents to promote the crystallisation kinetics of PLA and achieve high crystallinity ratios. Fourth will be about the strategies to limit the O₂ permeability of PLA through additives, a higher crystallinity ratio or processing strategies. Finally, recent works on the biodegradation of PLA will be reported and most noticeably the products from Carbiolice which allow PLA to be suitable for home-composting.

The second chapter will deal with the synthesis and use of novel symmetrical fatty bis-amide nucleating agents. In a first part, the synthesis of the compounds will be reported and the effect of the fatty chain along with the spacer between the amide functions on the thermal properties of these compounds will be discussed. Then, the study will focus on the efficiency of these bis-amides as nucleating agents for PLA. One particular compound synthesised from stearic acid and 1,4-diaminobutane will display the best performance and allow to achieve crystallinity ratios above 50% along with heat deflection temperature nearing 120°C.

Since increasing the crystallinity degree of PLA also increases its brittleness, chapter 3 will be dealing with polymeric additives based on poly(methyl ricinoleate) which has been reported an efficient rubber to toughen PLA. Taking advantage of the alkene function on every repetition motive, chemistry will be performed to bring additional chemical functions such as epoxides or cyclic carbonates to study both the effect on the mechanical properties of PLA and on its O₂ permeability. Two different grades of poly(methyl ricinoleate) will be used, one synthesised from a highly pure monomer and one obtained from an 85% pure monomer, and the differences in performance using these two polymers and their derivatives will be discussed. The best polymer regarding the enhancement of the mechanical properties is the poly(methyl ricinoleate) synthesised from the 85% pure monomer, without any chemical functionalisation. The effect of the epoxides and cyclic carbonates are more noticeable on the O₂ barrier properties since they will limit the increase of permeability due to the addition of an immiscible polymer additive inside PLA. Therefore, the great potential of poly(methyl ricinoleate)-based additives makes them suitable for more sustainable PLA materials.

References

1. *Polymer handbook*. (Wiley, 1999).
2. *Commission notice — Commission guidelines on single-use plastic products in accordance with Directive (EU) 2019/904 of the European Parliament and of the Council on the reduction of the impact of certain plastic products on the environment*. (2021).
3. PlasticsEurope. *Plastics, Compelling facts 2006*. (2006).
4. PlasticsEurope. *Plastics, the facts 2020*. (2020).
5. Eriksen, M. *et al.* Plastic Pollution in the World's Oceans: More than 5 Trillion Plastic Pieces Weighing over 250,000 Tons Afloat at Sea. *PLOS ONE* **9**, e111913 (2014).
6. Jambeck, J. R. *et al.* Plastic waste inputs from land into the ocean. *Science* (2015) doi:10.1126/science.1260352.
7. Thompson, R. Environment: A journey on plastic seas. *Nature* **547**, 278–279 (2017).
8. Marturano, V., Cerruti, P. & Ambroggi, V. Polymer additives. *Phys. Sci. Rev.* **2**, (2017).
9. Barnes, D. K. A., Galgani, F., Thompson, R. C. & Barlaz, M. Accumulation and fragmentation of plastic debris in global environments. *Philos. Trans. R. Soc. B Biol. Sci.* **364**, 1985–1998 (2009).
10. Andrady, A. L. Microplastics in the marine environment. *Mar. Pollut. Bull.* **62**, 1596–1605 (2011).
11. Tsakona, M. & Rucevska, I. *Baseline report on plastic waste*. <https://www.basel.int/Implementation/Plasticwaste/PlasticWastePartnership/Consultationsandmeetings/1stPWPmeeting/tabid/8305/ctl/Download/mid/23074/Default.aspx?id=9&ObjID=22886> (2020).
12. Mülhaupt, R. Green Polymer Chemistry and Bio-based Plastics: Dreams and Reality. *Macromol. Chem. Phys.* **214**, 159–174 (2013).
13. Demirbas, A. Biorefineries: Current activities and future developments. *Energy Convers. Manag.* **50**, 2782–2801 (2009).
14. Clark, J. H. Chapter 1 Green and Sustainable Chemistry: An Introduction. 1–11 (2016) doi:10.1039/9781782625940-00001.
15. Graedel, T. Green Chemistry in an industrial ecology context. *Green Chem.* **1**, G126–G128 (1999).

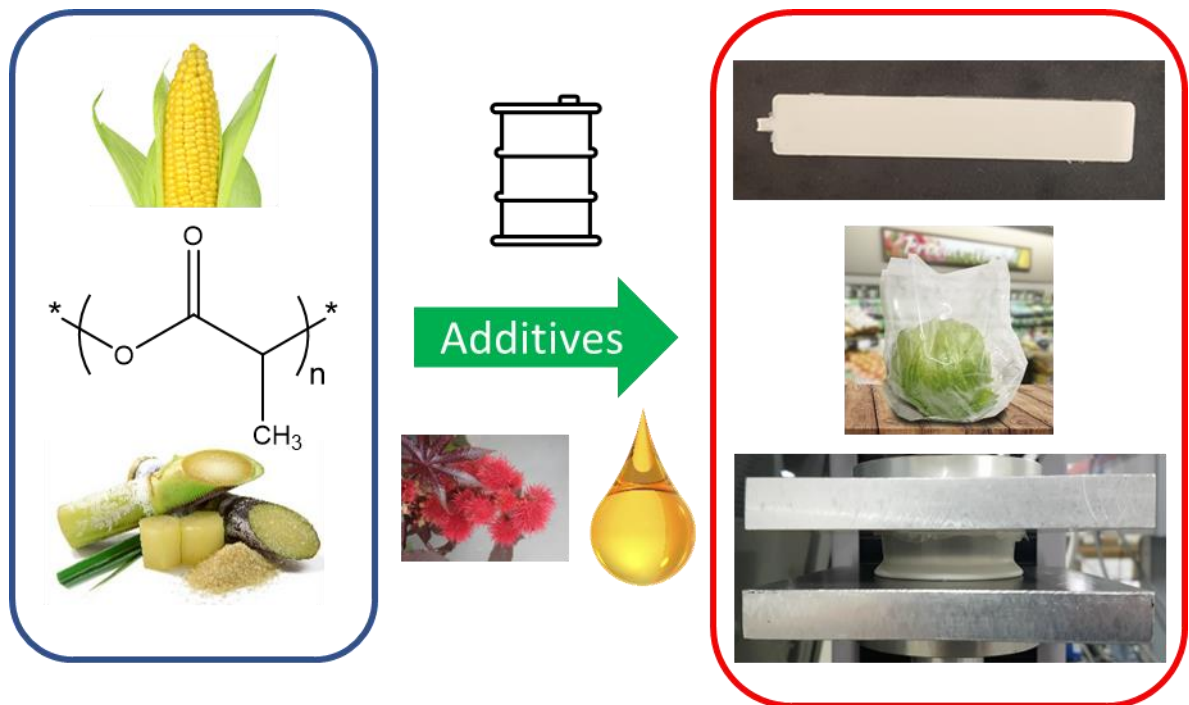
General introduction

16. European Bioplastics. <https://www.european-bioplastics.org/>.
17. Plastics - the Facts 2021 • Plastics Europe. *Plastics Europe* <https://plasticseurope.org/knowledge-hub/plastics-the-facts-2021/>.
18. Thaïlande : Total Corbion PLA démarre son usine de bioplastiques d'une capacité de 75 000 tonnes par an. *TotalEnergies.com*
<https://totalenergies.com/fr/medias/actualite/communiqués/thaïlande-total-corbion-pla-demarre-son-usine-de-bioplastiques-dune-capacite-de-75-000-tonnes-par>.
19. Polylactic Acid (PLA) Market | 2022 - 2026 | MarketsandMarkets.
<https://www.marketsandmarkets.com/Market-Reports/polylactic-acid-pla-market-29418964.html>.

Chapter I:

Poly(lactide): from a bio-based monomer to a potentially industrial polymer

Assets, drawbacks and industrial challenges



Contents

1. Poly(lactic acid), from a bio-based monomer to an economically viable polymer	10
1.1. From a green synthesis to an industrially available polymer.....	10
a. Lactic acid production and industrial stakes	10
b. PLA synthesis and production	12
1.2. PLA properties	17
a. Chemical structure and thermal transitions	17
b. Crystallographic properties and crystallisation behaviour	18
c. Processability.....	20
d. Mechanical properties	22
e. Gas permeation properties	23
f. End of life.....	26
2. PLA materials as food packaging: original drawbacks and requirements	31
2.1. Mechanical properties	31
2.2. Thermal properties.....	32
2.3. Gas barrier properties	32
2.4. End of life – Degradation and collection.....	33
3. Improving the properties of PLA through additives	34
3.1. Limiting the brittleness of PLA	34
a. Plasticisers: lowering the Tg below service temperature	36
b. Synthetic copolymers	37
c. Blending with soft low Tg polymers	44
d. Global summary and perspectives	60
3.2. Improving the heat deflection temperature of PLA.....	60
a. Enhancing the crystallisation kinetics (NAs, plasticisers...)	61
b. Stereocomplexation	67

3.3.	Tuning the O ₂ gas barrier properties.....	70
a.	Improving the crystallisation rate	70
b.	Specific additives	72
c.	Multi-layer films	76
3.4.	Improving the biodegradation of PLA materials	78
4.	Summary and strategy presentation for the research project	79
5.	References	82

1. Poly(lactic acid), from a bio-based monomer to an economically viable polymer

1.1. From a green synthesis to an industrially available polymer

a. Lactic acid production and industrial stakes

In 2021, about 2.42 million tons of bio-based polymers have been produced, which represents 0.7% of the 367 million tons of produced plastics in the world^{1,2}. In these 2.42 million tons, both traditional polyolefins such as poly(ethylene) along with novel polymers such as poly(lactide), poly(butylene-adipate-terephthalate), poly(hydroxyalkanoate)s, poly(butylene succinate), etc. are included. Among all these polymers, only about half of them are considered as compostable or biodegradable². The polymer with the one of highest production tonnage is PLA with about 460,000 tons, and moreover, its price now nearing \$2/kg which makes it economically competitive compared to other commodity polymers such as poly(styrene) or poly(ethylene terephthalate)³.

PLA is a compostable linear aliphatic polyester obtained from lactic acid (2-hydroxypropanoic acid), a chiral monomer, which exists under a levogyre form, L(+)-Lactic acid, and a dextrogyre form D(-)-Lactic acid. Lactic acid is itself obtained through the bacterial fermentation of carbohydrates or through chemical synthesis using the traditional petrochemical industry⁴. The latter involves many routes such as the hydrolysis of lactonitrile by strong acids, lactonitrile itself obtained from acetaldehyde, base-catalysed degradation of sugars, oxidation of propylene glycol or hydrolysis of chloropropionic acid. This petrochemical path is disregarded since productions capacities remain low, productions costs are high and the chemical path is not stereoselective⁵. Indeed, the resulting lactic acid will be obtained under a racemic mixture of 50/50 L- and D- forms which is not of industrial interest.

The preferred route to produce lactic acid is therefore the biotechnological one. Lactic acid bacteria are used for such process and, depending on the strain, can selectively yield either L-Lactic acid or D-Lactic acid⁶. Such bacteria can be classified into two groups: homofermentative and heterofermentative. The heterofermentative bacteria produce lactic acid along with carbon dioxide, acetic acid, glycerol and ethanol, whilst the homofermentative strains give high yields of lactic acid with very little by-products and are therefore more commonly used in the industry⁷.

The first generation sources for lactic acid production include sugar sources which span from corn, sugar cane, potato, tapioca seeds⁸. More recently, NatureWorks (Cargill Dow)⁹ and Total-Corbion¹⁰ are developing new industrial processes which allow the use of second-generation feedstocks *i.e.* lignocellulosic materials such as corn stover, wheat straw, wood chips or bagasse¹¹ while also exploring third generation feedstock based on algae and seaweed technology¹². Such third generation of feedstock is still however under development and requires some optimisations to manage the production of lactic acid that could be sold at a reasonable price¹³.

From all the first- or second-generation sources, starch is recuperated and then through hydrolysis is converted into glucose (90% yield), dextrose or sucrose. This carbohydrate is transformed into lactic acid through the bacterial fermentation process with approximately a 85% yield^{4,8}, giving between 300,000 - 400,000 tons of produced lactic acid per year in the United States, according to reports from 2016^{14,15} (Fig. I. 1). The leading companies for lactic acid and PLA production are NatureWorks and Total-Corbion, which have recently announced the opening of new plants in Thailand, with an expected annual production of 75,000 metric tons of PLA in the case of Total-Corbion^{16,17}.

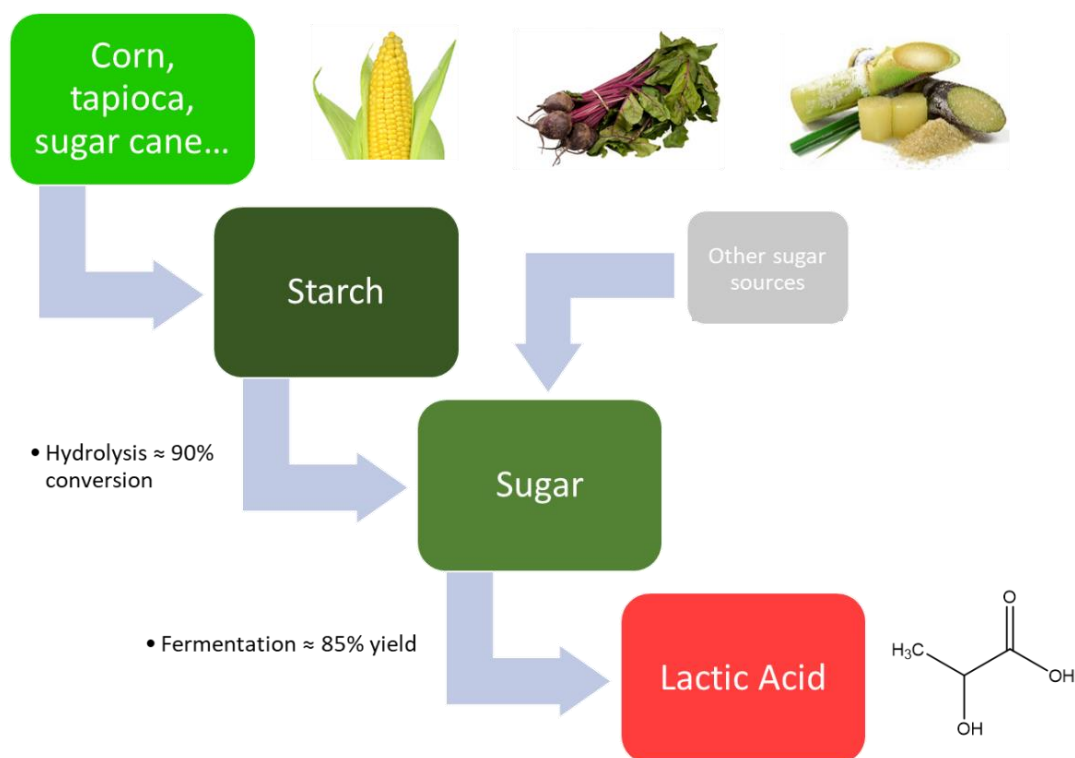


Fig. I. 1: Transformation process of first-generation feedstock to lactic acid

b. PLA synthesis and production

Three different methods can be used to transform lactic acid into high molar mass PLA: direct polycondensation, direct polycondensation using a solvent which allows an azeotropic dehydration or ring-opening polymerisation using a lactide dimer intermediate¹⁸ (Fig. 1. 2). Direct polycondensation seems to be the most obvious route thanks to the hydroxyl group and the carboxylic acid moiety borne by PLA. However, the molar masses obtained using this process are too low to be of interest, due to the combination of the need to remove the water condensate to shift the equilibrium along with a low reactivity of the formed secondary hydroxyl group of the monomer. Therefore, there is a necessity to use chain coupling agents to increase the molar mass. Such agents increase drastically both the cost of production of PLA and the synthesis step therefore rendering this path not very interesting from an industrial point of view^{4,18,19}. The same can be said when this strategy is employed to synthesise telechelic oligomers of PLA using a diol or a diacid to start the polymerisation. These oligomers can be used as prepolymers to achieve higher molar masses using chain extenders such as diisocyanates²⁰ or bis(amino-ether)s²¹, respectively yielding lactic acid based poly(ester-urethane) and poly(ester-amide) polymers. The synthesised final polymer must be further washed to eliminate unreacted chain coupling agents which complexifies the making process.

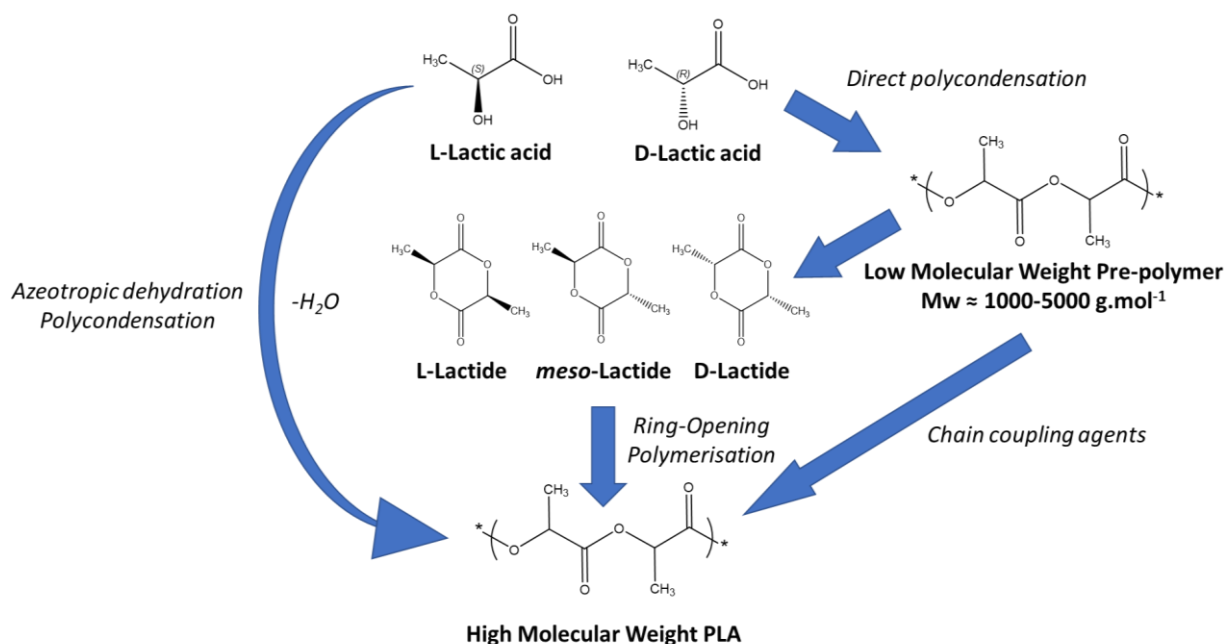


Fig. 1. 2: Pathways to synthesise high molar mass PLA

The approach involving an azeotropic distillation during the polymerisation has been used by Mitsui Toatsu Chemicals, Inc.²². The idea behind this technology is to allow the azeotropic

distillation of the condensate to shift the transesterification equilibrium towards the formation of the polymer. The reaction time is about 30-40h at 130°C which consumes a lot of time and energy therefore making this process unsuitable to produce cheap PLA. Moreover, high loadings of catalyst are also required to successfully reach high molar mass PLA, such catalysts having been reported to enhance the degradation of PLA during processing²³, favour hydrolysis or being toxic²⁴. Phosphoric acid or pyrophosphoric acid are therefore required to deactivate the catalyst and then strong acids such as sulfuric acid can be used to precipitate and filter the catalyst²⁵. All these extra steps complexify the synthesis of PLA and are not industrially suitable.

The most common PLA synthesis route is through the ROP of a lactide intermediate. Such lactide is obtained through a two-step procedure: first, PLA oligomers are formed by the direct condensation of lactic acid monomer units, and then, the more stable cyclic dimer lactide is formed through “end-biting” and “back-biting” depolymerisation. Both steps are conducted under heating and reduced pressure to eliminate the water formed during the oligomerisation process^{26,27}. However, lactic acid is a chiral monomer which leads to different enantiomers during the production of the lactide (Fig. I. 3). Such particularity involves multiple possibilities regarding the tacticity of the final polymer. Indeed, PLA can be atactic, syndiotactic or isotactic depending on the lactide quality used as the starting material. The optical purity of the final polymer has a direct effect on its thermal properties such as its melting point. PLA with less than 93% purity will remain amorphous and will not be able to crystallise.

The key point before the polymerisation is the separation of the stereoisomers to make sure to obtain the most optically pure PLA. Thankfully, the L-or D-Lactide have a different melting point than *meso*-Lactide and the racemic mixture (50%mol of L-Lactide and 50%mol of D-Lactide), respectively 97°C, 53°C and 125°C, allowing them to be separated²⁸. The common way used in the industry is a purification step by vacuum distillation which allows to recuperate water along with the separated lactide. Also, at the next step, the polymer reactor allows unreacted lactide to be recuperated and re-used for a new polymerisation, therefore limiting any waste regarding the monomer materials (Fig. I. 4).

Regarding the purification matter, another advantage is the use of the biorefinery route to produce lactic acid. Historically, such route yields a highly optically pure monomer, the L-Lactic acid although new bacterial strains allow to get highly pure D-Lactic acid as well^{14,15,29}.

Chapter 1

In the case of lactides derived from oil derivatives, a racemic mixture is obtained therefore requiring stereoselective catalysts to produce polymers with a controlled stereochemistry (Fig. 1. 7). Therefore, most lactides produced will be either the (S,S)-Lactide or so-called L(+)-lactide or the (R,R)-Lactide, the so-called D(-)-Lactide. The lactide is then used to conduct a ring opening polymerisation to yield PLA.

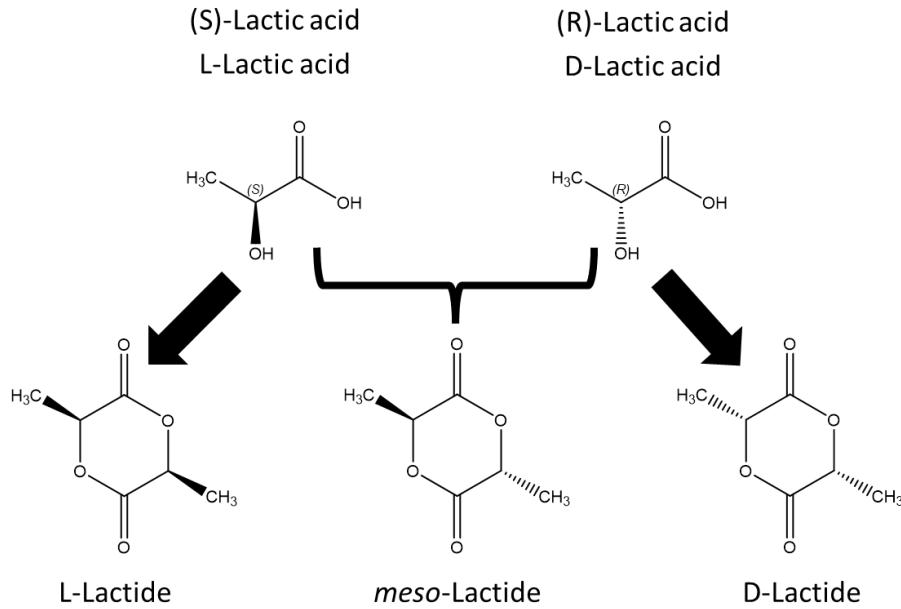


Fig. 1. 3: Enantiomeric and diastereoisomeric lactide structures obtained from lactic acid

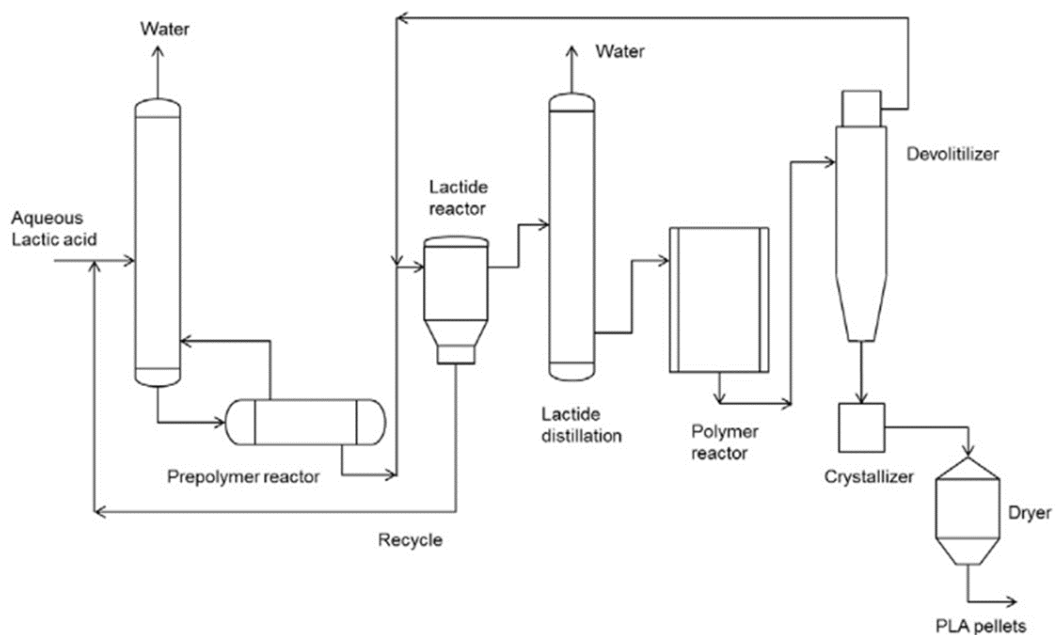


Fig. 1. 4: NatureWorks LLC commercial process for producing high molar mass PLA, reproduced from Castro-Aguirre et al.⁷ with permission from Elsevier

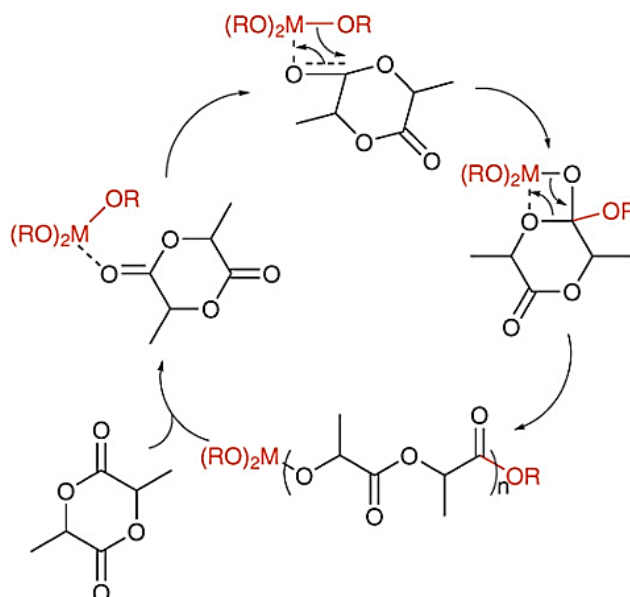


Fig. I. 5: Coordination-insertion mechanism of lactide polymerization using metal-alkoxide catalysts. Reproduced from Thomas C.M.³⁰ with permission from the Royal Society of Chemistry

Metal catalysts such as tin(II) bis(2-ethylhexanoate), zinc(II) lactate or aluminium(III) isopropoxide are commonly used for the high scale industrial synthesis of PLA from lactides but are not stereoselective³⁰ and work through a coordination-insertion mechanism³¹ (Fig. I. 5). Tin(II) bis(2-ethylhexanoate) supported by aluminium oxide remains the most commonly used catalytic system as it presents the highest catalytic effect, is soluble in organic solvents and allows polymerisation up to 180°C³². Jointly, lauryl alcohol is used as the initiator of the polymerisation. However, this catalyst remains toxic to aquatic life and has a reprotoxic effect³³. Extensive research is required to find alternatives such as organo-catalysts such as 1,5,7-triazabicyclo[4.4.0]dec-5-ene (TBD), 1,8-diazabicyclo[5.4.0]undec-7-ene (DBU), 7-methyl-1,5,7-triazabicyclo[4.4.0]dec-5-ene (MTBD), 4-(dimethylamino)pyridine (DMAP), 4-pyrrolidinopyridine (PPY), thioureas etc which allow the polymerisation to take place at lower temperatures and display short reaction times (approximately 1min for TBD used at 0.1mol%)²⁹. Thanks to the high optical purity of the lactides, the ROP will give highly enantiopure isotactic PLA grades poly(L-Lactide) (PLLA) or poly(D-Lactide) (PDLA) (Fig. I. 6). For historical reasons, PLLA remains the most common type of synthesised PLA, although an interest in producing PDLA has been developed recently due to the potential of PLA stereocomplexes, a co-crystal made of PLLA and PDLA chains^{34,35}.

Chapter 1

To avoid the purification problems brought by the chirality of lactic acid and with the growing interest towards PLA stereocomplexes, extensive research has been conducted towards high stereo-selective catalysts. The main focus is to use racemic lactide as the starting material as it is impossible to separate the two enantiomers in such mixture and therefore its polymerisation with traditional ROP catalysts will lead to an atactic polymer. The review from Thomas and the book chapter from Osten *et al.* clearly highlight the different types of catalysts developed to obtain selectively the achievable structures of PLA^{30,36} (Fig. I. 7). Works on chiral aluminium-based Schiff base catalyst systems demonstrated the effect of the ligand towards the preference of the catalyst towards either L-Lactide or D-Lactide. As first exemplified by Spassky *et al.*, these single-site catalysts³⁷ work through two different mechanisms: either a chain-end control mechanism³⁸ or a site control mechanism³⁹. Namely, the chain-end control operates through the control of the next inserted monomer through the stereoconfiguration of the last repeating unit in the growing polymer chain, whereas the site control mechanism operates through the configuration of the ligands on the catalyst site.

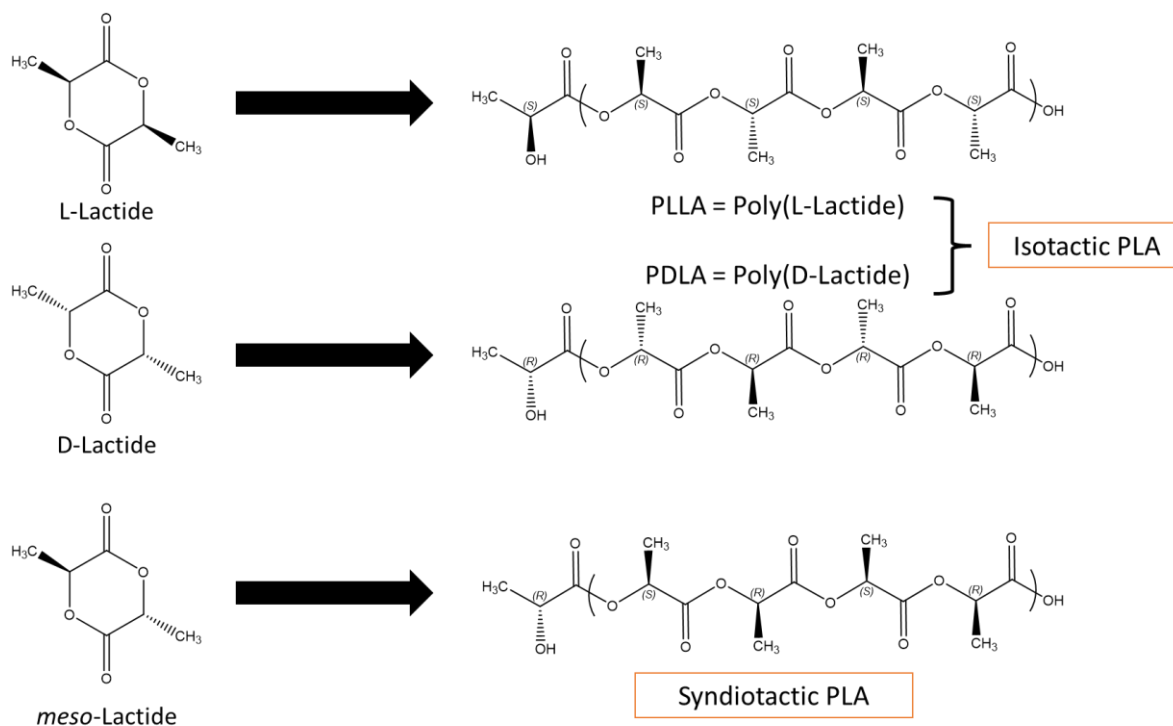


Fig. I. 6: Achievable stereocontrolled PLA grades from pure lactides

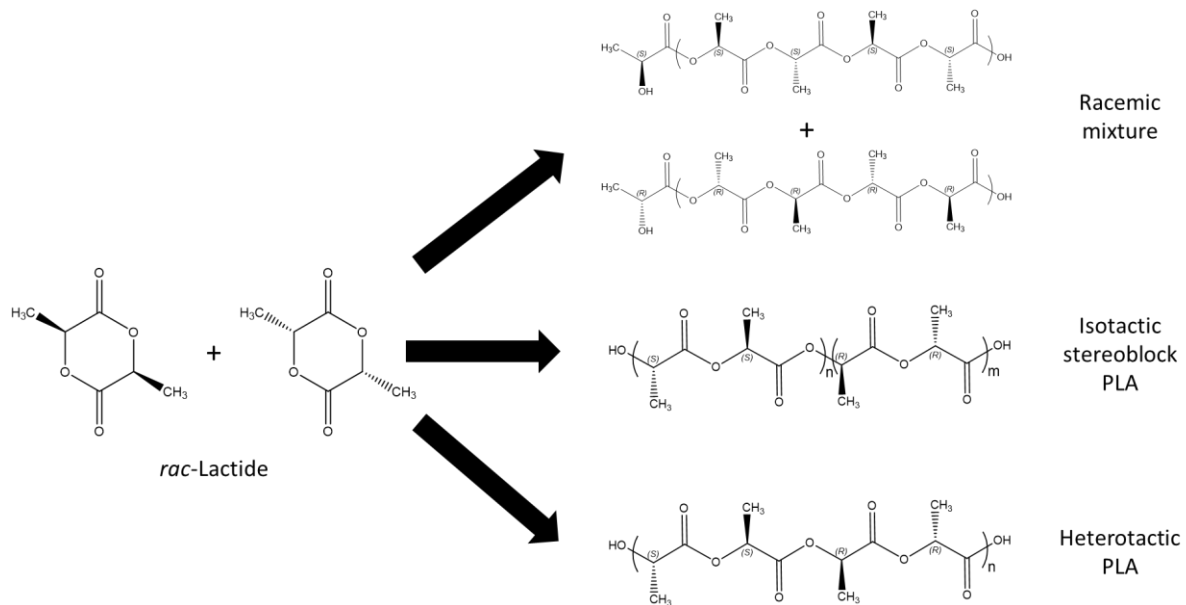


Fig. 1. 7: PLA stereochemistry obtained from a racemic lactide mixture with stereoselective metal catalysts

For the rest of the study, the emphasis will be specifically put on isotactic PLLA due to its high availability and its potential regarding its thermal properties and mechanical properties.

1.2. PLA properties

a. Chemical structure and thermal transitions

As previously mentioned, PLA is made from lactic acid, which is a chiral monomer, therefore implying tacticity issues for the obtained polymer. Depending on its tacticity, PLA will not display the same thermal properties. Atactic PLA is amorphous and only displays a glass transition temperature ranging from 55°C to 60°C which depends on the molar mass of PLA according to the Flory-Fox equation:

$$Tg = Tg^{\infty} - \frac{K}{Mn}$$

Where Tg^{∞} is the Tg at infinite molecular weight, K a constant expressing the excess of free volume of the end groups for polymer chains and Mn the number average molar mass. Values of Tg^{∞} and K are reported as 57-58°C and 5.50×10^4 °C.mol.g⁻¹ according to Jamshidi *et al.*⁴⁰.

PLAs which are at least 93% optically pure are semi-crystalline polymers with a Tg of 55°C and a melting point temperature ranging from 130°C to 180°C depending on both the molar mass and the optical purity⁴¹⁻⁴⁴. A final transition reported for PLA is its β -transition at -45°C

Chapter 1

upon which PLA is strictly brittle⁴⁵. Regarding the melting behaviour of PLA, Tsuji and Ikada found that the equilibrium melting point of PLA would increase with the molar mass up to a maximum value of 215°C⁴⁶ by using the Hoffman-Weeks extrapolation; although a more commonly reported and accepted value is 207°C reported by Kricheldorf *et al.*⁴. The melting enthalpy for a 100% crystalline PLA is 93.7J.g⁻¹ as calculated by Fischer *et al.* and is the commonly accepted value⁴⁷. The crystallinity ratio of PLA can be calculated using the DSC according to the following formula:

$$\chi_c = \frac{\Delta H_m - \Delta H_{cc}}{\Delta H_{m,0}}$$

With:

- χ_c = the crystallinity of the PLLA sample
- ΔH_m = the measured melting enthalpy
- ΔH_{cc} = the measured cold crystallisation enthalpy
- $\Delta H_{m,0}$ = the melting enthalpy of 100% crystalline PLA, 93.7 J/g

One particular feature of PLA is however its slow crystallisation kinetics. PLA crystallises between 90°C and 135°C following a dumb-bell shape behaviour, *i.e.* the fastest crystallisation rates are observed between 105°C and 125°C with a maximum between 110°C and 115°C⁴¹. The crystallisation half-time $t_{1/2}$ has been reported over 35mins for a commercial PLA (NatureWorks 3001D) at 115°C⁴⁸. Other studies also showed that a higher molar mass would also slow even more the crystallisation kinetics of PLA along with the amount of impurity^{41,42,44,47,49-52}. This characteristic is a major drawback to the use of PLA as fast industrial processing conditions do not allow enough time for PLA materials to crystallise.

b. Crystallographic properties and crystallisation behaviour

Semi-crystalline PLA has been reported to crystallise under four different forms. The two most ones are the α and the α' (also known as δ) phases. These two phases are the ones primarily formed by simply cooling PLA from the melt or during annealing and are quite similar in terms of crystalline structure, therefore justifying the α and the α' denominations. These two crystalline forms are reported to have a helical structure with a 10_3 parameter which indicates ten repeat units in three turns and have both orthorhombic crystal cells⁵³⁻⁵⁶. The

difference however appears while looking at the cell parameters of these two phases. Reports for the α phase give $a=10.86\text{\AA}$, $b=6.16\text{\AA}$ and $c=28.86\text{\AA}$ whereas for the α' , $a=10.80\text{\AA}$, $b=6.20\text{\AA}$ and $c=28.80\text{\AA}$. Since the ratio of the a and b parameters of the α phase is equal to $\sqrt{3}$, the helices of this phase verify a strictly packed hexagonal fashion whereas the α' phase is slightly distorted^{56,57}. These two phases also do not form at the same temperatures with PLA cooled from the melt. It is typically reported that the α' phase forms at temperatures below 120°C whereas the α phase forms above 100°C ⁵⁸ (Fig. 1. 8). The α' form is reported to melt before the α phase upon heating and, moreover, to transform into the α form upon heating; such phenomenon can be observed by the presence of a small exotherm in the DSC⁵⁷ or by a slight change of the XRD pattern of the sample⁵⁹.

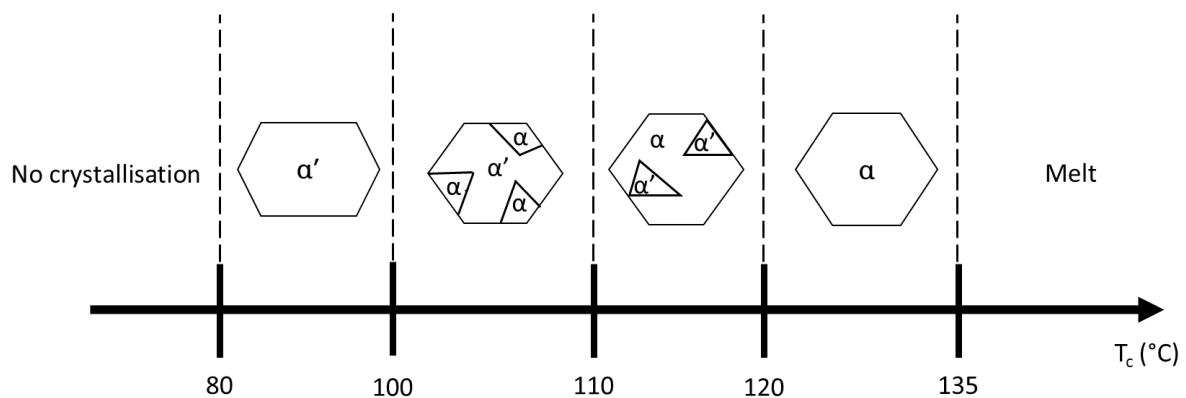


Fig. 1. 8: Formation of the crystalline phases of PLA when cooled from the melt

The β form of PLA is less common than the α' form and the α form. It is typically formed from α crystals in fibres that are being stretched or during the formation of thin films. The helix conformation is changed to 3_1 and the crystalline cell is now the one of a trigonal cell unit with the cell parameters $a=b=10.66\text{\AA}$ and $c=8.8\text{\AA}$ and $\alpha=\beta=90^\circ$ and $\gamma=120^\circ$ ^{55,60,61}.

The γ phase of PLA is less common due to the very specific conditions at which it can be created. It is specifically obtained from epitaxial crystallisation in hexamethylbenzene at 140°C ⁶². Two antiparallel helices are packed in an orthorhombic unit cell with parameters as follow: $a=9.95\text{\AA}$, $b=6.25\text{\AA}$ and $c=8.8\text{\AA}$. Unfortunately, the properties of this particular phase have not been studied.

The last known crystalline phase of PLA is the stereocomplex form. It is obtained from the co-crystallisation of an equimolar mixture of PLLA and PDLA³⁵. The stereocomplex is formed of left-handed and right-handed threefold helices. The parameters of the trigonal unit cell are

Chapter 1

$a=b=14.98\text{\AA}$ and $c= 8.7\text{\AA}$ and $\alpha=\beta=90^\circ$ and $\gamma=120^\circ$. The most noticeable feature of these stereocomplexes is their high melting point around 220°C , which is about 50°C higher than what can be obtained with PLA homopolymers. This is of particular interest since it can offer a solution to the low thermal resistance of PLA materials.

Regarding its crystalline morphology, PLA has been reported to crystallise under the form of non-banded 3D spherulites as observed by polarised optical microscopy (PLOM) by Vasanthakumari *et al.*⁶³ (Fig. I. 9) although Kalb and Pennings reported the formation of 2D axialites at a low degree of supercooling⁵². The density of spherulites has also been observed to decrease with a decreasing T_c , whereas the spherulite growth follows the bell-shape trend described for the crystallisation half-time of PLA described earlier. By applying the Avrami equation, the n exponent value is reported between 2 and 3.2, depending on the crystallisation conditions⁴⁴. Typically, the Avrami exponent can be separated into two terms:

$$n = n_d + n_n$$

Where n_d represents the dimensionality of the growing crystal (1, 2 or 3) which corresponds to 1D, 2D or 3D entities, and n_n represents the time dependence of the nucleation (0 or 1), being either instantaneous (0) or sporadic (1). For polymers, the value of n_d is 2 or 3 corresponding to 2D lamellar aggregates or 3D radial lamellae. The case of n_n is somehow less discrete since the nucleation dependence is rarely fully instantaneous or sporadic⁶⁴.

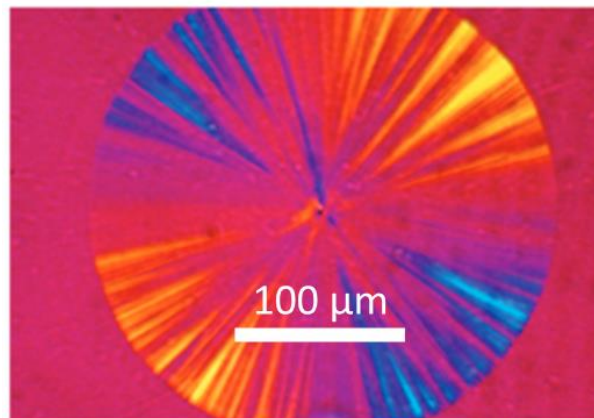


*Fig. I. 9: PLOM micrograph during the isothermal crystallisation of PLLA after 8 mins at 140°C (Adapted with permission from Castillo *et al.*⁶⁵. Copyright 2010 American Chemical Society)*

c. Processability

As mentioned above, PLA has a T_g around $55\text{--}60^\circ\text{C}$ and a melting temperature that can go up to 180°C . When considering the processing of PLA to make objects, one should take into

account these two fundamental characteristics. In the case of fully amorphous PLA, processing above the T_g will be enough to manufacture objects. In the case of semi-crystalline grades of PLA, the processing temperature should be higher than the melting temperature. However, the processing time should not be too long nor the temperature too high since it was reported PLA was subject to degradation in the melt state^{66–68}. Typically, PLA will undergo degradation at temperatures above 200°C resulting in the formation of acetaldehyde, carbon monoxide along with lactide and oligomers^{69–71}. The common technique for continuously processing PLA is the extrusion. Depending on the PLA grade, the melt-flow index will play an important role on determining the processing temperature. High molar mass PLAs will have lower MFIs therefore requiring a higher processing temperature to lower their viscosity. Unfortunately though, PLA is also a moisture sensitive polymer and therefore needs to be dried before being processed with NatureWorks recommending PLA should bear less than 250ppm of moisture content prior to extrusion. Speranza *et al.* studied the thermal and hydrolytic degradation of PLA in the molten state using rheology. They found PLA undergoes a significant change of viscosity especially when it has not been dried but their work was not correlated to any change in molar mass⁶⁶. Mysiukiewicz *et al.* investigated the processing parameters of different PLA grades and their impact on the PLA's properties. They concluded high temperatures and high rotation speeds greatly reduced the molar mass of PLA. However, they also reported the lower viscosity PLA grades were the ones which displayed least a loss of molar mass⁷². Shojaeiarani *et al.* showed the effect of reprocessing PLA by extrusion and observed a 80% reduction in molar mass after 5 cycles along with a lower T_g and a lower viscosity⁷³. This implies precautions should be taken when processing PLA otherwise the final properties of the material will be hampered.

Multiple techniques of polymer processing can also be used to make all sorts of objects such as injection-moulding, stretch-blow moulding, film casting, thermoforming, foaming or fibre-spinning⁷⁴. Many challenges remain in order to adapt the processing conditions to PLA. Indeed, all these processes are optimised for well-known and used polymers such as polyolefins or PET, which do not have the same melt strength, shrinking ability and viscosity as PLA. The injection-moulding technique can so far be successfully used to produce amorphous PLA objects at fast production rates, given the PLA piece can be cooled to 25°C–30°C prior to ejection. PLA films have also been successfully produced although such

production is more complicated than for PET or PP since PLA shows lower melt strength. The obtention of such films allows the use of thermoforming, which can be achieved using materials and techniques used for PET, high impact polystyrene and oriented polystyrene, using a lower temperature range (80-110°C)⁷⁵. More challenges still remain regarding stretch-blow moulding and extrusion blown film as processing optimisations still remain to be used for the first and for the second, the impossibility to create a stable bubble with neat PLA and therefore requiring the use of additives⁷⁶.

d. Mechanical properties

At room temperature, PLA is known to be a stiff and brittle polymer. Typical semi-crystalline PLA displays a Young's modulus around 3.5-4GPa, a tensile strength around 60 MPa and a typical strain at break of 4-7% at room temperature^{77,78}. Such properties are highly dependent on the molar mass and the stereochemistry of PLA as, for instance, the tensile strength of PLA can vary from 15.5 to 80 and even 150MPa with molar masses going respectively from 50,000 to over 150,000 and 200,000, along with a modulus that increases by a factor two⁷⁹. During a tensile test, PLA samples will break in the elastic zone and display no plastic behaviour. This is a similar behaviour than PS for instance which also displays such brittle behaviour at room temperature. However, it is clearly poorer than other commodity polymers such as PET, HDPE or PP that display high abilities to sustain a mechanical deformation or stress without breaking⁸⁰⁻⁸² (Table I. 1).

Table I. 1: Mechanical properties of PLA and other commodity polymers

Properties	PLA	PS	PET	HDPE	PP
Young's modulus (GPa)	3.5-4	3.0-3.5	2.8-4.1	0.6-1.4	1.1-1.3
Tensile strength	60	45	57	18-35	21-37
Strain at break (%)	4-7	3	300	100-1000	100-600
Impact strength – Notched IZOD (J.m⁻¹)	26	21	59	21-214	27-1068
Heat deflection temperature (°C)	55	75	71	60-90	100-120

One final factor also to consider is the thermal resistance of PLA, expressed by its heat deflection temperature (HDT). This value gives an idea of the temperature at which, under a

certain load, the polymer material will start to deform. In the case of PLA, this is another drawback as it is measured close to its T_g , meaning that above 55°C, no thermal application of PLA can be considered. This HDT however highly depends on the degree of crystallisation of the polymer. Tabi *et al.* have shown the relationship between the HDT of PLA and its crystallinity ratio. Namely, the HDT of PLA can go from 55°C in the case of a 3% crystallinity ratio polymer to 80-100°C for crystallinity ratios of 40-45%⁸³. They later discussed the importance of the crystalline phase, especially the two most common that are the α' and the α phases. The results asserted the α phase plays a predominant role in enhancing the HDT as temperature of 151°C be obtained, whereas with the α' phase, the HDT is never higher than 100°C even at high crystallinity ratios (45%)⁸⁴. All in all, PLA has similar properties than PS but then suffers from major disadvantages compared to other common polymers, which display significantly better mechanical properties. Fig. I. 10 summarises the different states of PLA according to temperature and displays the narrow range of temperature upon which PLA materials may be used.

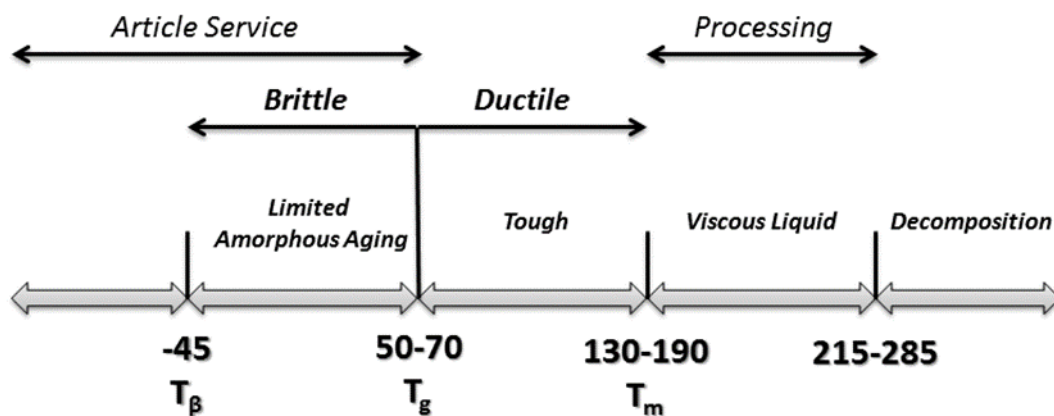


Fig. I. 10: Metastable states of high molar mass PLLA

e. Gas permeation properties

The permeation mechanism of a low molar mass solute inside a polymer follows a “solubilisation-diffusion” model⁸⁵. Typically, the penetrant will penetrate the polymer matrix into an available hole due to free volume and then a gap will open towards another available hole thanks to transient chain motion and finally the gap will close⁸⁶ (Fig. I. 11).



Fig. 1. 11: Schematic representation of the mechanism of the of a penetrant transport in a polymeric material

The permeability of such penetrant in a polymer can be expressed as follow:

$$P = D \times S$$

With P= the permeability coefficient of the penetrant through the matrix, D= the diffusion coefficient of the penetrant through the matrix and S= the solubility of the penetrant inside the matrix. This formula can further be developed using Fick's first law, supposing a concentration gradient which is linear with the distance, Fick's second law and Henry's law regarding the concentration of a gas. By supposing a steady state, the resulting formula can be used to measure the permeation:

$$P = \frac{Q \times L}{A \times t \times \Delta p}$$

Where Q is the amount of penetrant, L the thickness of the film/material, A the area of diffusion, t the time and Δp the pressure differential on the two sides of the material.

Typical parameters influencing the permeability can be divided into two categories that are the intrinsic and extrinsic factors. Extrinsic factors include the temperature, the relative humidity, the nature of the permeant whereas intrinsic factors include the chemical composition, the stiffness of the polymer chains, the polarity and the crystallinity ratio⁸⁷. Typical values of O₂ permeability for PLA range around 30-80x10⁻³ cm³.m.m⁻².day⁻¹.atm⁻¹ at temperatures ranging from 5°C to 58°C as reported by Sonchaeng *et al.* in their review⁸⁸, although Drieskens *et al.* reported higher values ranging from 132-590x10⁻³ cm³.m.m⁻².day⁻¹.atm⁻¹ in their work regarding the effect of crystallinity⁸⁹. Unfortunately, the

criteria to define a polymer as barrier or permeant varies depending on the targeted use. Polymer films with an oxygen permeability lower than $5 \times 10^{-3} \text{cm}^3 \cdot \text{m} \cdot \text{m}^{-2} \cdot \text{day}^{-1} \cdot \text{atm}^{-1}$ are considered as high barrier materials for food packaging⁹⁰. Wang *et al.* further refined the classification of a barrier grade material regarding oxygen to try to discriminate the different polymers (Table I. 2). Typical polyolefins such as HDPE, oriented PP and PS display very poor oxygen barrier behaviours with permeability values above $2000 \times 10^{-3} \text{cm}^3 \cdot \text{m} \cdot \text{m}^{-2} \cdot \text{day}^{-1} \cdot \text{atm}^{-1}$ for HDPE and oPP and around $4500 \times 10^{-3} \text{cm}^3 \cdot \text{m} \cdot \text{m}^{-2} \cdot \text{day}^{-1} \cdot \text{atm}^{-1}$ for PS⁹¹. Other polymers such as oriented PET have permeability values $35 \times 10^{-3} \text{cm}^3 \cdot \text{m} \cdot \text{m}^{-2} \cdot \text{day}^{-1} \cdot \text{atm}^{-1}$ which makes it a more suitable candidate for barrier applications⁹¹. In this regard, PLA is therefore a better barrier polymer than one of its direct challengers which is PS, however, it remains not as efficient as oPET which is another material PLA can challenge.

Table I. 2: Classification of polymers depending on their O₂ barrier performance. Adapted from Wu *et al.*⁸⁷

Barrier grade	Oxygen permeability ($10^{-3} \text{cm}^3 \cdot \text{m} \cdot \text{m}^{-2} \cdot \text{day}^{-1} \cdot \text{atm}^{-1}$)	Polymer examples
Very high	<1.6	EvOH, PGA
High	1.6-16	PVOH
Medium	16-160	PHAs, oPET, crystallised PLA, Nylon 6
Low	160-1600	Amorphous PLA, PBS
Poor	>1600	HDPE, oPP, PS, PBAT, PCL

In the case of PLA, the O₂ permeability greatly depends on the crystallinity ratio, the crystalline phase and the crystalline morphology⁹²⁻⁹⁴. However, to understand the relationship between the crystallinity ratio of PLA and the observed permeability, it is necessary to develop the model of a semi-crystalline polymer. Traditionally, a semi-crystalline polymer is composed of crystalline domains called crystallites, in which the polymer chains are densely packed and organised, and an amorphous fraction which corresponds to the rest of the polymer chains. However, Nguyen *et al.* have discovered that, in the case of PLA and PET, a three-phase model was necessary⁹⁵. The amorphous fraction of these polymers is actually composed of a mobile amorphous fraction and a restricted or rigid amorphous fraction (Fig. I. 12). Namely, the mobile amorphous fraction is the amorphous part of the polymer between crystallites whereas the rigid amorphous fraction is stuck within the

crystallites of these polymers, in this case, between the crystalline regions of the formed spherulites.

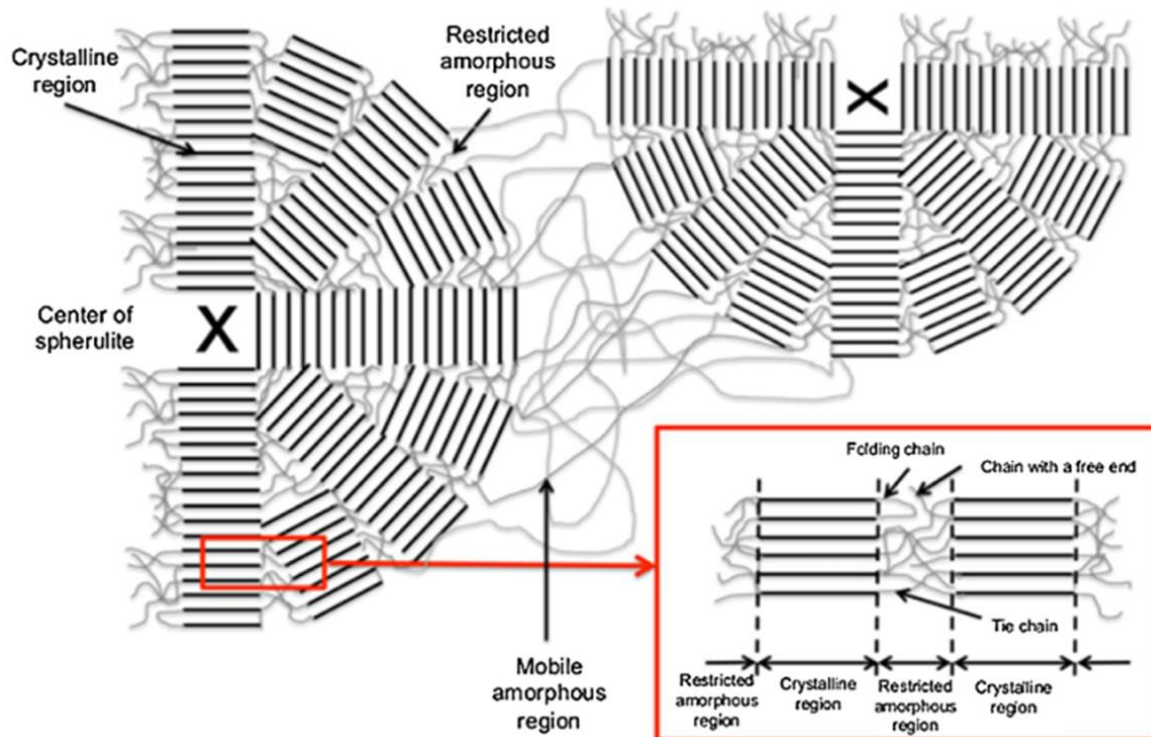


Fig. 1. 12: A possible schematic representation of the crystalline fraction (CF), the restricted amorphous fraction (RAF), and the mobile amorphous fraction (MAF), reproduced from Sonchaeng *et al.*⁸⁸ with the permission of Elsevier

Further studies by Del Rio *et al.* and Fernandes Nassar *et al.* actually showed an evolution of the quantity of these two amorphous regions during crystallisation and, more importantly, the O₂ permeability would actually be highly influenced by the amount of rigid amorphous fraction, which produces a lot of free volume holes⁹⁶. The authors concluded the best way to enhance the barrier properties during the crystallisation of PLA was to find a crystallisation process which would limit the formation of the rigid amorphous fraction⁹⁷.

f. End of life

PLA is often valued as being more environmentally friendly than other polymers such as PP, PE, PS or PET. It is also one of its major assets as, for instance, PLA is used for medical applications, in particular for bioresorbable materials. Indeed, PLA and especially PLLA is known to degrade in body fluids without being toxic to the living as such body can produce enzymes to deal with L-Lactic acid as it is a natural molecule produced from the muscles during

an effort⁹⁸. Due to its polyester nature and structure, PLA's main degradation mechanism is through hydrolysis⁹⁹. Jung *et al.* showed PLA would degrade slowly in neutral pH conditions and its rate of degradation would improve in acidic conditions and even more in alkaline conditions¹⁰⁰. More precisely, the effect of the acid-base catalysis was evaluated to be ten times faster when the pH value changed by just one unit¹⁰¹. The degradation mechanism was found to happen through the hydrolysis of random ester functions either on the chain-end or at the core of the PLA chain. More specifically, De Jong *et al.* showed the degradation of PLA in alkaline conditions happened through a progressive release of lactide¹⁰² (Fig. I. 13), whereas lactic acid is the directly formed product in acidic conditions⁹⁹ (Fig. I. 14).

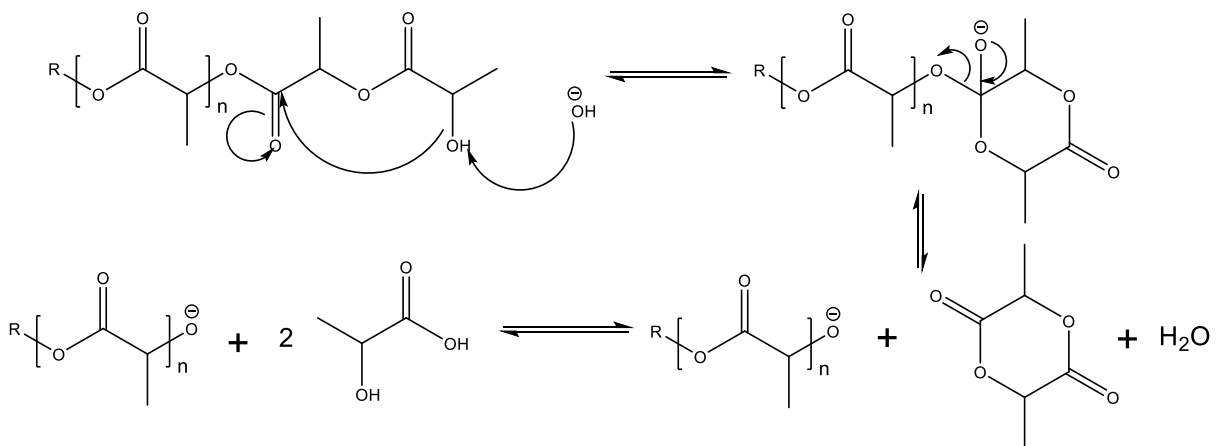


Fig. I. 13: Degradation mechanism of PLA in alkaline conditions

Chapter 1

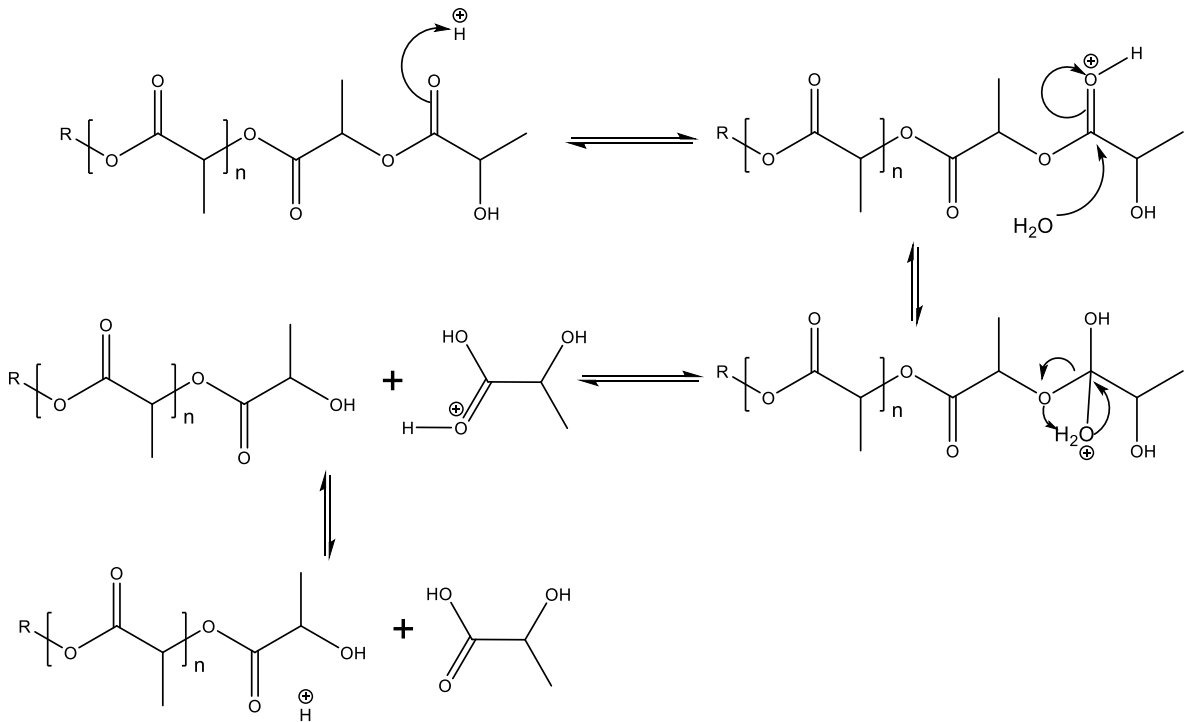


Fig. 1. 14: Degradation mechanism of PLA in acidic conditions

Multiple factors can influence the degradation of PLA such as the pH, the temperature, the shape and thickness of the sample, the crystallinity ratio and the molar mass of PLA.^{25,103} Typically, a higher molar mass PLA will degrade slower than lower grades as they have higher chain entanglement and therefore resist better to chain cleavage^{104–106}. Regarding the effect of the degree of crystallisation, highly crystalline PLA will degrade at a slower rate than the amorphous PLA since the amorphous fraction was found to be more prone to hydrolysis than the crystalline fraction^{107,108}. Such phenomenon is due to the higher chain packing density in the crystalline regions that prevent water uptake. The effect of temperature was reported by multiple studies and show an enhanced degradation when the temperature reached 55°C¹⁰⁹. This is explained thanks to the Tg of PLA that is of 55°C meaning that at temperatures near or above the Tg, the chain mobility will greatly increase, therefore allowing a higher water uptake along with a second effect on the reaction kinetics which are favoured by a higher temperature and result in a higher water activity towards the ester bonds. Once the molar mass of PLA is sufficiently low (below $M_n=10,000 \text{ g.mol}^{-1}$), microorganisms consume the small PLA chains and transforms them into carbon dioxide, water, and humus. Such microorganisms can be microbes, enzymes (Proteinase K, pronase)¹¹⁰ or fungi¹¹¹. However, these results are observed in laboratories and PLA seems not to degrade this well when left in natural environments¹¹².

According to the NF EN-13432 standard, PLA is a compostable polymer if degraded in industrial conditions in which conditions can reach up to 65°C with a relative humidity higher than 60%^{113,114}. However, multiple studies have shown it does not easily degrade when left in other media such as sea water, home-compost or in the raw environment and may take years to fully degrade¹¹⁴⁻¹¹⁷. Indeed, in such media, essential conditions, which directly influence the degradation rate, such as the pH, the temperature, or the present microorganisms, change a lot. Plastics can find themselves in the Arctic ocean where the water temperature reaches values below 0°C¹¹⁸ and therefore show very little degradation. The same can be said about soils and landfills which can either display neutral, acidic or basic conditions¹¹⁹. In these cases, PLA will likely behave as regular polymers and display physical fragmentation into small plastic parts rather chemical degradation into lactic acid. Chamas *et al.* compared the degradation rate of various common plastics in the environment in their perspective paper¹¹⁵. They considered different media such as in landfill/soil/compost, in marine environment, in biological conditions or under sunlight. These categories represent the four main degradation conditions for polymer degradation experiments which are: on land without exposure to sunlight, in water (fresh water or marine) with exposure to sunlight, in a lab using enzymes or microbes, or exclusively under sunlight exposure and air (Fig. I. 15). Surprisingly, the degradation rate of PLA without fillers nor accelerating conditions was shown to be similar to traditional oil-based polymers such as PET, HDPE, LDPE, or PP in marine conditions. On land, the trend was better looking as PLA shows to degrade about twenty times faster, about 21µm.year⁻¹ compared to 1µm.year⁻¹ for HDPE . This remains slow however and PLA should be properly collected and recycled rather than discarded.

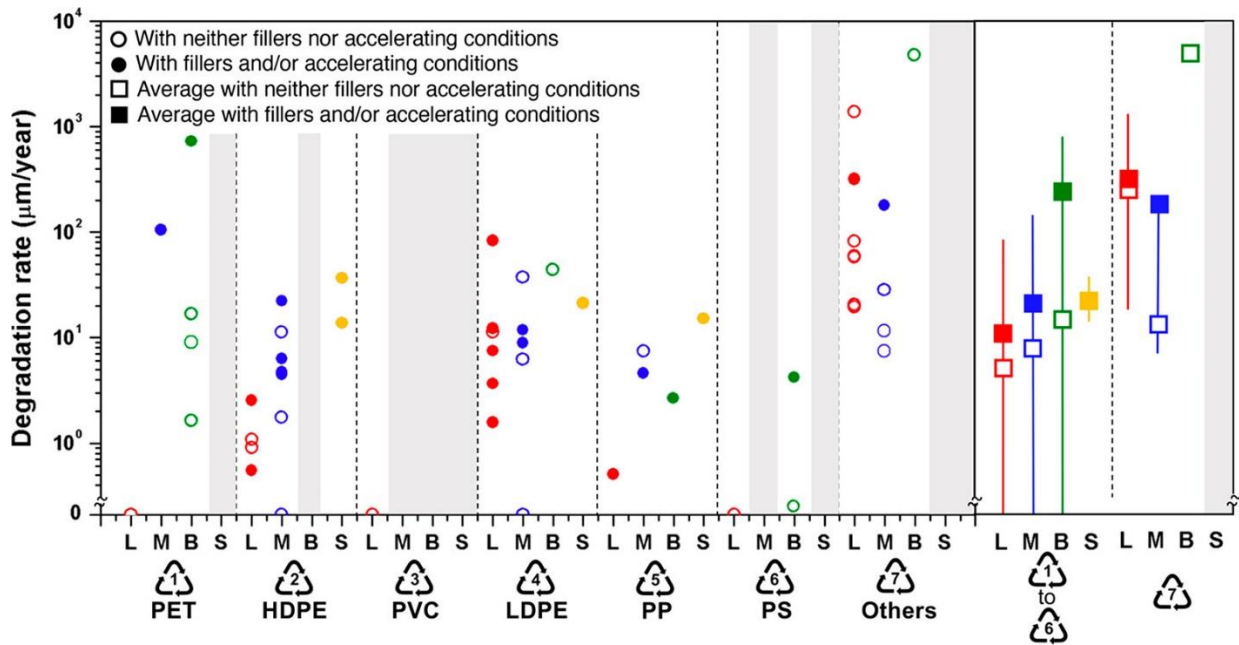


Fig. 1. 15: Specific surface degradation rates for various plastics, in $\mu\text{m}\cdot\text{year}^{-1}$. Vertical columns represent different environmental conditions (L, landfill/compost/soil; M, marine; B, biological; S, sunlight) and plastic types (represented by their resin identification codes). Plastics type 7, “others”, corresponds to various nominally biodegradable plastics. The range and average value for plastic types 1–6 are shown on the right as lines and squares, respectively, as well as for biodegradable “others”. Data points representing degradation rates that were unmeasurably slow are shown on the x-axis. Gray columns represent combinations for which no data were found. Reproduced from Chamas *et al.*¹¹⁵ under CC-BY license

As previously mentioned, PLA suffers from a loss of mechanical properties during reprocessing due to a decrease of molar mass⁷³ involving the need for fresh PLA to be used to make “directly recycled” PLA with suitable properties. Moreover, PLA objects are often produced with additives which would need to be compatible if mechanically recycled together, adding more to the complexity of the task. Fortunately, chemical recycling of PLA is already a mastered process which can be easily implemented. Regarding the life cycle analysis of such process, Piemonte *et al.* concluded it would cost less energy to regenerate PLA from chemical recycled lactic acid than freshly produced lactic acid from traditional sources¹²⁰. Multiple pathways are suggested going from pyrolysis to regenerate the lactide (although such solution bears risk as high temperatures can trigger racemisation or epimerisation), hydrolysis or alcoholysis to regenerate lactic acid or alkyl lactates as reported in the review from McKeown and Jones¹²¹.

Unfortunately, the recycling of PLA is not economically viable yet as the volumes of PLA materials are still too low to represent any interest. This has strong implications since the latest trend in some countries is to switch to plastics that are biodegradable or have an

established recycling circle. In the case of PLA, neither of these criteria are satisfied therefore limiting the will of plastic manufacturers to use PLA unless more research and development is conducted to improve its biodegradability.

2. PLA materials as food packaging: original drawbacks and requirements

As mentioned in the general introduction, packaging is currently the biggest application market for polymers as about 40% of produced polymers are designed for such use. Such high use involves requirements depending on the targeted application of such materials. Here, the focus will be put on food packaging, one of the widest and most global applications. Food packaging has the specificity to satisfy seven main criteria as explained by Dole and his collaborators in their book. Food packaging materials should preserve the quality of the food, prevent any microbiological contamination, preserve the integrity of the packaging and its content; prevent chemical risks and contamination, be environmentally friendly, respect technical and economic specifications from both the manufacturer and the consumer and finally interact and transmit information to the consumer¹²².

The following lines will confront the aforementioned PLA characteristics to some food packaging requirements and highlight the needs to be able to produce sustainable PLA packaging. The focus will be put on the mechanical, thermal, gas barrier and degradation properties which are the main deadlocks that prevent the use of PLA as a food packaging material.

2.1. Mechanical properties

The first and foremost requirement of a food packaging is to protect food's integrity from outside damage. Therefore, food packaging should be behaving as a physical barrier for accidental contact and contamination. As such, the considered material has to show suitable mechanical resistance to offer that level of protection, either through tensile, impact or vertical compression testing¹²³. Typical food packaging can sustain a certain level of deformation without breaking, which would compromise the integrity of the packed food. Also, since most food packaging containers are used below room temperature, the mechanical properties of the different materials should be considered at these temperatures¹²⁴. In this

regard, neat PLA is unsuitable to be used as a packaging material due to its high brittleness at room temperature and below. Therefore, work on enhancing such mechanical properties is necessary to satisfy the relevant mechanical resistance criteria.

2.2. Thermal properties

As previously mentioned, PLA has a very bad thermal behaviour if processed too quickly. The heat deflection temperature of neat PLA objects produced in industrial conditions is reported around 55°C, therefore excluding common food preservation techniques such as pasteurisation or sterilisation. Since pasteurisation is typically conducted at temperatures ranging from 60°C to 100°C and sterilisation at temperatures above 100°C¹²⁵, the use of PLA as such is indeed excluded since such temperature would compromise the integrity of the packaging. Through previously mentioned strategies, it is of particular interest to enhance the heat deflection temperature of PLA as it is possible to reach values above 100°C as for PLA grades currently commercialised by Total Corbion¹²⁶. This would therefore allow to use PLA for packing food, which requires such thermal treatment for its preservation and further go towards replacing traditionally used non-biodegradable commodity polymers.

2.3. Gas barrier properties

The gas barrier properties of packaging materials must satisfy different criteria depending on the targeted application. Indeed, different properties are required depending on the type of food which will be preserved (Fig. I. 16). Typically, the most studied gases are water vapour, O₂ and CO₂ as they play the most fundamental roles for food preservation¹²⁷. For instance, the presence O₂ will decrease the shelf-life of products by ways of oxidation, modification of organoleptic properties, and the growth of aerobic microorganisms¹²⁸. In the case of fresh food such as vegetables or fruit, both the O₂ and CO₂ exchanges must be considered. Through the respiration phenomenon, these products will naturally absorb O₂ and release CO₂ and therefore the packaging must allow a satisfactory respiration rate for the food to preserve longer by avoiding fermentation processes to take place. The same can be said about the water vapour permeation, which should be designed to maintain a specific moisture rate, for

instance either by blocking any water from coming in or out in the case of delicatessen, or by allowing water to regularly come in to preserve fresh food¹²³.

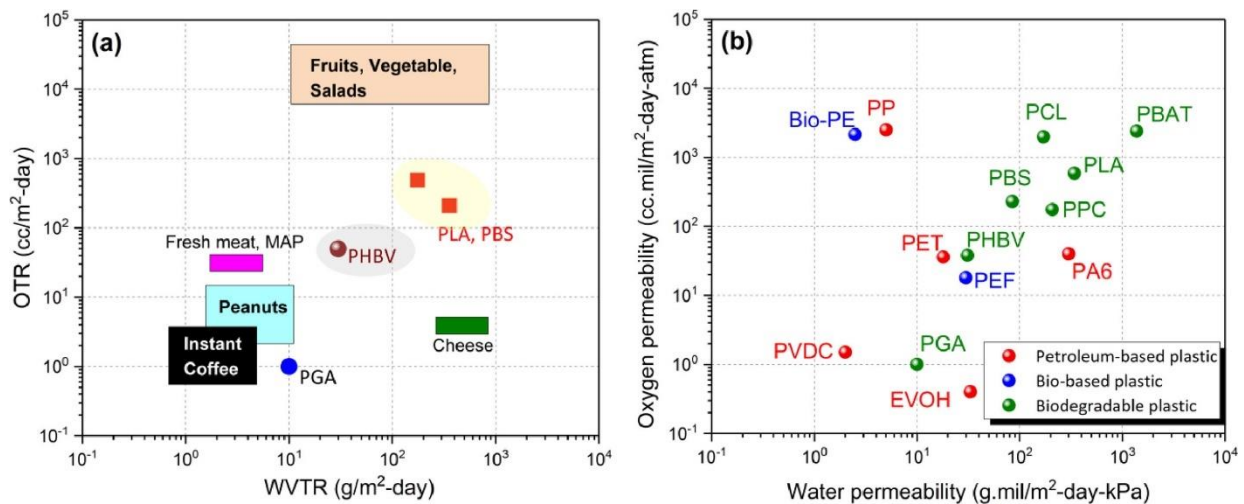


Fig. 1.16: (a) Requirements of barrier properties for different food packaging applications and a comparison between oxygen/water transition rate of selected biodegradable polymers at $25\ \mu\text{m}$ and food packaging barrier requirements. (b) The oxygen/moisture permeability of different polymers. (Copyright 2022, Adapted from Wu et al.⁸⁷ with permission from Elsevier)

2.4. End of life – Degradation and collection

In April 2021, the French 3R decree (Reduction, Reuse, and Recycling) regarding plastic materials was published. The decree is part of a global strategy to reduce plastic waste by getting rid of single use plastics by 2040. Only plastics which are industrially collected and recycled or biodegradable in home-compost or other environmental compartments, will be allowed to be used¹²⁹. This particularly regards food packaging since the used materials are single-use plastics. At this point, PLA does not satisfy these criteria since a proper collection and recycle circuit does not exist. As well, it is only certified as industrially compostable therefore not satisfying the end-of-life criteria. However, solutions regarding that matter are being developed. Citeo, the French organism in charge of managing and planning the future of packages, is currently studying how feasible and the impact of creating a new collection and recycling circuit specific to PLA¹³⁰.

3. Improving the properties of PLA through additives

3.1. Limiting the brittleness of PLA

The brittleness of PLA is probably the main drawback to its global use. As described before, PLA is a very brittle material at room temperature resulting on low impact strength and low elongation at break and yields through crazing. In other words, PLA will break under low energy impacts as opposed to tough materials which absorb a large amount of energy before failure. However, at a threshold temperature depending on the sample's geometry, the structure and morphology of the sample and the speed of testing, a polymer can undergo a brittle-ductile transition. Below such temperature, the polymer will break in a brittle manner, whereas it will break in a ductile fashion above (Fig. I. 17). The aim of the research focussing on the toughening of PLA is therefore to lower this transition temperature in order to have a ductile fracture behaviour of PLA samples at their service temperature.

The brittleness of polymers can be evaluated through multiple mechanical testing techniques such as impact testing, tensile testing, or vertical compression resistance testing. Impact testing is a high-speed test opposite to the more conventional tensile test which uses moderate rates of loadings and yields the well-known uniaxial stress vs strain curves. Vertical compression testing is a more delicate test to interpret as also it imposes an uniaxial moderate rate of deformation but generates a geometry change of the sample which results in a non-linear behaviour at high strain (Fig. I. 18). Consequently, although mechanical improvements can be measured by tensile testing and compression testing, the impact test is required to confirm the fracture behaviour of a material. The impact strength is not however a fundamental material property (compared to Young's modulus for instance) since impact test values greatly depend on the type of test (notched/unnotched Charpy or Izod test) and the geometry of the sample.

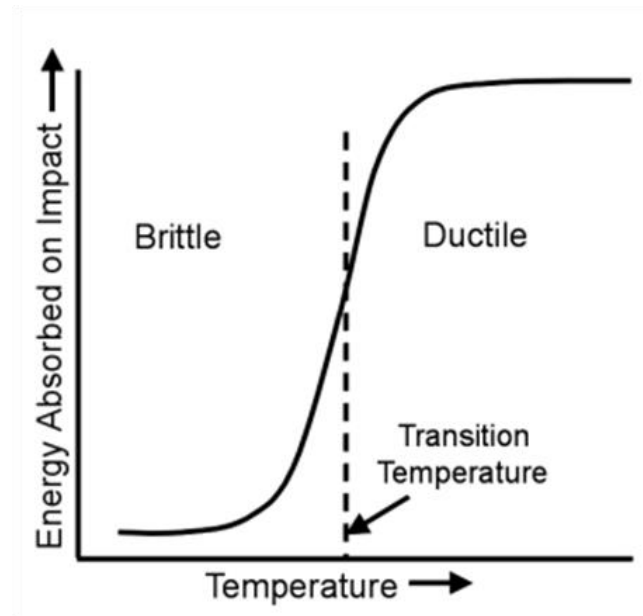


Fig. I. 17: Evidence of a brittle-ductile transition depending on the temperature

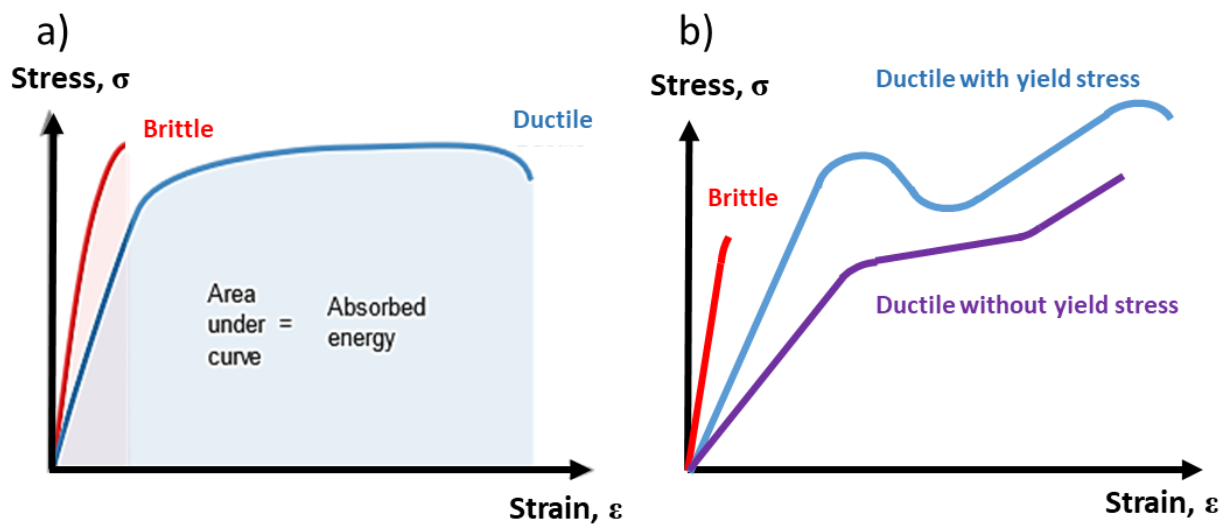


Fig. I. 18: Typical stress-strain curves of brittle and ductile materials for: a) tensile testing and b) compression testing

Multiple solutions have been designed to improve the toughness of PLA through strategies previously developed for other brittle polymeric materials such as PS which has widespread uses. Such strategies that can be applied for PLA are the use of plasticisers, the addition of fillers, copolymerisation and/or melt-blending with flexible polymers¹³¹.

Chapter 1

a. Plasticisers: lowering the T_g below service temperature

A cheap and easy technique to work on the brittleness of PLA is to use plasticisers to lower its T_g. This is a commonly used technique, originally to facilitate the processing of many polymer materials, which also has the effect of making them more flexible when they would otherwise be too stiff and brittle and break too easily¹³² such as poly(vinyl chloride) when used for garden hoses¹³³. In order to decrease the T_g, the plasticiser must be miscible in the polymer matrix. The idea relies upon the fact that the brittle-ductile transition temperature of PLA is around its T_g (50-60°C range), therefore, lowering the T_g of the polymer so that it will be lower than the temperature at which the material is used will cause the brittle material to behave then as a ductile material as the service temperature will then be in the ductile behaviour temperature range of the plasticised material. The efficiency of a plasticiser directly depends of the loading levels, its molar mass, and its miscibility with the polymer. Plasticisers can either be simple molecules, oligomers, or even low molar mass polymers if miscible. Their efficiency is directly evaluated through the depression of the T_g and the enhancement in mechanical properties, for instance the elongation at break. Low molecular weight plasticisers tend to have a higher efficiency but are however more subject to migration overtime, leading to a dramatic loss of mechanical properties. High molar mass plasticisers show a lower plasticising efficiency but are less subject to migration, leading to sustained mechanical properties overtime.

Regarding PLA, many plasticisers have been tested^{78,82,134,135}. Amongst the most popular are poly(ethylene oxide)¹³⁶, low molar mass PLA¹³⁷, triethyl citrate¹³⁸ and other citrate esters¹³⁹, glycerol, glycerol triacetate, glucose monoesters, partial fatty acid esters¹³⁹ and bishydroxymethyl malonate¹⁴⁰. Poly(ethylene oxide) is probably one of the best enhancers as Nijenhuis *et al.* reported a very high elongation at break could be achieved, over 500% using a high molar mass PEG (M_w=4x10⁶ g.mol⁻¹) at a 20wt% loading¹⁴¹. This was explained by the fact that for this particular blend, the T_g was measured around room temperature, therefore bringing the brittle-ductile transition to such temperature. The tensile strength decreases by a factor three accounting for the softening of the polymer matrix (unfortunately, there is no value of modulus reported). Also, the measured degradation rate was the fastest at 20wt% loading at 37°C compared to the other blends. Martin and Avérous tried using oligomeric lactic acid (20wt%), which resulted in a T_g of 18°C, a crystallinity ratio of 24% (compared to 1% for

neat PLA), an elongation at break of 200% along with a drop of modulus by a 2.7 factor from 2050 MPa to 744 MPa. Similarly, the use of citrate esters at high loadings resulted in an improved elongation at break (over 300%) but with a very high softening of the material which is not suitable⁸². Vegetable oils and their derivatives have also been considered as plasticisers for PLA such as epoxidized palm oil¹⁴², soybean oil¹⁴³, sunflower oil¹⁴⁴ or epoxidized oleic acid derivatives¹⁴⁵. Although reduction of the Tg and improved elongation at break are reported around 200% with just 5wt% of plasticiser, the material loses too much in terms of stiffness and the impact strength is not as greatly improved as it would be expected^{134,145}.

Other strategies are therefore required to toughen PLA better rather than just improving its flexibility. Regarding the considered plasticisers, many also showed migration problems which would cause the material to become hard and stiff again. The following two parts are therefore dedicated to the so-called “rubber” toughening of PLA through two strategies, using block copolymers or directly melt-blending two homopolymers. The idea of these techniques is to disperse microscopic (or nanoscopic) particles of an immiscible low Tg polymer inside the hard polymer matrix. Here, the toughening mechanism is different, unlike plasticisers, the Tg of the hard polymer should remain the same due to the immiscibility of polymers or blocks between one another. The toughening effect is obtained through the deformation of these soft particles that will absorb the impact energy and limit the crack propagation¹⁴⁶.

b. Synthetic copolymers

Developed in this part, the first strategy consists in the incorporation of low Tg polymeric motives directly linked to PLA chains through the use of block copolymers. The dispersion of the low Tg polymer blocks relies upon the well-known fact that immiscible block copolymers will self-assemble, the final morphology depending on the volume fraction of the blocks (Fig. I. 19). Such technique is highly efficient but however suffers from high costs which are not compatible with industrial applications requiring low production costs and lowering the price of PLA materials.

Random copolymers have been considered using ring-opening copolymerisation to achieve high molar mass copolymers. Such copolymers have shown to improve the mechanical properties of PLA, as in the case of copolymerised lactide with ϵ -caprolactone¹⁴⁷, trimethylene carbonate¹⁴⁸, or ricinoleic acid¹⁴⁹. Such candidates are actually promising thanks

Chapter 1

to the low T_g of their homopolymers (-60°C for poly(caprolactone), -20°C for poly(trimethylene carbonate) and -80°C for poly(ricinoleic acid)) which would allow to expect a significant decrease of the T_g of PLA when randomly copolymerised with such monomers. The copolymerisation of lactic acid and ϵ -caprolactone (80/20 to 40/60) led to copolymers displaying elongation at break higher than 100% with, however a decrease in modulus and tensile strength was observed. The copolymerisation of lactic acid and 30wt% of trimethylene carbonate improved the toughness to $100 \text{ MJ}\cdot\text{m}^{-3}$ as compared to the 2.5 for neat PLA and brought the elongation at break to 375% compared to 6%, again, however, with a huge decrease in modulus (factor two) and tensile strength (30% decrease). Despite really promising results regarding the toughening of PLA, it was also reported for all of these solutions that, due to the randomness of the repeating units, the thermal properties of PLA would be lost, even using pure L-Lactic acid or L-Lactide as the monomer. Such characteristic is not suitable since the thermal resistance of PLA is one of its major drawbacks, therefore, another solution such as using block copolymers appears to be more suitable.

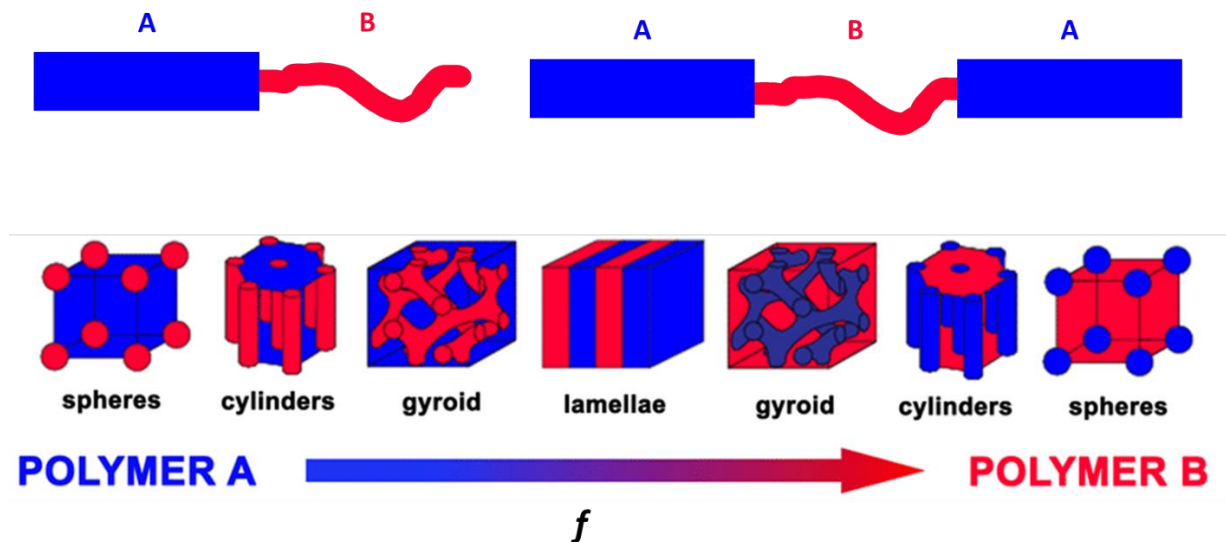


Fig. 1. 19: Block copolymer morphology depending on the volume fraction of one polymer between another with: A – Hard polymer block and B – Soft polymer block

Block copolymers can be synthesised using a wide range of chemical paths, contrary to random copolymers for which the used monomers must be able to polymerise through ring-opening polymerisation or direct polycondensation. The strategy of using block copolymers is already well-known with high impact resistance polystyrene which is either a triblock copolymer of styrene-butadiene-styrene, or the well-known acrylonitrile-butadiene-styrene terpolymer. In the literature, multiple block architectures for PLA have been reported that can

be traditional AB or ABA block copolymers or even multi-block copolymers involving bio-based or oil-based monomers. Here, only block copolymers that have been used as the sole material and not as compatibilizer are described¹⁵⁰.

The Hillmyer group reported many PLA-based copolymers to try to solve the brittleness of PLA. First, a PLA-*b*-poly(isoprene)-*b*-PLA was produced with different compositions which exhibited a broad range of morphologies such as the spherical, cylindrical, and lamellar morphology. The cylindrical phased-forming copolymer displayed the best elongation at break which was over 650%. Unfortunately, such performance came with low Young's modulus and tensile strength, whatever the copolymer composition¹⁵¹. Then, Pitet and Hillmyer successfully synthesised a poly(D,L-Lactide)-*b*-poly(butadiene)-*b*-poly(D,L-Lactide) copolymer using the ring opening polymerisation of 1,5-cyclooctadiene to synthesise the hydroxyl-terminated poly(butadiene) which was used as the macroinitiator for the PLA blocks. The volume fraction of PLA ranged from 0.24 to 0.89 allowing the authors to study multiple ordered-state morphologies and thermo-mechanical properties. The most noticeable feature comes with the 0.89 volume fraction of PLA sample which displayed a modulus of 1.3GPa, a yield strength of 38MPa, a tensile strength of 33MPa and an elongation at break of 42%¹⁵². The team synthesised a graft copolymer system, the poly(1,5-cyclooctadiene-*co*-5-norbornene-2-methanol-*graft*-D,L-lactide) (PCNL) which displayed an elongation at break over 200% with just 5wt% of rubber in the backbone¹⁵³. Delgado and Hillmyer went a step forward by synthesising a poly(D,L-Lactide)-*b*-poly(butadiene)-*b*-poly(D,L-Lactide) hydroxy-terminated block copolymer upon which 2-ureido-4[1H]-pyrimidinone segments could be grafted (UPy) (Fig. I. 20). Noticeable mechanical improvements could be noticed for copolymers containing at least 90wt% of PLA to reach elongations at break around 13%. The addition of UPy motives increased the elongation at break to 20% for copolymers containing 97wt% of PLA with a modulus of 2.1GPa and an energy absorption value of 9.3MJ.m⁻³. The effect of the UPy group was further studied by changing their amount on the toughest copolymer. With only one UPy function, the elongation at break increased to 58 with a storage modulus still close to 2GPa and the absorbed energy went up to 14MJ.m⁻³¹⁵⁴.

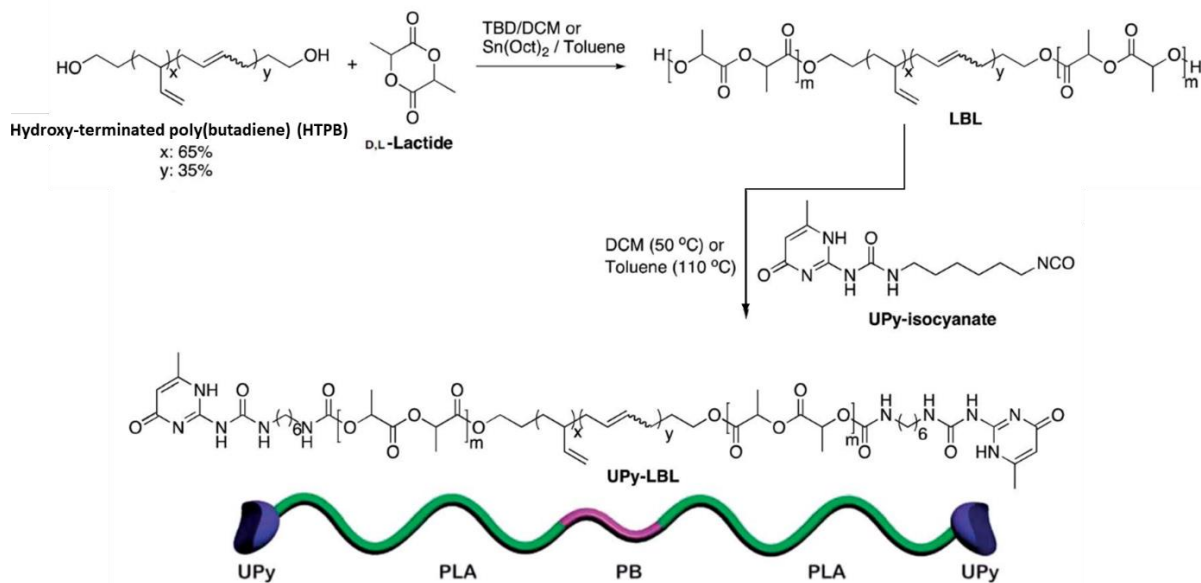


Fig. I. 20: Synthesis of hydroxy-terminated block copolymers (LBL) and UPy-functionalised block copolymers (UPy-LBL), adapted from Delgado and Hillmyer¹⁵⁴ with permission from The Royal Society of Chemistry

The sequential ring-opening polymerisation of lactones was also a strategy used to synthesise telechelic triblock copolymers based on lactide. PLA blocks were grown on a telechelic macroinitiator synthesised from the ring-opening polymerisation of a lactone with a diol as initiator to obtain hydroxyl functionalised end chains (Fig. I. 21). Lactones such as glycolide, β -butyrolactone, ϵ -caprolactone, or trimethylene carbonate among many others have been used and are well presented in the review by Diaz and Mehrkhodavandi regarding the synthesis of copolymers using lactones¹⁵⁵ and Becker *et al.* for the investigation of the mechanical properties of PLA bearing systems¹⁵⁶. In a first example, trimethylene carbonate along with ϵ -caprolactone and glycolide were copolymerised with lactide at different molar ratios to obtain ABA triblocks with A remaining PLA¹⁵⁷. 21mol% of TMC allowed the triblocks to have an elongation at break 50% but with a tensile yield strength down to 36MPa from 62 MPa but also showed a decrease in the T_g to 33°C. As a further study, the effect of the stereochemistry of PLA was investigated by Zhang *et al.* on PLA-*b*-PTMC-*b*-PLA triblocks with however low PLA content (from 10mol% to 42mol%). Amorphous PLA blocks at 35mol% content gave an elongation at break of 130% with a very low modulus of 16MPa. Higher Young's modulus and tensile strength were obtained when L-Lactide or D-Lactide were used to synthesise the PLA blocks due to the ability of such blocks to crystallise but with low elongation at break. Eventually, equimolar mixtures of PLLA-*b*-PTMC-*b*-PLLA and PDLA-*b*-

PTMC-*b*-PDLA were studied and gave improved mechanical and thermal properties due to the formation of stereocomplexes¹⁵⁸. Guerin *et al.* synthesised PLLA-*b*-PTMC diblocks, PLLA-*b*-PTMC-*b*-PLLA triblocks and 3-arm star PTMC-*b*-PLLA using sequential copolymerisation techniques. Elongation at break values above 200% could easily be obtained using 20wt% of PTMC with a modulus still around 2GPa, with the best composition bearing 27wt% of PTMC and achieving a 320% elongation at break¹⁵⁹.

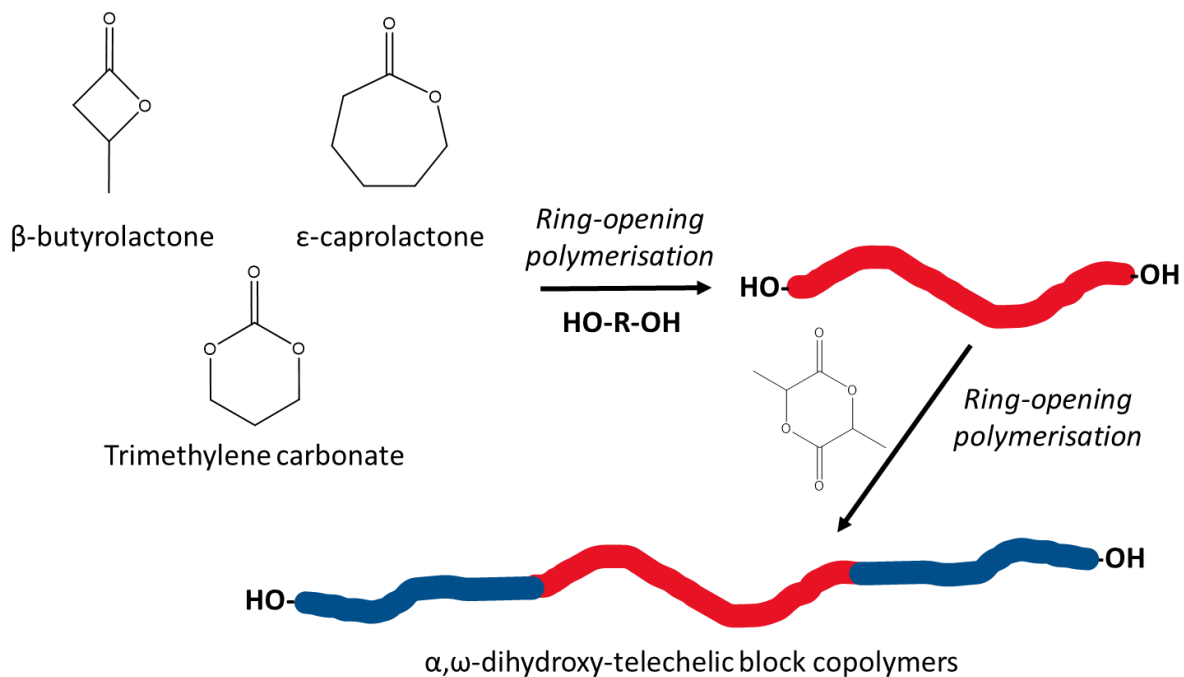


Fig. I. 21: Chemical pathway to synthesise PLA-*b*-XX-*b*-PLA triblock copolymers using sequential ring-opening polymerisation

The block copolymer system of PLA with poly(ϵ -caprolactone) is another intensively studied solution to enhance the mechanical properties of PLA. As mentioned previously, random copolymers of PLA-poly(ϵ -caprolactone) are amorphous while block copolymers displays dual melting behaviours corresponding to the two polymer phases¹⁶⁰. Qian *et al.* synthesised ABA triblocks with compositions ranging from 89/11 to 28/72 mol/mol of L-Lactide and ϵ -caprolactone. The elongation at break was brought over 400% with at least 30mol% of ϵ -caprolactone, going up to nearly 800% for a 50/50 mixture with the tensile strength diminishing from 63MPa to 38MPa (40MPa at 30mol% of ϵ -caprolactone)¹⁶¹. Multi-block copolymers have also been synthesised but the best performance that was achieved gave a remarkable elongation at break over 500% but a modulus of 165MPa which is very low¹⁶⁰. More recently, the effect of the stereochemistry of the PLA blocks was also studied for

Chapter 1

PLA-*b*-poly(ϵ -caprolactone)-*b*-PLA triblocks. PLLA-*b*-poly(ϵ -caprolactone)-*b*-PLLA and PDLA-*b*-poly(ϵ -caprolactone)-*b*-PDLA triblocks were synthesised separately with different block lengths and then blended in a 1:1 PLLA/PDLA ratio. The separate triblocks showed remarkable elongation at break over 800% with a tensile strength of 36MPa and a high toughness of 160MJ.m⁻³ for the sample bearing 11kDa of poly(ϵ -caprolactone)(21%) and 40kDa of PDLA (79%). The mixture of this triblock and its PLLA-based counterpart was also the one which gave the best mechanical properties with an elongation at break of 600%, a tensile modulus of 36MPa. The thermal properties of the blends were also better than the triblocks alone due to the formation of stereocomplexes which improved the thermal resistance of the enantiomeric blends¹⁶².

Regarding other available biodegradable building blocks, PLA has been polymerised using poly(hydroxyalkanoate)s especially poly(3-hydroxybutyrate) as the mid-block. The first PLA-*b*-PHA system was reported by Haynes *et al.* by growing a PLLA block on a commercially available PHA polymer with a weight ratio of PLLA of 80%. Modifications were observed on the T_g, which decreased to -2°C¹⁶³. Triblock copolymers made of PLLA-*b*-poly(3-hydroxybutyrate)-*b*-PLLA were prepared using the ring-opening polymerisation of β -butyrolactone with the presence of 1,4-butanediol and then the use of the synthesised telechelic hydroxyl-terminated initiator to polymerise PLA. The mid-block initiator exhibited a T_g ranging from -6°C to 5°C allowing to hope for a toughening effect with PLLA. The modulus increased from 30MPa to 160MPa with an increasing PLLA content whereas the elongation at break gradually decreased from 200% to 86%¹⁶⁴. The stereochemistry effect of PLA was also studied on PLLA-*b*-poly(3-hydroxybutyrate)-*b*-PDLA triblocks. Such triblocks exhibit a high melting point above 200°C which is characteristic of the stereocomplexes which are formed. However, the tensile testing revealed poor tensile strength and modulus (33MPa and 548MPa) with an elongation at break of just 11%, showing very limited interest for these systems¹⁶⁵.

One of the most extensively studied triblock system involving PLA is with poly(ethylene oxide) as it is both biocompatible and hydrophilic. Multiple examples range from diblock or triblock copolymers to multiple block copolymers¹⁶⁶⁻¹⁶⁸. Unfortunately, these will not be reported here as they were mainly used as compatibilizers for PLA/poly(ethylene oxide) blends or as additives in PLA^{150,169,170}.

Plant oils and their derivatives are also being extensively researched as such bio-based resources offer many chemical opportunities. The main examples as copolymers come from castor oil derivatives. The Hillmyer group synthesised a block copolymer of PLA-*b*-poly(ricinoleic acid) to improve the compatibility of PLA with castor oil blends with results which will be discussed further¹⁷¹. The example of a triblock used as a sole material comes from Lebarbé *et al.* who synthesised a PLLA-*b*-poly(ricinoleic acid)-*b*-PLLA copolymer starting from 1,3-propanediol affording a telechelic poly(ricinoleic acid) (PRic) upon which PLLA blocks were grown using ring-opening polymerisation of L-Lactide (Fig. I. 22).

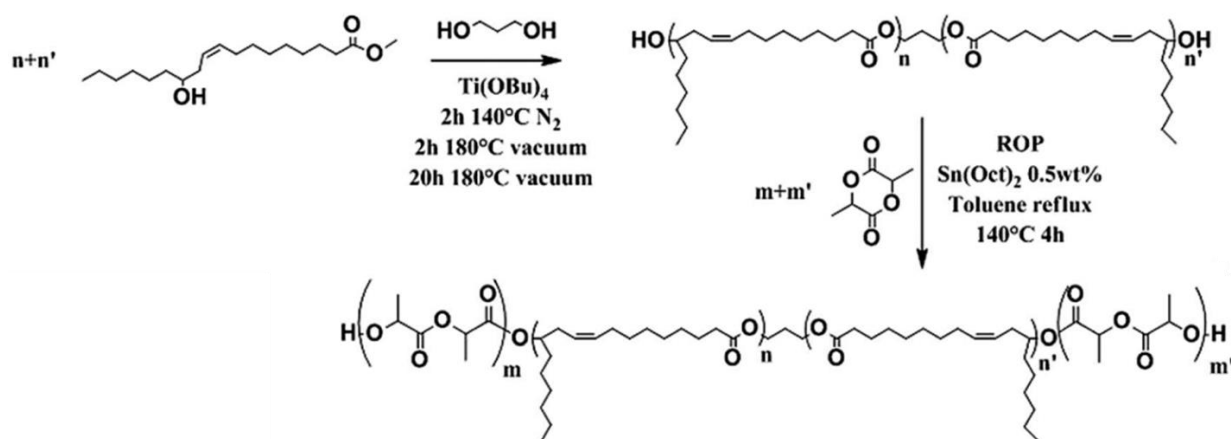


Fig. I. 22: Two-step procedure to PLLA-*b*-PRic-*b*-PLLA triblock copolymers, adapted from Lebarbé *et al.*¹⁷² with permission from The Royal Society of Chemistry

The weight ratio between the PLLA blocks and the PRic blocks varied from 83/17 to 35/65 by playing on the length of the PLLA blocks. Tensile tests were conducted and 17wt% of PRic allowed to reach 98% of elongation at break with only a 25% loss of Young's modulus compared to neat PLLA and decreased yield stress and stress at break. 29wt% of PRic gave similar results with a higher modulus than the 17wt% copolymer. Moreover, annealing treatments showed high crystallinity ratios above 55% could still be obtained, demonstrating the advantage of block copolymers against plasticisers^{172,173}. Other examples regarding plant oils will be developed in the blend part as many bio-based polymers are now directly incorporated in PLA to obtain a toughening effect.

c. Blending with soft low Tg polymers

A final technique to greatly enhance the mechanical properties of a brittle polymer is to blend a “soft”, low Tg, immiscible homopolymer polymer into it. Such low Tg polymer should, nonetheless, have a good interfacial adhesion/compatibility with the hard polymer matrix. The soft domains will then be able to limit the crazing by absorbing the deformation or create interfaces that will require extra energy to break and therefore also limit crazing. This is the typical strategy used for high impact poly(styrene) which has poly(butadiene) incorporated inside its matrix. Many polymers have been tested, both non-biodegradable and biodegradable leading to a very extensive literature^{78,82,150,174–176}. In this part, both will be distinguished although the emphasis will be put on polymers that will preserve the compost degradation properties of PLA.

i. **Non-biodegradable polymer blends**

Melt blending homopolymers is an economically viable and easy way to greatly improve the properties of PLA. This is also a way of keeping PLA production prices to a low as very cheap oil-based polymers can be incorporated through such a way. A very extensive literature exists regarding such polymer blends, however, since the scope of this project was to focus on bio-based and sustainable additives for PLA, only the most prominent examples will be reported here. Complete reports can be found in multiple reviews which cover the subject of the toughening of PLA^{78,82,131,150,174–177}.

Poly(ethylene oxide) (PEO)

One of the most used polymers with PLA is high molar mass poly(ethylene oxide) which is not miscible with PLA opposite to its low molar mass counterpart which has already been described as a plasticiser for PLA¹⁷⁸. Kim *et al.* mixed high molar mass poly(ethylene oxide) with PLLA (40/60 weight ratio) and obtained an elongation at break of 280% with a tensile modulus of 17 MPa. The addition of poly(vinyl acetate) as a compatibilizer further increased the performance to 410%¹⁷⁹. Polymer blends prepared by Li *et al.* showed an increase of modulus and tensile strength along with a decrease of the elongation at break when the molar mass of poly(ethylene oxide) increased. The work enlightens a sweet spot between 5wt% and 15wt% loadings with a 10,000g.mol⁻¹ poly(ethylene oxide) where an elongation at break of 300% could be achieved¹⁸⁰. Finally, Eom *et al.* made blends containing 1, 3 and 5wt% of poly(ethylene oxide). The impact strength was increased from 9.9 kJ.m⁻² to 11.6 kJ.m⁻² and the

elongation at break from 13% to 24% with little variation of the tensile strength. Such results are encouraging but highlight the need for a compatibilizer to achieve a better performance¹⁷⁸.

Poly(ethylene) (PE)

PE is one of the most produced polymers and is known for its flexibility. PLA/PE blends have been studied and have shown these two polymers are immiscible. The group of Hillmyer extensively studied such blends with the presence or not of block copolymers as compatibilizers. Significant increases in impact toughness were obtained with 19wt% low density PE and 5wt% PLLA-*b*-PE copolymers as compatibilizers with a value of 760 J.m⁻¹ compared to just 12 J.m⁻¹ for neat PLLA (Fig. I. 23). The use of harder and stiffer high density PE, the improvement was limited to 64 J.m⁻¹ which is much lower¹⁸¹⁻¹⁸³.

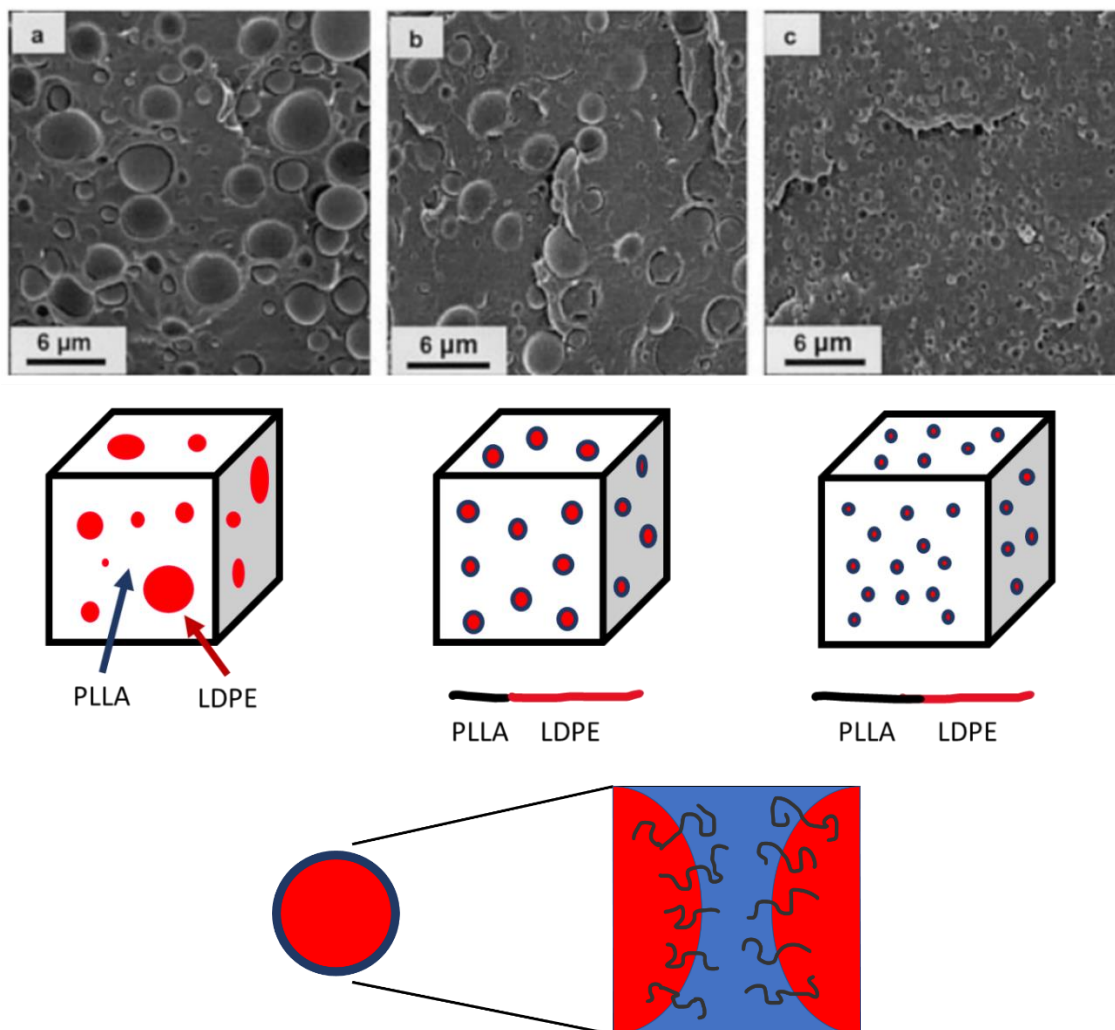


Fig. I. 23: Effect of PLLA-*b*-LDPE block copolymer on the interfacial compatibility of PLLA/PE blends. SEM images adapted from Anderson et al.¹⁸¹, copyright 2003 John Wiley & Sons, Inc

Natural rubber (NR)

Natural rubber or *cis*-1,4-poly(isoprene) is an impact modifier obtained from renewable resources which displays high toughness, biocompatibility, and low cost. Neat PLA/NR had an elongation at break of 200% with 10wt% of NR with relatively high modulus and tensile strength (2.0 GPa and 40 MPa)¹⁸⁴. The use of epoxidized NR as compatibilizer allowed to obtain a 16-time higher impact strength value than neat PLA. The effect of the compatibilizer could be seen by a reduction of the diameter of the particles by SEM (Fig. 1. 24)¹⁸⁵. Finally, a more recent worked used low amounts of NR-*g*-maleic anhydride as a compatibilizer which proved more efficient¹⁸⁶. Other strategies involved using sulphur to trigger dynamic vulcanisation to partially crosslink PLA with NR which resulted in high impact strength (25kJ.m⁻²) and high strain at break (125%)¹⁸⁷. Epoxidized hydrogenated NR was also considered and gave blends with an impact strength of 32.4 kJ.m⁻² and an elongation at break of 348% while retaining high tensile strength above 40 MPa¹⁸⁸.

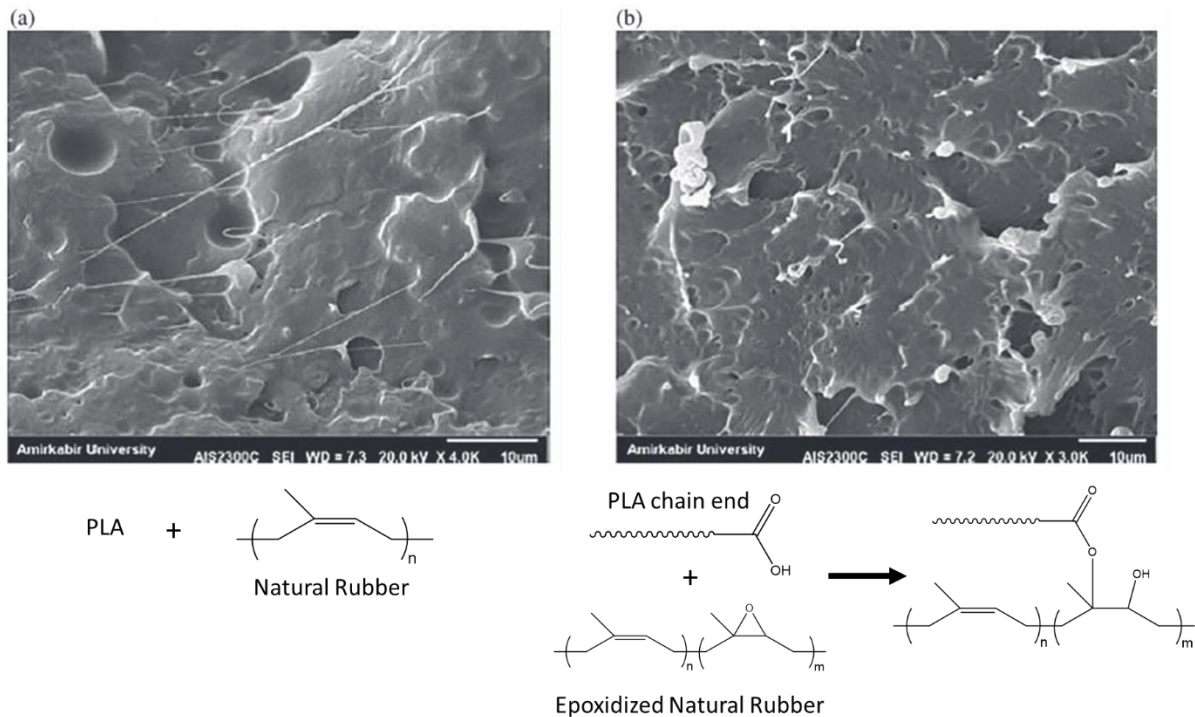


Fig. 1. 24: SEM images of impact fractured surfaces of PLA/NR (a) and PLA/NR/Epoxidized NR (b) blends at magnifications of $\times 4000$ and $\times 3000$, respectively, with the chemical reaction of epoxidized rubber with PLA chains. Adapted, with permission, from Nematollahi et al.¹⁸⁵, copyright 2019 John Wiley & Sons, Inc

Ethylene-co-vinyl acetate (EVA)

EVA is a copolymer made of ethylene and vinyl acetate which is widely used in the plastic industry showing high flexibility and toughness. PLA is actually miscible with poly(vinyl acetate) and immiscible with poly(ethylene), therefore, the compatibility between PLA and EVA can be tuned by changing the ethylene/vinyl acetate ratio in the copolymer. The effect of the amount of vinyl acetate was studied by Ma *et al.* in PLA/EVA blends of 80/20 weight ratio. They found there needs to be content of vinyl acetate between 40% and 70% in the EVA copolymer to have a toughening effect of the blend. When the right conditions were met, the impact strength was brought from 3 kJ.m⁻² to 50-60 kJ.m⁻² and the strain at break from 4% to 300-350% while the modulus was kept at 2.4-2.7 GPa¹⁸⁹. PLA/EVA blends using various compatibilizers have also been reported and show improved ductility and impact strength¹³⁵. Finally, Tábi investigated the effect of annealing on PLA/EVA blends and found that over 65 kJ.m⁻² notched Charpy impact strength can be achieved with only 15 wt% EVA. The dominant crystalline phase was the disordered α' form as such results were obtained for an annealing temperature of 80°C¹⁹⁰.

Acrylic and styrene-based copolymers

Worthy examples can be reported regarding the use of such copolymers as they constitute the traditionally used impact modifiers for brittle polymers such as poly(styrene). The most well-known systems are the styrene-butadiene-styrene (SBS) copolymer, or the acrylonitrile-butadiene-styrene (ABS) terpolymer. SBS and hydrogenated SBS were first reported as good impact strength enhancers by improving it by a 2.5 factor¹⁹¹. Epoxidized SBS was also prepared at different epoxidation levels to enhance the compatibility between PLA and SBS and resulted in blends having an impact strength of 891 J.m⁻¹ and an elongation at break of 254% and a modulus of 1.1 GPa (1.6 GPa for their neat PLA) (70/30 PLA/epoxidized SBS with 35.8% of epoxy groups)¹⁹². ABS was also considered as an impact modifier for PLA. Li and Shimizu prepared blends PLA/ABS blends with and without the use of a compatibilizer, the reactive styrene/acrylonitrile/glycidyl methacrylate copolymer (SAN-GMA) along with a catalyst. 70/30 PLA/ABS blends showed an improved impact strength of 64 kJ.m⁻² which could be further improved to 124 kJ.m⁻² (twice as high as neat PLA) using 5wt% of SAN-GMA and 0.2phr of catalyst, the elongation at break being limited to 24% though (Fig. I. 25)¹⁹³. Such system is so

promising that NatureWorks started commercializing a PLA blended with an ABS-based toughening agent: Blendex™ 338¹⁷⁶.

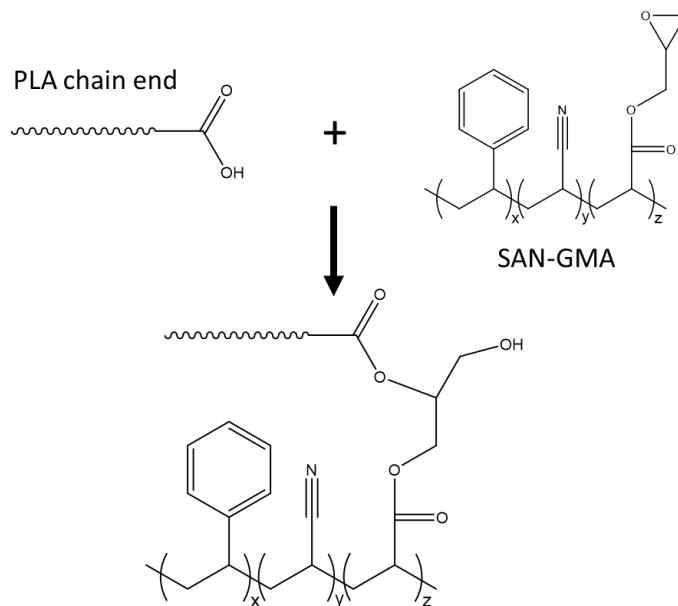


Fig. 1. 25: Use of glycidyl methacrylate rubber functionalisation for the reactive compatibilization of PLA binary blends

Core-shell impact enhancers using poly(methyl methacrylate) (PMMA) as the shell were developed based on the fact that PLA/PMMA blends are miscible¹⁹⁴. Such polymers are low Tg rubbery core cross-linked with a hard shell which offers compatibility and good interfacial adhesion with PLA. Methyl methacrylate-ethyl acrylate core-shell copolymers (ACR) blends with PLA (80/20 weight ratio PLA/ACR) had an impact strength of 77.1 kJ.m⁻², up from 2.8 kJ.m⁻² and an elongation at break of 94% but with a noticeable decrease of modulus and tensile strength¹⁹⁵. Glycidyl methacrylate-functionalized (GACR) were prepared by Li *et al.* 75/25 blends of PLA/GACR allowed to obtain an impact strength of 83.5 kJ.m⁻² with neat PLA but with a dramatic decrease of modulus and tensile strength¹⁹⁶. A final system of methyl methacrylate-butadiene-styrene (MBS) blended with PLA was reported. 25wt% of MBS in PLA resulted in an impact strength of 97.2 kJ.m⁻² vs 4.7 kJ.m⁻² for neat PLA, with a strain at break of 300% but a tensile strength down from 70 MPa to 34 MPa along with a modulus down to 720 MPa from 1800 MPa¹⁹⁷.

The study above demonstrates the research efficiency to find strong toughening agents for PLA using well-known chemistry of olefinic, acrylic and styrenic polymers. The introduction of reactive functions allowed to create covalent bonds between PLA and the impact modifiers,

therefore improving the interfacial adhesion between the two phases and resulting in improved impact strength properties. The success of such technology has resulted in commercially available impact modifiers such as Elvaloy, BioMax® Strong and Biostrength™ from the DuPont Company and Arkema.

Despite the high efficiency of such impact modifiers, the degradation properties of PLA are hampered as such additives will not be able either to degrade in the environment or in regulated conditions such industrial compost plants. Thus, one of the main features of PLA is suppressed and such additives do not constitute a viable long-term solution. Therefore, the more recent scope of research has been focussing on more sustainable second-generation bio-based impact modifier additives that are compostable and/or biodegradable.

ii. **Compostable and biodegradable polymer blends**

Many polyesters are available to be blended with PLA to enhance its properties (Fig. I. 26). Such polyesters display flexibility, biodegradability, crystallinity, and many characteristics which are suitable to tailor the properties of PLA.

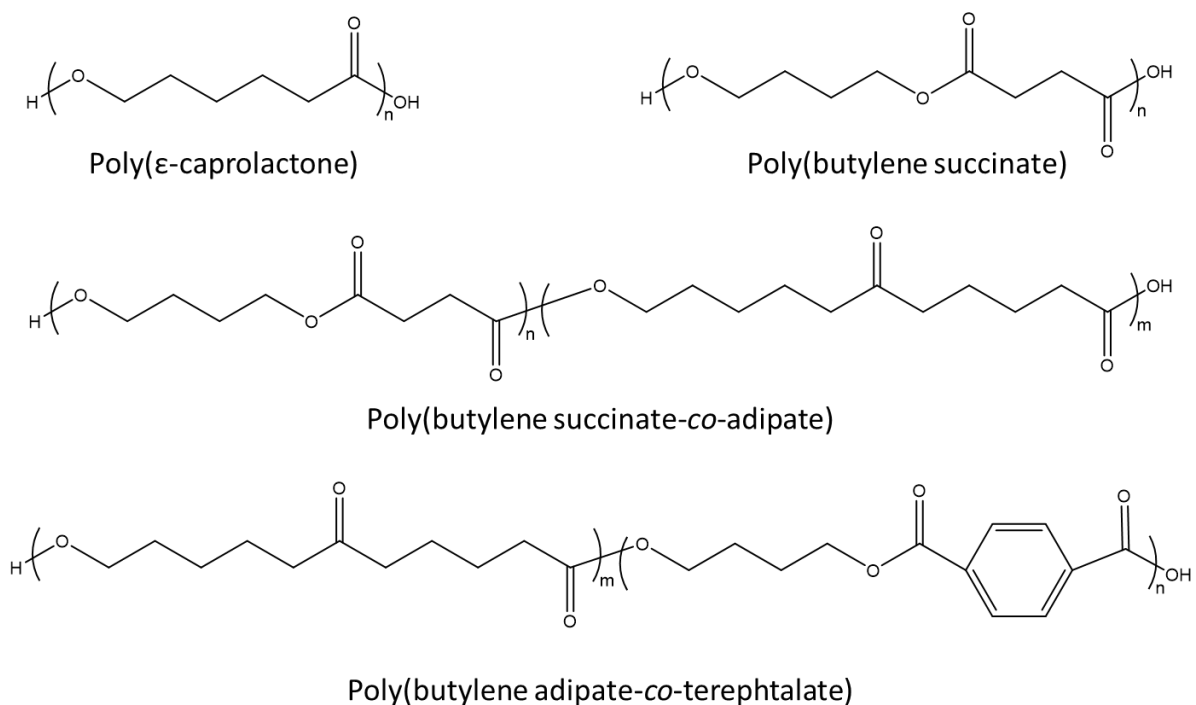


Fig. I. 26: Structure of polyesters as potential toughening agents for PLA

Poly(ε-caprolactone) (PCL)

Although it originates from petrochemical derivatives, PCL is a promising candidate for blending with PLA as it displays excellent ductility and flexibility due to its low T_g (-60°C) and

its semi-crystalline nature (melting temperature range 55-70°C). Unfortunately, due to a very high immiscibility between PCL and PLA, non-compatibilized blends only showed marginal ductility improvements at very high loadings (>60wt% of PCL) which implied a significant loss of modulus and tensile strength, thus emphasising the need for the use of compatibilizers^{198,199}. However, as Fortelny *et al.* underline in their review, opposite results have also been reported with PLA/PCL that showed improved ductility and flexibility. The authors of the review concluded that in the case of pure PLA/PCL blends, there is a very fine dependence of the critical particle size of PCL to induce enhanced toughness, the blend composition, and the crystallinity ratio of PLA in the considered samples. Such conclusions show the existence of a very narrow window of particle size (0.3-0.6µm) upon which toughened blends can be obtained, even more emphasising the need to use compatibilizers to obtain a fine particle phase structure more easily²⁰⁰. To do so, three main strategies are available that are: the use of block or graft copolymers, reactive compatibilization or more recently, nanofillers.

Dell'Erba *et al.* used PLLA-*b*-PCL-*b*-PLLA as compatibilizers for multiple PLA/PCL blend compositions which showed a decrease of the size of the PCL particles²⁰¹. The effect of PCL-*b*-PLLA diblock copolymers of various compositions was studied by Xiang *et al.* in 80/20 PLA/PCL blends. The addition of 5wt% of copolymers greatly enhanced the elongation at break to over 150%, with rather stable tensile strength, but unfortunately, no impact testing was conducted²⁰². Poly(ethylene oxide)-*b*-(poly(propylene oxide))-*b*-poly(ethylene oxide) were found to be even better compatibilizers in 70/30 PLA/PCL blends as a high increase in fracture energy was noticed when using 2wt% of them. Morphological studies showed a partial miscibility of the blend with the addition of such compatibilizer^{203,204}. Unfortunately, this strategy only showed moderate enhancements in mechanical properties of PLA/PCL blends even for more recent studies^{200,205}.

Reactive compatibilization showed more promising results and was studied for blends ranging from 15-35wt% content of PCL in PLA. In a first example, Wang *et al.* used triphenyl phosphine (2 phr) to trigger a transesterification reaction between PLA and PCL chains during melt-blending of an 80/20 PLA/PCL blend. The elongation at break was brought up to over 120% for the compatibilized blends vs 28% otherwise with a low tensile modulus of 147 MPa²⁰⁶. Dicumyl peroxide was also used to generate reactive free radicals during melt-

blending to generate random compatibilization through grafting and crosslinking. In the case of 70/30 weight ratio PLA/PCL blend, the compatibilized blend showed an elongation at break over 130% and a notched IZOD impact strength three times higher than neat PLA. AFM studies confirmed the decrease in size of the PCL domains with increasing dicumyl peroxide content and little effect of the processing method^{207,208}. Isocyanate reactive agents have also been used for reactive compatibilization, in particular lysine triisocyanate. Isocyanate moieties can indeed react with hydroxyl groups borne by the chain-ends of PLA and PCL and generate *in-situ* urethane groups as linkers between the polymer chains (Fig. I. 27). Takayama *et al.* used such compound to show improved mechanical performance and impact strength due to a better compatibility of the phases^{209,210}. Harada *et al.* also tested lysine triisocyanate along with other commercially available multifunctional isocyanates and epoxides. They concluded lysine triisocyanate was the best compound for reactive compatibilization and achieved an elongation at break of 268% and an impact strength nearly nine times higher than the neat PLA/PCL blend (80/20) while maintaining good tensile strength (47.3 MPa)²¹¹.

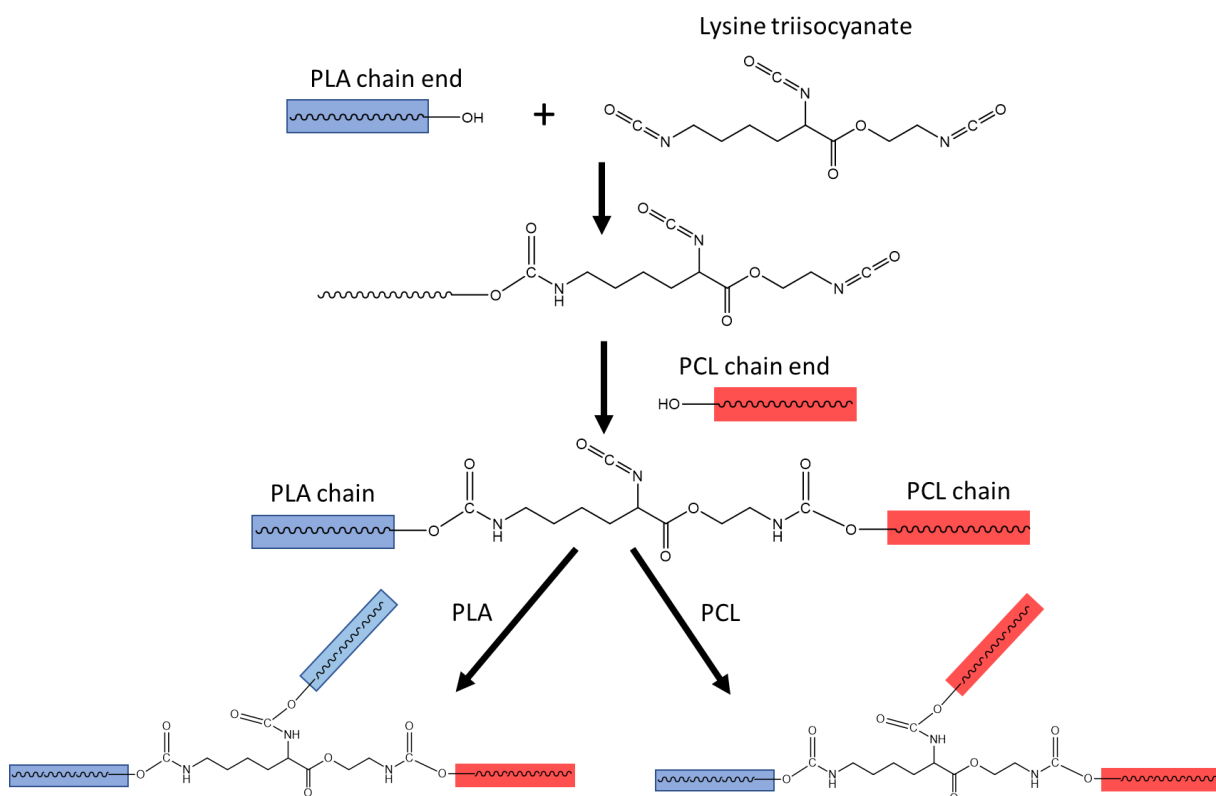


Fig. I. 27: Reactive compatibilization of PLA and PCL using lysine triisocyanate

Later, the influence of the PLA matrix's crystallinity ratio was studied. It was shown that higher crystallinity ratios in compatibilized blends would actually result in a higher impact

strength whereas such impact strength would decrease for non-compatibilized blends. This was explained by a change in the impact fracture process: for amorphous samples, the fracture process is dominated by crazing whereas it is dominated by shear yielding in the case of crystallised samples, therefore involving a higher volume of the PLA matrix and resulting in improved toughness^{212,213}. Other strategies involving glycidyl methacrylate²¹⁴ and maleic-anhydride-grafted PLA²¹⁵ have been reported but display lower performances than those described. This study shows the possibility of achieving high performing PLA/PCL blends rather than using chemically modified PLA polymers.

Poly(butylene adipate-co-terephthalate) (PBAT)

Blends with poly(butylene adipate-co-terephthalate) (PBAT) are becoming more and more interesting due to the increasing production of this polymer. Indeed, reports for 2021 showed it actually overtook PLA in terms of production. It is a flexible and fully biodegradable copolyester, which displays a strain at break over 700%²¹⁶. Unfortunately, its price remains high, and it still relies heavily on oil-based monomers. Jiang *et al.* produced blends containing 5, 10, 15 and 20wt% of PBAT in PLA. The fracture mode of PLA became fully ductile from very small loadings and showed a phase separation. The tensile strength was only reduced from 62 MPa to 47 MPa at the highest loading while allowing extensions above 200% with only 5wt% of PBAT. Yet, the impact strength was not really improved due to the phase separation of the blend²¹⁶.

To overcome this feature, compatibilizers were used to enhance the mechanical properties of the blend such as PLA-*b*-PBAT-*b*-PLA triblock copolymers, epoxide functionalised polymers, free-radical initiators, or tetrabutyl citrate¹⁷⁶. The triblock strategy allowed the authors of the study to increase the elongation at break of their 70/30 weight ratio PLA/PBAT blend from 22% to 166% using 5wt% of triblock while retaining the tensile strength²¹⁷.

The use of glycidyl methacrylate allowed the reaction of the epoxide groups with the -OH and -COOH terminated polymer chains of PLA and PBAT during the extrusion process used for the blending; therefore creating very small amounts of covalent bonds between the two phases through the apparition of random terpolymers. This allowed a better interfacial compatibility between the two phases. The optimised mixing ratio with 5wt% of compatibilizer and 25wt% of PBAT allowed to enhance the impact strength value from 21 J.m⁻¹ to 77 J.m⁻¹ with an increased modulus, although the elongation at break remained low at 6.5%

vs 4.5%²¹⁸. In another study using only 10wt% of PBAT, 5wt% was also reported as the sweet spot for the compatibilizer's loading, giving samples with an elongation at break of 190% and an impact strength which tripled compared to neat PLA²¹⁹. A commercial additive, Joncryl® ADR 4368, was used by Al-Itry *et al.* in 80/20 PLA/PBAT blends with an optimal amount of compatibilizer of 0.5wt% which gave an elongation at break of 135% and a modulus of 1.1 GPa against 1.3 GPa^{67,220}.

Free radical initiators can be used to trigger random reactions to create cross-linked architectures which will form a strong cross-linked interface (Fig. I. 28). Coltelli *et al.* showed the effect of the peroxide content on 75/25 PLA/PBAT blends and reported an optimal amount of 0.2wt%²²¹. In a 80/20 PLA/PBAT blend, 0.5wt% of dicumyl peroxide allowed to obtain materials showing better mechanical properties as in the previous example with an elongation at break of 250% with an increased impact strength of 110 J.m⁻¹ compared to 60 J.m⁻¹ for the original blend and a higher tensile strength²²².

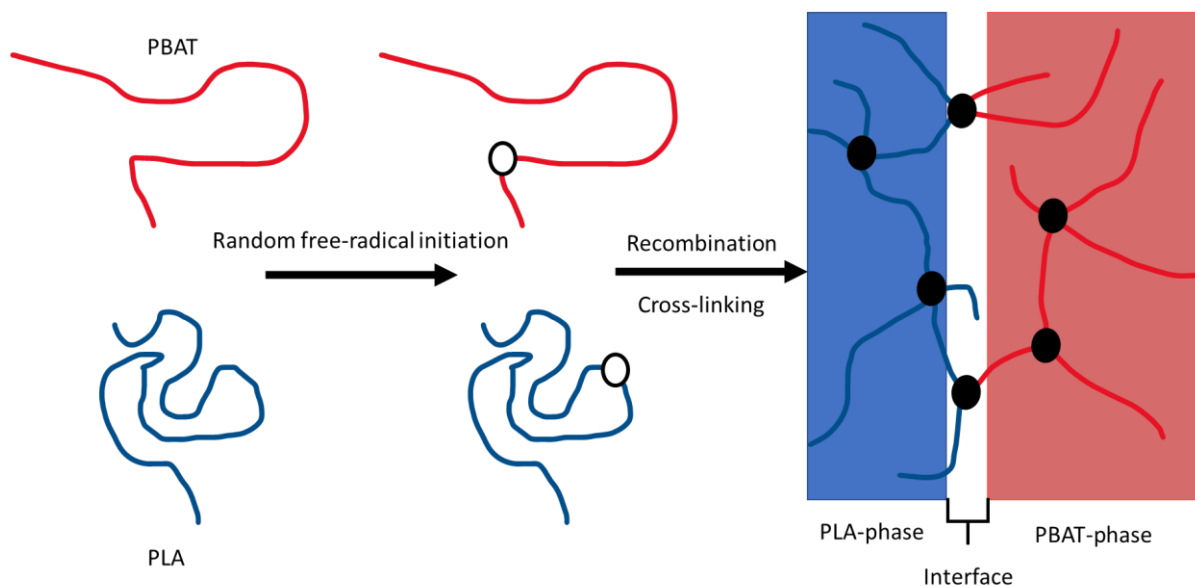


Fig. I. 28: Effect of radical coupling reactions of PLA/PBAT blends

A more recent study involves a transesterification process using tetrabutyl citrate in a 70/30 PLA/PBAT blend. 0.5wt% of the citrate gave an elongation at break of 300% with a tensile strength of 45MPa and an impact strength up to 9 kJ.m⁻² as opposed to 2.5 kJ.m⁻² for neat PLA and 3.5 kJ.m⁻² for the blend without citrate²²³.

Finally, 1wt% of cellulose nanocrystals were used as interfacial fillers in 75/25 PLA/PBAT blends. Such fillers induced a morphology change in the blend from dispersed spheres to a co-

continuous morphology resulting in highly improved impact strength (95 J.m^{-1} vs 21 J.m^{-1}) with a stable modulus around 2.5 GPa and an elongation at break of 145%²²⁴.

Through these examples, it is shown that compatibilizers are required to obtain a good combination of ductility, toughness, and strength. PLA/PBAT blends are commercialised by BASF under the tradename Ecovio® offering a wide range of properties depending on their exact composition^{176,225}. Unfortunately, the price competitiveness of such high potential blends is still quite poor as their price is reported around \$5/kg.

Poly(butylene succinate) (PBS)

PBS is now a bio-based and biodegradable semi-crystalline polymer originating from succinic acid with a T_g around -32°C and a melting point reported at 114°C . It also displays excellent flexibility and biodegradability which could be retained in PLA/PBS blends²²⁶. Park and Im studied various PLA/PBS blends which displayed a single T_g over every blend composition, accounting for a high compatibility of the amorphous phases. PBS was found to increase the crystallisation rate of PLA due to phase separation and was reported for crystallised blends with more than 40wt% of PBS^{227,228}. On the other hand, Wang *et al.* reported immiscible PLLA/PBS blends for 20wt% of PBS. A high elongation at break of 250% was reported with a modulus of 2.9 GPa but with a low improvement of impact strength (3.7 kJ.m^{-2} vs 2.5 kJ.m^{-2} for neat PLLA). In the same paper, the addition of 0.1wt% of dicumyl peroxide improved the impact strength to 30 kJ.m^{-2} while retaining similar elongation at break and modulus²²⁹. Ji *et al.* reported similar enhancement using dicumyl peroxide²³⁰. Other studies did not report such mechanical improvement without using any compatibilizer^{231,232}, therefore strategies to enhance the compatibility of the two polymers were developed. Lysine triisocyanate was used by Harada *et al.* for 90/10 PLA/PBS blends resulting in an elongation at break of 225% and an impact strength of $55\text{-}60 \text{ kJ.m}^{-2}$ whereas the compatibilized 80/20 blend did not break during the impact strength test²³³. The use of epoxide-based compatibilizers was also reported and led to high mechanical enhancement^{226,234-236} which was not the case when a PLLA-*b*-PBS-*b*-PLLA triblock copolymer was synthesised and used as a compatibilizer²³⁷; the copolymer strategy being efficient when a three-arm star-block copolymer was synthesised²³⁶. More recently, a ternary blend of PLA/PBS/PBAT was reported by Wu *et al.* using a slight amount of peroxide. A blend composition of 40/60/20 PLA/PBS/PBAT with 0.3phr of peroxide was reported to achieve a 1000 J.m^{-1} impact strength with an elongation at break around 100%

and a modulus of 1.3 GPa but a tensile strength of 34 MPa²³⁸. These examples show the high potential of such polymer blend which is however disregarded due to the high cost of production of PBS.

Poly(butylene succinate-co-adipate) (PBSA)

Similar to PBS, PBSA is another flexible and biodegradable polyester with a reported elongation at break around 300%. Lee and Lee prepared PLA/PBSA blends resulting in poor mechanical properties due to the high incompatibility of the two polymers²³⁹. First reporting the same behaviour²⁴⁰, Ojijo *et al.* also studied the effect of using triphenyl phosphine as a reactive compatibilizer in blends containing from a 90/10 to a 50/50 weight ratio of PLA/PBSA. An elongation at break of 230% and an impact strength of 11.4 kJ.m⁻² were obtained for the 70/30 blend using 2wt% of triphenyl phosphine. For the 90/10 blend, the elongation at break was only 140% but the impact strength was higher and reached 16 kJ.m⁻², nearly a three-time higher value than neat PLA. The tensile strength was also close to that of neat PLA²⁴¹. The same team used a commercially available chain extender, Joncryl® ADR 4368 CS, bearing pendant epoxy groups. The use of 0.6wt% of such additive allowed a 60/40 weight ratio PLA/PBSA blend to display an impact strength of 38.4 kJ.m⁻² and an elongation at break of 179% with a modulus of 2.4 GPa²⁴², showing the potential of this polymer but that more research is required to tune the properties of its blend with PLA.

Biopolymers (poly(hydroxyalkanoate)s, starch, chitosan)

Recently, a renewed interest has been devoted to the use of biopolymers to enhance the properties of PLA. Such polymers are typically poly(hydroxyalkanoate)s (PHA)s starch, chitosan or proteins.

Poly(hydroxyalkanoate)s, or PHAs, are promising biodegradable, aliphatic, and bio-based polymers for the toughening of PLA. These polymers are so-called microbial polymers as they are produced by microorganisms. PHAs are actually copolymers containing minor amounts of other hydroxyalkanoate motives depending on the production process^{243,244}. The mechanical properties of PHAs are closely correlated to their structure, which can bear from three to over fourteen carbon atoms. The most common PHAs are poly(3-hydroxybutyrate), poly(3-hydroxyvalerate), poly(3-hydroxybutyrate-co-3-hydroxyhexanoate), poly(3-hydroxybutyrate-co-3-hydroxyvalerate), and poly(3-hydroxyoctanoate) (Fig. I. 29).

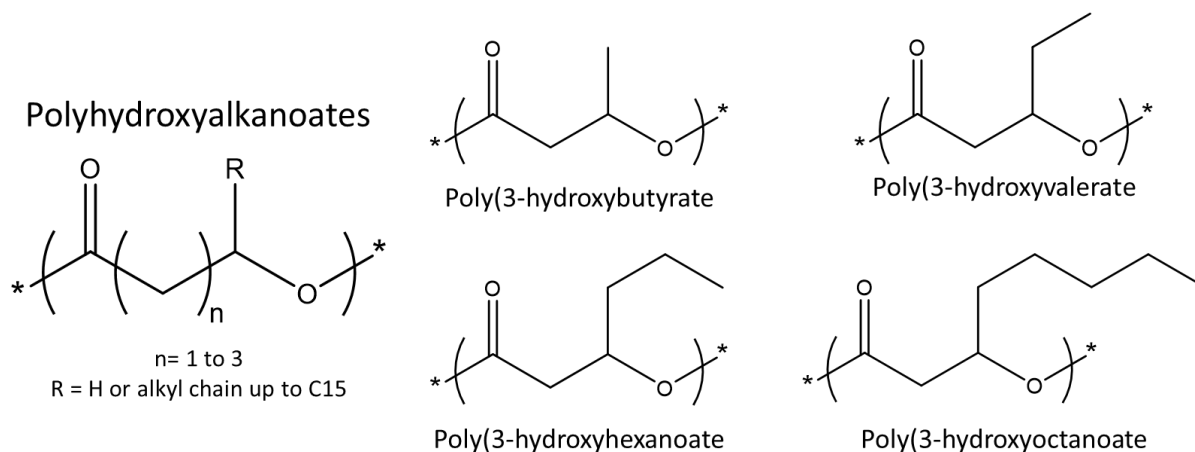


Fig. 1. 29: General structure of PHAs with a few common motives

A commercial poly(3-hydroxybutyrate) copolymer with other PHAs (Nodax) as blended with PLA and 10wt% was sufficient to improve the ductility and impact strength by one order of magnitude²⁴⁵. Another PHA, poly(3-hydroxybutyrate-co-3-hydroxyvalerate) was blended with PLA which did not result in highly improved mechanical properties even at high loadings of PHA²⁴⁶. More recently, Burzic *et al.* tested two grades of commercially available PHAs (undisclosed composition) and managed to get an un-notched impact strength of 80 kJ.m^{-2} from 19 kJ.m^{-2} for an 80/20 weight ratio of PLA/PHA although the resulting elongation at break only improved to 4%. The same paper also reported the effect of annealed samples which gave an improved impact strength up to 115 kJ.m^{-2} up from 55 kJ.m^{-2} for annealed neat PLA²⁴⁷. More recently, Arrieta *et al.* reported PLA/ poly(3-hydroxybutyrate) blends using acetyl-tri-n-butyl citrate as a plasticiser in a 63.75/21.25/15 weight ratio blend. The resulting fibre materials had a depressed Tg of 26°C with an elongation at break of 105% compared to the unplasticized blend which had an elongation at break of 55% and a Tg of 51°C ²⁴⁸. Also, Bian *et al.* tested poly(3-hydroxybutyrate-co-4-hydroxybutyrate) with and without dicumyl peroxide and/or triallyl isocyanurate to enhance the compatibility of the two polymers. Using 0.2wt% of these two compounds in 70/30 blends, an elongation at break of 251% could be achieved with a modulus of 1.1 GPa (5% and 2.0 GPa for neat PLA). This is still close to the performance achieved by the neat blend, which showed an elongation at break of 186% and a modulus of 1.2 GPa, therefore underlying the good compatibility of this PHA with PLA²⁴⁹. These examples amongst many others show the great potential of PLA/PHA blends which properties can be tuned depending on the PHA grade used.

Jacobsen and Fritz were the first to blend PLA with starch to reduce the cost of PLA-based materials while enhancing its flexibility. They realised they could only use up to 10wt% of native starch due to the semicrystalline character of the additive²⁵⁰. Since then, many studies have focussed on using modified starch materials (thermoplastic starch) with plasticisers to obtain an effect on the properties of PLA²⁵¹. Martin and Avérous used such thermoplastic starch with glycerol and showed the rigidity of the material was controlled by the amount of glycerol and emphasised the need for compatibilization due to the poor mechanical properties which were obtained¹³⁷. Li and Huneault reported various results using sorbitol and glycerol, with or without chain extenders which resulted in improved ductility at the expense of tensile strength which dramatically decreased^{252,253}. The ductility of PLA/thermoplastic starch blends was enhanced using PLA-*graft*-maleic anhydride or thermoplastic starch-*graft*-maleic anhydride with a plasticiser^{254–256}.

Chitosan or β -(1,4)-2-amino-2-deoxy-D-glucopyranose has the great advantage of being available, biocompatible, biodegradable, non-toxic and shows antimicrobial properties. It is the deacetylated derivative of chitin, the major component of crustaceans' shells (shrimps, squids, crabs etc.). Typical use of chitosan with PLA is to enhance the flexibility of PLA. A work reporting blends of chitosan and PLA is from Suyatma *et al.* in which 10, 20 or 30wt% of PLA is incorporated into chitosan. The mechanical properties of the blends are better than neat PLA, however they still remain very unsatisfactory in terms of elongation at break. Fimbeau *et al.* prepared PLA/chitosan films using poly(ethylene oxide) as a plasticiser. Enhanced properties were obtained due to the use of the plasticiser as reported previously in this chapter²⁵⁷. Works by Bonilla *et al.* and Claro *et al.* on PLA films containing 10wt% of chitosan showed an improved strength and ductility compared to neat PLA films^{258,259}. Such materials show potential not only due to their flexibility but also thanks to their high biodegradability.

Other biodegradable polymers

A commercial polyamide elastomer (PEBAX 2533) based on polyamide 12 (22wt%) and poly(tetramethylene oxide) (78wt%) was also used for blends with PLA. Partial miscibility was reported between PLLA and PEBAX due to the good interactions between PLLA and the soft polyether and the hydrogen bonding between the amide functions of PEBAX and the ester functions of PLLA. The blend could exhibit an elongation at break of 161% for only 5wt% of PEBAX along with a very small decrease of modulus from 1.5 GPa to 1.8 GPa²⁶⁰. Multiple long-

Chapter 1

chain polyamides were tested by Raj *et al.* where polyamide 12 proved to enhance the mechanical properties of PLA the best with an elongation at break over 150% at 30wt% loadings and an impact strength up to 27 kJ.m^{-2} from 18 kJ.m^{-2} for neat PLA. At 40wt%, polyamide 12 and polyamide 10-12 could increase the impact strength to $33\text{-}38 \text{ kJ.m}^{-2}$, both compositions retaining high tensile strength²⁶¹. Zhang *et al.* produced ternary PLA/PEBA/ethylene-methyl acrylate-glycidyl methacrylate blends. A 70/10/20 weight ratio blend exhibited an impact strength of 550 J.m^{-1} with an elongation at break of 60% while showing a modulus of 1.9 GPa and a tensile strength of 45 MPa due to a very good interfacial adhesion of the components²⁶². More recently, Xia *et al.* chemically modified PEBA with glycidyl methacrylate and then blended the PEBA grafted with glycidyl methacrylate with PLA. The use of 30wt% of this polymer resulted in an impact strength of 78.3 kJ.m^{-2} and an elongation at break of 310%²⁶³.

Lebarbé *et al.* developed a series of bio-based polyesters and poly(ester-amides) to act as toughening agents for PLLA. The incorporation of 10wt% of the most promising compound allowed the blend to show highly improved elongation at break of 155% and a modulus of 900MPa (vs 4% and 1500MPa for neat PLLA) (Fig. I. 30). Unfortunately, the impact strength only showed very little improvement compared to other reported values in the literature^{264,265}.

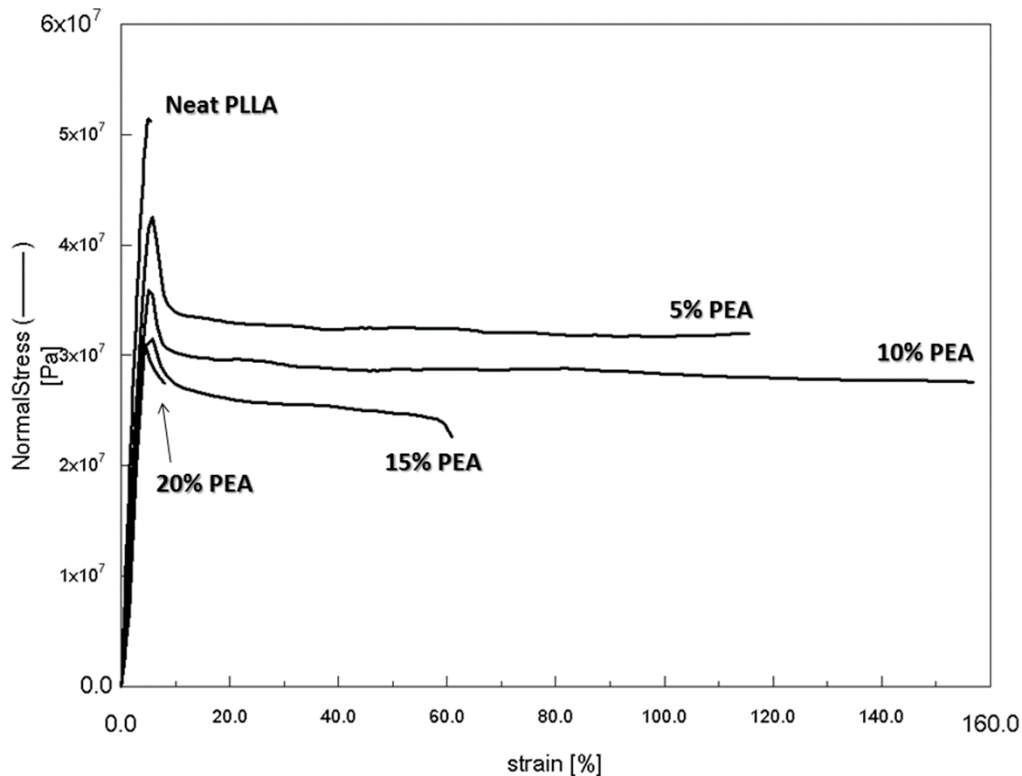


Fig. 1. 30: Tensile stress vs strain curves for PLLA blends with different poly(ester-amide) contents. Reproduced from Lebarbé et al.²⁶⁵ with permission from Elsevier, copyright 2015

The same team later studied the influence of a bio-based polyester structure made from sebacic acid, 1,10-decanediol and a dimer fatty acid Pripol 1009[®] with a varying amount of alkyl dangling chains. The obtained additives had a constant T_g around -50°C but a melting point which would span from -5°C to 78°C . A good compromise could be found with the compound containing 70mol% of dangling chains which displayed at 10wt% an elongation at break of 360% and an impact strength of $6\text{kJ}\cdot\text{m}^{-2}$ and at 20wt% an even higher impact strength of $10\text{kJ}\cdot\text{m}^{-2}$ with a lower elongation at break of 250%. This was remarkable given the impact strength of PLLA was reported at $2.5\text{kJ}\cdot\text{m}^{-2}$, however, the modulus was divided by two and gave values around between 700 and 850MPa ²⁶⁶. Finally, in collaboration with the ITERG, direct blends of PLLA with poly(methyl ricinoleate) were reported as having mechanical properties as 10wt% loadings allowed the blend to exhibit an elongation at break of 155% with a modulus of 1200MPa , and a tensile strength of 44MPa for a blend with a crystallinity ratio of 46% which demonstrates the high potential and efficiency of castor oil derivatives for the toughening of PLA²⁶⁷.

Chapter 1

For the sake of mentioning them, PLA-based fibre composites have recently gained an interest due to their low price, high availability from annually renewable resources and biodegradability. Various examples include jute, kenaf, bamboo, straw, miscanthus etc. Such materials have been found to enhance the mechanical properties of PLA at room temperature in terms of impact strength, stiffness, elongation at break and in some cases to a very low extent, a slight effect on the crystallisation rate. Challenges remain regarding the optimal fibre length, the dispersion of the fibre and its wettability with the PLA resin and the processing conditions and techniques of such composites. The readers are referred to the available literature from Siakeng *et al.* and Sangeetha *et al.* regarding such materials for more information^{268,269}.

d. Global summary and perspectives

The very extensive literature regarding the toughening of PLA offers multiple possibilities, especially regarding the use of bio-based and biodegradable modifiers²⁶⁹. The main remaining challenge is to preserve the compostable characteristic of PLA to get more sustainable materials while preserving a low cost of production. Hopefully, the examples reported above showed the possibility to use biodegradable polyesters which would be highly suitable materials.

The ester linkage is prone to hydrolysis which leads to believe it can undergo natural degradation in a compost medium or in the environment. Also, most of the reported polyester materials are mostly obtained from renewable resources derived from the biomass, for instance, PBAT, PBS, PHAs or poly(methyl ricinoleate) and can be used at low loadings, especially in the case of the latter polymer. Other challenges remain regarding PLA which will be dealt with in the coming parts.

3.2. Improving the heat deflection temperature of PLA

The low heat deflection temperature of PLA is a well-known phenomenon which is still a major drawback for the use of PLA-based materials above 55°C. This is due to the fact that the T_g of PLA is between 55°C and 60°C and that, although optically pure PLA grades (PLLA or PDLA) are semi-crystalline polymers, their crystallisation kinetics are very slow leading to materials with very low crystallinity ratios when made at high production speeds. Indeed, multiple strategies have been developed to try to enhance this behaviour, either by trying to

modify the T_g of PLA, take advantage of its stereocomplexation, improve its crystallinity ratio, or even by adding solid fibres^{138,270}.

a. **Enhancing the crystallisation kinetics (NAs, plasticisers...)**

A typical problem of PLA is its slow crystallisation kinetics. Since the industrial production of PLA pieces is about a few seconds long, PLA does not have the time to crystallise, even in favourable conditions (mould set between 100°C and 130°C)²⁷¹. As described in the part dealing with the crystallisation of PLA, the crystallisation phenomenon of a polymer can be divided into two major components: the nucleation and the crystal growth. Both components are at play in defining the low crystallisation kinetics of PLA⁴⁴ and the different kinetics enhancement strategies can play a role on a single or both components. The thermal annealing of the PLA objects can be a solution, however, it is still not compatible with fast production rates as this process requires several minutes to obtain a sufficiently high crystallinity ratio that would improve greatly the heat deflection temperature²⁷².

Nucleating agents

A first common strategy to enhance the crystallisation kinetics is to use nucleating agents. Nucleating agents are small organic molecules or inorganic compounds that will highly promote the crystallisation phenomenon when mixed inside a polymer by increasing the nucleation density to very high levels. This concept is already well-known from their use with polyolefins such as high density polyethylene or isotactic polypropylene^{273–275}. Tested nucleating agents for PLA are numerous¹³⁵ and involve mineral and organic compounds such as minerals²⁷⁶, oxides^{277,278}, hydrazide compounds^{279–281} or amides^{282–289} (Fig. I. 31).

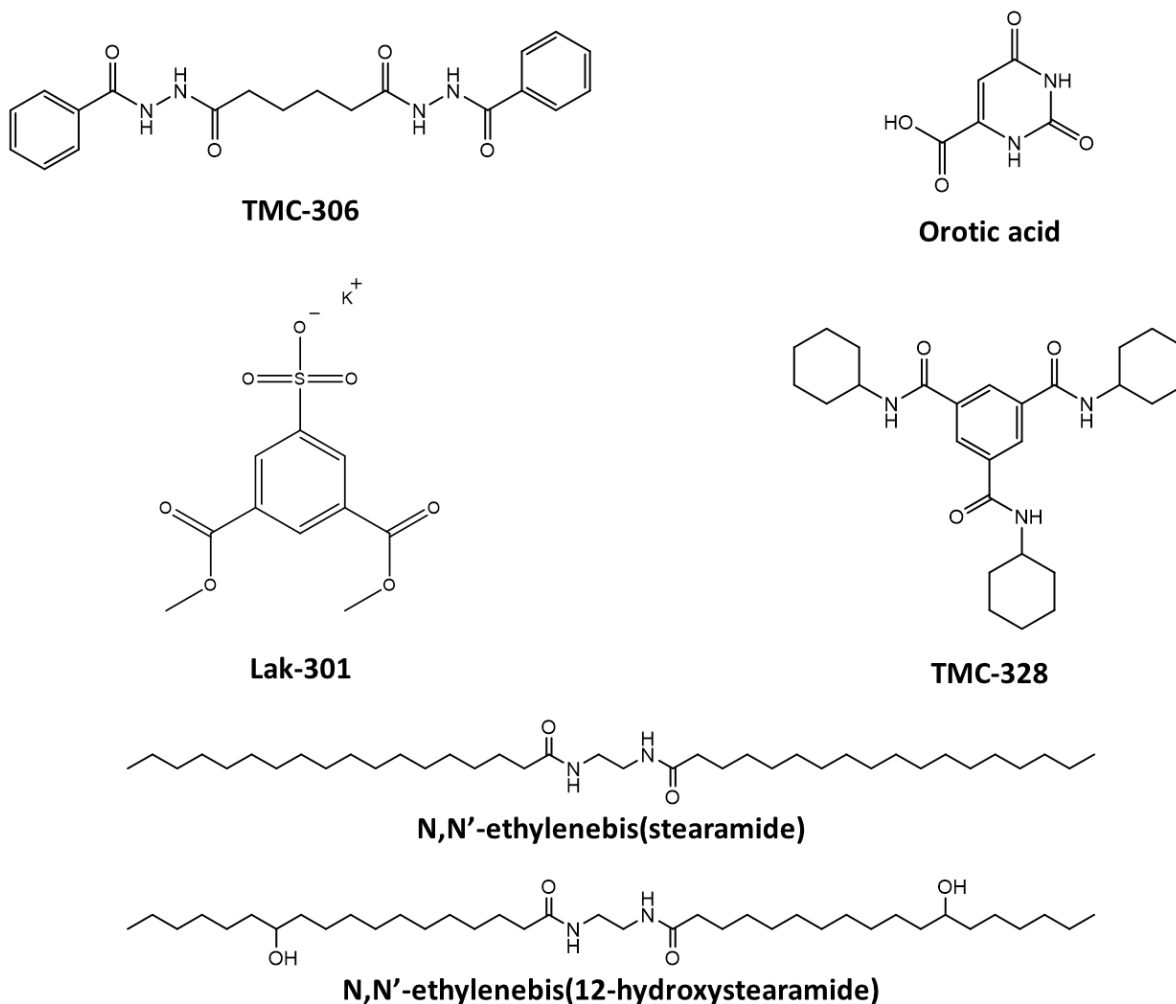


Fig. 1. 31: Commonly reported organic nucleating agents for PLA

Kolstad was the first to report the use of 6wt% talc in PLLA which increased the nucleation density by 500 times, leading to a seven-fold reduction of $t_{1/2}$ at 110°C to less than a minute²⁹⁰. Harris and Lee reported such performance using only 2wt% of talc at 115°C with a $t_{1/2}$ down from 38.2 min for neat PLA to 0.6 min⁴⁸. Li and Huneault showed that for 1wt% of talc, the optimum crystallisation temperature would drop to 100°C and decrease $t_{1/2}$ to 90 seconds²⁹¹. The influence of the size of talc particles was later discussed by Petchwattana *et al.*, which concluded that the smaller particles of talc of 1µm were the most efficient. However, the highest HDT of 139°C was only achieved using 10wt% of talc (precise injection-moulding conditions not disclosed)²⁹². Clay has also been considered as a mineral nucleating agent as it has been used to improve the thermal, mechanical, biodegradation and barrier properties of PLA²⁹³. A study found that 4wt% of nanoclay could increase the crystallisation rate from 36% for neat PLA to 49% after 1.5h at 110°C, which is not much²⁹⁴. A more profound study into the kinetics of PLA/clay systems concluded that the effect of clay is rather moderate on the

crystallisation kinetics of PLA and that talc makes a much better nucleating agent in comparison²⁹⁵.

Organic nucleating agents can also be used. They are typically low molecular weight compounds that can crystallise at a higher temperature than the polymer therefore providing organic nucleation sites. Compared to inorganic fillers, they can be more finely dispersed inside the polymer matrix in the molten state. Various nitrogen bearing compounds have been considered as such. Nam *et al.* reported the use of N,N'-ethylenebis(12-hydroxystearamide) (EBHS) as a nucleating agent with PLA. Optical micrographs showed the evidence of trans-crystallites which was proof of an epitaxial growth of PLA crystallites from the surface of EBHS. They also demonstrated the effect of the nucleating agent at crystallisation temperatures of 110°C and 130°C. Moreover, a clear trend of faster crystallisation rates was measured at 110°C with just 1wt% of EBHS²⁹⁶. Xing *et al.* observed a similar effect using the same compound which resulted in a very high nucleation density (Fig. I. 32)²⁸⁸. A very similar compound that is N,N'-ethylenebis(stearamide) (EBS) was also tested as a nucleating agent. 2wt% of EBS brought the $t_{1/2}$ down to 1.8 min from 38.2 min, which was however less efficient than talc⁴⁸. The performances of EBS and EBHS were compared by Xing *et al.* They showed that EBHS was the better nucleating agent at 125°C and 1wt% in PLA, both through isothermal DSC measurements and by polarised optical micrographs although it has a lower melting point than EBS (142°C vs 146°C). Such difference was attributed to a better hydrogen bond interaction between PLA and EBHS due to the presence of the hydroxyl groups²⁸⁴. Saitou and Yamaguchi further studied these two agents and did not see a clear difference between the two in isothermal crystallisation kinetics at 100°C when the loading was lower than 0.7wt%²⁸⁷. These two bio-based nucleating agents show such promising performances that patents were filled regarding heat resistant PLA formulations^{297–299}.

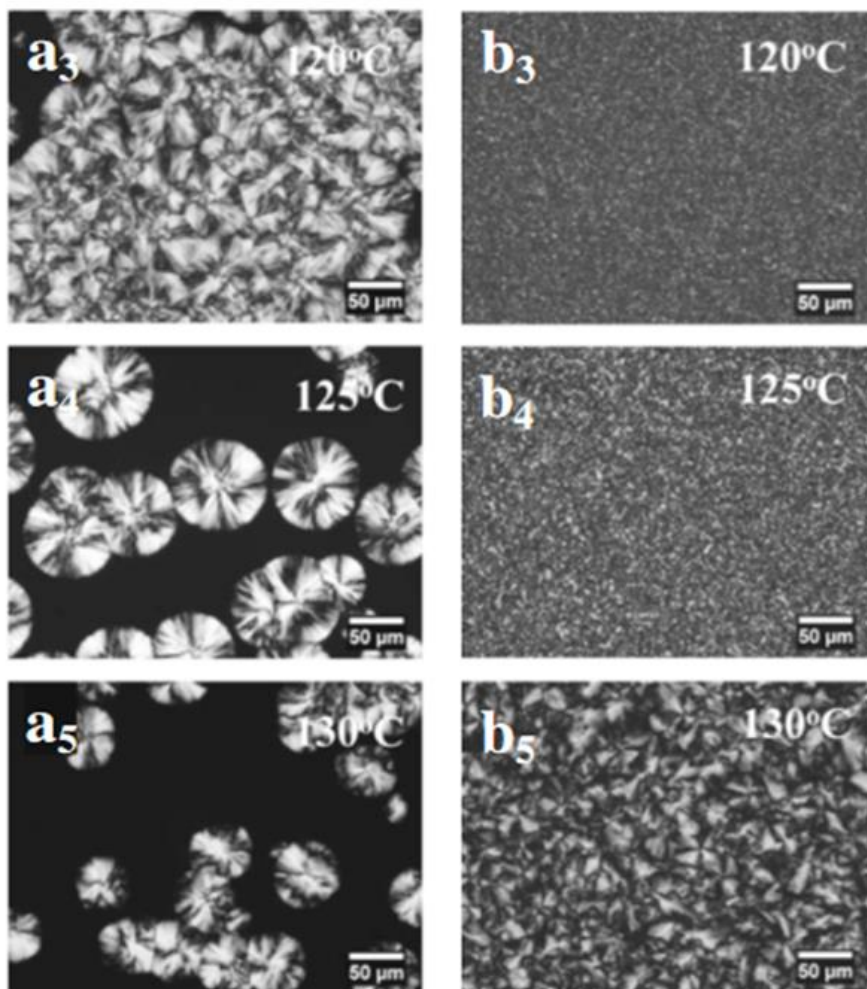


Fig. 1.32: Polarised Optical Microscopy micrographs of neat PLLA (a_3 - a_5) and PLLA/ N,N' -ethylenebis(12-hydroxystearamide) (b_3 - b_5) at selected temperatures for 90 mins. Adapted from Xing *et al.*²⁸⁸ with permission from Springer-Verlag Berlin Heidelberg, copyright 2015

Other compounds include orotic acid which was melt-blended at a 0.3wt% loading. Isothermal crystallisation was performed at 120°C and $t_{1/2}$ was reduced to 40 secs from over 10 mins³⁰⁰ although another study reported a lower effect using 0.5wt%²⁸⁵. Hydrazide compounds are also reported as efficient nucleating agents. Qi *et al.* synthesised a series of aliphatic diacyl adipic dihydrazides with different alkyl moieties which were added into PLA at 1wt% loadings. The $t_{1/2}$ values were reduced to 2.8-5 mins depending on the alkyl moieties, the octyl substituent being the most efficient³⁰¹. A commercially available dihydrazide compound N,N' -dibenzoyladipohydrazide (TMC-306) brought $t_{1/2}$ down to 0.5 min from 8.1 min at 120°C at a 0.5wt% loading. In the similar study, a homemade bisoxalamide molecule, N,N' -(ethane-1,2-diyl)bis(N -phenyloxalamide), gave a $t_{1/2}$ of 0.6 min²⁸⁵. Similar linear oxalamide compounds were studied by Roy *et al.* and reported a $t_{1/2}$ of 2.7 minutes compared to 17.7 minutes for neat PLA at 2wt% loading³⁰² and similar derivatives are also reported in

patents³⁰³. Derivatives of 1,3,5-trialkyl-benzenetricarboxylamides (BTAs) are also reported. 0.8wt% was found to be the optimal loading with the butyl substituents. A $t_{1/2}$ of 0.8 mins was obtained during isothermal crystallisation at 120°C as compared to 18 min for neat PLA. It was further decreased to 0.6 mins at 105°C showing the high efficiency of such components³⁰⁴. A similar compound, N,N',N''-tricyclohexyl-1,3,5-benzene-tricarboxylamide (TMC-328) also showed similar efficiency with a heat deflection temperature above 140°C³⁰⁵. Among other very efficient compounds are precipitated barium sulfate³⁰⁶, uracyle ($t_{1/2}$ 1 min at 120°C vs 16.8 min)³⁰⁷, zinc phenylphosphate ($t_{1/2}$ = 0.62 min at 115°C at 2wt% loading)³⁰⁸, and a potassium salt of dimethyl 5-sulfoisophthalate (Lak-301) which reduced the $t_{1/2}$ to 0.28 in at 120°C in PLA/miscanthus/Lak-301 blends (89/10/1)³⁰⁹. Due to the incredible number of papers, we refer the readers to other extensive reviews regarding nucleating agents such as the one from Tábi *et al*¹³⁵.

The extensive research conducted on nucleating agents for PLA has managed to discover very efficient compounds that greatly promote the crystallisation of PLA, through a very high nucleation efficiency. Very simple and cheap commercially available compounds are reported which opens the way for PLA with nucleating agents to obtain PLA materials with enhanced thermal properties.

Plasticisers

Jointly, another strategy to help PLA crystallise is the use of plasticisers. Thanks to such compounds, the chain mobility of PLA can be enhanced and therefore crystallise more easily. Another reported effect is directly linked to the nature of the plasticisers. Indeed, esters and especially citrates are reported to boost the crystal growth^{138,298,310}. Most plasticisers have already been described in the part regarding the toughening of PLA. Their performance regarding the improvement of crystallisation kinetics is however worth mentioning in some cases. Low molar mass poly(ethylene oxide) ($M_n=200 \text{ g}\cdot\text{mol}^{-1}$) was used by Chieng *et al.* who reported an increased crystallinity ratio for sheets obtained by hot pressing at 160°C for 10 mins (above 55% for a poly(ethylene oxide) content from 1wt% to 5wt%)³¹¹. Muller *et al.* used poly(ethylene oxide)s with higher molar masses from $M_n= 1000 \text{ g}\cdot\text{mol}^{-1}$ to $5000 \text{ g}\cdot\text{mol}^{-1}$ to avoid phase separation and also reported increased crystallinity ratios during dynamic DSC cooling³¹². More recently, triblock copolymers of PLA-*b*-poly(ethylene oxide)-*b*-PLA were also reported to induce a higher crystallinity ratio when blended with PLA³¹³. Citrate ester were

also reported to influence the crystallisation degree of PLA. Acetyl triethyl citrate was reported by Li and Huneault as having a slight effect when combined with a nucleating agent such as talc²⁹¹. Labrecque *et al.* showed high amounts of triethyl, tributyl citrate or acetyl triethyl citrate improved the crystallisation kinetics of PLA although this was most noticeable on the cold crystallisation of the mixture³¹⁴. Similar observations were reported by Ljungberg *et al.*¹⁴⁰.

Polymer blends

Like the plasticisers, this part will cover the effect of polymers blended with PLA, most of which have already been discussed regarding their effect of the mechanical properties of PLA.

Hao *et al.* studied the evolution of the Tg of miscible PLA/poly(methyl methacrylate) blends. Though the crystallinity ratio of the blends was not improved, the Tg did increase with increasing contents of PMMA reaching 74°C for 50/50 blends³¹⁵. The poly(ester-amide) impact enhancers reported by Lebarbé *et al.* also showed they improved the crystallisation kinetics of PLA by bringing the $t_{1/2}$ to 1.72 min from 6.12 min for neat PLLA at 110°C²⁶⁵. Similarly, their polyester containing 70% of dimer fatty acid showed a $t_{1/2}$ down to 1.60 min and 1.17 min during isothermal crystallisation at 110°C at 10wt% and 20wt% loadings²⁶⁶. Diblock PLLA-*b*-PCL copolymers were studied by Castillo *et al.* and reported to have faster crystallisation kinetics with a growing amount of PCL up to 10wt%⁶⁵. Cock *et al.* reported the higher crystallisation degree of PLA/PCL blends due to the nucleating effect of PCL during the supercooling of the PLA matrix³¹⁶. Poly(3-hydroxybutyrate) was also reported to enhance the crystallisation kinetics of PLA with a crystallinity ratio of 22% compared to 3% for neat PLA³¹⁷. Guo *et al.* reported a heat deflection temperature of 133°C using 50wt% of poly(oxymethylene) in PLA³¹⁸. Quero *et al.* studied the isothermal crystallisation of PLA/PBAT blends with and without the use of acetyl tributyl citrate. The combined effect of the plasticiser and PBAT slightly reduced the half-time crystallisation of the blend³¹⁹. Shibata *et al.* studied the thermal behaviour of PLA/PBS and PLA/poly(butylene succinate-co-L-lactate) (PBSL) blends. They found both polymers would increase the crystallinity ratio of the blend for samples injection moulded at 40°C. Furthermore, isothermal crystallisation measurements allowed them to report $t_{1/2}$ down to 3.1 min for PBSL at 10wt% loadings from 12.5 min for neat PLLA at 110°C. PBS only had a slight effect at 5wt% with a $t_{1/2}$ reported at 9.6 min³²⁰.

Biopolymers (starch, chitin, silk, cellulose) have also been considered for PLA. As previously described for the mechanical properties' enhancement, starch or thermoplastic starch has

been tested. PLA blends with corn starch had a $t_{1/2}$ of 1.5-3.2 min at 100°C compared to 14 min for neat PLA but remained lower than the one induced by talc³²¹. Chitin was reported by Rizvi *et al.* to enhance the crystallisation kinetics of PLA as 1wt% was sufficient to obtain a crystallinity degree above 40% by compression moulding at 180°C for 10 min³²². Silk was also reported to act as a nucleating agent with just 1wt% in PLA. No effect could be measured by non-isothermal DSC studies; however, a difference clearly appeared by polarised optical microscopy during an isothermal, crystallisation at 120°C. A maximum crystallisation rate was found at 107°C with a $t_{1/2}$ around 2 min compared to over 10 min for neat PLA³²³. Cellulose crystals are also a reported nucleating agent with lower efficiency than chitin or silk^{324,325}, even when it was chemically modified through esterification³²⁶.

Some notable examples combine the use of a plasticiser along with a nucleating agent or a polymer acting as such. Singh *et al.* reported the use of triethyl citrate at 20wt% with 1wt% of chitin nanocrystals which showed high crystallinity ability through the DSC and polarised optical microscopy¹³⁸.

b. Stereocomplexation

Adding low molar mass PLA to high molar mass PLLA or PDLA has been suggested in the mechanical reinforcement part so that it would act as a plasticiser on PLA. Yin *et al.* used small amounts of a high melting point PLLA (187°C) blended, in such a way that it would not melt, inside a PLLA matrix ($T_m=168^\circ\text{C}$). Using such technique, the authors managed to enhance greatly the crystallisation kinetics of the PLLA matrix bringing the $t_{1/2}$ down to 24 sec from over 15 min. This technique was more efficient than blending PDLA or talc at the same weight ratio (5wt%)³²⁷. Di Lorenzo and Androsch studied the effect of low molar mass highly pure PLLA in PLLA containing 4mol% of D-lactide on the crystallisation kinetics. They found such incorporation enhanced the crystallisation kinetics of the high molar mass PLLA as the low molar mass PLLA would crystallise first and therefore induce the crystallisation of the higher molar mass PLLA.³²⁸

Thanks to new efficient production means, PDLA has become a very affordable grade of PLA. Combined with the need to enhance the thermal behaviour of PLA-based materials, the path of stereocomplexes has been highly considered³²⁹. Stereocomplexes are formed from the equimolar mixture of PLLA and PDLA chains which co-crystallise in a new arrangement (Fig. I. 33). Also, since stereocomplexes form at a higher temperature than PLA homocrystals (220-

240°C)^{35,330}, they might act as nucleating agents on top of adding to the thermal stability of PLA.

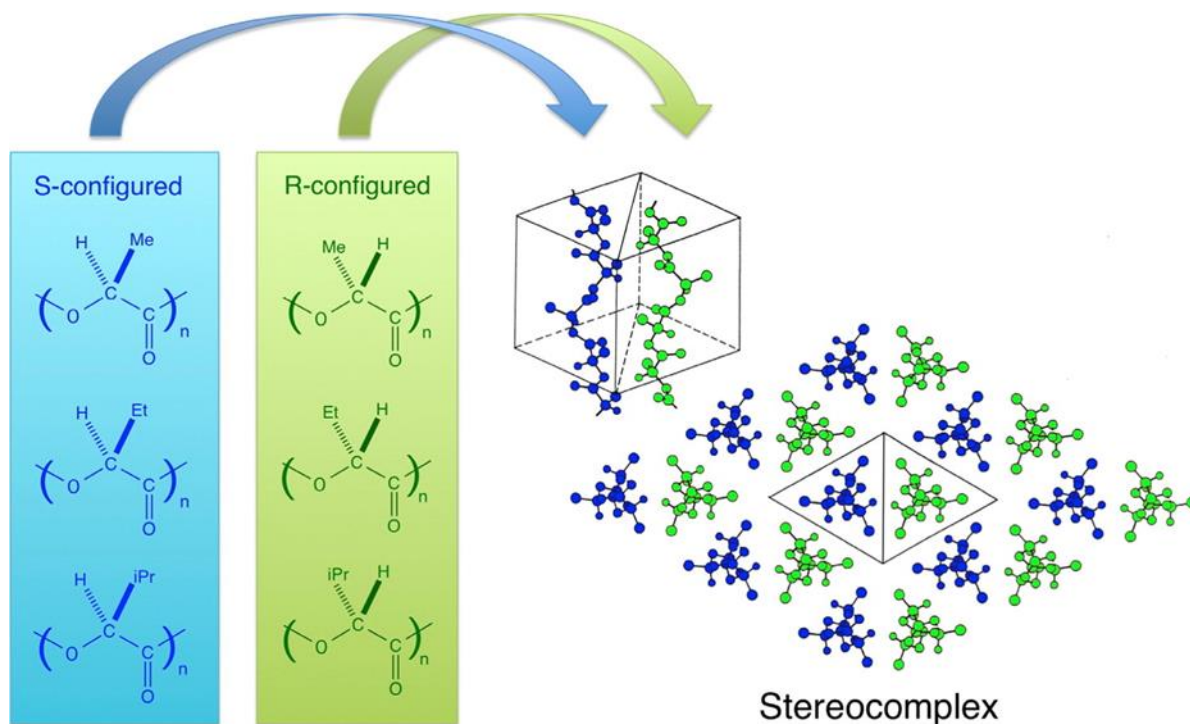


Fig. 1. 33: Stereocomplex formation using PLLA and PDLA, reproduced from Tsuji³³¹ with permission from Elsevier

To support this hypothesis, the study from Brochu *et al.* reported a higher spherulite density along with a larger homocrystalline fraction. The authors concluded that PLLA crystals can grow through epitaxy on previously formed stereocomplexes' lamellae³³². Anderson and Hillmyer studied the effect of the molar mass of PDLA in 97/3 weight ratios PLLA/PDLA blends on the crystallisation kinetics of PLLA and the formation of stereocomplexes. They found that a PDLA with an M_n of 14,000 $\text{g}\cdot\text{mol}^{-1}$ was the most efficient and resulted in a $t_{1/2}$ of less than 1 min at 140°C (vs 17 min for neat PLLA) and close performance was achieved using only 1wt%. The presence of stereocomplexes was proven using the DSC and polarised optical microscopy³³³. Tsuji *et al.* further confirmed such observations by studying the amount of stereocomplexes formed. They noticed a difference in behaviour between the isothermal and non-isothermal crystallisation, the amount of PDLA was ten times higher to have an effect on the isothermal crystallisation kinetics, whereas only 1wt% was necessary for non-isothermal crystallisation³³⁴. These studies conclude with the fact that at one point, stereocomplexation is hindered by the homocrystallisation of PLLA and PDLA. Studies have also found that the stereocomplex formation was highly dependent on the processing method. Narita *et al.* mixed

10wt% of PDLA in 90wt% PLLA by extrusion and observed that the stereocomplexes will be the most efficient to enhance the crystallisation of PLLA only if melted in the temperature range of 228-238°C. This was attributed to the formation of very small size stereocomplexes resulting in a larger number amount of crystallites. Partially melted stereocomplexes at lower temperatures or stereocomplexes melted above 240°C did not display the same efficiency³³⁵. Such study was consistent with what had been observed previously by Yamane and Sasai who did not see any nucleation effect on PLLA when a 95wt% PLLA/5wt% PDLA blend was heated above 240°C³³⁶. More recently, Samsuri *et al.* used the formation of different size stereocomplex particles to prove their influence on the nucleation of PLLA³³⁷.

Extensive research has been conducted since 2013 and has recently been published in a review by Chen *et al.* in which they report the thermal properties and behaviour of diverse PLA materials holding stereocomplexes³²⁹. Globally, the higher the stereocomplex fraction and degree of crystallinity, the higher the heat deflection temperature of the PLA material. Various strategies have been developed to trigger the formation of stereocomplexes and obtain PLA materials with enhanced thermal properties. PLLA/PDLA blends were prepared in a 50/50 weight ratio by Zhang *et al.* and injection-moulded in a mould set at 120°C. The reported Vicat softening temperature (another type of test to assess the thermal resistance of a material) was 164°C for unannealed samples containing homocrystals and stereocomplexes (29-34% crystallinity ratio of homopolymers and 5-6% crystallinity ratio of stereocomplexes) and further went up to 199°C after annealing at 210°C which produced only stereocomplexes (stereocomplexes' crystallinity ratio of 55%), therefore demonstrating the better thermal behaviour of pure stereocomplexes in PLA materials³³⁸. Another work further demonstrated the potential for heat resistance of stereocomplexes by increasing the Vicat softening temperature from 61°C to 196°C by just increasing the crystallisation degree of stereocomplexes from 2% to 35%³³⁹. The highest Vicat softening temperature was reported at 212°C by Liu *et al.* by injection moulding at 210°C in a mould set at 190°C. The material developed contained a mixture of high optically pure content PLA stereocomplexes with 20wt% of low optically pure ones with a reported stereocomplex crystallinity ratio of 40%. In comparison, the low optically pure stereocomplex PLA material had a softening temperature of 164°C³⁴⁰.

Chapter 1

For the sake of mentioning them, block copolymers using PLLA or PDLA with a polymer which can have a toughening effect have also been developed. Such polymers include PEO, PMMA, PCL, PHB, or PBAT. The idea is to develop a polymeric system which can display both enhanced mechanical properties along with high heat resistance thanks to the formation of stereocomplexes. Moreover, in some of the works previously mentioned, the higher crystallinity ratio of PLA materials resulted in a higher toughening effect of the toughening agent. We refer the readers to the review from Li *et al.* which deals with such materials³⁴¹.

The strategy involving stereocomplexes is of particular interest as better thermomechanical properties can be achieved for PLA materials due to their faster rate of crystallisation and their nucleating effect on PLLA and PDLA. There are severe drawbacks however which are the high processing temperatures which are required due to the high melting point and the high temperature formation range of the stereocomplexes, which also implies the thermal degradation of the PLLA/PDLA chains. Finally, although the production is now increasing, the price of PDLA remains higher than PLLA and therefore renders this strategy less economically attractive.

Various research has been conducted on improving the thermal behaviour of PLA. The different occurrences have reported efficient solutions which however imply the use of the correct processing conditions to obtain PLA materials with good thermal behaviour. As a simple solution, nucleating agents seems to be a simple and cheap way of achieving such goal.

3.3. Tuning the O₂ gas barrier properties

As mentioned in the part dealing with the general properties of PLA, it was clear that in order to obtain suitable food packaging properties, the gas barrier properties of PLA will have to be modified, either through a reinforcement of the barrier behaviour towards O₂ or water vapour or, on the contrary, greatly enhance the permeability of gases for fresh vegetables or fruit.

a. Improving the crystallisation rate

A first way of enhancing the gas barrier properties of PLA is to enhance its crystallinity ratio. Multiple studies have reported that the gas permeability of PLA will decrease when the crystallinity ratio increases^{89,94,97,342,343}. For instance, Guinault *et al.* measured O₂ and helium

permeabilities respectively reduced by two and three with crystallinity ratios above 40%⁹⁴. Later, their team showed the impact of the crystalline phase on the O₂ permeability. In the case of the presence of the α' phase, no reduction of O₂ permeability could be noticed and only the presence of the α phase would result in a reduction of the O₂ permeability. This was however specific to O₂ since the permeability of helium decreased with increasing ratios of crystallinity³⁴². More interestingly, Fernandes Nassar *et al.* showed a link between the process used to make PLA crystallise and the O₂ permeability⁹⁷. In their work, the authors obtained crystalline PLA sheets either directly from the melt or from the glassy state through annealing. Each time, the crystallisation conditions were selected to specifically obtain either the α' form or the α form of crystalline PLA. They concluded that the O₂ permeability of PLA films crystallised from the melt would display better barrier behaviours, about 2.5 times less permeable to O₂ when the crystallinity ratios were over 35%, whatever the selected crystallisation temperature (85°C, supposed to favour the α' form or 130°C supposed to favour the α form). An outstanding feature was, however, the permeability obtained for a sample crystallised from the glassy state at 130°C for 20 mins which gave the lowest O₂ permeability of $0.58 \times 10^{-18} \text{ m}^3 \cdot \text{m} \cdot \text{m}^{-2} \cdot \text{s}^{-1} \cdot \text{Pa}^{-1}$ compared to the original $2.30 \times 10^{-18} \text{ m}^3 \cdot \text{m} \cdot \text{m}^{-2} \cdot \text{s}^{-1} \cdot \text{Pa}^{-1}$ for neat PLA. The authors therefore concluded that to obtain the best O₂ barrier properties, PLA should be pre-nucleated and quickly annealed for a short amount of time from the glassy state at 130°C.

Unfortunately, the authors could not clearly state the predominance of either the α' or the α form in their samples. In fact, to fully understand the impact of the crystallisation degree on the barrier properties of PLA, it is necessary to decorelate the effect of the increasing crystallinity ratio and the excess of free volume formed with the rigid amorphous part of the material. Sangroniz *et al.* compared the transport properties of PLLA and a mixture of PLLA/PDLA (50/50) producing stereocomplexes for which the rigid amorphous fraction (RAF) is very small. They proved that the RAF content increases with the crystallinity ratio in PLLA, therefore leading to the creation of free volume which overcame the effect of the increased crystallinity ratio of the barrier performance. This was not the case for stereocomplexes therefore leading to a lower O₂ permeability³⁴⁴, such lower permeability at similar crystallinity ratios than PLA homopolymers being reported in other studies and the role of the stereocomplexes was also defined as increasing the tortuosity of the polymer material on top

of limiting the free volume³²⁹. In another study, Bai *et al.* changed the shape of the PLLA crystallites from spherulites to shish-kebab-like crystals using TMC-328 as a nucleating agent. The obtained PLA material has an O₂ permeability 500 times lower than neat amorphous PLA (new value of $1.91 \times 10^{-20} \text{ m}^3 \cdot \text{m} \cdot \text{m}^{-2} \cdot \text{s}^{-1} \cdot \text{Pa}^{-1}$). Such low value was obtained thanks to the parallel-aligned crystals with interlocked boundaries which greatly limited the diffusion of O₂ inside the material (Fig. I. 34)³⁴⁵.

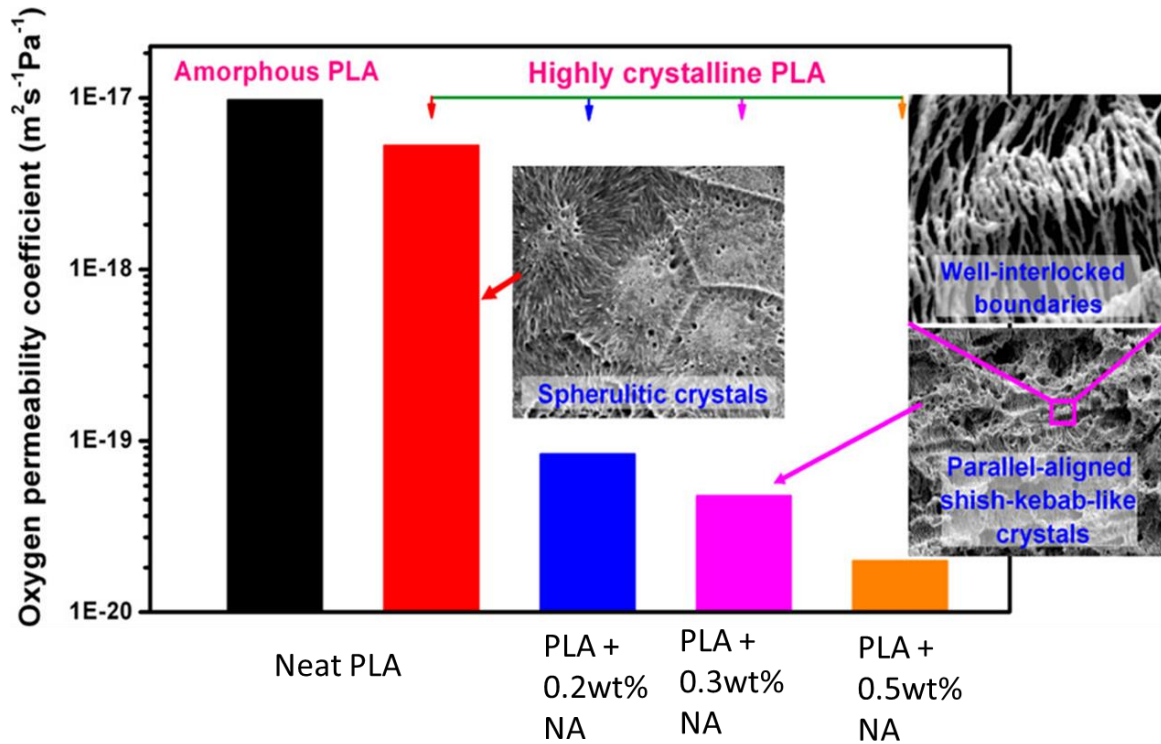


Fig. I. 34: O₂ permeability measurements on PLA samples with different crystalline morphologies. Reproduced from Bai *et al.*³⁴⁵ with permission from the American Chemical Society, Copyright 2014

The O₂ barrier properties of PLA do not only depend on its crystallinity ratio but are also highly dependent on the crystal morphology and the ratio between the crystalline, the rigid amorphous fraction and the mobile amorphous fraction of the material. Enhancing the crystallisation degree of PLA materials is however a very simple and efficient way of tuning their gas barrier properties.

b. Specific additives

The use of additives to tune the gas barrier properties of PLA has been widely studied. Depending on the nature of the additive, it is possible to predict the evolution of the permeability through the following equation:

$$\ln(P) = \varphi_1 * \ln(P_1) + \varphi_2 * \ln(P_2)$$

With P = the permeability of the penetrant through the blend, φ_1 = the volume fraction of component 1, φ_2 = the volume fraction of component 2, P_1 = the permeability of the penetrant through component 1 and P_2 = the permeability of the penetrant through component 2. In case of an immiscible blend, the Maxwell model can be used to predict the permeability through the following equation:

$$\ln(P) = \frac{P_d + 2 \times P_c - 2 \times \varphi_d \times (P_d - P_c)}{P_d + 2 \times P_c - \varphi_d \times (P_d - P_c)}$$

With P = the permeability of the penetrant through the blend, φ_d = the volume fraction of the dispersed phase, P_c = the permeability of the penetrant through the continuous phase and P_d = the permeability of the penetrant through the dispersed phase^{346–348}. The considered additives can either be fillers, or polymers^{87,88,349}. Plasticisers are disregarded as they increase chain mobility inside a polymer matrix which results in increased permeability values as demonstrated with acetyl tributyl citrate by Courgneau *et al.* even with the addition of talc as a nucleating agent to increase the crystallinity ratio³⁵⁰.

Fillers are a very efficient way of increasing the barrier behaviour of PLA. Fillers will intercalate between the polymer chains of PLA therefore reducing the free volume and also increasing the tortuosity of the path through the polymer for penetrants (Fig. I. 35). Among the most widely used fillers are montmorillonites (MMTs) which are hydrated alumina-silica layered clays. Guo *et al.* used multiple fillers such as MMT, organomodified MMT, halloysite nanotubes and organomodified halloysite nanotubes. The halloysite nanotubes did not have any effect on the O_2 permeability, whereas the organomodified MMT divided by 2 the permeability of the samples³⁵¹. In another work, Ortenzi *et al.* used silane-modified nanosilica and MMT. An 81% reduction in O_2 permeability ($2.35 \times 10^{-19} \text{ m}^3 \cdot \text{m} \cdot \text{m}^{-2} \cdot \text{s}^{-1} \cdot \text{Pa}^{-1}$) using epoxy-silane modified nanosilica at 1wt% was achieved along with a very high crystallinity ratio of 67%, also contributing to such performance³⁵². In a recent study, halloysite nanotubes were shown to reduce the O_2 permeability by a 1.5 factor at 3wt% loading, however with a rather wide standard deviation³⁵³. Graphene and graphene oxide have also been used as fillers for PLLA. Graphene sheets were incorporated with a compatibilization step involving melt-condensation of lactic acid oligomers, resulting in a reduction of 45% of the O_2 permeability³⁵⁴. Graphene oxide and graphene nanoplatelets were tested by Pinto *et al.* and 0.4wt% of them,

in separate mixtures, allowed the permeability to be reduced to $1.2 \times 10^{-18} \text{ m}^3 \cdot \text{m} \cdot \text{m}^{-2} \cdot \text{s}^{-1} \cdot \text{Pa}^{-1}$ from $3.8 \times 10^{-18} \text{ m}^3 \cdot \text{m} \cdot \text{m}^{-2} \cdot \text{s}^{-1} \cdot \text{Pa}^{-1}$ for neat PLLA³⁵⁵.

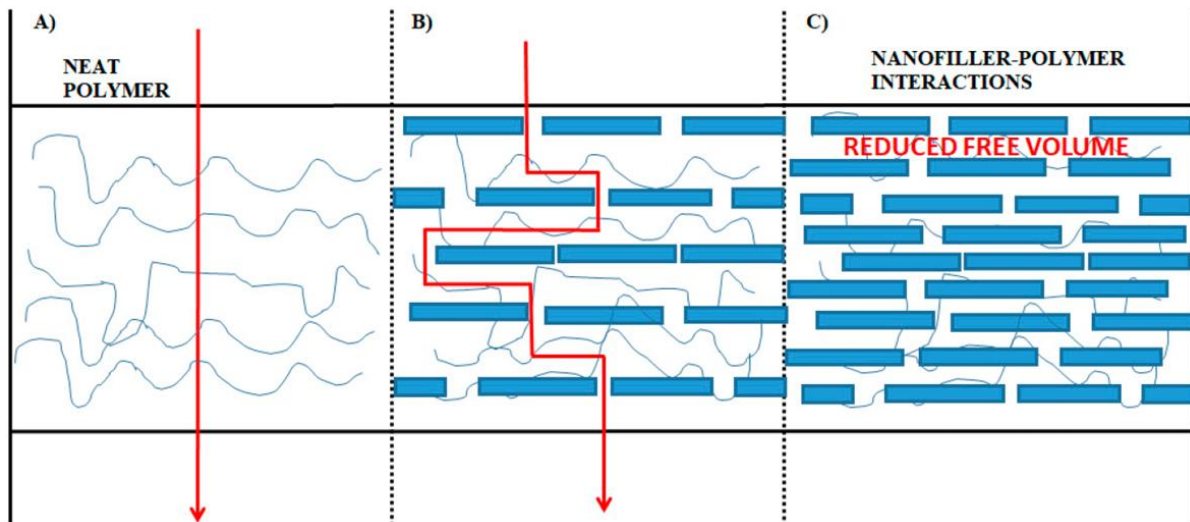


Fig. 1. 35: Simplified drawing of the “tortuous path” produced by the incorporation of nanocomposite fillers into a polymer matrix. (A) Neat polymer (diffusing gas molecules follow a pathway perpendicular to the film orientation); (B) non-interacting nanocomposite (impermeable platelets hinders direct diffusion); (C) interacting nanocomposite (the polymer strands are “immobilized” at the polymer–nanofiller interface and the overall free volume available is reduced). Reproduced from Marano *et al.*³⁵⁶ under a Creative Common CC-BY License

Regarding polymers, Lagaron *et al.* defined chemical criteria to determine whether such chemical moiety in a repeating unit would favour or not the permeability of O₂. The best results were obtained with -OH pendant groups such as the ones found with EVOH and amongst the worst groups were linear aliphatic polyolefins such as PE and even worse, repeating units containing alkyl dangling chains. Their discussion regarding the macromolecular architecture reported that polymers bearing dangling chains or branching along with atactic polymers would give lower barrier performances³⁵⁷. Moreover, the morphology of the blend is of prime importance, as a discontinuous morphology is expected to have a higher permeability than a co-continuous morphology⁸⁶.

Blends of PLA with poly(vinylacetate-co-vinyl alcohol) were prepared by Razavi *et al.* with various amounts of vinyl alcohol. The O₂ permeability was divided by a factor 2 for a copolymer containing 15mol% of vinyl alcohol at a 5wt% loading in PLA compared to neat PLA³⁵⁸. PHAs have also been blended with PLA especially poly(3-hydroxybutyrate) and poly(3-hydroxybutyrate-co-3-hydroxyvalerate). The incorporation of 15wt% of poly(3-hydroxybutyrate) reduced the O₂ transmission rate by 1.5 compared to neat PLA³⁵⁹. In another

study, 25wt% of poly(3-hydroxybutyrate-co-3-hydroxyvalerate) led to a reduction by 2.5 of the oxygen permeability. Different additives were also tested with this blend but did not improve the performance further than the neat blend³⁶⁰. Polypropylene carbonate is one of the most efficient polymers blended with PLA to reduce the O₂ permeability. In blends containing 40wt% of PLA, the O₂ permeability was reduced by 63% without the use of a compatibilizer³⁶¹. PBSA was blended with PLA and crotonic acid functionalised PLA for which N,N'-dicyclohexylcarbodiimide was used as a coupling reagent. The neat PLA/PBSA blend resulted with an increased O₂ permeability while the blend with functionalised PLA led to a 35% decrease³⁶². Chitosan was reported as a biopolymer with interesting barrier properties. It was grafted on oligomeric(lactic acid) and blended with PLLA. 5wt% of such additive resulted in a O₂ permeability reduction of 82% while keeping good mechanical properties³⁶³. Gum arabic was also tested through lactic acid-*grafted*-gum arabic taking advantage of the available -OH and -NH₂ pendant groups. The oxygen permeability was reduced by a factor ten, whatever the loading of the additive (3, 5, or 10wt%). Such performance was attributed to the dispersion of the additive increasing the tortuosity of the O₂ path and the reduction of the solubility of O₂ due to a uniform dispersion³⁶⁴. The effect of cellulose microcrystals and nanocrystals was studied by Sanchez-Garcia *et al.* and Espino-Pérez *et al.* with a focus on the size of the cellulose derivatives. Cellulose microcrystals did not have any effect on the barrier properties³⁶⁵, whereas cellulose nanocrystals decreased the O₂ permeability by a factor 10 in samples loaded at 5wt%³⁶⁶. Such results were not observed by Espino-Pérez *et al.* who did not notice a clear reduction of the O₂ permeability³⁶⁷.

Unfortunately, PLA blends with other polymers, which are reported to enhance its mechanical properties, return unsatisfactory O₂ barrier behaviours. Moreover it is hard to apprehend the true impact of the different additives since the conditions (temperature, relative humidity) are not always stated and may have an impact on the measured values, especially regarding the hydrophilic additives. Other techniques are therefore required to trigger an enhancement of such properties. This was the case with PLA/PBS and PLA/PBAT blends for instance. Such blends have been reported as having interesting mechanical properties, however the O₂ permeability properties were unsatisfactory. Works on such blends to trigger an *in-situ* fibrillation have demonstrated the possibility to reduce drastically the O₂ permeability. For a 80/20 PLA/PBS blend, the permeability was reduced to 2.0×10^{-19}

$\text{m}^3 \cdot \text{m}^{-2} \cdot \text{s}^{-1} \cdot \text{Pa}^{-1}$ which is three times lower than the permeability of neat PBS³⁶⁸. PLA/PBAT blends with a 50/50 PLA/PBAT weight ratio had an O_2 permeability which was similar to the one of neat PLA although the O_2 permeability of PBAT is originally five times higher³⁶⁹. Zhou *et al.* later reported an O_2 permeability nine times lower than neat PLLA using the same strategy with PLA/PBAT blends of 85/15 weight ratio with enhanced mechanical properties³⁷⁰.

c. Multi-layer films

Multi-layer extrusion is a common technique to superpose multiple polymer layers in a sandwich-like fashion and obtain a film presenting the characteristics of all the polymeric materials used. Regarding the permeability, it can be calculated as such:

$$\frac{1}{P} = \sum_{i=1}^n \frac{\phi_i}{P_i}$$

Where P is the general permeance, ϕ_i is the volume fraction of polymer i and P_i the permeability of the polymer composing the layer i . A typical technique is to use an expensive high barrier polymer such as ethylene vinyl alcohol (EVOH) as a middle layer to obtain high barrier properties along with a polyolefin (PE, PP) which will have a low water vapour permeability due to its highly hydrophobic nature.

Regarding PLA, only few polymers have been reported for multi-layer film production. Among these polymers are PBS, poly(3-hydroxybutyrate-co-3-hydroxyvalerate), cellulose, and fish gelatine. For the PLA/PBS system, films of $225\mu\text{m}$ were prepared containing 2049 layers with layers of PBS about 45nm thick. The O_2 permeability was only slightly affected with a 28% decrease, the most noticeable effect being on the CO_2 permeability which was decreased by nearly a factor 2.5³⁷¹. Boufarguine *et al.* produced multilayered PLA/poly(3-hydroxybutyrate-co-3-hydroxyvalerate) films (Fig. I. 36) and measured the helium permeability. The amount of layers did not have a great influence since a 35% decrease of permeability was observed whatever the amount of layers³⁷².

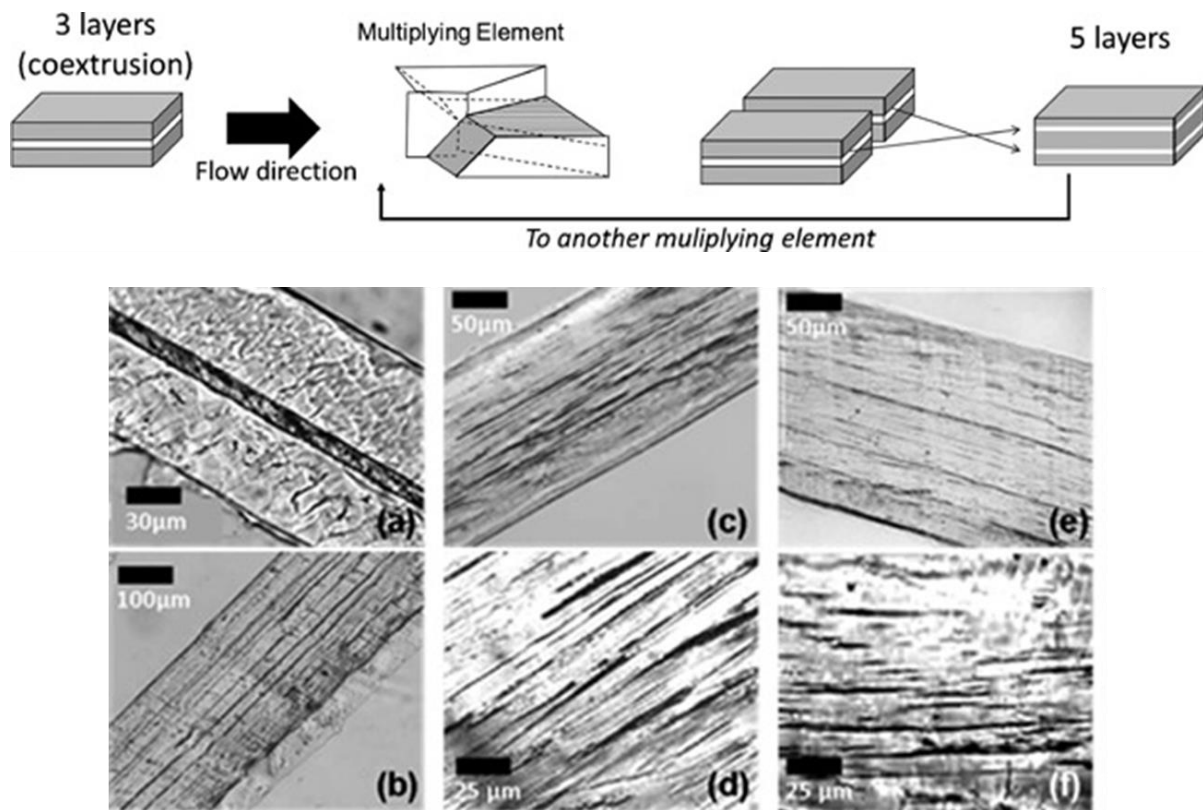


Fig. 1. 36: Schematic of the multilayer co-extrusion process (top). Optical micrographs of multilayered films a) 3 layers, (b) 17 layers, (c)(d: zoom) 129 layers, (e)(f: zoom) 2049 layers (bottom). Reproduced from Boufarguine *et al.*³⁷² with permission from John Wiley & Sons, copyright 2013

Fish gelatine has been considered as an alternative to mammalian gelatine as it is highly available from the fish processing industry. Gelatine typically displays a highly hydrophobic behaviour and superior barrier characteristics. The triple layer film displayed an O_2 permeability of $5.8 \times 10^{-19} \text{ m}^3 \cdot \text{m} \cdot \text{m}^{-2} \cdot \text{s}^{-1} \cdot \text{Pa}^{-1}$ making it one of the lowest values reported for fully bio-based systems³⁷³. Nanocellulose was also used to produce three-layered films. The measured O_2 permeability with nanocellulose crystals decreased to $1 \times 10^{-19} \text{ m}^3 \cdot \text{m} \cdot \text{m}^{-2} \cdot \text{s}^{-1} \cdot \text{Pa}^{-1}$, 80 times lower than neat PLA in this study³⁷⁴. Li *et al.* prepared alternating multilayer PLA films with layers containing a nucleating agent, TMC-300 and layers containing the same nucleating agent along with graphene sheets. The 16-layer film exhibited particular morphology which resulted in a very low O_2 permeability of $7 \times 10^{-20} \text{ m}^3 \cdot \text{m} \cdot \text{m}^{-2} \cdot \text{s}^{-1} \cdot \text{Pa}^{-1}$, one of the lowest permeability reported³⁷⁵.

These last examples show the high performances that can be achieved with the multi-layer extrusion technique of PLA-based films. More importantly, some of the most efficient examples regarding the O_2 barrier behaviour are based on renewable and biodegradable materials, some of which can be obtained easily in great quantities such as fish gelatine.

3.4. Improving the biodegradation of PLA materials

As reported by Ghosh and Jones, PLA is only suitable for degradation in industrial composting conditions and anaerobic conditions, meaning it does not satisfy the standards regarding the biodegradation in home compost, marine, fresh water, and soil environments¹¹⁶. As previously mentioned, new regulations require single-use plastic materials to be much more sustainable than before, especially regarding their end-of-life¹²⁹.

Studies regarding the degradation of polymers have emphasised the effect of additives on the biodegradability of compostable or biodegradable polymers in other environmental compartments. Sedničková *et al.* concluded in their study that blends with high PLA contents are not suitable for home-composting and should be treated in industrial composting systems. Indeed, the most easily degradable parts of the blend will disappear first leaving a lot of PLA left to degrade, which takes a very long time in such conditions³⁷⁶. Factors influencing the degradation of PLA blends are typically the morphology and the hydrophilicity of the filler/additive^{377,378}. Plasticisers such as poly(ethylene oxide) or citrates are reported to enhance the degradability of PLA *in vivo*³⁷⁹. Starch has been reported to enhance the biodegradability of PLA as films of PLA blended with starch were reported to disintegrate in 21 days in compost³⁸⁰. This was explained by the fact that starch increases the water uptake of PLA and also disrupts the crystalline structure of PLA resulting in more of the amorphous phase³⁸¹. Such behaviour was also reported regarding gelatine and ternary blends containing PLA/starch/gelatine were found to degrade faster than neat PLA³⁸². PLA/PBS blends-based materials have been buried in soil to assess their degradability and the presence of PBS was found to slightly enhance the degradation of the material due to the phase separation. Only high content blends showed a very high degradation rate though³⁸³. The degradation of a PLA/poly(3-hydroxybutyrate-co-3-hydroxyhexanoate) blend was also studied in seawater in the powder form. The higher the PLA content, the lower the biodegradation, yet, after 28 days, a 60/40 weight ratio blend showed a biodegradation of 26%³⁸⁴. PLA/poly(3-hydroxybutyrate) blends (75/25) were shown to degrade in home-composting conditions in less than a month. The plasticisers such as poly(ethylene oxide) and acetyl tributyl citrate further enhanced the degradation rate³⁸⁵. However, for PLA/PBAT blends, studies have shown no positive evolution on the biodegradation rate neither for neat blends^{386,387} nor compatibilized blends³⁸⁸. Gaps still need to be filled regarding the biodegradation

performance of novel PLA-based materials, especially regarding blends which are a promising way to obtain satisfactory mechanical properties.

Research also focussed on microorganisms, which would be able to degrade PLA and the polymers used for blending. The interested readers are referred to the reviews published by Garrison *et al.*, Qi *et al.*, and Rosli *et al.* dealing with such subject^{111,377,381}. One of the most efficient and recent developments is due to a French company called Carbiolice. Carbiolice has developed a master-batch to make PLA materials, such as objects or films, suitable for home-compost. They also patented a process which allows the making of PLA and PLA/PBAT (85/15) materials such as films or thicker objects. The master batch contains enzymes that have the ability to depolymerise PLA such as Savinase[®], Esperase[®], or Everlase[®] supplied by Novozymes, the world leader in enzyme production. The master-batch is produced using a low Tg or low melting polymer such as PBAT, PBSA, PHAs or PCL for instance. Some polysaccharide (gum arabic) is also included to serve as feedstock for the enzymes. The resulting so-called master batch is then incorporated into PLA at loadings between 0.5wt% and 15wt% (5wt% disclosed in the examples) resulting in better mechanical, impact strength and melt-flow properties^{310,389–392}. The master batch is commercialised under the tradename Evanesto[®] and 60µm films made of PLA and Evanesto[®] have satisfied the French standard NF T51-800 regarding home-compost ability of plastic materials³⁹³.

Promising solutions exist to make PLA-based materials more sustainable in regard to their after-use environmental impact. There is indeed quite a potential for new solutions by taking advantage of strategies like the one developed by Carbiolice and apply it to other high potential materials and possibly even further enhance their degradability. This is fundamental in the case of PLA since research is conducted to enhance its thermal resistance, which will be achieved through high crystallinity ratios, which will hamper greatly the degradation rate of PLA-based materials.

4. Summary and strategy presentation for the research project

The current state-of-the-art shows a very rich literature regarding PLA, both due to the long-time lasting research along with more recent gain of interest towards economically viable sustainable materials. Nowadays, PLA remains the sole fully bio-based and industrially

Chapter 1

compostable polymer which is sufficiently cheap to position itself as an economically viable alternative to oil-based, non-degradable commodity polymers.

Multiple strategies have been developed to challenge the historical drawbacks to the use of PLA such as its brittleness, low heat deflection temperature and medium-low barrier properties. Easily implementable solutions are achievable using the common extrusion process for mixing. This way, PLA can be blended with additives such as impact enhancing polymers which will allow PLA to undergo a brittle-ductile transition and have a completely different mechanical behaviour at room temperature. Other types of additives also have an effect on the thermal behaviour of PLA with nucleating agents being a simple and easy solution to dramatically improve the crystallisation rate of PLA. Furthermore, some reported studies have emphasised a joint-effect regarding the use of toughening agents and highly crystallised PLA, as such materials with high crystallisation degrees would benefit from an even higher toughening effect using the same toughening agent. This was mainly due to an increased phase separation of the two components of the blend thanks to the crystallisation of the PLA phase.

However, finely tuning the properties of PLA remains a challenge as some beneficial effects might be detrimental in some cases, for instance, the addition of a toughening agent inside a PLA matrix was reported to increase the gas permeability of the material. Studies remain to be made to assess the effect of the combination of a toughening agent and a nucleating agent on the barrier properties of PLA and assess whether the higher crystallinity ratio effect will be enough to counteract the addition of an immiscible phase.

Lately, the stereocomplex solution is gaining momentum due to the decreasing production price of PDLA. PLA stereocomplexes have been reported to have a higher crystallisation rate than PLA homopolymers along with better barrier properties. Their use remains a challenge since it involves higher processing temperatures and a very fine control on the temperature conditions to obtain optimal nucleating conditions. More research is currently underway to promote the use of such high-potential material. Overall, some impact resistant and heat resistant materials are already commercially available proving the efficiency of some solutions¹⁷⁷.

In our project, we will focus on two simple solutions to tune the properties of the PLLA homopolymer, the most widely available. The first strategy consists in using novel amide-

based nucleating agents to enhance the crystallinity ratio of PLA materials. Such nucleating agents would be derived from C18 fatty acids and a linear aliphatic diamine as such structure was reported in the literature to be highly efficient. Not only would this strategy enhance the heat deflection temperature of PLA, but it would also potentially enhance the barrier properties of such materials. In parallel, work will be conducted using a reported toughening agent that is poly(methyl ricinoleate). This fully bio-based polyester was highly efficient in modifying the mechanical behaviour of PLLA at low loadings and is therefore of high interest. Moreover, it has the advantage of bearing an alkene function, therefore opening the possibility for post-functionalisation which could enhance the toughening effect and open the way to new functionalities which could further be exploited (Fig. I. 37).

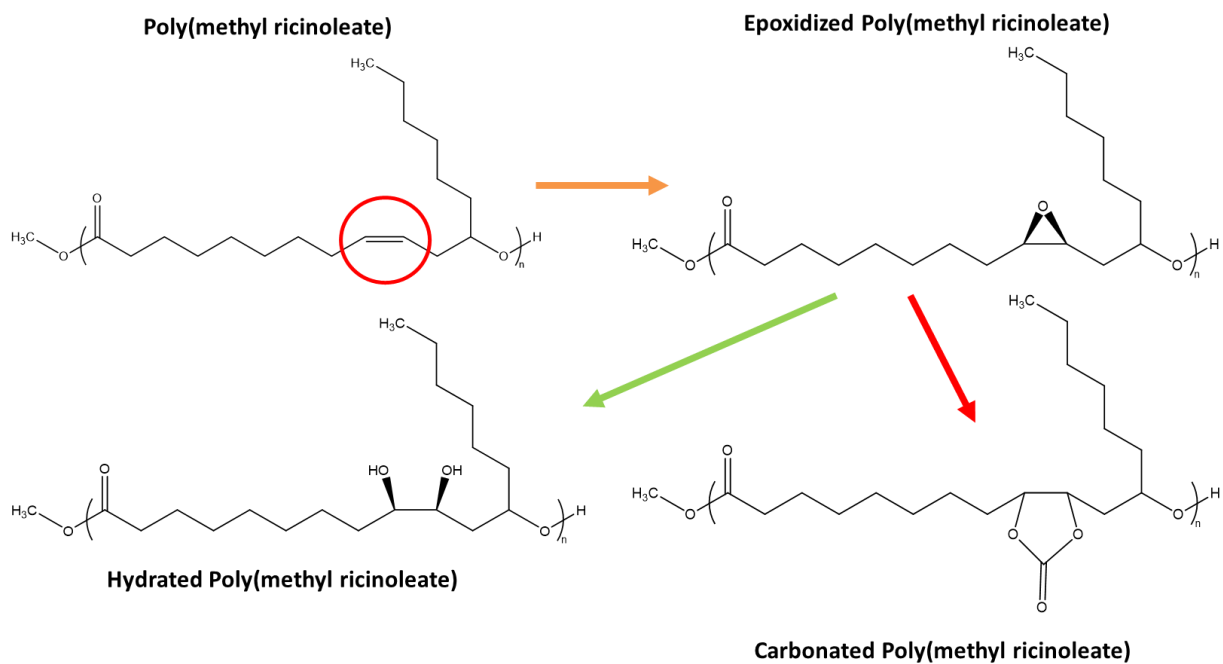


Fig. I. 37: Potential chemical modifications for poly(methyl ricinoleate)

5. References

1. Plastics - the Facts 2021 • Plastics Europe. *Plastics Europe* <https://plasticseurope.org/knowledge-hub/plastics-the-facts-2021/>.
2. European Bioplastics. <https://www.european-bioplastics.org/>.
3. Polylactic Acid (PLA) Market | 2022 - 2026 | MarketsandMarkets. <https://www.marketsandmarkets.com/Market-Reports/polylactic-acid-pla-market-29418964.html>.
4. Kricheldorf, H. R., Kreiser-Saunders, I., Jürgens, C. & Wolter, D. Polylactides - Synthesis, characterization and medical application. *Macromol. Symp.* **103**, 85–102 (1996).
5. Datta, R. & Henry, M. Lactic acid: recent advances in products, processes and technologies — a review. *J. Chem. Technol. Biotechnol.* **81**, 1119–1129 (2006).
6. Madhavan Nampoothiri, K., Nair, N. R. & John, R. P. An overview of the recent developments in polylactide (PLA) research. *Bioresour. Technol.* **101**, 8493–8501 (2010).
7. Castro-Aguirre, E., Iñiguez-Franco, F., Samsudin, H., Fang, X. & Auras, R. Poly(lactic acid)—Mass production, processing, industrial applications, and end of life. *Adv. Drug Deliv. Rev.* **107**, 333–366 (2016).
8. Facts and Statistics - IfBB - Institute for bioplastics and biocomposites. <https://www.ifbb-hannover.de/en/facts-and-statistics.html>.
9. NatureWorks | Where Ingeo Comes From. <https://www.natureworkslc.com/What-is-Ingeo/Where-Ingeo-Comes-From>.
10. Discovering a sustainable resource for bioplastics. <https://www.corbion.com/about-corbion/innovation/alternative-feedstock>.
11. Rajgarhia, V. *et al.* Genetically Modified Yeast Species, and Fermentation Processes Using Genetically Modified Yeast. (2016).
12. Druon, A. & Patinier, S. Method for the production of a microalgal biomass of optimised sensory quality. (2018).
13. Grasa, E. T., Ögmundarson, Ó., Gavala, H. N. & Sukumara, S. Commodity chemical production from third-generation biomass: a techno-economic assessment of lactic acid production. *Biofuels Bioprod. Biorefining* **15**, 257–281 (2021).
14. Alexandri, M., Schneider, R., Mehlmann, K. & Venus, J. Recent Advances in D-Lactic Acid Production from Renewable Resources: Case Studies on Agro-Industrial Waste Streams. *Food Technol. Biotechnol.* **57**, 293–304 (2019).
15. Klotz, S., Kuenz, A. & Prüße, U. Nutritional requirements and the impact of yeast extract on the D -lactic acid production by *Sporolactobacillus inulinus*. *Green Chem.* **19**, 4633–4641 (2017).
16. NatureWorks | NatureWorks Passes Final Authorization Milestone for New Fully Integrated Ingeo PLA Manufacturing Plant in Thailand. <https://www.natureworkslc.com/News-and-Events/Press-Releases/2021/2021-08-09-NatureWorks-Final-Authorization-Ingeo-PLA-Plant-Thailand>.
17. Thaïlande : Total Corbion PLA démarre son usine de bioplastiques d'une capacité de 75 000 tonnes par an. *TotalEnergies.com* <https://totalenergies.com/fr/medias/actualite/communiqués/thaïlande-total-corbion-pla-demarre-son-usine-de-bioplastiques-dune-capacite-de-75-000-tonnes-par>.
18. Hartmann, M. H. High Molecular Weight Polylactic Acid Polymers. in *Biopolymers from Renewable Resources* (ed. Kaplan, D. L.) 367–411 (Springer, 1998). doi:10.1007/978-3-662-03680-8_15.
19. Hyon, S.-H., Jamshidi, K. & Ikada, Y. Synthesis of polylactides with different molecular weights. *Biomaterials* **18**, 1503–1508 (1997).
20. Hiltunen, K., Seppälä, J. V. & Härkönen, M. Lactic acid based poly(ester-urethane)s: The effects of different polymerization conditions on the polymer structure and properties. *J. Appl. Polym. Sci.* **64**, 865–873 (1997).
21. Tuominen, J. & Seppälä, J. V. Synthesis and Characterization of Lactic Acid Based Poly(ester–amide). *Macromolecules* **33**, 3530–3535 (2000).
22. Ajioka, M., Enomoto, K., Suzuki, K. & Yamaguchi, A. The basic properties of poly(lactic acid) produced by the direct condensation polymerization of lactic acid. *J. Environ. Polym. Degrad.* **3**, 225–234 (1995).
23. Wojtczak, E., Kubisa, P. & Bednarek, M. Thermal stability of polylactide with different end-groups depending on the catalyst used for the polymerization. *Polym. Degrad. Stab.* **151**, 100–104 (2018).
24. Garlotta, D. A Literature Review of Poly(Lactic Acid). *J. Polym. Environ.* **9**, 63–84 (2001).
25. Naser, A. Z., Deiab, I. & Darras, B. M. Poly(lactic acid) (PLA) and polyhydroxyalkanoates (PHAs), green alternatives to petroleum-based plastics: a review. *RSC Adv.* **11**, 17151–17196 (2021).

26. Yoo, D. K., Kim, D. & Lee, D. S. Synthesis of lactide from oligomeric PLA: Effects of temperature, pressure, and catalyst. *Macromol. Res.* **14**, 510–516 (2006).
27. Cunha, B. L. C. *et al.* Lactide: Production Routes, Properties, and Applications. *Bioengineering* **9**, 164 (2022).
28. Groot, W., van Krieken, J., Sliemers, O. & de Vos, S. Production and Purification of Lactic Acid and Lactide. in *Poly(Lactic Acid)* 1–18 (John Wiley & Sons, Ltd, 2010). doi:10.1002/9780470649848.ch1.
29. Masutani, K. & Kimura, Y. Chapter 1 PLA Synthesis. From the Monomer to the Polymer. in *Poly(lactic acid) Science and Technology: Processing, Properties, Additives and Applications* 1–36 (The Royal Society of Chemistry, 2015). doi:10.1039/9781782624806-00001.
30. Thomas, C. M. Stereocontrolled ring-opening polymerization of cyclic esters: synthesis of new polyester microstructures. *Chem Soc Rev* **39**, 165–173 (2010).
31. Dittrich, V. W. & Schulz, R. C. Kinetik und Mechanismus der ringöffnenden Polymerisation von L(–)-Lactid. *Angew. Makromol. Chem.* **15**, 109–126 (1971).
32. Pretula, J., Slomkowski, S. & Penczek, S. Polylactides—Methods of synthesis and characterization. *Adv. Drug Deliv. Rev.* **107**, 3–16 (2016).
33. Stannous Octoate - ECHA. <https://echa.europa.eu/fr/brief-profile/-/briefprofile/100.005.554>.
34. Cartier, L., Okihara, T. & Lotz, B. Triangular Polymer Single Crystals: Stereocomplexes, Twins, and Frustrated Structures. *Macromolecules* **30**, 6313–6322 (1997).
35. Okihara, T. *et al.* Crystal structure of stereocomplex of poly(L-lactide) and poly(D-lactide). *J. Macromol. Sci. Part B* **30**, 119–140 (1991).
36. Osten, K. M., Aluthge, D. C. & Mehrhodavandi, P. Ligand Design in Enantioselective Ring-opening Polymerization of Lactide. in *Ligand Design in Metal Chemistry* 270–307 (John Wiley & Sons, Ltd, 2016). doi:10.1002/9781118839621.ch10.
37. Spassky, N., Wisniewski, M., Pluta, C. & Le Borgne, A. Highly stereoselective polymerization of rac-(D,L)-lactide with a chiral Schiff's base/aluminium alkoxide initiator. *Macromol. Chem. Phys.* **197**, 2627–2637 (1996).
38. Dove, A. P. *et al.* Synthetic, Structural, Mechanistic, and Computational Studies on Single-Site β -Diketiminato Tin(II) Initiators for the Polymerization of rac-Lactide. *J. Am. Chem. Soc.* **128**, 9834–9843 (2006).
39. H. Chisholm, M., J. Patmore, N. & Zhou, Z. Concerning the relative importance of enantiomeric site vs. chain end control in the stereoselective polymerization of lactides: reactions of (R, R-salen)- and (S, S-salen)-aluminium alkoxides LAIOCH 2 R complexes (R = CH₃ and S = -CHMeCl). *Chem. Commun.* **0**, 127–129 (2005).
40. Jamshidi, K., Hyon, S.-H. & Ikada, Y. Thermal characterization of polylactides. *Polymer* **29**, 2229–2234 (1988).
41. He, Y. *et al.* DSC analysis of isothermal melt-crystallization, glass transition and melting behavior of poly(l-lactide) with different molecular weights. *Eur. Polym. J.* **43**, 4431–4439 (2007).
42. Androsch, R., Di Lorenzo, M. L. & Schick, C. Effect of molar mass on enthalpy relaxation and crystal nucleation of poly(l-lactic acid). *Eur. Polym. J.* **96**, 361–369 (2017).
43. Avérous, L. Chapter 21 - Polylactic Acid: Synthesis, Properties and Applications. in *Monomers, Polymers and Composites from Renewable Resources* (eds. Belgacem, M. N. & Gandini, A.) 433–450 (Elsevier, 2008). doi:10.1016/B978-0-08-045316-3.00021-1.
44. Müller, A. J., Ávila, M., Saenz, G. & Salazar, J. CHAPTER 3 Crystallization of PLA-based Materials. in *Poly(lactic acid) Science and Technology: Processing, Properties, Additives and Applications* 66–98 (The Royal Society of Chemistry, 2015). doi:10.1039/9781782624806-00066.
45. Henton, D. E., Gruber, P., Lunt, J. & Randall, J. Polylactic acid technology. in *Natural Fibers, Biopolymers, and Biocomposites* 527–577 (2005).
46. Tsuji, H. & Ikada, Y. Properties and morphologies of poly(l-lactide): 1. Annealing condition effects on properties and morphologies of poly(l-lactide). *Polymer* **36**, 2709–2716 (1995).
47. Fischer, E. W., Sterzel, H. J. & Wegner, G. Investigation of the structure of solution grown crystals of lactide copolymers by means of chemical reactions. *Kolloid-Z. Z. Für Polym.* **251**, 980–990 (1973).
48. Harris, A. M. & Lee, E. C. Improving mechanical performance of injection molded PLA by controlling crystallinity. *J. Appl. Polym. Sci.* **107**, 2246–2255 (2008).
49. Miyata, T. & Masuko, T. Crystallization behaviour of poly(l-lactide). *Polymer* **39**, 5515–5521 (1998).
50. Androsch, R., Iqbal, H. M. N. & Schick, C. Non-isothermal crystal nucleation of poly(l-lactic acid). *Polymer* **81**, 151–158 (2015).

Chapter 1

51. Saeidlou, S., Huneault, M. A., Li, H. & Park, C. B. Poly(lactic acid) crystallization. *Prog. Polym. Sci.* **37**, 1657–1677 (2012).
52. Kalb, B. & Pennings, A. J. General crystallization behaviour of poly(l-lactic acid). *Polymer* **21**, 607–612 (1980).
53. Santis, P. D. & Kovacs, A. J. Molecular conformation of poly(S-lactic acid). *Biopolymers* **6**, 299–306 (1968).
54. Kobayashi, J. *et al.* Structural and optical properties of poly lactic acids. *J. Appl. Phys.* **77**, 2957–2973 (1995).
55. Hoogsteen, W., Postema, A. R., Pennings, A. J., Ten Brinke, G. & Zugenmaier, P. Crystal structure, conformation and morphology of solution-spun poly(L-lactide) fibers. *Macromolecules* **23**, 634–642 (1990).
56. Wasanasuk, K. *et al.* Crystal Structure Analysis of Poly(l-lactic Acid) α Form On the basis of the 2-Dimensional Wide-Angle Synchrotron X-ray and Neutron Diffraction Measurements. *Macromolecules* **44**, 6441–6452 (2011).
57. Wasanasuk, K. & Tashiro, K. Crystal structure and disorder in Poly(l-lactic acid) δ form (α' form) and the phase transition mechanism to the ordered α form. *Polymer* **52**, 6097–6109 (2011).
58. Kawai, T. *et al.* Crystallization and Melting Behavior of Poly (l-lactic Acid). *Macromolecules* **40**, 9463–9469 (2007).
59. Zhang, J., Tashiro, K., Tsuji, H. & Domb, A. J. Disorder-to-Order Phase Transition and Multiple Melting Behavior of Poly(L-lactide) Investigated by Simultaneous Measurements of WAXD and DSC. *Macromolecules* **41**, 1352–1357 (2008).
60. Puiggali, J. *et al.* The frustrated structure of poly(l-lactide). *Polymer* **41**, 8921–8930 (2000).
61. Lotz, B. A. Single Crystals of the Frustrated β -Phase and Genesis of the Disordered α' -Phase of Poly(l-lactic acid). *ACS Macro Lett.* **4**, 602–605 (2015).
62. Cartier, L. *et al.* Epitaxial crystallization and crystalline polymorphism of polylactides. *Polymer* **41**, 8909–8919 (2000).
63. Vasanthakumari, R. & Pennings, A. J. Crystallization kinetics of poly(l-lactic acid). *Polymer* **24**, 175–178 (1983).
64. Lorenzo, A. T., Arnal, M. L., Albuerno, J. & Müller, A. J. DSC isothermal polymer crystallization kinetics measurements and the use of the Avrami equation to fit the data: Guidelines to avoid common problems. *Polym. Test.* **26**, 222–231 (2007).
65. Castillo, R. V., Müller, A. J., Raquez, J.-M. & Dubois, P. Crystallization Kinetics and Morphology of Biodegradable Double Crystalline PLLA-b-PCL Diblock Copolymers. *Macromolecules* **43**, 4149–4160 (2010).
66. Speranza, V., De Meo, A. & Pantani, R. Thermal and hydrolytic degradation kinetics of PLA in the molten state. *Polym. Degrad. Stab.* **100**, 37–41 (2014).
67. Al-Itry, R., Lamnawar, K. & Maazouz, A. Improvement of thermal stability, rheological and mechanical properties of PLA, PBAT and their blends by reactive extrusion with functionalized epoxy. *Polym. Degrad. Stab.* **97**, 1898–1914 (2012).
68. Aoyagi, Y., Yamashita, K. & Doi, Y. Thermal degradation of poly[(R)-3-hydroxybutyrate], poly[ϵ -caprolactone], and poly[(S)-lactide]. *Polym. Degrad. Stab.* **7** (2002).
69. Kopinke, F.-D., Remmler, M., Mackenzie, K., Möder, M. & Wachsen, O. Thermal decomposition of biodegradable polyesters—II. Poly(lactic acid). *Polym. Degrad. Stab.* **53**, 329–342 (1996).
70. McNeill, I. C. & Leiper, H. A. Degradation studies of some polyesters and polycarbonates—1. Polylactide: General features of the degradation under programmed heating conditions. *Polym. Degrad. Stab.* **11**, 267–285 (1985).
71. McNeill, I. C. & Leiper, H. A. Degradation studies of some polyesters and polycarbonates—2. Polylactide: Degradation under isothermal conditions, thermal degradation mechanism and photolysis of the polymer. *Polym. Degrad. Stab.* **11**, 309–326 (1985).
72. Mysiukiewicz, O., Barczewski, M., Skórczewska, K. & Matykiewicz, D. Correlation between Processing Parameters and Degradation of Different Polylactide Grades during Twin-Screw Extrusion. *Polymers* **12**, 1333 (2020).
73. Shojaeiarani, J., Bajwa, D. S., Rehovsky, C., Bajwa, S. G. & Vahidi, G. Deterioration in the Physico-Mechanical and Thermal Properties of Biopolymers Due to Reprocessing. *Polymers* **11**, 58 (2019).
74. Lim, L.-T., Auras, R. & Rubino, M. Processing technologies for poly(lactic acid). *Prog. Polym. Sci.* **33**, 820–852 (2008).
75. Richard F. Grossman, Nwabunma, D. & Engelmann, S. Thermoformed Packaging Made of PLA. in *Advanced Thermoforming* 227–231 (John Wiley & Sons, Ltd, 2012). doi:10.1002/9781118207086.ch32.
76. Lim, L.-T., Cink, K. & Vanyo, T. Processing of Poly(Lactic Acid). in *Poly(Lactic Acid)* 189–215 (John Wiley & Sons, Ltd, 2010). doi:10.1002/9780470649848.ch14.

77. Södergård, A. & Stolt, M. Properties of lactic acid based polymers and their correlation with composition. *Prog. Polym. Sci.* **27**, 1123–1163 (2002).
78. Farah, S., Anderson, D. G. & Langer, R. Physical and mechanical properties of PLA, and their functions in widespread applications — A comprehensive review. *Adv. Drug Deliv. Rev.* **107**, 367–392 (2016).
79. Van de Velde, K. & Kiekens, P. Biopolymers: overview of several properties and consequences on their applications. *Polym. Test.* **21**, 433–442 (2002).
80. Paesano, A. *Handbook of Sustainable Polymers for Additive Manufacturing*. (CRC Press, 2022). doi:10.1201/9781003221210.
81. Ncube, L. K., Ude, A. U., Ogunmuyiwa, E. N., Zulkifli, R. & Beas, I. N. Environmental Impact of Food Packaging Materials: A Review of Contemporary Development from Conventional Plastics to Polylactic Acid Based Materials. *Materials* **13**, 4994 (2020).
82. Anderson, K. S., Schreck, K. M. & Hillmyer, M. A. Toughening Polylactide. *Polym. Rev.* **48**, 85–108 (2008).
83. Tabi, T., Sajo, I. E., Szabo, F., Luyt, A. S. & Kovacs, J. G. Crystalline structure of annealed polylactic acid and its relation to processing. *Express Polym. Lett.* **4**, 659–668 (2010).
84. Tábi, T., Hajba, S. & Kovács, J. G. Effect of crystalline forms (α' and α) of poly(lactic acid) on its mechanical, thermo-mechanical, heat deflection temperature and creep properties. *Eur. Polym. J.* **82**, 232–243 (2016).
85. Ghosal, K. & Freeman, B. D. Gas separation using polymer membranes: an overview. *Polym. Adv. Technol.* **5**, 673–697 (1994).
86. Dhoot, S. N., Freeman, B. D. & Stewart, M. E. Barrier Polymers. in *Encyclopedia of Polymer Science and Technology* (American Cancer Society, 2002). doi:10.1002/0471440264.pst025.
87. Wu, F., Misra, M. & Mohanty, A. K. Challenges and new opportunities on barrier performance of biodegradable polymers for sustainable packaging. *Prog. Polym. Sci.* **117**, 101395 (2021).
88. Sonchaeng, U. *et al.* Poly(lactic acid) mass transfer properties. *Prog. Polym. Sci.* **86**, 85–121 (2018).
89. Drieskens, M. *et al.* Structure versus properties relationship of poly(lactic acid). I. Effect of crystallinity on barrier properties. *J. Polym. Sci. Part B Polym. Phys.* **47**, 2247–2258 (2009).
90. Dong, T. *et al.* Biodegradable high oxygen barrier membrane for chilled meat packaging. *J. Appl. Polym. Sci.* **132**, (2015).
91. Permeability Properties of Plastics and Elastomers (Second Edition). in *Permeability Properties of Plastics and Elastomers (Second Edition)* (ed. Massey, L. K.) 601 (William Andrew Publishing, 2003). doi:10.1016/B978-1-884207-97-6.50102-9.
92. Auras, R., Harte, B. & Selke, S. An Overview of Poly(lactides) as Packaging Materials. *Macromol. Biosci.* **4**, 835–864 (2004).
93. Cocca, M., Lorenzo, M. L. D., Malinconico, M. & Frezza, V. Influence of crystal polymorphism on mechanical and barrier properties of poly(l-lactic acid). *Eur. Polym. J.* **47**, 1073–1080 (2011).
94. Guinault, A., Sollogoub, C., Domenek, S., Grandmontagne, A. & Ducruet, V. Influence of crystallinity on gas barrier and mechanical properties of PLA food packaging films. *Int. J. Mater. Form.* **3**, 603–606 (2010).
95. Nguyen, T. L., Bédoui, F., Mazeran, P.-E. & Guigon, M. Mechanical investigation of confined amorphous phase in semicrystalline polymers: Case of PET and PLA. *Polym. Eng. Sci.* **55**, 397–405 (2015).
96. del Río, J., Etxeberria, A., López-Rodríguez, N., Lizundia, E. & Sarasua, J. R. A PALS Contribution to the Supramolecular Structure of Poly(l-lactide). *Macromolecules* **43**, 4698–4707 (2010).
97. Fernandes Nassar, S. *et al.* Multi-scale analysis of the impact of polylactide morphology on gas barrier properties. *Polymer* **108**, 163–172 (2017).
98. da Silva, D. *et al.* Biocompatibility, biodegradation and excretion of polylactic acid (PLA) in medical implants and theranostic systems. *Chem. Eng. J.* **340**, 9–14 (2018).
99. Lucas, N. *et al.* Polymer biodegradation: Mechanisms and estimation techniques — A review. *Chemosphere* **73**, 429–442 (2008).
100. Jung, J. H., Ree, M. & Kim, H. Acid- and base-catalyzed hydrolyses of aliphatic polycarbonates and polyesters. *Catal. Today* **115**, 283–287 (2006).
101. Pierre, T. St. & Chiellini, E. Review : Biodegradability of Synthetic Polymers Used for Medical and Pharmaceutical Applications: Part 1— Principles of Hydrolysis Mechanisms. *J. Bioact. Compat. Polym.* **1**, 467–497 (1986).
102. de Jong, S. J. *et al.* New insights into the hydrolytic degradation of poly(lactic acid): participation of the alcohol terminus. *Polymer* **42**, 2795–2802 (2001).
103. Larrañaga, A. & Lizundia, E. A review on the thermomechanical properties and biodegradation behaviour of polyesters. *Eur. Polym. J.* 109296 (2019) doi:10.1016/j.eurpolymj.2019.109296.
104. Saha, S. K. & Tsuji, H. Effects of molecular weight and small amounts of d-lactide units on hydrolytic degradation of poly(l-lactic acid)s. *Polym. Degrad. Stab.* **91**, 1665–1673 (2006).

Chapter 1

105. Burkersroda, F. von, Schedl, L. & Göpferich, A. Why degradable polymers undergo surface erosion or bulk erosion. *Biomaterials* **23**, 4221–4231 (2002).
106. Tsuji, H. & Miyauchi, S. Enzymatic Hydrolysis of Poly(lactide)s: Effects of Molecular Weight, L-Lactide Content, and Enantiomeric and Diastereoisomeric Polymer Blending. *Biomacromolecules* **2**, 597–604 (2001).
107. Tsuji, H. & Miyauchi, S. Poly(l-lactide): VI Effects of crystallinity on enzymatic hydrolysis of poly(l-lactide) without free amorphous region. *Polym. Degrad. Stab.* **71**, 415–424 (2001).
108. Tsuji, H. & Miyauchi, S. Poly(l-lactide): 7. Enzymatic hydrolysis of free and restricted amorphous regions in poly(l-lactide) films with different crystallinities and a fixed crystalline thickness. *Polymer* **42**, 4463–4467 (2001).
109. Itävaara, M., Karjomaa, S. & Selin, J.-F. Biodegradation of polylactide in aerobic and anaerobic thermophilic conditions. *Chemosphere* **46**, 879–885 (2002).
110. Watanabe, M., Kawai, F., Tsuboi, S., Nakatsu, S. & Ohara, H. Study on Enzymatic Hydrolysis of Polylactic Acid by Endogenous Depolymerization Model. *Macromol. Theory Simul.* **16**, 619–626 (2007).
111. Qi, X., Ren, Y. & Wang, X. New advances in the biodegradation of Poly(lactic) acid. *Int. Biodeterior. Biodegrad.* **117**, 215–223 (2017).
112. Rocca-Smith, J. R. *et al.* Beyond Biodegradability of Poly(lactic acid): Physical and Chemical Stability in Humid Environments. *ACS Sustain. Chem. Eng.* **5**, 2751–2762 (2017).
113. NF EN 13432. *Afnor EDITIONS* <https://www.boutique.afnor.org/fr-fr/norme/nf-en-13432/emballage-exigences-relatives-aux-emballages-valorisables-par-compostage-et/fa049121/454>.
114. Haider, T. P., Völker, C., Kramm, J., Landfester, K. & Wurm, F. R. Plastics of the Future? The Impact of Biodegradable Polymers on the Environment and on Society. *Angew. Chem. Int. Ed.* **58**, 50–62 (2019).
115. Chamas, A. *et al.* Degradation Rates of Plastics in the Environment. *ACS Sustain. Chem. Eng.* (2020) doi:10.1021/acssuschemeng.9b06635.
116. Ghosh, K. & Jones, B. H. Roadmap to Biodegradable Plastics—Current State and Research Needs. *ACS Sustain. Chem. Eng.* **9**, 6170–6187 (2021).
117. Karamanlioglu, M., Preziosi, R. & Robson, G. D. Abiotic and biotic environmental degradation of the bioplastic polymer poly(lactic acid): A review. *Polym. Degrad. Stab.* **137**, 122–130 (2017).
118. Doi, Y., Kanesawa, Y., Tanahashi, N. & Kumagai, Y. Biodegradation of microbial polyesters in the marine environment. *Polym. Degrad. Stab.* **36**, 173–177 (1992).
119. Mergaert, J., Webb, A., Anderson, C., Wouters, A. & Swings, J. Microbial degradation of poly(3-hydroxybutyrate) and poly(3-hydroxybutyrate-co-3-hydroxyvalerate) in soils. *Appl. Environ. Microbiol.* **59**, 3233–3238 (1993).
120. Piemonte, V., Sabatini, S. & Gironi, F. Chemical Recycling of PLA: A Great Opportunity Towards the Sustainable Development? *J. Polym. Environ.* **21**, 640–647 (2013).
121. McKeown, P. & Jones, M. D. The Chemical Recycling of PLA: A Review. *Sustain. Chem.* **1**, 1–22 (2020).
122. Dole, P. *Les 7 fonctions de l'emballage*. (Lavoisier-Tec & doc, 2018).
123. Siracusa, V., Rocculi, P., Romani, S. & Rosa, M. D. Biodegradable polymers for food packaging: a review. *Trends Food Sci. Technol.* **19**, 634–643 (2008).
124. Auras, R. A., Singh, S. P. & Singh, J. J. Evaluation of oriented poly(lactide) polymers vs. existing PET and oriented PS for fresh food service containers. *Packag. Technol. Sci.* **18**, 207–216 (2005).
125. Bimbenet, J. J. & Loncin, M. *Bases of food process engineering*. (1995).
126. TotalEnergies Corbion. <https://www.totalenergies-corbion.com/luminy-pla-portfolio/>.
127. Siracusa, V. Food Packaging Permeability Behaviour: A Report. *Int. J. Polym. Sci.* **2012**, e302029 (2012).
128. Germain, Y. Polymer films with controlled permeability for food packaging. *Ind. Aliment. Agric. Fr.* (1997).
129. *Décret n° 2021-517 du 29 avril 2021 relatif aux objectifs de réduction, de réutilisation et de réemploi, et de recyclage des emballages en plastique à usage unique pour la période 2021-2025*. 2021-517 (2021).
130. Emballages en PLA : un 1er test pour comprendre les conditions de leur compostage. *CITEO* <https://livepreview.citeo.com/le-mag/emballages-en-pla-un-1er-test-pour-comprendre-les-conditions-de-leur-compostage>.
131. Zhao, X. *et al.* Super tough poly(lactic acid) blends: a comprehensive review. *RSC Adv.* **10**, 13316–13368 (2020).
132. Mascia, L. & Xanthos, M. An overview of additives and modifiers for polymer blends: Facts, deductions, and uncertainties. *Adv. Polym. Technol.* **11**, 237–248 (1992).
133. Godwin, A. D. PLASTICIZERS. in *Applied Polymer Science: 21st Century* (eds. Craver, C. D. & Carraher, C. E.) 157–175 (Pergamon, 2000). doi:10.1016/B978-008043417-9/50011-8.

134. Bocqué, M., Voirin, C., Lapinte, V., Caillol, S. & Robin, J.-J. Petro-based and bio-based plasticizers: Chemical structures to plasticizing properties. *J. Polym. Sci. Part Polym. Chem.* **54**, 11–33 (2016).
135. Tábi, T., Ageyeva, T. & Kovács, J. G. Improving the ductility and heat deflection temperature of injection molded Poly(lactic acid) products: A comprehensive review. *Polym. Test.* **101**, 107282 (2021).
136. Chaos, A. *et al.* Plasticization of poly(lactide) with poly(ethylene glycol): Low weight plasticizer vs triblock copolymers. Effect on free volume and barrier properties. *J. Appl. Polym. Sci.* **137**, 48868 (2020).
137. Martin, O. & Avérous, L. Poly(lactic acid): plasticization and properties of biodegradable multiphase systems. *Polymer* **42**, 6209–6219 (2001).
138. Singh, S., MasPOCH, M. L. & Oksman, K. Crystallization of triethyl-citrate-plasticized poly(lactic acid) induced by chitin nanocrystals. *J. Appl. Polym. Sci.* **0**, 47936 (2019).
139. Jacobsen, S. & Fritz, H. G. Plasticizing polylactide—the effect of different plasticizers on the mechanical properties. *Polym. Eng. Sci.* **39**, 1303–1310 (1999).
140. Ljungberg, N. & Wesslén, B. Preparation and Properties of Plasticized Poly(lactic acid) Films. *Biomacromolecules* **6**, 1789–1796 (2005).
141. Nijenhuis, A. J., Colstee, E., Grijpma, D. W. & Pennings, A. J. High molecular weight poly(l-lactide) and poly(ethylene oxide) blends: thermal characterization and physical properties. *Polymer* **37**, 5849–5857 (1996).
142. Chieng, B. W., Ibrahim, N. A., Then, Y. Y. & Loo, Y. Y. Epoxidized Vegetable Oils Plasticized Poly(lactic acid) Biocomposites: Mechanical, Thermal and Morphology Properties. *Molecules* **19**, 16024–16038 (2014).
143. Chieng, B. W., Chieng, B. W., Ibrahim, N. A., Ibrahim, N. A. & Loo, Y. Y. Bioplasticizer Epoxidized Vegetable Oils–Based Poly(Lactic Acid) Blends and Nanocomposites. in *Handbook of Composites from Renewable Materials* 205–231 (John Wiley & Sons, Ltd, 2017). doi:10.1002/9781119441632.ch112.
144. Santos, E. F., Oliveira, R. V. B., Reiznautt, Q. B., Samios, D. & Nachtigall, S. M. B. Sunflower-oil biodiesel-oligoesters/polylactide blends: Plasticizing effect and ageing. *Polym. Test.* **39**, 23–29 (2014).
145. Ferri, J. M. *et al.* Plasticizing effect of biobased epoxidized fatty acid esters on mechanical and thermal properties of poly(lactic acid). *J. Mater. Sci.* **51**, 5356–5366 (2016).
146. Wang, J., Zhang, X., Jiang, L. & Qiao, J. Advances in toughened polymer materials by structured rubber particles. *Prog. Polym. Sci.* 101160 (2019) doi:https://doi.org/10.1016/j.progpolymsci.2019.101160.
147. Hiljanen-Vainio, M., Kylmä, J., Hiltunen, K. & Seppälä, J. V. Impact modification of lactic acid based poly(ester-urethanes) by blending. *J. Appl. Polym. Sci.* **63**, 1335–1343 (1997).
148. Ruckenstein, E. & Yuan, Y. Molten Ring-Open Copolymerization of L-Lactide and Cyclic Trimethylene Carbonate. in *Solution and Surface Polymerization* (CRC Press, 2019).
149. Slivniak, R. & Domb, A. J. Lactic Acid and Ricinoleic Acid Based Copolyesters. *Macromolecules* **38**, 5545–5553 (2005).
150. Rasal, R. M., Janorkar, A. V. & Hirt, D. E. Poly(lactic acid) modifications. *Prog. Polym. Sci.* **35**, 338–356 (2010).
151. Frick, E. M., Zalusky, A. S. & Hillmyer, M. A. Characterization of Polylactide-b-polyisoprene-b-polylactide Thermoplastic Elastomers. *Biomacromolecules* **4**, 216–223 (2003).
152. Pitet, L. M. & Hillmyer, M. A. Combining Ring-Opening Metathesis Polymerization and Cyclic Ester Ring-Opening Polymerization To Form ABA Triblock Copolymers from 1,5-Cyclooctadiene and d,l-Lactide. *Macromolecules* **42**, 3674–3680 (2009).
153. Theryo, G., Jing, F., Pitet, L. M. & Hillmyer, M. A. Tough Polylactide Graft Copolymers. *Macromolecules* **43**, 7394–7397 (2010).
154. Delgado, P. & Hillmyer, M. Combining block copolymers and hydrogen bonding for poly(lactide) toughening. *RSC Adv.* **4**, 13266–13273 (2014).
155. Diaz, C. & Mehrkhodavandi, P. Strategies for the synthesis of block copolymers with biodegradable polyester segments. *Polym. Chem.* **12**, 783–806 (2021).
156. Becker, J. M., Pounder, R. J. & Dove, A. P. Synthesis of Poly(lactide)s with Modified Thermal and Mechanical Properties. *Macromol. Rapid Commun.* **31**, 1923–1937 (2010).
157. Grijpma, D. W. & Pennings, A. J. (Co)polymers of L-lactide, 1. Synthesis, thermal properties and hydrolytic degradation. *Macromol. Chem. Phys.* **195**, 1633–1647 (1994).
158. Zhang, Z., Grijpma, D. W. & Feijen, J. Triblock Copolymers Based on 1,3-Trimethylene Carbonate and Lactide as Biodegradable Thermoplastic Elastomers. *Macromol. Chem. Phys.* **205**, 867–875 (2004).
159. Guerin, W. *et al.* Macromolecular engineering via ring-opening polymerization (1): L-lactide/trimethylene carbonate block copolymers as thermoplastic elastomers. *Polym. Chem.* **4**, 1095–1106 (2013).
160. Jeon, O., Lee, S.-H., Kim, S. H., Lee, Y. M. & Kim, Y. H. Synthesis and Characterization of Poly(l-lactide)-Poly(ϵ -caprolactone) Multiblock Copolymers. *Macromolecules* **36**, 5585–5592 (2003).

Chapter 1

161. Qian, H., Bei, J. & Wang, S. Synthesis, characterization and degradation of ABA block copolymer of l-lactide and ε-caprolactone. *Polym. Degrad. Stab.* **7** (2000).
162. Mulchandani, N. *et al.* Toughened PLA-b-PCL-b-PLA triblock copolymer based biomaterials: effect of self-assembled nanostructure and stereocomplexation on the mechanical properties. *Polym. Chem.* **12**, 3806–3824 (2021).
163. Haynes, D., Abayasinghe, N. K., Harrison, G. M., Burg, K. J. & Smith, D. W. In Situ Copolyesters Containing Poly(L-lactide) and Poly(hydroxyalkanoate) Units. *Biomacromolecules* **8**, 1131–1137 (2007).
164. Hiki, S., Miyamoto, M. & Kimura, Y. Synthesis and characterization of hydroxy-terminated [RS]-poly(3-hydroxybutyrate) and its utilization to block copolymerization with l-lactide to obtain a biodegradable thermoplastic elastomer. *Polymer* **41**, 7369–7379 (2000).
165. Aluthge, D. C. *et al.* PLA-PHB-PLA Triblock Copolymers: Synthesis by Sequential Addition and Investigation of Mechanical and Rheological Properties. *Macromolecules* **46**, 3965–3974 (2013).
166. Wang, S., Cui, W. & Bei, J. Bulk and surface modifications of polylactide. *Anal. Bioanal. Chem.* **381**, 547–556 (2005).
167. Lee, S.-H., Kim, S. H., Han, Y.-K. & Kim, Y. H. Synthesis and characterization of poly(ethylene oxide)/polylactide/poly(ethylene oxide) triblock copolymer. *J. Polym. Sci. Part Polym. Chem.* **40**, 2545–2555 (2002).
168. Luo, W., Li, S., Bei, J. & Wang, S. Synthesis and characterization of poly(L-lactide)-poly(ethylene glycol) multiblock copolymers. *J. Appl. Polym. Sci.* **84**, 1729–1736 (2002).
169. Rathi, S. *et al.* Toughening semicrystalline poly(lactic acid) by morphology alteration. *Polymer* **52**, 4184–4188 (2011).
170. Rathi, S. R. *et al.* Effect of midblock on the morphology and properties of blends of ABA triblock copolymers of PDLA-mid-block-PDLA with PLLA. *Polymer* **53**, 3008–3016 (2012).
171. Robertson, M. L., Paxton, J. M. & Hillmyer, M. A. Tough Blends of Polylactide and Castor Oil. *ACS Appl. Mater. Interfaces* **3**, 3402–3410 (2011).
172. Lebarbé, T., Ibarboure, E., Gadenne, B., Alfos, C. & Cramail, H. Fully bio-based poly(l-lactide)-b-poly(ricinoleic acid)-b-poly(l-lactide) triblock copolyesters: investigation of solid-state morphology and thermo-mechanical properties. *Polym. Chem.* **4**, 3357 (2013).
173. Cramail, H., Lebarbe, T., Gadenne, B. & Alfos, C. Novel Biobased Pre-Polymers and Uses Thereof for Preparing Polymers Which Are of Use as Additives in a Poly(lactic Acid) Matrix. (2014).
174. Krishnan, S., Pandey, P., Mohanty, S. & Nayak, S. K. Toughening of Polylactic Acid: An Overview of Research Progress. *Polym.-Plast. Technol. Eng.* **55**, 1623–1652 (2016).
175. Wang, M., Wu, Y., Li, Y.-D. & Zeng, J.-B. Progress in Toughening Poly(Lactic Acid) with Renewable Polymers. *Polym. Rev.* **57**, 557–593 (2017).
176. Hamad, K., Kaseem, M., Ayyoob, M., Joo, J. & Deri, F. Polylactic acid blends: The future of green, light and tough. *Prog. Polym. Sci.* **85**, 83–127 (2018).
177. Nagarajan, V., Mohanty, A. K. & Misra, M. Perspective on Polylactic Acid (PLA) based Sustainable Materials for Durable Applications: Focus on Toughness and Heat Resistance. *ACS Sustain. Chem. Eng.* **4**, 2899–2916 (2016).
178. Eom, Y., Choi, B. & Park, S. A Study on Mechanical and Thermal Properties of PLA/PEO Blends. *J. Polym. Environ.* **27**, 256–262 (2019).
179. Kim, K.-S. *et al.* Crystallization behavior and mechanical properties of poly(ethylene oxide)/poly(L-lactide)/poly(vinyl acetate) blends. *J. Appl. Polym. Sci.* **82**, 3618–3626 (2001).
180. Li, F.-J., Liang, J.-Z., Zhang, S.-D. & Zhu, B. Tensile Properties of Polylactide/Poly(ethylene glycol) Blends. *J. Polym. Environ.* **23**, 407–415 (2015).
181. Anderson, K. S., Lim, S. H. & Hillmyer, M. A. Toughening of polylactide by melt blending with linear low-density polyethylene. *J. Appl. Polym. Sci.* **89**, 3757–3768 (2003).
182. Wang, Y. & Hillmyer, M. A. Polyethylene-poly(L-lactide) diblock copolymers: Synthesis and compatibilization of poly(L-lactide)/polyethylene blends. *J. Polym. Sci. Part Polym. Chem.* **39**, 2755–2766 (2001).
183. Anderson, K. S. & Hillmyer, M. A. The influence of block copolymer microstructure on the toughness of compatibilized polylactide/polyethylene blends. *Polymer* **45**, 8809–8823 (2004).
184. Alias, N. F. & Ismail, H. An overview of toughening polylactic acid by an elastomer. *Polym.-Plast. Technol. Mater.* **58**, 1399–1422 (2019).
185. Nematollahi, M., Jalali-Arani, A. & Modarress, H. High-performance bio-based poly(lactic acid)/natural rubber/epoxidized natural rubber blends: effect of epoxidized natural rubber on microstructure, toughness and static and dynamic mechanical properties. *Polym. Int.* **68**, 439–446 (2019).

186. Klinkajorn, J. & Tanrattanakul, V. Compatibilization of poly(lactic acid)/epoxidized natural rubber blend with maleic anhydride. *J. Appl. Polym. Sci.* **137**, 48297 (2020).
187. Yuan, D., Chen, K., Xu, C., Chen, Z. & Chen, Y. Crosslinked bicontinuous biobased PLA/NR blends via dynamic vulcanization using different curing systems. *Carbohydr. Polym.* **113**, 438–445 (2014).
188. Tissanan, W., Chanthateyanonth, R., Yamaguchi, M. & Phinyocheep, P. Improvement of mechanical and impact performance of poly(lactic acid) by renewable modified natural rubber. *J. Clean. Prod.* **276**, 123800 (2020).
189. Ma, P. *et al.* Toughening of poly(lactic acid) by ethylene-co-vinyl acetate copolymer with different vinyl acetate contents. *Eur. Polym. J.* **48**, 146–154 (2012).
190. Tábi, T. The application of the synergistic effect between the crystal structure of poly(lactic acid) (PLA) and the presence of ethylene vinyl acetate copolymer (EVA) to produce highly ductile PLA/EVA blends. *J. Therm. Anal. Calorim.* **138**, 1287–1297 (2019).
191. Yang, J., Nie, S. & Zhu, J. A comparative study on different rubbery modifiers: Effect on morphologies, mechanical, and thermal properties of PLA blends. *J. Appl. Polym. Sci.* **133**, (2016).
192. Wang, Y., Wei, Z. & Li, Y. Highly toughened polylactide/epoxidized poly(styrene-*b*-butadiene-*b*-styrene) blends with excellent tensile performance. *Eur. Polym. J.* **85**, 92–104 (2016).
193. Li, Y. & Shimizu, H. Improvement in toughness of poly(l-lactide) (PLLA) through reactive blending with acrylonitrile–butadiene–styrene copolymer (ABS): Morphology and properties. *Eur. Polym. J.* **45**, 738–746 (2009).
194. Canetti, M., Cacciamani, A. & Bertini, F. Miscible blends of polylactide and poly(methyl methacrylate): Morphology, structure, and thermal behavior. *J. Polym. Sci. Part B Polym. Phys.* **52**, 1168–1177 (2014).
195. Li, W. *et al.* The Effect of Core–Shell Ratio of Acrylic Impact Modifier on Toughening PLA. *Adv. Polym. Technol.* **36**, 491–501 (2017).
196. Li, W. *et al.* Toughening of polylactide with epoxy-functionalized methyl methacrylate–butyl acrylate copolymer. *Polym. Bull.* **71**, 2881–2902 (2014).
197. Zhang, H. *et al.* Toughening of polylactide by melt blending with methyl methacrylate–butadiene–styrene copolymer. *J. Appl. Polym. Sci.* **125**, E550–E561 (2012).
198. López-Rodríguez, N., López-Arraiza, A., Meaurio, E. & Sarasua, J. r. Crystallization, morphology, and mechanical behavior of polylactide/poly(ϵ -caprolactone) blends. *Polym. Eng. Sci.* **46**, 1299–1308 (2006).
199. Imre, B. & Pukánszky, B. Compatibilization in bio-based and biodegradable polymer blends. *Eur. Polym. J.* **49**, 1215–1233 (2013).
200. Fortelny, I., Ujcic, A., Fambri, L. & Slouf, M. Phase Structure, Compatibility, and Toughness of PLA/PCL Blends: A Review. *Front. Mater.* **6**, (2019).
201. Dell’Erba, R., Groeninckx, G., Maglio, G., Malinconico, M. & Migliozi, A. Immiscible polymer blends of semicrystalline biocompatible components: thermal properties and phase morphology analysis of PLLA/PCL blends. *Polymer* **42**, 7831–7840 (2001).
202. Xiang, S. *et al.* Toughening modification of PLLA with PCL in the presence of PCL-*b*-PLLA diblock copolymers as compatibilizer. *Polym. Adv. Technol.* **30**, 963–972 (2019).
203. Vilay, V., Mariatti, M., Ahmad, Z., Pasomsouk, K. & Todo, M. Improvement of microstructures and properties of biodegradable PLLA and PCL blends compatibilized with a triblock copolymer. *Mater. Sci. Eng. A* **527**, 6930–6937 (2010).
204. Wachirahuttapong, S., Thongpin, C. & Sombatsompop, N. Effect of PCL and Compatibility Contents on the Morphology, Crystallization and Mechanical Properties of PLA/PCL Blends. *Energy Procedia* **89**, 198–206 (2016).
205. Finotti, P. F. M., Costa, L. C. & Chinelatto, M. A. Effect of the Chemical Structure of Compatibilizers on the Thermal, Mechanical and Morphological Properties of Immiscible PLA/PCL Blends. *Macromol. Symp.* **368**, 24–29 (2016).
206. Wang, L., Ma, W., Gross, R. A. & McCarthy, S. P. Reactive compatibilization of biodegradable blends of poly(lactic acid) and poly(ϵ -caprolactone). *Polym. Degrad. Stab.* **59**, 161–168 (1998).
207. Semba, T., Kitagawa, K., Ishiaku, U. S., Kotaki, M. & Hamada, H. Effect of compounding procedure on mechanical properties and dispersed phase morphology of poly(lactic acid)/polycaprolactone blends containing peroxide. *J. Appl. Polym. Sci.* **103**, 1066–1074 (2007).
208. Semba, T., Kitagawa, K., Ishiaku, U. S. & Hamada, H. The effect of crosslinking on the mechanical properties of polylactic acid/polycaprolactone blends. *J. Appl. Polym. Sci.* **101**, 1816–1825 (2006).
209. Takayama, T., Todo, M. & Arakawa, K. Characterization of Impact Fracture Behavior of Biodegradable PLA/PCL Polymer Blend. *Key Eng. Mater.* **326–328**, 1569–1572 (2006).

Chapter 1

210. Takayama, T., Todo, M., Tsuji, H. & Arakawa, K. Effect of LTI content on impact fracture property of PLA/PCL/LTI polymer blends. *J. Mater. Sci.* **41**, 6501–6504 (2006).
211. Harada, M., Iida, K., Okamoto, K., Hayashi, H. & Hirano, K. Reactive compatibilization of biodegradable poly(lactic acid)/poly(ϵ -caprolactone) blends with reactive processing agents. *Polym. Eng. Sci.* **48**, 1359–1368 (2008).
212. Bai, H. *et al.* Tailoring Impact Toughness of Poly(l-lactide)/Poly(ϵ -caprolactone) (PLLA/PCL) Blends by Controlling Crystallization of PLLA Matrix. *ACS Appl. Mater. Interfaces* **4**, 897–905 (2012).
213. Takayama, T., Todo, M. & Tsuji, H. Effect of annealing on the mechanical properties of PLA/PCL and PLA/PCL/LTI polymer blends. *J. Mech. Behav. Biomed. Mater.* **4**, 255–260 (2011).
214. Chee, W. K., Ibrahim, N. A., Zainuddin, N., Abd Rahman, M. F. & Chieng, B. W. Impact Toughness and Ductility Enhancement of Biodegradable Poly(lactic acid)/Poly(ϵ -caprolactone) Blends via Addition of Glycidyl Methacrylate. *Adv. Mater. Sci. Eng.* **2013**, e976373 (2013).
215. Gardella, L., Calabrese, M. & Monticelli, O. PLA maleation: an easy and effective method to modify the properties of PLA/PCL immiscible blends. *Colloid Polym. Sci.* **292**, 2391–2398 (2014).
216. Jiang, L., Wolcott, M. P. & Zhang, J. Study of Biodegradable Poly(lactide)/Poly(butylene adipate-co-terephthalate) Blends. *Biomacromolecules* **7**, 199–207 (2006).
217. Ding, Y., Lu, B., Wang, P., Wang, G. & Ji, J. PLA-PBAT-PLA tri-block copolymers: Effective compatibilizers for promotion of the mechanical and rheological properties of PLA/PBAT blends. *Polym. Degrad. Stab.* **147**, 41–48 (2018).
218. Kumar, M., Mohanty, S., Nayak, S. K. & Rahail Parvaiz, M. Effect of glycidyl methacrylate (GMA) on the thermal, mechanical and morphological property of biodegradable PLA/PBAT blend and its nanocomposites. *Bioresour. Technol.* **101**, 8406–8415 (2010).
219. Zhang, N., Wang, Q., Ren, J. & Wang, L. Preparation and properties of biodegradable poly(lactic acid)/poly(butylene adipate-co-terephthalate) blend with glycidyl methacrylate as reactive processing agent. *J. Mater. Sci.* **44**, 250–256 (2009).
220. Al-Itry, R., Lamnawar, K. & Maazouz, A. Rheological, morphological, and interfacial properties of compatibilized PLA/PBAT blends. *Rheol. Acta* **53**, 501–517 (2014).
221. Coltelli, M.-B., Bronco, S. & Chinea, C. The effect of free radical reactions on structure and properties of poly(lactic acid) (PLA) based blends. *Polym. Degrad. Stab.* **95**, 332–341 (2010).
222. Ma, P. *et al.* In-situ compatibilization of poly(lactic acid) and poly(butylene adipate-co-terephthalate) blends by using dicumyl peroxide as a free-radical initiator. *Polym. Degrad. Stab.* **102**, 145–151 (2014).
223. Lin, S., Guo, W., Chen, C., Ma, J. & Wang, B. Mechanical properties and morphology of biodegradable poly(lactic acid)/poly(butylene adipate-co-terephthalate) blends compatibilized by transesterification. *Mater. Des. 1980-2015* **36**, 604–608 (2012).
224. Mohammadi, M., Heuzey, M.-C., Carreau, P. J. & Taguet, A. Interfacial localization of CNCs in PLA/PBAT blends and its effect on rheological, thermal, and mechanical properties. *Polymer* **233**, 124229 (2021).
225. Siegenthaler, K. O., Künkel, A., Skupin, G. & Yamamoto, M. Ecoflex® and Ecovio®: Biodegradable, Performance-Enabling Plastics. in *Synthetic Biodegradable Polymers* (eds. Rieger, B. *et al.*) 91–136 (Springer, 2012). doi:10.1007/12_2010_106.
226. Aliotta, L., Seggiani, M., Lazzeri, A., Gigante, V. & Cinelli, P. A Brief Review of Poly (Butylene Succinate) (PBS) and Its Main Copolymers: Synthesis, Blends, Composites, Biodegradability, and Applications. *Polymers* **14**, 844 (2022).
227. Park, J. W. & Im, S. S. Phase behavior and morphology in blends of poly(L-lactic acid) and poly(butylene succinate). *J. Appl. Polym. Sci.* **86**, 647–655 (2002).
228. Park, S. B., Hwang, S. Y., Moon, C. W., Im, S. S. & Yoo, E. S. Plasticizer effect of novel PBS ionomer in PLA/PBS ionomer blends. *Macromol. Res.* **18**, 463–471 (2010).
229. Wang, R., Wang, S., Zhang, Y., Wan, C. & Ma, P. Toughening modification of PLLA/PBS blends via in situ compatibilization. *Polym. Eng. Sci.* **49**, 26–33 (2009).
230. Ji, D. *et al.* Morphology, rheology, crystallization behavior, and mechanical properties of poly(lactic acid)/poly(butylene succinate)/dicumyl peroxide reactive blends. *J. Appl. Polym. Sci.* **131**, (2014).
231. Bhatia, A., Gupta, R. K., Bhattacharya, S. N. & Choi, H. J. Compatibility of biodegradable poly (lactic acid) (PLA) and poly (butylene succinate) (PBS) blends for packaging application. **19**, 7 (2007).
232. Hassan, E., Wei, Y., Jiao, H. & Muho, Y. Dynamic Mechanical Properties and Thermal Stability of Poly(lactic acid) and Poly(butylene succinate) Blends Composites. *J. Fiber Bioeng. Inform.* **6**, 85–94 (2013).
233. Harada, M. *et al.* Increased impact strength of biodegradable poly(lactic acid)/poly(butylene succinate) blend composites by using isocyanate as a reactive processing agent. *J. Appl. Polym. Sci.* **106**, 1813–1820 (2007).

234. Xue, B. *et al.* A Facile Fabrication of High Toughness Poly(lactic Acid) via Reactive Extrusion with Poly(butylene Succinate) and Ethylene-Methyl Acrylate-Glycidyl Methacrylate. *Polymers* **10**, 1401 (2018).
235. Su, S., Kopitzky, R., Tolga, S. & Kabasci, S. Polylactide (PLA) and Its Blends with Poly(butylene succinate) (PBS): A Brief Review. *Polymers* **11**, 1193 (2019).
236. Zhang, B., Sun, B., Bian, X., Li, G. & Chen, X. High Melt Strength and High Toughness PLLA/PBS Blends by Copolymerization and in Situ Reactive Compatibilization. *Ind. Eng. Chem. Res.* **56**, 52–62 (2017).
237. Supthanyakul, R., Kaabbuathong, N. & Chirachanchai, S. Poly(l-lactide- b -butylene succinate- b -l-lactide) triblock copolymer: A multi-functional additive for PLA/PBS blend with a key performance on film clarity. *Polym. Degrad. Stab.* **142**, 160–168 (2017).
238. Wu, F., Misra, M. & Mohanty, A. K. Super Toughened Poly(lactic acid)-Based Ternary Blends via Enhancing Interfacial Compatibility. *ACS Omega* **4**, 1955–1968 (2019).
239. Lee, S.-M. & Lee, J.-W. Characterization and processing of Biodegradable polymer blends of poly(lactic acid) with poly(butylene succinate adipate). *Korea-Aust. Rheol. J.* **17**, 71–77 (2005).
240. Ojijo, V., Sinha Ray, S. & Sadiku, R. Role of Specific Interfacial Area in Controlling Properties of Immiscible Blends of Biodegradable Polylactide and Poly[(butylene succinate)-co-adipate]. *ACS Appl. Mater. Interfaces* **4**, 6690–6701 (2012).
241. Ojijo, V., Sinha Ray, S. & Sadiku, R. Toughening of Biodegradable Polylactide/Poly(butylene succinate-co-adipate) Blends via in Situ Reactive Compatibilization. *ACS Appl. Mater. Interfaces* **5**, 4266–4276 (2013).
242. Ojijo, V. & Ray, S. S. Super toughened biodegradable polylactide blends with non-linear copolymer interfacial architecture obtained via facile in-situ reactive compatibilization. *Polymer* **80**, 1–17 (2015).
243. Sudesh, K., Abe, H. & Doi, Y. Synthesis, structure and properties of polyhydroxyalkanoates: biological polyesters. *Prog. Polym. Sci.* **25**, 1503–1555 (2000).
244. Addagada, L., Pathak, P., Shahid, M. K. & Rout, P. R. Microbial Polyhydroxyalkanoates (PHAs): A Brief Overview of Their Features, Synthesis, and Agro-Industrial Applications. in *Advances in Agricultural and Industrial Microbiology: Volume 1: Microbial Diversity and Application in Agroindustry* (eds. Nayak, S. K., Baliyarsingh, B., Mannazzu, I., Singh, A. & Mishra, B. B.) 217–236 (Springer Nature, 2022). doi:10.1007/978-981-16-8918-5_12.
245. Noda, I., Satkowski, M. M., Dowrey, A. E. & Marcott, C. Polymer alloys of Nodax copolymers and poly(lactic acid). *Macromol. Biosci.* **4**, 269–275 (2004).
246. Zembouai, I. *et al.* Poly(3-Hydroxybutyrate-co-3-Hydroxyvalerate)/Polylactide Blends: Thermal Stability, Flammability and Thermo-Mechanical Behavior. *J. Polym. Environ.* **22**, 131–139 (2014).
247. Burzic, I. *et al.* Impact modification of PLA using biobased biodegradable PHA biopolymers. *Eur. Polym. J.* **114**, 32–38 (2019).
248. Arrieta, M. P., López, J., López, D., Kenny, J. M. & Peponi, L. Development of flexible materials based on plasticized electrospun PLA–PHB blends: Structural, thermal, mechanical and disintegration properties. *Eur. Polym. J.* **73**, 433–446 (2015).
249. Bian, Y. *et al.* Toughening mechanism behind intriguing stress–strain curves in tensile tests of highly enhanced compatibilization of biodegradable poly(lactic acid)/poly(3-hydroxybutyrate-co-4-hydroxybutyrate) blends. *RSC Adv.* **4**, 41722–41733 (2014).
250. Jacobsen, S. & Fritz, H. G. Filling of poly(lactic acid) with native starch. *Polym. Eng. Sci.* **36**, 2799–2804 (1996).
251. Zaaba, N. F. & Ismail, H. A review on tensile and morphological properties of poly (lactic acid) (PLA)/thermoplastic starch (TPS) blends. *Polym.-Plast. Technol. Mater.* **58**, 1945–1964 (2019).
252. Li, H. & Huneault, M. A. Effect of chain extension on the properties of PLA/TPS blends. *J. Appl. Polym. Sci.* **122**, 134–141 (2011).
253. Li, H. & Huneault, M. A. Comparison of sorbitol and glycerol as plasticizers for thermoplastic starch in TPS/PLA blends. *J. Appl. Polym. Sci.* **119**, 2439–2448 (2011).
254. Huneault, M. A. & Li, H. Preparation and properties of extruded thermoplastic starch/polymer blends. *J. Appl. Polym. Sci.* **126**, E96–E108 (2012).
255. Wootthikanokkhan, J. *et al.* Effect of blending conditions on mechanical, thermal, and rheological properties of plasticized poly(lactic acid)/maleated thermoplastic starch blends. *J. Appl. Polym. Sci.* **124**, 1012–1019 (2012).
256. Ma, P., Hristova-Bogaerds, D. G., Schmit, P., Goossens, J. G. P. & Lemstra, P. J. Tailoring the morphology and properties of poly(lactic acid)/poly(ethylene)-co-(vinyl acetate)/starch blends via reactive compatibilization. *Polym. Int.* **61**, 1284–1293 (2012).

Chapter 1

257. Fimbeau, S., Grelier, S., Copinet, A. & Coma, V. Novel biodegradable films made from chitosan and poly(lactic acid) with antifungal properties against mycotoxinogen strains. *Carbohydr. Polym.* **65**, 185–193 (2006).
258. Bonilla, J., Fortunati, E., Vargas, M., Chiralt, A. & Kenny, J. M. Effects of chitosan on the physicochemical and antimicrobial properties of PLA films. *J. Food Eng.* **119**, 236–243 (2013).
259. Claro, P. I. C. *et al.* Biodegradable Blends with Potential Use in Packaging: A Comparison of PLA/Chitosan and PLA/Cellulose Acetate Films. *J. Polym. Environ.* **24**, 363–371 (2016).
260. Zhang, W., Chen, L. & Zhang, Y. Surprising shape-memory effect of polylactide resulted from toughening by polyamide elastomer. *Polymer* **50**, 1311–1315 (2009).
261. Raj, A., Prashantha, K. & Samuel, C. Compatibility in biobased poly(L-lactide)/polyamide binary blends: From melt-state interfacial tensions to (thermo)mechanical properties. *J. Appl. Polym. Sci.* **137**, 48440 (2020).
262. Zhang, K., Nagarajan, V., Misra, M. & Mohanty, A. K. Supertoughened Renewable PLA Reactive Multiphase Blends System: Phase Morphology and Performance. *ACS Appl. Mater. Interfaces* **6**, 12436–12448 (2014).
263. Xia, Y. *et al.* Highly toughened poly(lactic acid) blends prepared by reactive blending with a renewable poly(ether-block-amide) elastomer. *J. Appl. Polym. Sci.* **138**, 50097 (2021).
264. Lebarbé, T. *et al.* Methyl 10-undecenoate as a raw material for the synthesis of renewable semi-crystalline polyesters and poly(ester-amide)s. *Polym. Chem.* **3**, 2842 (2012).
265. Lebarbé, T., Grau, E., Alfos, C. & Cramail, H. Fatty acid-based thermoplastic poly(ester-amide) as toughening and crystallization improver of poly(l-lactide). *Eur. Polym. J.* **65**, 276–285 (2015).
266. Lebarbé, T., Grau, E., Gadenne, B., Alfos, C. & Cramail, H. Synthesis of Fatty Acid-Based Polyesters and Their Blends with Poly(L-lactide) as a Way To Tailor PLLA Toughness. *ACS Sustain. Chem. Eng.* **3**, 283–292 (2015).
267. Cramail, H., Lebarbe, T., Gadenne, B. & Alfos, C. Use of polymers as additives in a polymer matrix. (2017).
268. Siakeng, R. *et al.* Natural fiber reinforced polylactic acid composites: A review. *Polym. Compos.* **40**, 446–463 (2019).
269. Sangeetha, V. h., Deka, H., Varghese, T. o. & Nayak, S. k. State of the art and future perspectives of poly(lactic acid) based blends and composites. *Polym. Compos.* **39**, 81–101 (2018).
270. Jin, F.-L., Hu, R.-R. & Park, S.-J. Improvement of thermal behaviors of biodegradable poly(lactic acid) polymer: A review. *Compos. Part B Eng.* **164**, 287–296 (2019).
271. De Santis, F., Pantani, R. & Titomanlio, G. Nucleation and crystallization kinetics of poly(lactic acid). *Thermochim. Acta* **522**, 128–134 (2011).
272. Srihep, Y., Nealey, P. & Turng, L.-S. Effects of annealing time and temperature on the crystallinity and heat resistance behavior of injection-molded poly(lactic acid). *Polym. Eng. Sci.* **53**, 580–588 (2013).
273. Hoffmann, K., Huber, G. & Mäder, D. Nucleating and clarifying agents for polyolefins. *Macromol. Symp.* **176**, 83–92 (2001).
274. Libster, D., Aserin, A. & Garti, N. Advanced nucleating agents for polypropylene. *Polym. Adv. Technol.* **18**, 685–695 (2007).
275. Fillon, B., Thierry, A., Lotz, B. & Wittmann, J. C. Efficiency scale for polymer nucleating agents. *J. Therm. Anal.* **42**, 721–731 (1994).
276. Helanto, K., Talja, R. & Rojas, O. J. Talc reinforcement of polylactide and biodegradable polyester blends via injection-molding and pilot-scale film extrusion. *J. Appl. Polym. Sci.* **n/a**, 51225.
277. Khaki, A., Garmabi, H., Javadi, A. & Yahyae, N. Effect of Crystallinity, Crystal Polymorphism, and Graphene Oxide Nanosheets on the Barrier Properties of Poly(l-lactic acid). *Eur. Polym. J.* (2019) doi:10.1016/j.eurpolymj.2019.05.047.
278. Shojaeiarani, J., Bajwa, D., Jiang, L., Liaw, J. & Hartman, K. Insight on the influence of nano zinc oxide on the thermal, dynamic mechanical, and flow characteristics of Poly(lactic acid)–zinc oxide composites. *Polym. Eng. Sci.* **0**, (2019).
279. Liu, H. *et al.* A novel aryl hydrazide nucleator to effectively promote stereocomplex crystallization in high-molecular-weight poly(L-lactide)/poly(D-lactide) blends. *Polymer* 122873 (2020) doi:10.1016/j.polymer.2020.122873.
280. Schultz, N. E., Song, L. & Li, F. Composés D'hydrazide Appropriés Pour La Nucléation De Polymère D'acide Polylactique. (2016).
281. Xing, Q., Wang, Z., Li, R., Dong, X. & Wang, D. Effect of solubility of a hydrazide compound on the crystallization behavior of poly(L-lactide). *RSC Adv.* **6**, 113377–113389 (2016).
282. Leoné, N. *et al.* Improving Processing, Crystallization, and Performance of Poly-L-lactide with an Amide-Based Organic Compound as Both Plasticizer and Nucleating Agent. *ACS Omega* **4**, 10376–10387 (2019).

283. Aliotta, L. *et al.* Effect of nucleating agents on crystallinity and properties of poly (lactic acid) (PLA). *Eur. Polym. J.* **93**, 822–832 (2017).
284. Xing, Q., Zhang, X., Dong, X., Liu, G. & Wang, D. Low-molecular weight aliphatic amides as nucleating agents for poly (L-lactic acid): Conformation variation induced crystallization enhancement. *Polymer* **53**, 2306–2314 (2012).
285. Feng, Y. *et al.* The crystallization behavior of poly(lactic acid) with different types of nucleating agents. *Int. J. Biol. Macromol.* **106**, 955–962 (2018).
286. Nanthananon, P., Seadan, M., Pivsa-Art, S. & Suttiruengwong, S. Enhanced crystallization of poly (lactic acid) through reactive aliphatic bisamide. *IOP Conf. Ser. Mater. Sci. Eng.* **87**, 012067 (2015).
287. Saitou, K. & Yamaguchi, M. Transparent poly(lactic acid) film crystallized by annealing beyond glass transition temperature. *J. Polym. Res.* **27**, 104 (2020).
288. Xing, Q. *et al.* Tailoring crystallization behavior of poly (l-lactide) with a low molecular weight aliphatic amide. *Colloid Polym. Sci.* **293**, 3573–3583 (2015).
289. Yueagyen, P. & Lertworasirikul, A. Effect of Poly(Hexamethylene Succinamide) on Crystallization of Poly(L-Lactic Acid). *Key Engineering Materials* vol. 751 302–307 /KEM.751.302 (2017).
290. Kolstad, J. J. Crystallization kinetics of poly(L-lactide-co-meso-lactide). *J. Appl. Polym. Sci.* **62**, 1079–1091 (1996).
291. Li, H. & Huneault, M. A. Effect of nucleation and plasticization on the crystallization of poly(lactic acid). *Polymer* **48**, 6855–6866 (2007).
292. Petchwattana, N., Covavisaruch, S. & Petthai, S. Influence of talc particle size and content on crystallization behavior, mechanical properties and morphology of poly(lactic acid). *Polym. Bull.* **71**, 1947–1959 (2014).
293. Sinha Ray, S., Yamada, K., Okamoto, M., Ogami, A. & Ueda, K. New Polylactide/Layered Silicate Nanocomposites. 3. High-Performance Biodegradable Materials. *Chem. Mater.* **15**, 1456–1465 (2003).
294. Nam, J. Y., Sinha Ray, S. & Okamoto, M. Crystallization Behavior and Morphology of Biodegradable Polylactide/Layered Silicate Nanocomposite. *Macromolecules* **36**, 7126–7131 (2003).
295. Nam, P. H., Ninomiya, N., Fujimori, A. & Masuko, T. Crystallization characteristics of intercalated poly(L-lactide)/organo-modified montmorillonite hybrids. *Polym. Eng. Sci.* **46**, 39–46 (2006).
296. Nam, J. Y. *et al.* Morphology and crystallization kinetics in a mixture of low-molecular weight aliphatic amide and polylactide. *Polymer* **47**, 1340–1347 (2006).
297. Yoshida, Y. & Obuchi, S. POLYLACTIC ACID RESIN COMPOSITION AND FILM THEREFROM. 9 (2001).
298. Takenaka, A. & Nomoto, S. Biodegradable resin composition. 15 (2010).
299. Onishi, H., 大西英明, Morishita, T. & 森下健. Polylactic acid resin composition and resin molded article thereof. (2013).
300. Qiu, Z. & Li, Z. Effect of Orotic Acid on the Crystallization Kinetics and Morphology of Biodegradable Poly(L-lactide) as an Efficient Nucleating Agent. *Ind. Eng. Chem. Res.* **50**, 12299–12303 (2011).
301. Qi, Z. *et al.* Effect of aliphatic diacyl adipic dihydrazides on the crystallization of poly(lactic acid). *J. Appl. Polym. Sci.* **132**, (2015).
302. Roy, M. *et al.* On the nucleation of polylactide by melt-soluble oxalamide based organic compounds. *Polymer* 122680 (2020) doi:10.1016/j.polymer.2020.122680.
303. Rastogi, S., DESHMUKH, Y., MA, P. & WILSENS, C. Nucleating agents for biopolymers. (2013).
304. Wang, T. *et al.* Effect of 1,3,5-trialkyl-benzenetricarboxylamide on the crystallization of poly(lactic acid). *J. Appl. Polym. Sci.* **130**, 1328–1336 (2013).
305. Zhang, X. *et al.* Effect of nucleating agents on the crystallization behavior and heat resistance of poly(l-lactide). *J. Appl. Polym. Sci.* **133**, (2016).
306. Yang, J. *et al.* Crystallization and Rheological Properties of the Eco-friendly Composites Based on Poly (lactic acid) and Precipitated Barium Sulfate. *J. Polym. Environ.* **27**, 2739–2755 (2019).
307. Pan, P. *et al.* Nucleation Effects of Nucleobases on the Crystallization Kinetics of Poly(L-lactide). *Macromol. Mater. Eng.* **297**, 670–679 (2012).
308. Wu, N. & Wang, H. Effect of zinc phenylphosphonate on the crystallization behavior of poly(l-lactide). *J. Appl. Polym. Sci.* **130**, 2744–2752 (2013).
309. Nagarajan, V., Zhang, K., Misra, M. & Mohanty, A. K. Overcoming the Fundamental Challenges in Improving the Impact Strength and Crystallinity of PLA Biocomposites: Influence of Nucleating Agent and Mold Temperature. *ACS Appl. Mater. Interfaces* **7**, 11203–11214 (2015).
310. Dalibey, M. A. & Arnault, C. Matière plastique à haute teneur en pla comprenant un ester de citrate. (2020).

Chapter 1

311. Chieng, B. W., Ibrahim, N. A., Yunus, W. M. Z. W. & Hussein, M. Z. Plasticized poly(lactic acid) with low molecular weight poly(ethylene glycol): Mechanical, thermal, and morphology properties. *J. Appl. Polym. Sci.* **130**, 4576–4580 (2013).
312. Muller, J., Jiménez, A., González-Martínez, C. & Chiralt, A. Influence of plasticizers on thermal properties and crystallization behaviour of poly(lactic acid) films obtained by compression moulding. *Polym. Int.* **65**, 970–978 (2016).
313. Jariyasakoolroj, P., Rojanaton, N. & Jarupan, L. Crystallization behavior of plasticized poly(lactide) film by poly(l-lactic acid)-poly(ethylene glycol)-poly(l-lactic acid) triblock copolymer. *Polym. Bull.* **77**, 2309–2323 (2020).
314. Labrecque, L. V., Kumar, R. A., Davé, V., Gross, R. A. & McCarthy, S. P. Citrate esters as plasticizers for poly(lactic acid). *J. Appl. Polym. Sci.* **66**, 1507–1513 (1997).
315. Hao, X., Kaschta, J., Liu, X., Pan, Y. & Schubert, D. W. Entanglement network formed in miscible PLA/PMMA blends and its role in rheological and thermo-mechanical properties of the blends. *Polymer* **80**, 38–45 (2015).
316. Cock, F., Cuadri, A. A., García-Morales, M. & Partal, P. Thermal, rheological and microstructural characterisation of commercial biodegradable polyesters. *Polym. Test.* **32**, 716–723 (2013).
317. D'Amico, D. A., Iglesias Montes, M. L., Manfredi, L. B. & Cyras, V. P. Fully bio-based and biodegradable polylactic acid/poly(3-hydroxybutyrate) blends: Use of a common plasticizer as performance improvement strategy. *Polym. Test.* **49**, 22–28 (2016).
318. Guo, X., Zhang, J. & Huang, J. Poly(lactic acid)/polyoxymethylene blends: Morphology, crystallization, rheology, and thermal mechanical properties. *Polymer* **69**, 103–109 (2015).
319. Quero, E., Müller, A. J., Signori, F., Coltelli, M.-B. & Bronco, S. Isothermal Cold-Crystallization of PLA/PBAT Blends With and Without the Addition of Acetyl Tributyl Citrate. *Macromol. Chem. Phys.* **213**, 36–48 (2012).
320. Shibata, M., Inoue, Y. & Miyoshi, M. Mechanical properties, morphology, and crystallization behavior of blends of poly(l-lactide) with poly(butylene succinate-co-l-lactate) and poly(butylene succinate). *Polymer* **47**, 3557–3564 (2006).
321. Ke, T. & Sun, X. Melting behavior and crystallization kinetics of starch and poly(lactic acid) composites. *J. Appl. Polym. Sci.* **89**, 1203–1210 (2003).
322. Rizvi, R., Cochrane, B., Naguib, H. & Lee, P. C. Fabrication and characterization of melt-blended polylactide-chitin composites and their foams. *J. Cell. Plast.* **47**, 283–300 (2011).
323. Pandey, A. K., Katiyar, V., Sasaki, S. & Sakurai, S. Accelerated crystallization of poly(l-lactic acid) by silk fibroin nanodisc. *Polym. J.* **1** (2019) doi:10.1038/s41428-019-0229-9.
324. Mathew, A. P., Oksman, K. & Sain, M. The effect of morphology and chemical characteristics of cellulose reinforcements on the crystallinity of polylactic acid. *J. Appl. Polym. Sci.* **101**, 300–310 (2006).
325. Herrera, N., Mathew, A. P. & Oksman, K. Plasticized polylactic acid/cellulose nanocomposites prepared using melt-extrusion and liquid feeding: Mechanical, thermal and optical properties. *Compos. Sci. Technol.* **106**, 149–155 (2015).
326. Shojaeiarani, J., Bajwa, D. S. & Hartman, K. Esterified cellulose nanocrystals as reinforcement in poly(lactic acid) nanocomposites. *Cellulose* **26**, 2349–2362 (2019).
327. Yin, H.-Y. *et al.* Enhancing Thermomechanical Properties and Heat Distortion Resistance of Poly(l-lactide) with High Crystallinity under High Cooling Rate. *ACS Sustain. Chem. Eng.* **3**, 654–661 (2015).
328. Di Lorenzo, M. L. & Androsch, R. Accelerated crystallization of high molar mass poly(l/d-lactic acid) by blending with low molar mass poly(l-lactic acid). *Eur. Polym. J.* **100**, 172–177 (2018).
329. Chen, Q., Auras, R. & Uysal-Unalan, I. Role of stereocomplex in advancing mass transport and thermomechanical properties of polylactide. *Green Chem.* **24**, 3416–3432 (2022).
330. Tsuji, H. *et al.* Stereocomplex crystallization, homocrystallization, and polymorphism of enantiomeric copolyesteramides poly(lactic acid-co-alanine)s from the melt. *Polym. Cryst.* **3**, e10094 (2020).
331. Tsuji, H. Poly(lactic acid) stereocomplexes: A decade of progress. *Adv. Drug Deliv. Rev.* **107**, 97–135 (2016).
332. Brochu, S., Prud'homme, R. E., Barakat, I. & Jerome, R. Stereocomplexation and Morphology of Polylactides. *Macromolecules* **28**, 5230–5239 (1995).
333. Anderson, K. S. & Hillmyer, M. A. Melt preparation and nucleation efficiency of polylactide stereocomplex crystallites. *Polymer* **47**, 2030–2035 (2006).
334. Tsuji, H., Takai, H. & Saha, S. K. Isothermal and non-isothermal crystallization behavior of poly(l-lactic acid): Effects of stereocomplex as nucleating agent. *Polymer* **47**, 3826–3837 (2006).
335. Narita, J., Katagiri, M. & Tsuji, H. Highly Enhanced Nucleating Effect of Melt-Recrystallized Stereocomplex Crystallites on Poly(l-lactic acid) Crystallization. *Macromol. Mater. Eng.* **296**, 887–893 (2011).

336. Yamane, H. & Sasai, K. Effect of the addition of poly(D-lactic acid) on the thermal property of poly(L-lactic acid). *Polymer* **44**, 2569–2575 (2003).
337. Samsuri, M., Iswaldi, I. & Purnama, P. The Effect of Stereocomplex Polylactide Particles on the Stereocomplexation of High Molecular Weight Polylactide Blends. *Polymers* **13**, 2018 (2021).
338. Zhang, Z.-C. *et al.* Inducing Stereocomplex Crystals by Template Effect of Residual Stereocomplex Crystals during Thermal Annealing of Injection-Molded Polylactide. *Ind. Eng. Chem. Res.* **55**, 10896–10905 (2016).
339. Zhang, Z.-C. *et al.* Enhanced Heat Deflection Resistance via Shear Flow-Induced Stereocomplex Crystallization of Polylactide Systems. *ACS Sustain. Chem. Eng.* **5**, 1692–1703 (2017).
340. Liu, Z. *et al.* Stereocomplex-type polylactide with bimodal melting temperature distribution: Toward desirable melt-processability and thermomechanical performance. *Polymer* **169**, 21–28 (2019).
341. Li, Z., Tan, B. H., Lin, T. & He, C. Recent advances in stereocomplexation of enantiomeric PLA-based copolymers and applications. *Prog. Polym. Sci.* **62**, 22–72 (2016).
342. Guinault, A., Sollogoub, C., Ducruet, V. & Domenek, S. Impact of crystallinity of poly(lactide) on helium and oxygen barrier properties. *Eur. Polym. J.* **48**, 779–788 (2012).
343. Dong, T. *et al.* Thermal and barrier properties of stretched and annealed polylactide films. *Polym. Sci. Ser. A* **57**, 738–746 (2015).
344. Sangroniz, A. *et al.* Influence of the Rigid Amorphous Fraction and Crystallinity on Polylactide Transport Properties. *Macromolecules* **51**, 3923–3931 (2018).
345. Bai, H. *et al.* Significantly Improving Oxygen Barrier Properties of Polylactide via Constructing Parallel-Aligned Shish-Kebab-Like Crystals with Well-Interlocked Boundaries. *Biomacromolecules* **15**, 1507–1514 (2014).
346. Connolly, T. M. & Turner, J. C. R. Two-phase diffusion. *Chem. Eng. Sci.* **34**, 319–323 (1979).
347. Panapitiya, N. *et al.* Compatibilized Immiscible Polymer Blends for Gas Separations. *Materials* **9**, 643 (2016).
348. Mannan, H. A. *et al.* Recent Applications of Polymer Blends in Gas Separation Membranes. *Chem. Eng. Technol.* **36**, 1838–1846 (2013).
349. Domenek, S., Fernandes-Nassar, S. & Ducruet, V. Rheology, Mechanical Properties, and Barrier Properties of Poly(lactic acid). in *Synthesis, Structure and Properties of Poly(lactic acid)* (eds. Di Lorenzo, M. L. & Androsch, R.) 303–341 (Springer International Publishing, 2018). doi:10.1007/12_2016_17.
350. Courgneau, C. *et al.* Effect of crystallization on barrier properties of formulated polylactide. *Polym. Int.* **61**, 180–189 (2012).
351. Guo, Y. *et al.* Effects of clay platelets and natural nanotubes on mechanical properties and gas permeability of Poly (lactic acid) nanocomposites. *Polymer* **83**, 246–259 (2016).
352. Ortenzi, M. A. *et al.* Evaluation of crystallinity and gas barrier properties of films obtained from PLA nanocomposites synthesized via “in situ” polymerization of L-lactide with silane-modified nanosilica and montmorillonite. *Eur. Polym. J.* **66**, 478–491 (2015).
353. Risyon, N. P., Othman, S. H., Basha, R. K. & Talib, R. A. Characterization of polylactic acid/halloysite nanotubes bionanocomposite films for food packaging. *Food Packag. Shelf Life* **23**, 100450 (2020).
354. Ambrosio-Martín, J. *et al.* Synergistic effect of lactic acid oligomers and laminar graphene sheets on the barrier properties of polylactide nanocomposites obtained by the in situ polymerization pre-incorporation method. *J. Appl. Polym. Sci.* **133**, (2016).
355. Pinto, A. M., Cabral, J., Tanaka, D. A. P., Mendes, A. M. & Magalhães, F. D. Effect of incorporation of graphene oxide and graphene nanoplatelets on mechanical and gas permeability properties of poly(lactic acid) films. *Polym. Int.* **62**, 33–40 (2013).
356. Marano, S., Laudadio, E., Minelli, C. & Stipa, P. Tailoring the Barrier Properties of PLA: A State-of-the-Art Review for Food Packaging Applications. *Polymers* **14**, 1626 (2022).
357. Lagaron, J. M., Catalá, R. & Gavara, R. Structural characteristics defining high barrier properties in polymeric materials. *Mater. Sci. Technol.* **20**, 1–7 (2004).
358. Razavi, S. M., Dadbin, S. & Frounchi, M. Oxygen-barrier properties of poly(lactic acid)/poly(vinyl acetate-co-vinyl alcohol) blends as biodegradable films. *J. Appl. Polym. Sci.* **125**, E20–E26 (2012).
359. Armentano, I. *et al.* Processing and characterization of plasticized PLA/PHB blends for biodegradable multiphase systems. *Express Polym. Lett.* **9**, 583–596 (2015).
360. Jost, V. Blending of Polyhydroxybutyrate-co-valerate with Polylactic Acid for Packaging Applications – Reflections on Miscibility and Effects on the Mechanical and Barrier Properties. *Chem. Biochem. Eng. Q.* **29**, 221–246 (2015).
361. Sun, Q., Mekonnen, T., Misra, M. & Mohanty, A. K. Novel Biodegradable Cast Film from Carbon Dioxide Based Copolymer and Poly(Lactic Acid). *J. Polym. Environ.* **24**, 23–36 (2016).

Chapter 1

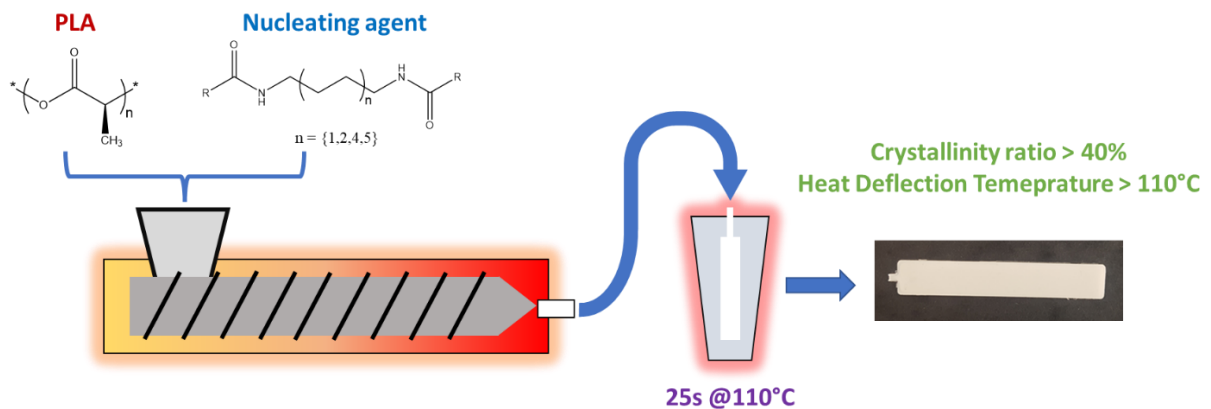
362. Yang, X., Xu, H., Odelius, K. & Hakkarainen, M. Poly(lactide)-g-poly(butylene succinate-co-adipate) with High Crystallization Capacity and Migration Resistance. *Materials* **9**, 313 (2016).
363. Pal, A. K. & Katiyar, V. Nanoamphiphilic Chitosan Dispersed Poly(lactic acid) Bionanocomposite Films with Improved Thermal, Mechanical, and Gas Barrier Properties. *Biomacromolecules* **17**, 2603–2618 (2016).
364. Tripathi, N. & Katiyar, V. PLA/functionalized-gum arabic based bionanocomposite films for high gas barrier applications. *J. Appl. Polym. Sci.* **133**, (2016).
365. Sanchez-Garcia, M. D., Gimenez, E. & Lagaron, J. M. Morphology and barrier properties of solvent cast composites of thermoplastic biopolymers and purified cellulose fibers. *Carbohydr. Polym.* **71**, 235–244 (2008).
366. Sanchez-Garcia, M. D. & Lagaron, J. M. On the use of plant cellulose nanowhiskers to enhance the barrier properties of polylactic acid. *Cellulose* **17**, 987–1004 (2010).
367. Espino-Pérez, E. *et al.* Influence of chemical surface modification of cellulose nanowhiskers on thermal, mechanical, and barrier properties of poly(lactide) based bionanocomposites. *Eur. Polym. J.* **49**, 3144–3154 (2013).
368. Xie, L. *et al.* From Nanofibrillar to Nanolaminar Poly(butylene succinate): Paving the Way to Robust Barrier and Mechanical Properties for Full-Biodegradable Poly(lactic acid) Films. *ACS Appl. Mater. Interfaces* **7**, 8023–8032 (2015).
369. Evstatiev, M., Simeonova, S., Friedrich, K., Pei, X.-Q. & Formanek, P. MFC-structured biodegradable poly(l-lactide)/poly(butylene adipate-co-terephthalate) blends with improved mechanical and barrier properties. *J. Mater. Sci.* **48**, 6312–6330 (2013).
370. Zhou, S.-Y. *et al.* Super-Robust Poly(lactide) Barrier Films by Building Densely Oriented Lamellae Incorporated with Ductile in Situ Nanofibrils of Poly(butylene adipate-co-terephthalate). *ACS Appl. Mater. Interfaces* **8**, 8096–8109 (2016).
371. Messin, T. *et al.* Biodegradable PLA/PBS multilayer membrane with enhanced barrier performances. *J. Membr. Sci.* **598**, 117777 (2020).
372. Boufarguine, M., Guinault, A., Miquelard-Garnier, G. & Sollogoub, C. PLA/PHBV Films with Improved Mechanical and Gas Barrier Properties. *Macromol. Mater. Eng.* **298**, 1065–1073 (2013).
373. Hosseini, S. F., Javidi, Z. & Rezaei, M. Efficient gas barrier properties of multi-layer films based on poly(lactic acid) and fish gelatin. *Int. J. Biol. Macromol.* **92**, 1205–1214 (2016).
374. Le Gars, M. *et al.* High-Barrier and Antioxidant Poly(lactic acid)/Nanocellulose Multilayered Materials for Packaging. *ACS Omega* (2020) doi:10.1021/acsomega.0c01955.
375. Li, C. *et al.* Enhancing the Oxygen-Barrier Properties of Polylactide by Tailoring the Arrangement of Crystalline Lamellae. *ACS Sustain. Chem. Eng.* **6**, 6247–6255 (2018).
376. Sedničková, M. *et al.* Changes of physical properties of PLA-based blends during early stage of biodegradation in compost. *Int. J. Biol. Macromol.* **113**, 434–442 (2018).
377. Garrison, T., Murawski, A. & Quirino, R. Bio-Based Polymers with Potential for Biodegradability. *Polymers* **8**, 262 (2016).
378. Petinakis, E. *et al.* Biodegradation and thermal decomposition of poly(lactic acid)-based materials reinforced by hydrophilic fillers. *Polym. Degrad. Stab.* **95**, 1704–1707 (2010).
379. Rosa-Ramírez, H. D. L., Aldas, M., Ferri, J. M., López-Martínez, J. & Samper, M. D. Modification of poly(lactic acid) through the incorporation of gum rosin and gum rosin derivative: Mechanical performance and hydrophobicity. *J. Appl. Polym. Sci.* **n/a**, 49346 (2020).
380. Taiatele, I. *et al.* Abiotic Hydrolysis and Compostability of Blends Based on Cassava Starch and Biodegradable Polymers. *J. Polym. Environ.* **27**, 2577–2587 (2019).
381. Rosli, N. A., Karamanlioglu, M., Kargarzadeh, H. & Ahmad, I. Comprehensive exploration of natural degradation of poly(lactic acid) blends in various degradation media: A review. *Int. J. Biol. Macromol.* **187**, 732–741 (2021).
382. Guzman-Sielicka, A., Janik, H. & Sielicki, P. Proposal of New Starch-Blends Composition Quickly Degradable in Marine Environment. *J. Polym. Environ.* **21**, 802–806 (2013).
383. Zhang, S. J., Tang, Y. W. & Cheng, L. H. Biodegradation Behavior of PLA/PBS Blends. *Adv. Mater. Res.* **821–822**, 937–940 (2013).
384. Sashiwa, H., Fukuda, R., Okura, T., Sato, S. & Nakayama, A. Microbial Degradation Behavior in Seawater of Polyester Blends Containing Poly(3-hydroxybutyrate-co-3-hydroxyhexanoate) (PHBHHx). *Mar. Drugs* **16**, 34 (2018).
385. Arrieta, M. P., López, J., Rayón, E. & Jiménez, A. Disintegrability under composting conditions of plasticized PLA-PHB blends. *Polym. Degrad. Stab.* **108**, 307–318 (2014).

386. Weng, Y.-X. *et al.* Biodegradation behavior of poly(butylene adipate-co-terephthalate) (PBAT), poly(lactic acid) (PLA), and their blend under soil conditions. *Polym. Test.* **32**, 918–926 (2013).
387. Tabasi, R. Y. & Ajji, A. Selective degradation of biodegradable blends in simulated laboratory composting. *Polym. Degrad. Stab.* **120**, 435–442 (2015).
388. Palsikowski, P. A., Kuchnier, C. N., Pinheiro, I. F. & Morales, A. R. Biodegradation in Soil of PLA/PBAT Blends Compatibilized with Chain Extender. *J. Polym. Environ.* **26**, 330–341 (2018).
389. Auclair, N., GUILLAUMONT, C., ARNAULT, C. & CHARPENTIER, Y. Procédé de Préparation d'un Mélange Maître Enzymé. (2021).
390. MACEDO, S., NOEL, M. & ARNAULT, C. Utilisation d'un mélange enzyme pour améliorer les propriétés mécaniques d'un article comprenant le mélange enzyme et un polymère biodégradable. (2021).
391. Auclair, N. & Arnault, C. Film multicouche transparent. (2019).
392. Arnault, C. Article multicouche enzymé. (2021).
393. Evanesto® ≡ Solution enzymatique PLA 100% compostable. *Carbiolice*
<https://www.carbiolice.com/evanesto-inside/>.

Chapter II:

Use of nucleating agents for PLA

Enhancing its heat deflection temperature and its gas barrier properties



Contents

1. Introduction	101
2. Fatty bis-amides from fatty acids as nucleating agents	103
2.1. Synthesis.....	103
a. Selection of long chain precursors and amines	103
b. Synthetic procedures	105
2.2. Chemical structure and thermal properties.....	108
3. Use with PLA to enhance its crystallisation kinetics	117
3.1. DSC preliminary analysis	117
3.2. Blending to make DMA samples in isothermal conditions	121
a. Melt-blending.....	121
b. Preliminary study: mould temperature screening.....	122
c. Optimisation: effect of time and loading.....	128
d. Crystallographic structure	135
4. Conclusion and perspectives	139
5. Experimental & SI	141
References	145

1. Introduction

PLA is a well-known bio-based polyester which unfortunately carries major drawbacks to its industrial use. One of the limiting properties of PLA is its low heat deflection temperature (HDT) which is reported around 55°C¹. Such low HDT is due to a T_g reported around 55°C-60°C and to the fact that, although PLA can be a semi-crystalline polymer, its crystallisation kinetics are too slow to get sufficiently high crystallinity ratios in fast-industrial production techniques such as the injection moulding process for instance¹⁻³. This constitutes a major issue to the use of PLA since no thermal application can be considered as such. Indeed, unless efficient means of making PLA crystallise are developed, the fast production of crystalline PLA materials cannot be achieved.

Another drawback linked to the low crystallinity ratios regards the gas barrier properties of PLA. As mentioned previously, PLA has got in between O₂ gas barrier properties meaning it can neither be considered as a barrier polymer nor a permeant polymer⁴. However, reports from Drieskens *et al.*, have shown the higher the crystallinity ratio, the better its barrier behaviour⁵. Typically, they put forward the fact that the O₂ permeability of PLA could be at least divided by two when crystallinity ratios above 40% were achieved compared to fully amorphous PLA.

Further studies by Cocca *et al.* later revealed that the crystalline form of PLA would also play an important role. Namely, PLA crystallised in the α form would exhibit better gas barrier properties (regarding the water vapour barrier properties) than the less packed α' form⁶. Guinault *et al.* then conducted a study regarding the O₂ and helium barrier properties of annealed PLA films while considering the morphology of PLA and its effects on the barrier properties. Their work showed the α' crystalline form would have very little effect on reducing the O₂ permeability, which would only decrease by nearly a factor 4 when the α crystalline form was present⁷. A further study by Fernandes Nassar *et al.* showed the barrier properties were also affected by the manufacturing process⁸. They compared the O₂ permeability of PLA films either crystallised from the melt or after annealing from the glassy state and realised the films crystallised from the melt would display better barrier behaviours, about 2.5 times less permeable to O₂ when the crystallinity ratios were over 35%, whatever the selected crystallisation temperature (85°C, supposed to favour the α' form or 130°C supposed to favour the α form). An outstanding feature was, however, the permeability obtained for a sample

Chapter 2

crystallised from the glassy state at 130°C for 20 mins which gave the lowest O₂ permeability. The authors therefore concluded that to obtain the best O₂ barrier properties, PLA should be pre-nucleated and quickly annealed for a short amount of time from the glassy state at 130°C. Unfortunately, the authors could not clearly state the predominance of either the α' or the α form in their samples.

In this part, we focused our strategy on the use of nucleating agents to enhance the crystallisation kinetics of PLA directly from the melt. As reported in Chapter 1, many compounds have been described as successful nucleating agents, more particularly fatty amide type compounds such as N,N'-ethylene bis(stearamide) (EBS) and N,N'-ethylene bis(12-hydroxystearamide) (EBHS)⁹⁻¹³ which have been reported to bring the t_{1/2} of PLA from over 30 minutes to less than 2 minutes at 1wt% loading. To our knowledge, we did not find further literature reporting the use of new C18 fatty amides as such. After further investigation, patents suggesting the efficiency of fatty amide nucleating agents with such structure were found. Takenaka *et al.* reported multiple formulations of PLA with a glycerol-based plasticiser and a nucleating agent along with a moulding process for sheets. The maximum crystallinity ratios obtained are lower than 35% using 0.5wt% of nucleating agent and 15wt% of plasticiser. Although fatty amides obtained from fatty acids with a pendant hydroxyl group are mentioned, only EBHS and N,N'-Hexamethylenebis-12-hydroxystearic acid amide are cited as potential examples. High loadings such as 3wt% regarding the amount of PLA are used in this invention¹⁴. Onishi *et al.* later reported multiple formulations of PLA with a glycerol fatty acid-based plasticiser and a nucleating agent along with a moulding process to obtain PLA films with high transparency and heat resistance. This time, only 0.4wt% of nucleating agent is used with 5wt% of plasticiser and the process mentions performances achieved with the formulation directly cooled from the melt, with a moulding time of 5s. The inventors did not however specifically focussed on most C18 fatty bis-amides, with exception to EBS, EBHS, N,N'-Hexamethylenebis-12-hydroxystearic acid amide and N,N'-Xylylenebis-12-hydroxystearic acid amide¹⁵.

Here, similar fatty bis-amide compounds were synthesised based on C18 fatty acids and a fully linear aliphatic diamine. The considered diamines have different chain lengths to change the distance between the two newly formed amide groups and to study the impact of such a

change. The synthesised bis-amide compounds were then mixed to a highly optically pure PLLA, referred to as PLA, to measure their effect on its crystallisation rate.

2. Fatty bis-amides from fatty acids as nucleating agents

2.1. Synthesis

a. Selection of long chain precursors and amines

Thanks to their versatility, a wide range of fatty acids or their derivatives are easily available to be tested. In the case of C18 fatty acids, 4 compounds were targeted for testing (Fig. II. 1).

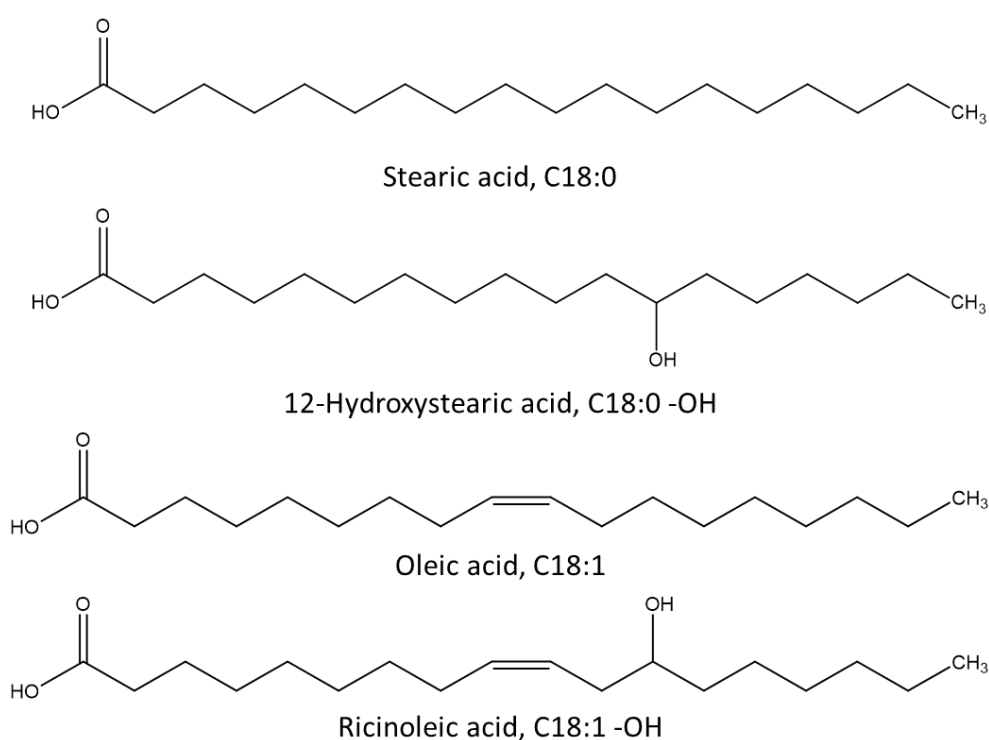


Fig. II. 1: Selected C18 fatty acids as precursors of bis-amides

The aim here is to see whether the characteristics of the fatty acids influence the efficiency of the obtained nucleating agents. The particular interest of these four compounds is to be able to use C18 fatty acids which are either fully saturated (stearic acid), have got a hydroxyl group in the C12 position (12-hydroxystearic acid), have an unsaturation between the C9 and the C10 (oleic acid) or a combination of both an unsaturation and a hydroxyl group (ricinoleic acid). More especially, stearic acid and 12-hydroxystearic acid have already been reported in the literature under the form of EBS and EBHS as mentioned previously.

Chapter 2

Along with this selection of fatty acids, a selection of 4 different diamines was used to make the reaction. Since compounds using ethylenediamine are already reported in the literature, the focus was put on using longer diamines which are respectively 1,4-diaminobutane (C4), 1,6-diaminohexane (C6), 1,10-diaminododecane (C10) and 1,12-diaminododecane (C12) (Fig. II. 2).

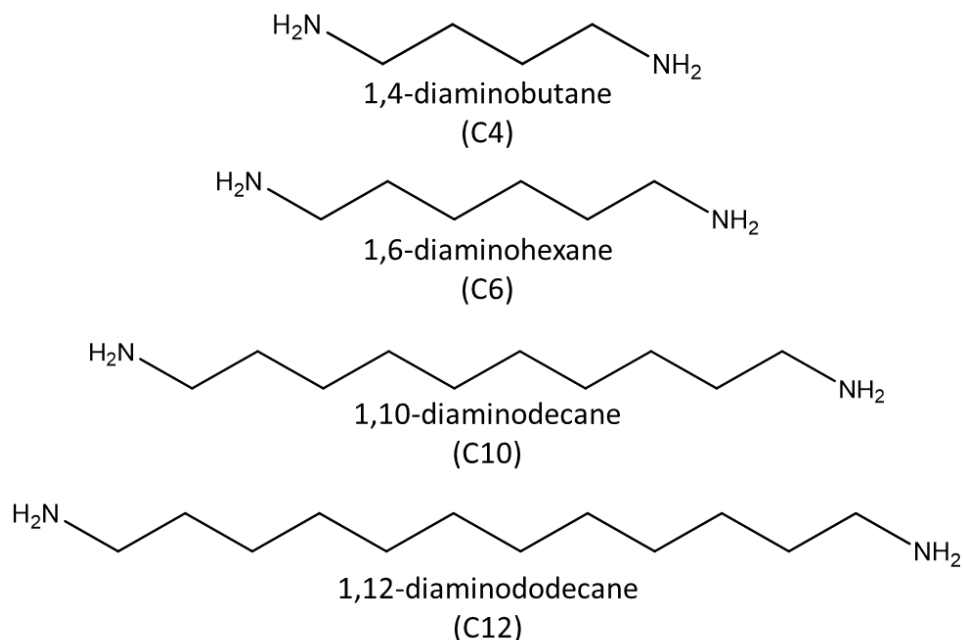


Fig. II. 2: Selected diamines for bis-amide synthesis

Here, the main objective is to evaluate the influence of the distance between the formed amide functions on the properties of the synthesised compounds, thanks to four different spacers. Also, these diamines were chosen to favour H-bonding intermolecular interactions. Indeed, in this configuration, an even number of carbon atoms will give amide groups which are oriented as shown in Fig. II. 3. As first reported by Hill and Walker¹⁶ then by Stempfle *et al.*¹⁷ in the case of polyamides, this configuration will lead to a maximum amount of H-bonding between the different amide groups bore by the different molecules. Therefore, rather high melting points are expected to be achieved with the synthesised bis-amides.

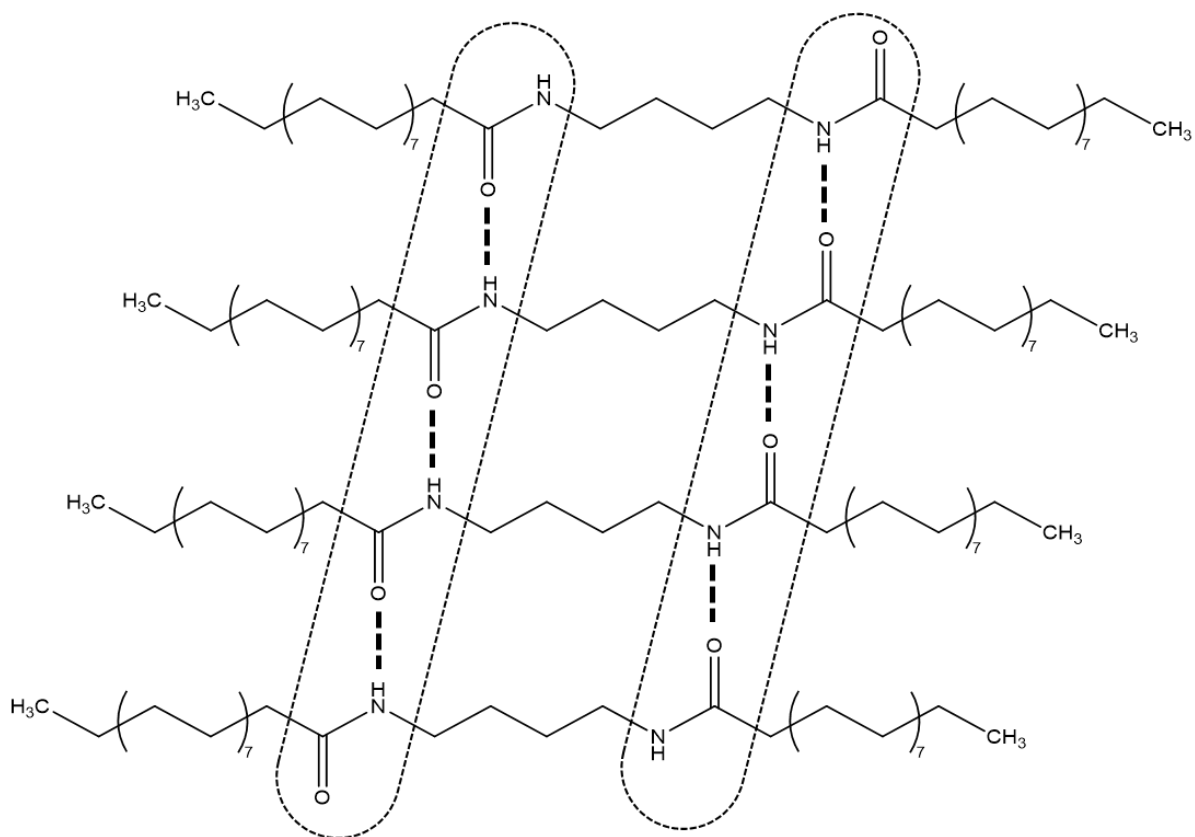


Fig. II. 3: Schematic orientation of the bis-amide compounds (C4-stearic bis-amide example) and the occurring H-bonding

b. Synthetic procedures

The classical route to synthesise amides from carboxylic acids involves transforming the carboxylic acid into a more reactive acyl chloride intermediate on which the amine can react. Such acyl chloride is typically formed using highly toxic compounds such as thionyl chloride, phosphorus trichloride or phosphorus pentachloride¹⁸. Depending on the available fatty acid derivatives, three different procedures to synthesise our fatty bis-amides were therefore tested. Starting from an acyl chloride derivative, the Schotten-Baumann procedure was used (Fig. II. 4) which proved to be the most effective in this case.

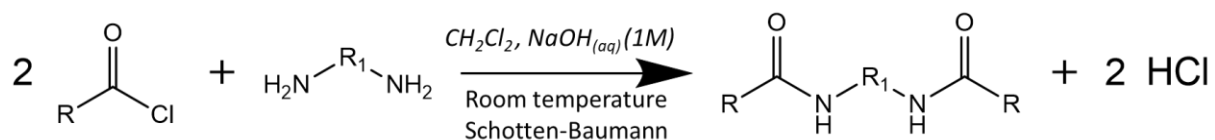


Fig. II. 4: Bis-amide synthesis according to the Schotten-Baumann procedure

Namely, equal molar amounts of acyl chloride and amine groups were put in an immiscible two-solvent system. The organic phase, a dichloromethane phase to solubilise the reactants, and an aqueous solution of sodium hydroxide to neutralise the formed hydrochloric acid and

move the equilibrium towards the amide formation, were used in equal volumes. Upon addition of the diamine on the acyl chloride, a white solid was formed corresponding to the precipitation of the formed bis-amide which is hardly soluble using this solvent system. After 2h, the solid was recovered and washed with dichloromethane, water and diethyl ether to remove any side products or unreacted reactants and dried. Yields from 34% to 66% were obtained.

For carboxylic acids, the amine was directly reacted on them according to the following simplified reaction scheme (Fig. II. 5). Usually, this synthesis is conducted in bulk at high temperatures above 150°C^{19–22} and involves the use of vacuum to remove the water formed through the condensation of the amine groups with the carboxylic acid groups.

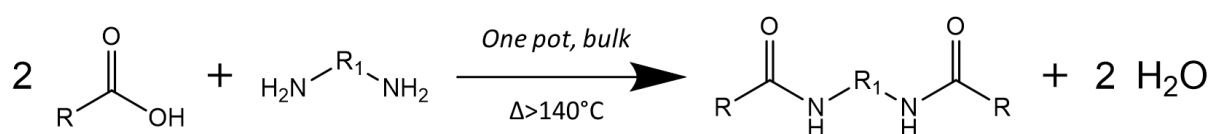


Fig. II. 5: Synthesis of bis-amides from fatty acids and a diamine

Equimolar amounts of carboxylic acid and amine groups were mixed together in a round bottom flask. The mixture was placed in an oil bath at 150°C with magnetic stirring. In the case of a hydroxyl substituted fatty acid reactant, the temperature was brought down to 140°C to avoid self-condensation and oligomerisation.

The mechanism of this reaction has been explained by Lanigan and Sheppard²³ (Fig. II. 6): upon mixing, the carboxylic acid and the primary amine form a carboxylate/ammonium salt due to the pKa of one another.

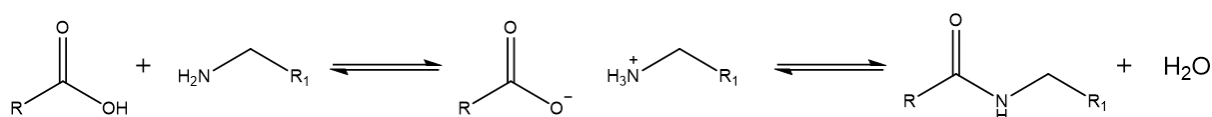


Fig. II. 6: Dual equilibrium during the formation of amides from carboxylic acids and primary amines

The formed ammonium salt is part of a dual equilibrium which can be shifted towards the amide formation by removing the water. In our case, this phenomenon was observed during the synthesis of our compounds when, upon heating, both reactants would mix in the liquid state and then form a solid as the temperature of the flask was still rising. Such solid would eventually melt when the temperature reached approximately 100°C. The evolution of the reaction could be followed using ¹H NMR spectroscopy in deuterated chloroform (CDCl₃) with

a few drops of 1,1,1,3,3,3-hexafluoro-2-propanol (HFIP) to allow the solubilisation of the reaction mixture and formed product. Total reaction times could range from 6h to more than 20h depending on the reactivity of the selected diamine. Indeed, the longer the carbon chain of an aliphatic diamine, the less reactive it is. In the case where the used diamine was too volatile, more was added during the reaction to compensate the loss. Upon completion, the reaction mixture was cooled to room temperature allowing it to crystallise, then recuperated and ground into a powder. This powder was then washed with ethanol and chloroform to eliminate side products and unreacted reactants and dried at 80°C under reduced pressure for 12h. Final yields from 55% to 93% were obtained.

Finally, in some cases, the methyl ester derivative was used for the synthesis as according to the scheme shown in Fig. II. 7. This path turned out to be the less efficient one since methyl esters are less reactive to form amides than their carboxylic acid counterparts and require the use of a catalyst as reported in different publications²⁴⁻²⁸. In our case, we decided to inspire ourselves from the synthetic path reported by Lebarbé *et al.*²⁷ for their poly(ester-amide) precursors. 1,5,7-triazabicyclo[4.4.0]dec-5-ene (TBD), a basic organic catalyst for aminolysis of esters as reported by Sabot *et al.*²⁵, was used at a 20% molar ratio vs the amount of methyl ester functions. One molar equivalent of diamine was mixed in bulk with two molar equivalents of methyl ester and the TBD as a catalyst in round-bottom flask with magnetic stirring at 120°C and using a condenser. The reaction time was around 3h upon which the reaction mixture was cooled to room temperature and washed with water and cold ethanol to remove the catalyst and side products and dried. Yields from 50 to 65% were obtained.

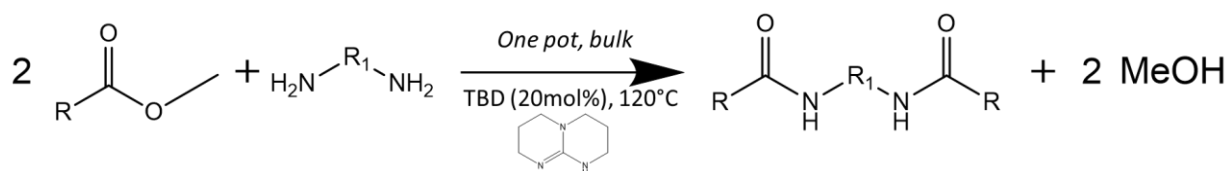


Fig. II. 7: Aminolysis of a methyl ester to form a bis-amide compound

The corresponding procedures for each fatty acid derivative and chosen diamines are reported in Table II. 1.

Table II. 1: Considered reaction procedures to synthesise bis-amide nucleating agents

Fatty acid	Diamines used	Derivative used
Stearic acid	C4, C6, C10, C12	Carboxylic acid
Oleic acid	C4, C6, C10, C12	Acyl chloride
12-hydroxystearic acid	C4, C6, C10, C12	Carboxylic acid
Ricinoleic acid	C4, C6, C10, C12	Methyl ester

For the rest of the discussion, the synthesised compounds will be named as such: CX-YYYY with X corresponding to the number of carbon atoms of the used diamine (*i.e.* 4, 6, 10 or 12) and YYYY corresponding to the name of the fatty acid derivative (*i.e.* Stear for stearic acid, 12-HSA for 12-hydroxystearic acid, Oleic for oleic acid or Ric for ricinoleic acid).

2.2. Chemical structure and thermal properties

As seen in Fig. II. 8 to Fig. II. 11, the signal shift of the methylene protons of the free amine could be observed and followed as well as signal shift of the methylene protons in alpha position of either the carboxylic acid, the methyl ester, or the acyl chloride.

Moreover, thanks to the addition of HFIP, the proton linked to the nitrogen atom of the amide group could be quantified in these spectra. Unfortunately, the proton signals corresponding to the HFIP would sometimes hide or give a bad baseline for the proton signals of the methylene groups in alpha of the newly formed amide functions. The degree of purity of the synthesised compounds was thus determined mainly using ^1H NMR, as shown in Fig. II. 8 for stearic based bis-amides, Fig. II. 9 for 12-hydroxystearic based bis-amides, Fig. II. 10 for oleyl chloride based bis-amides & Fig. II. 11 for methyl ricinoleate based bis-amides, using a mixture of CDCl_3 with a few drops of HFIP, necessary to improve the solubility of the synthesised bis-amides Stear and 12-HSA.

In every spectrum, a quadruplet appeared around 3.3ppm corresponding to proton H_e in Fig. II. 8, proton H_f in Fig. II. 9, proton H_g in Fig. II. 10 and proton H_h in Fig. II. 11. These protons show the formation of an amide bond and therefore that our reaction occurred and could be used to determine the degree of purity of the products along with the conversion. Unfortunately, in some of the spectra, these proton signals overlap with the proton signals of the HFIP and it is therefore impossible to analyse them. The -NH proton signal that appears

between 5.5 & 6ppm, depending on the sample, was used to evaluate the amount of amide groups formed. In most spectra, there was no residual proton signal around 2.7ppm corresponding to remaining free amine apart from the spectrum corresponding to the C4-Ric product in Fig. II. 11. In this spectrum, a signal corresponding to protons in alpha position of a primary amine was noticed; such signals would remain after washing. Using the SEC in THF, this signal was shown to correspond to the mono-amide intermediate of our desired product (evaluated at 14% by NMR and 10% by SEC). Such product would seem to have rather similar solubility properties to the bis-amide compound when both are mixed together, therefore making them nearly impossible to separate. The data determined by ^1H NMR and the SEC are summarised in Table II. 2.

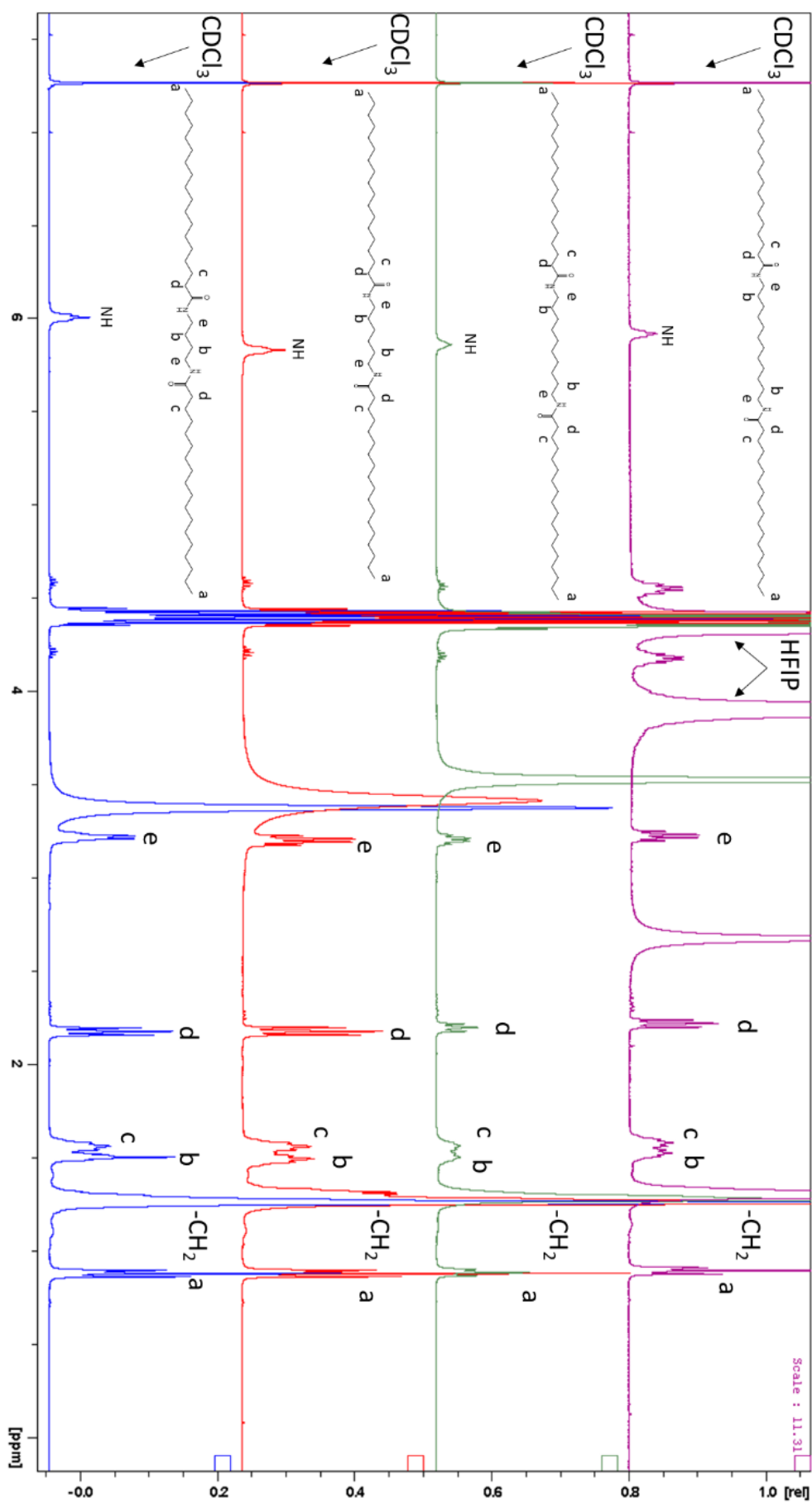


Fig. II. 8: ^1H NMR spectra of stearic acid based bis-amides in CDCl_3 with HFIP

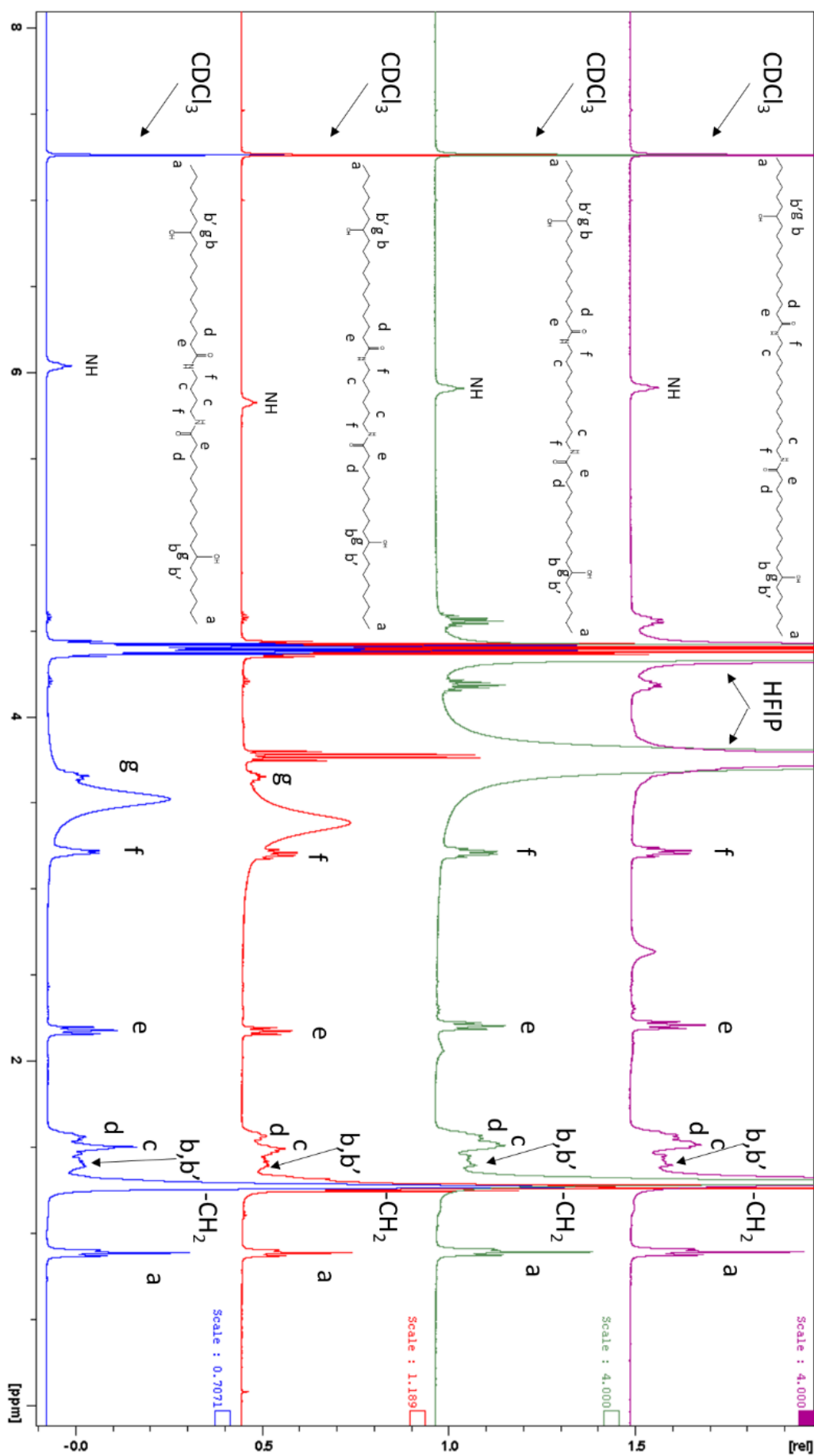


Fig. II. 9: ^1H NMR spectra of 12-hydroxystearic based bis-amides in CDCl_3 with HFIP

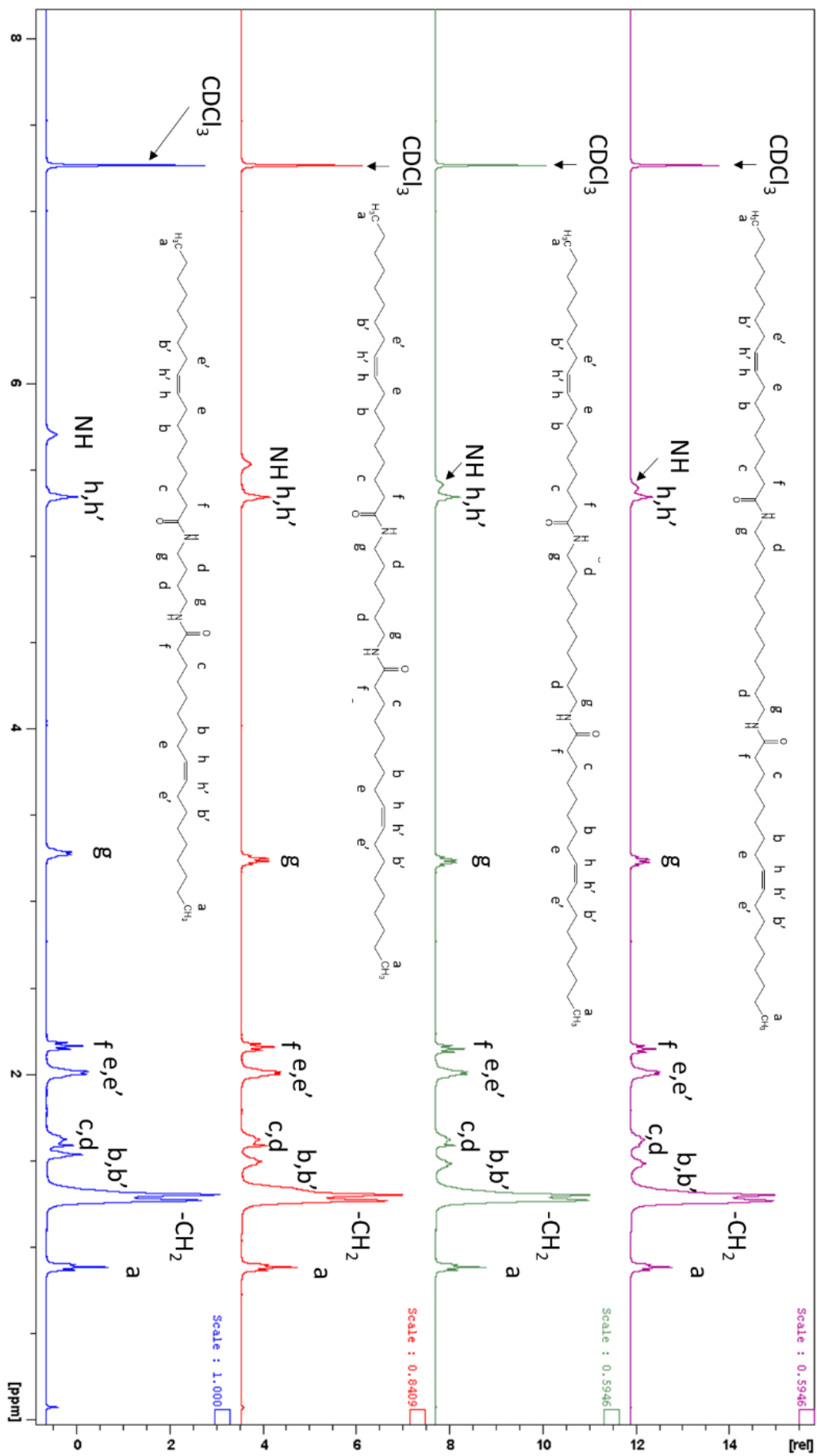


Fig. II. 10: ^1H NMR spectra of oleyl chloride based bis-amides in CDCl_3

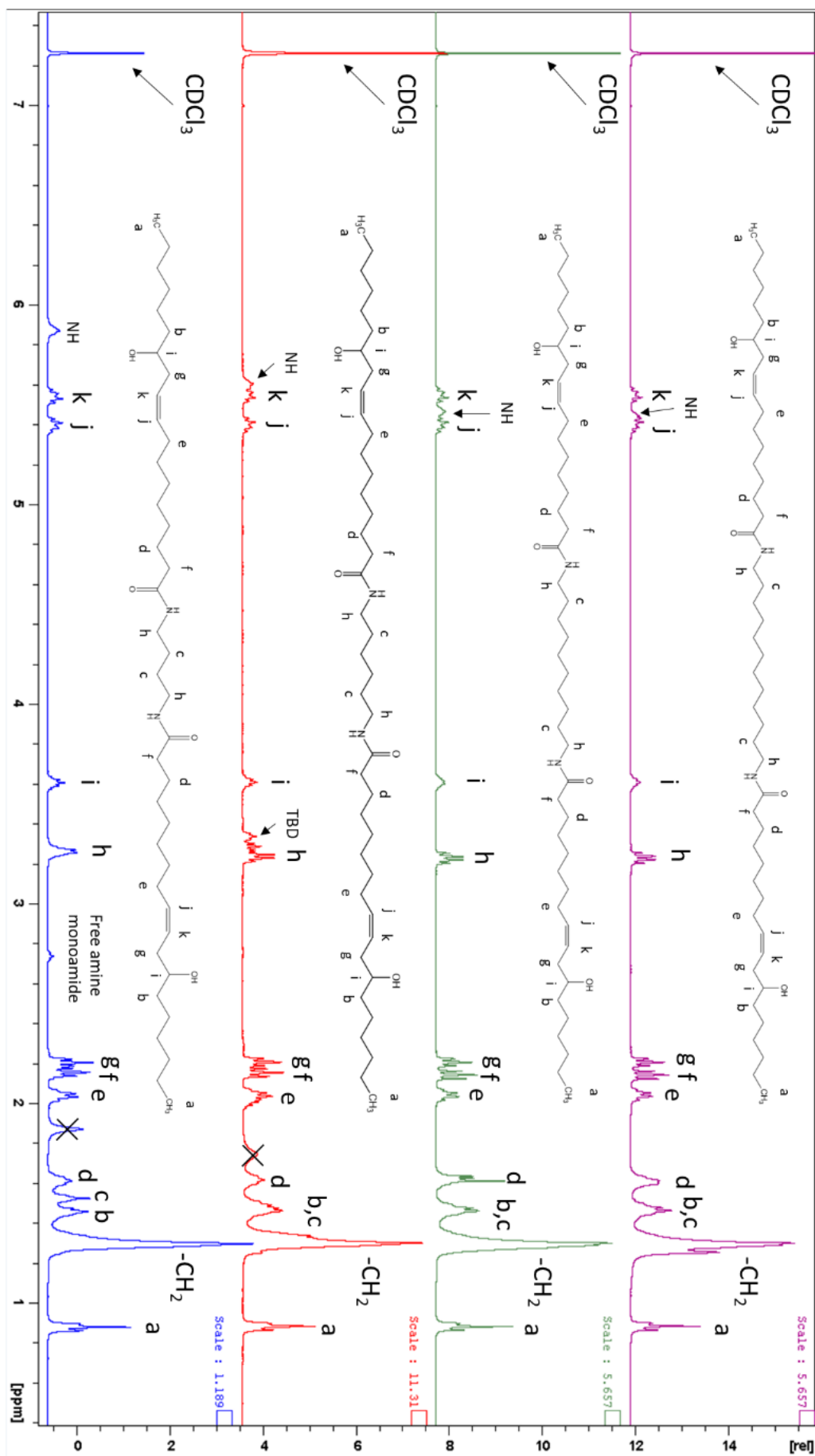


Fig. II. 11: ^1H NMR spectra of methyl ricinoleate based bis-amides in CDCl_3

Chapter 2

Unfortunately, due to the difficulty encountered to remove the TBD catalyst from the reaction mixture of the obtained products, high amounts of catalyst were still present and mixed with the ricinoleic derived bis-amides. This was the case with C6-Ric since it was found that this compound was highly soluble in the same solvents as TBD, including water to some extent, therefore leading to a very low yield and lower degree of purity (82%) of the final product.

The melting point and the crystallisation point of the synthesised products were then measured by means of the DSC and shown on Fig. II. 12 and Fig. II. 13.

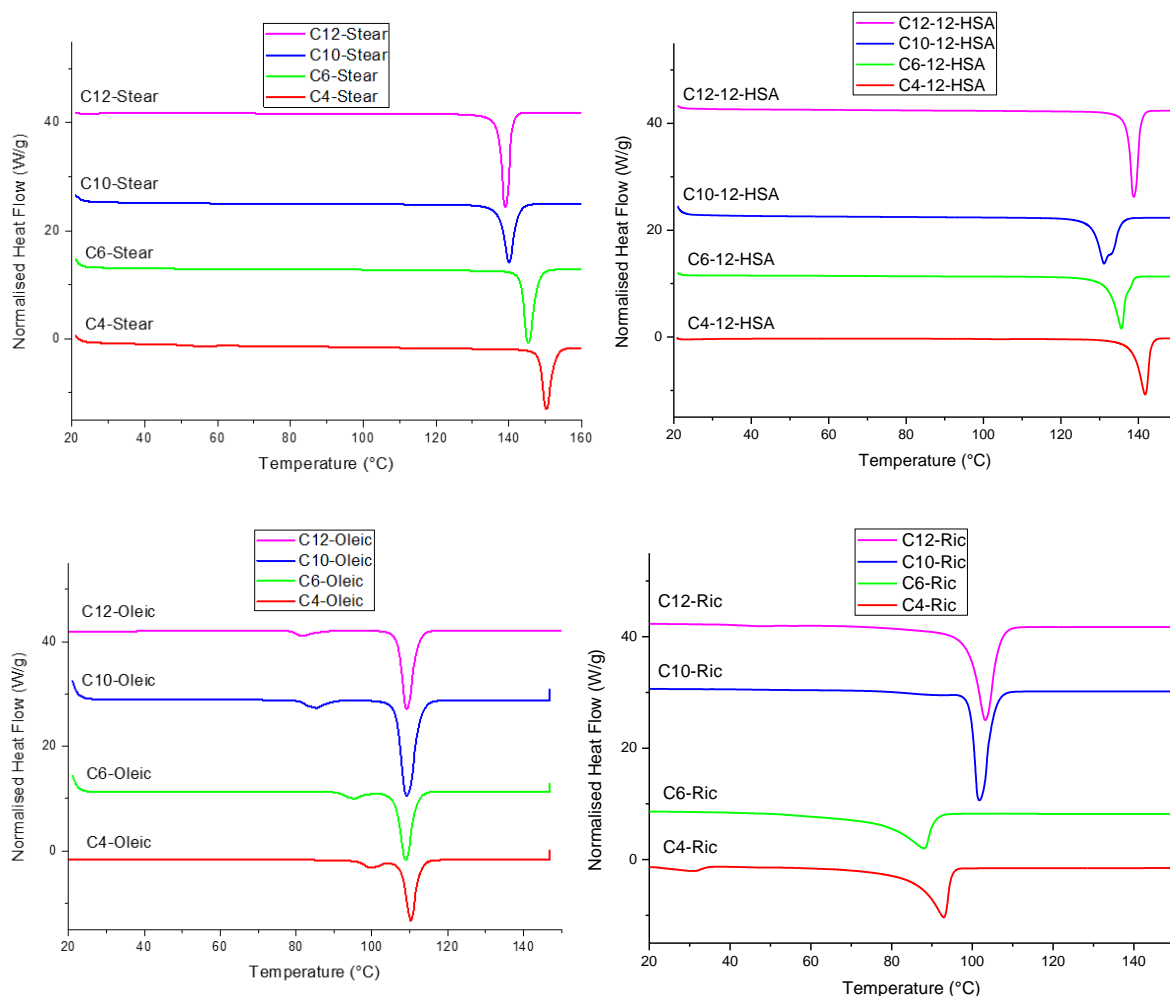


Fig. II. 12: DSC traces of the synthesised nucleating agents - 2nd heating, 10°C/min - Melting points

These thermal characteristics were respectively measured during the 2nd heating ramp at 10°C/min and during the cooling ramp at -10°C/min. All characteristics of the synthesised bis-amides are reported in Table II.2.

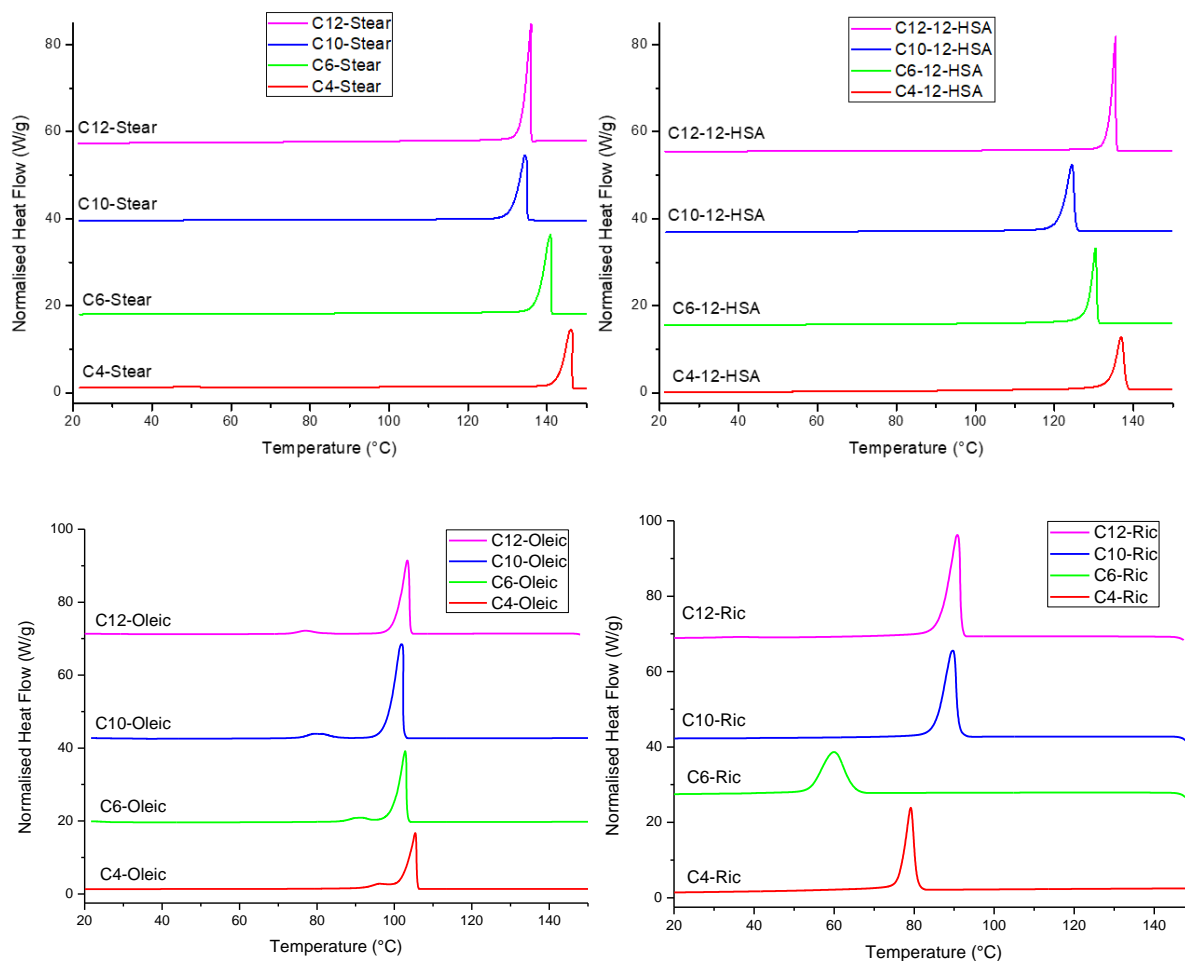


Fig. II. 13: DSC traces of the synthesised nucleating agents – cooling after 1st heating, $-10^{\circ}\text{C}/\text{min}$ - Crystallisation points

The thermograms corresponding to the stearic acid-based show very well-defined melting endotherms and crystallisation exotherms. For the 12-hydroxystearic acid derivatives, the C10-12-HSA and to some little extent the C6-12-HSA bis-amides seem to display overlapping melting peaks. This was attributed to the polymorphism of crystalline fatty derivatives which was reported in different studies^{29–31}. In the case of the oleic acid-based compounds, small second endotherms and exotherms could also be seen. The NMR spectra do not show any residual free amine, therefore the origin of these peaks was attributed to the polymorphism of the compounds due to the configuration of the fatty chain³¹. In the case of the ricinoleic-based bis-amides, broader melting peaks and crystallisation peaks were observed in the case of C4-Ric and C6-Ric, due to the lower purity and the presence of TBD or mono-amide.

Table II. 2: Degree of purity and thermal characteristics of the synthesised bis-amides

Fatty acid	Diamine	Purity _{NMR} (%) ^a	Purity _{SEC} (%) ^b	ΔH_m (kJ/mol) ^c	T _m (°C) ^c	T _c (°C) ^d
Stearic	C4	94	-	117.3	150	146
	C6	98	-	127.2	145	141
	C10	95	-	134.2	140	134
	C12	97	-	146.5	138	133
12-hydroxystearic	C4	93	-	84.2	142	137
	C6	96	-	89.4	136	130
	C10	95	-	113.4	131	125
	C12	95	-	149.6	139	136
Oleic	C4	98	-	62.0	110	105
	C6	98	-	72.5	109	103
	C10	98	-	94.6	109	102
	C12	97	-	105.3	109	103
Ricinoleic	C4	93	94	59.4	93	79
	C6	82	88	64.4	88	60
	C10	95	99	87.5	102	90
	C12	94	95	95.9	103	91

a) ¹H NMR, CDCl₃, 400MHz, b) SEC in THF vs PS, 40°C, 1mL/min, c) DSC 2nd heating 20°C to 190°C, 10°C/min, d) DSC cooling 190°C to 20°C, -10°C/min

Looking at the trend, the highest melting points are obtained for the stearic derived compounds, which corresponds to a fully aliphatic fatty C18 chain. The second most high melting points are obtained for the 12-hydroxystearic derived bis-amides then the oleic derivatives and finally the ricinoleic. It is possible to notice the effect of the fatty chain on the melting point of the bis-amides: a fully aliphatic and linear chain will provide the highest melting points whereas a substituted chain with a hydroxyl group and an unsaturation will lead to lower melting point values. This is in accordance with common knowledge relating to intermolecular interactions. The presence of an unsaturation will lead to less favourable packing of the molecules between themselves due to an effect on the chain configuration. This can also be true in the case of the presence of a hydroxyl group which might partially block the trans-trans configuration of the chains. Therefore, less energy will be required to break such assembly leading to lower melting points than in the case of the fully linear and aliphatic carbon chain.

Looking at the different amines used, namely the different chain spacers between the two amide groups, a trend for the stearic derivatives can be noticed showing that the longer the chain of the diamine, the lower the melting point. This was mainly attributed to the decreasing amide group content in the molecular chain, that is to say, a lower hydrogen-bond density due to the increase of the number of methylene groups with longer diamines. As also reported by Stempfle *et al.*¹⁷, van der Waals interactions between hydrocarbon segments only contribute to a minor role. This behaviour and melting point values have been also reported by Poopalam *et al.*³¹. As per a similar trend with non-fully aliphatic bis-amides, the DSC revealed nothing as such. In the case of the 12-hydroxystearic derivatives, the trend was verified for C4-12-HSA, C6-12-HSA and C10-12-HSA but the melting point of C12-12-HSA was higher than the one of C12-12-HSA. This can be explained by a more predominant effect of the hydrocarbon chains' intermolecular interactions between each other on the crystallisation process rather than the H-bonding effect between the amide groups. For all oleic derivatives, the melting point was rather similar and around 110°C. Finally, in the case of the ricinoleic based bis-amides, the trend was completely opposite, the longer the diamine chain, the higher the melting point. However, this to be further examined and discussed. Indeed, highly pure compounds could be due to difficulties during the purification step. Therefore, the low melting point and crystallisation point of C6-Ric could be explained by the presence of remaining TBD. For C4-Ric, an effect might be measured through the presence of 10 to 14% of mono-amide, as revealed by NMR and SEC, with a lower melting point.

3. Use with PLA to enhance its crystallisation kinetics

3.1. DSC preliminary analysis

Prior to mixing the synthesised nucleating agents with PLA using a mini extruder, some tests were run using the DSC by just mixing very small amounts of PLA with the synthesised bis-amide products. Prior to mixing, the PLA pellets were dried for at least 12h at 80°C under reduced pressure. To mix the nucleating agents with the PLA, a small aluminium container was used on a hot plate set at 200°C. About 1g of total mixture was produced, with a weight ratio of PLA/nucleating agents of 99/1. The two compounds were put in the hot container to melt at the open air at the same time, and, once all had melted, were mixed thanks to a metal

Chapter 2

spatula for stirring. Once the mixture seemed rather homogeneous, the container was taken off the hot plate and dropped on the cold practice bench to rapidly cool. Small bits of the formed PLA blends were then cut to be used as DSC samples. The 1st heating ramp was used to erase the thermal history of the sample. Using the -10°C/min cooling ramp, a dynamic crystallisation enthalpy could be measured. The obtained values allowed us to calculate a crystallinity ratio upon cooling using the following formula:

$$\chi_c = \frac{\Delta H_c}{\omega_{PLLA} * \Delta H_{m,0}}$$

With:

- χ_c = the crystallinity of the PLLA sample
- ΔH_c = the crystallisation enthalpy
- $\Delta H_{m,0}$ = the equilibrium melting enthalpy of PLLA, 93.7 J/g
- ω_{PLLA} = the weight fraction of PLLA in the sample

Upon the 2nd heating, the T_g and the T_m were measured and, using the cold crystallisation enthalpy and the melting enthalpy, another value of the crystallinity ratio could be calculated and compared to the one calculated upon cooling from the melt. This time, the formula used for the calculations was:

$$\chi_c = \frac{\Delta H_m - \Delta H_{CC}}{\omega_{PLLA} * \Delta H_{m,0}}$$

With:

- χ_c = the crystallinity of the PLLA sample
- ΔH_m = the measured melting enthalpy
- ΔH_{CC} = the measured cold crystallisation enthalpy
- $\Delta H_{m,0}$ = the equilibrium melting enthalpy of PLLA, 93.7 J/g
- ω_{PLLA} = the weight fraction of PLLA in the sample

The DSC data corresponding to the different samples is reported in Table II. 3.

Table II. 3: DSC results of preliminary samples of PLA + 1wt% of synthesised fatty NA

Fatty acid	Diamine	ΔH_c (J/g) ^a	ΔH_{cc} (J/g) ^b	ΔH_m (J/g) ^b	$\Delta H_{\alpha \rightarrow \beta}$ (J/g) ^b	$X_{c,m}$ (%) ^a	$X_{c,c}$ (%) ^b	T_g (°C) ^b	T_c (°C) ^a	T_m (°C) ^b
PLA	-	5.34	40.5	49.2	0.59	6	9	60	111	173
	C4	45.1	-	49.1	-	48	52	62	120	173
	C6	43.3	-	49.9	-	46	53	62	115	172
	C10	20.9	18.1	55.1	3.13	22	36	60	113	172
	C12	16.3	21.8	55.2	2.93	17	33	59	114	172
	C4	37.9	3.14	52.4	1.56	41	51	59	113	172
12-hydroxystearic	C6	44.5	-	55.9	-	48	60	62	113	173
	C10	12.7	24.9	53.8	4.10	14	27	60	113	172
	C12	12.9	23.0	51.6	3.62	14	27	60	114	172
	C4	14.7	26.4	52.5	3.57	16	24	59	112	171
	C6	9.84	30.2	52.5	5.44	11	18	60	112	172
	C10	12.2	28.4	53.7	4.96	13	22	60	112	172
Oleic	C12	13.6	27.0	54.1	5.43	15	23	60	112	172
	C4	9.17	36.2	55.4	3.50	10	17	59	115	171
	C6	3.59	45.8	52.4	2.63	4	4	58	110	168
	C10	8.98	38.9	56.7	3.50	10	15	59	114	172
	C12	7.27	40.6	54.7	3.54	8	11	59	112	171
	Ricinoleic	C4	9.17	36.2	55.4	3.50	10	17	59	115
C6		3.59	45.8	52.4	2.63	4	4	58	110	168
C10		8.98	38.9	56.7	3.50	10	15	59	114	172
C12		7.27	40.6	54.7	3.54	8	11	59	112	171

a) DSC cooling 190°C to 20°C, -10°C/min, b) DSC 2nd heating 20°C to 190°C, 10°C/min

Chapter 2

The results reported allow us to pre-determine the best nucleating agents from the ones synthesised. Neat PLA has very slow crystallisation kinetics, only a crystallinity ratio below 10% in controlled cooling conditions. Crystallinity ratios over 50% could be obtained with bis-amides based on stearic acid and 12-hydroxystearic acid in the same controlled cooling conditions. More precisely, such performance was achieved using the shorter diamines which are the C4-diamine and the C6-diamine. When the C10-diamine and the C12-diamine were used, there was also an enhancement in the crystallinity ratio, however, it was at least 20% lower than the ones previously described. Comparatively, the crystallinity ratios obtained using nucleating agents synthesised from either the oleic acid derivative or the ricinoleic acid derivative stayed below 25% therefore making these group of bis-amides the less efficient in these dynamic cooling conditions.

Looking at these performances in regard of the respective melting points and crystallisation points of the bis-amides, a clear effect of the thermal transitions on the nucleation efficiency can be seen. The most efficient nucleating agents have melting points and crystallisation points which are all above 130°C, which corresponds to the upper limit of the temperature window in which PLA will be able to crystallise. Indeed, neat PLA is reported to only be able to crystallise between 80°C and 130°C^{2,32,33}. Here, the best nucleating agents all crystallise before PLA starts crystallising or just as it would as observed by Nam *et al.* with EBHS⁹. This also explains why other nucleating agents from oleic acid derivatives or ricinoleic acid derivatives, all with crystallisation points in the low temperature range of crystallisation of PLA (Table II. 2), are not as efficient as the ones made from stearic acid and 12-hydroxystearic acid. In effect, we suggest that fully crystallised nucleating agents have created multiple nuclei in the PLA matrix therefore greatly enhancing the crystallisation kinetics by partially getting rid of the energy barrier required for nucleation during the crystallisation process of PLA. Moreover, if our compounds' dispersion in PLA is good, this would allow a very homogeneous nucleation and therefore limit the amount of time needed for crystalline growth since most of the PLA matrix would start crystallising at the same time.

However, just a difference in melting points and crystallisation points might not be sufficient as an explanation. In the case of 12-HSA derived bis-amides, a higher crystallisation point for the C12-bis-amide than for the C6-bis-amide was reported, although the C6-bis-amide remains the more efficient of the two. Intermolecular interactions could be at play here

since there is a 6-carbon atom difference in space between the amide functions of these two molecules. It therefore seems that closer amide functions would create more favourable interactions with the PLA matrix to promote the crystallisation phenomenon. This would also be in accordance with polarised optical microscopy reported by Nam *et al.*⁹ in which they noticed an epitaxial growth of oriented PLA crystals at the interface between the crystallised nucleating agent and the PLA melt. Far from this interface, the PLA would crystallise in its regular spherulite morphology.

3.2. Blending to make DMA samples in isothermal conditions

a. Melt-blending

Thanks to the preliminary DSC analysis, the focus was put on evaluating the efficiency of two specific families of our bis-amides which are the bis-amides obtained from stearic acid and the ones obtained from 12-hydroxystearic acid. Indeed, the highest crystallisation enthalpies upon cooling from the melt were measured with these two groups of nucleating agents and accordingly, the highest crystallisation ratios. To go further in this study, our nucleating agents were blended in PLA using a twin-screw mini extruder with a recirculating canal to properly mix the compounds and to use the injection moulding technique to produce DMA samples. These DMA samples would be used to test different isothermal moulding conditions and evaluate the performance of our nucleating agents in such isothermal conditions. The extruder was heated to 190°C and the screw rotation speed set to 100RPM. About 7g of compound were loaded to fill up the extruder. To do so, PLA pellets were mixed in a small container with the nucleating agent which came as a powder. The mixture was added in the extruder in such a way to have a similar and regular amount of powder with the pellets. Upon total addition, 5 mins were counted to ensure a good homogenous mixing of the compound before transferring it to the injection moulding device. For isothermal moulding conditions, three different mould temperatures were tested first: 95°C, 100°C and 110°C for PLA samples with a 1wt% of nucleating agent and held the sample inside the mould for 75s. Afterwards, a moulding temperature of 110°C was chosen and the composition of our samples was changed, namely, the amount of nucleating agent used was diminished, and also the moulding time was reduced from 75s to 25s which is the fastest time that can be reproducibly obtained using our apparatus. The idea here was to gather finer information about the

performance of our nucleating agents, how low could we go in terms of composition and how fast the injection moulding process could be to have highly crystallised PLA samples in favourable temperature conditions.

b. Preliminary study: mould temperature screening

Once the rectangular injection-moulded samples were obtained (Fig. II. 14), they were analysed by means of the DSC and dynamic mechanical analysis (DMA). The DSC analysis was used to measure the crystallinity ratio of the samples whereas the DMA was used to evaluate the thermo-mechanical behaviour of the considered samples. Indeed, in the case of PLA, the DMA gives a very good picture that reflects the low HDT. As shown in Fig. II. 15, highly amorphous PLA will display a huge drop of storage modulus (E') just after the temperature reaches 55-60°C.



Fig. II. 14: DMA samples of an injection moulded a) neat PLA, b) PLA + 1wt% Stear-C4 at 110°C for 75secs

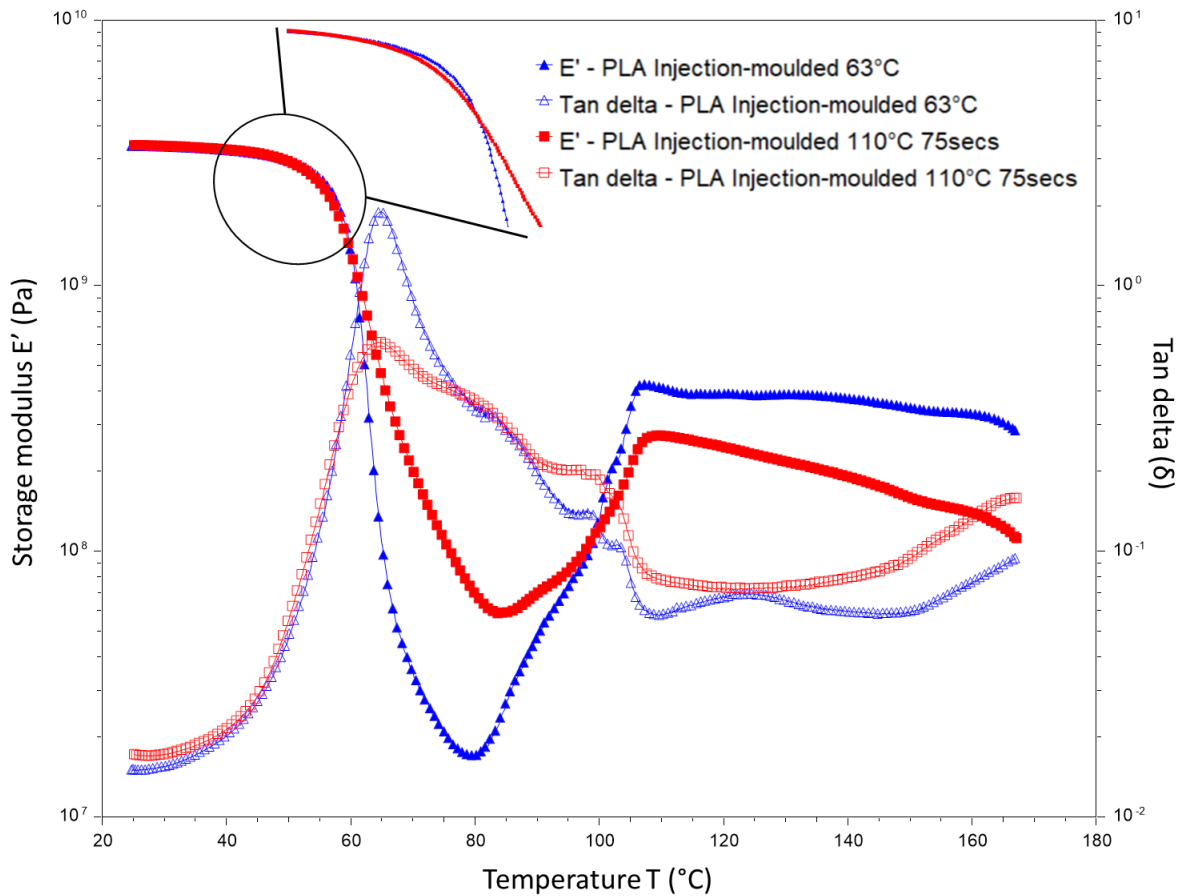


Fig. II. 15: Storage modulus (full symbols) and $\tan \delta$ (empty symbols) vs temperature (heating $3^\circ\text{C}/\text{min}$) of neat PLA injection moulded at 63°C (quenched - triangles) and 110°C for 1min 15s (hot - squares)

This is typical since the crystallisation kinetics of PLA are very slow, even though an optically pure grade of PLA that makes it semi-crystalline is used, PLA will not be able to crystallise during fast means of production such as injection moulding in a cold mould regarding the crystallisation temperature range of PLA. Therefore, as the temperature goes above the T_g of PLA, there will not be any crystalline segments holding the PLA chains, which are able to move between one another at such temperature. This leads to the observed fall of the storage modulus by more than a hundred-fold and the very high peak on $\tan \delta$. The increase later observed corresponds to the cold crystallisation of PLA starting around 80°C which can be verified using the DSC as shown in Fig. II. 16. The second sample represented in Fig. II. 15 is also PLA but injection-moulded at 110°C for 1min 15s which will be our reference time for preliminary testing of our nucleating agents. Here, the drop of modulus is not as strong as for the quenched amorphous sample thanks to a higher crystallinity ratio as shown in the data in Table II. 4.

Chapter 2

The so-called heat deflection temperature (HDT) is however incorrect since it was not measured according to any standards. Here, the temperature at which the storage modulus value is equal to a tenth of its value at 25°C is reported. Surprisingly, the onset temperature for the decrease of E' at the T_g is higher for the quenched PLA with the lower crystallinity ratio. We would have predicted the opposite since a higher onset temperature usually is proof of an increased thermal resistance, which is not the case here. We also did not expect to find the maximum of $\tan \delta$ at the same temperature; like the storage modulus temperature onset, we would have assumed a higher temperature for the more crystallised sample. However, when looking at the HDT criterion, a small increase from 63°C to 67°C could be noticed, which is nonetheless too low to make a real difference in terms of heat resistance. All in all, it seems just a 10% crystallinity ratio is insufficient to make a real difference for PLA in terms of thermal resistance and properties.

Fig. II. 16 gives us also an idea of the difference in thermal behaviour of the two samples. First of all, the cold crystallisation peaks differ since the one for the 110°C injection-moulded sample is narrower and starts at lower temperatures than the one for the 63°C injection-moulded PLA. Moreover, there is also a small exotherm present just before the melt endotherm in the 110°C moulded sample. This is known to be a solid-state transition from the α' form to the more stable α form of PLA prior to melting. This would suggest that our moulding will favour the creation of the α' crystalline form of PLA. This has been confirmed further by means of XRD (see Fig. II. 20 and Fig. II. 21).

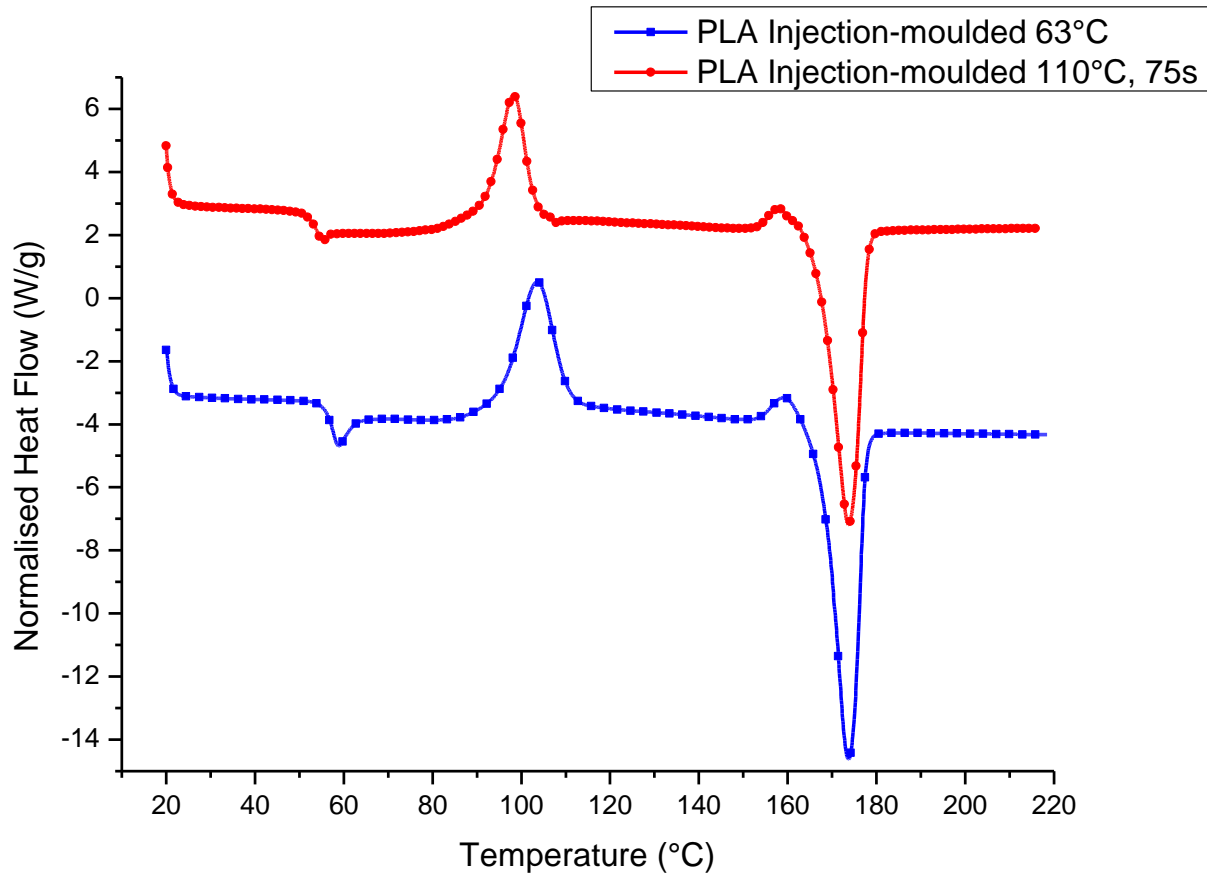


Fig. II. 16: DSC traces of PLA injection moulded at 63°C and 110°C for 1min 15s, 1st heating, 10°C/min

Table II. 4: DMA and DSC data for neat PLA moulded at 63°C and 110°C

Sample	Mould temperature (°C)	Onset E' (°C) ^a	Max tan δ (°C) ^a	HDT (°C) ^a	$\chi_{c,c}$ (%) ^b	T _g (°C) ^b	T _m (°C) ^b
Neat PLA	63	59.6	64.9	63	4	57	174
	110	56.7	64.5	67	15	54	174

a) DMA 25°C to 170°C 3°C/min – 1Hz – 0.1% strain, b) DSC 1st heating 20°C to 190°C, 10°C/min

At first, to test the efficiency of our nucleating agents, the composition was set to 99 parts of PLA and 1 part of NA per weight. The moulding time was set to 1min 15s and only the mould temperature was changed. The samples were analysed through the DSC and the DMA, and the results are reported in Table II. 5.

Table II. 5: Thermal and thermo-mechanical analysis of injection moulded samples in different isothermal conditions

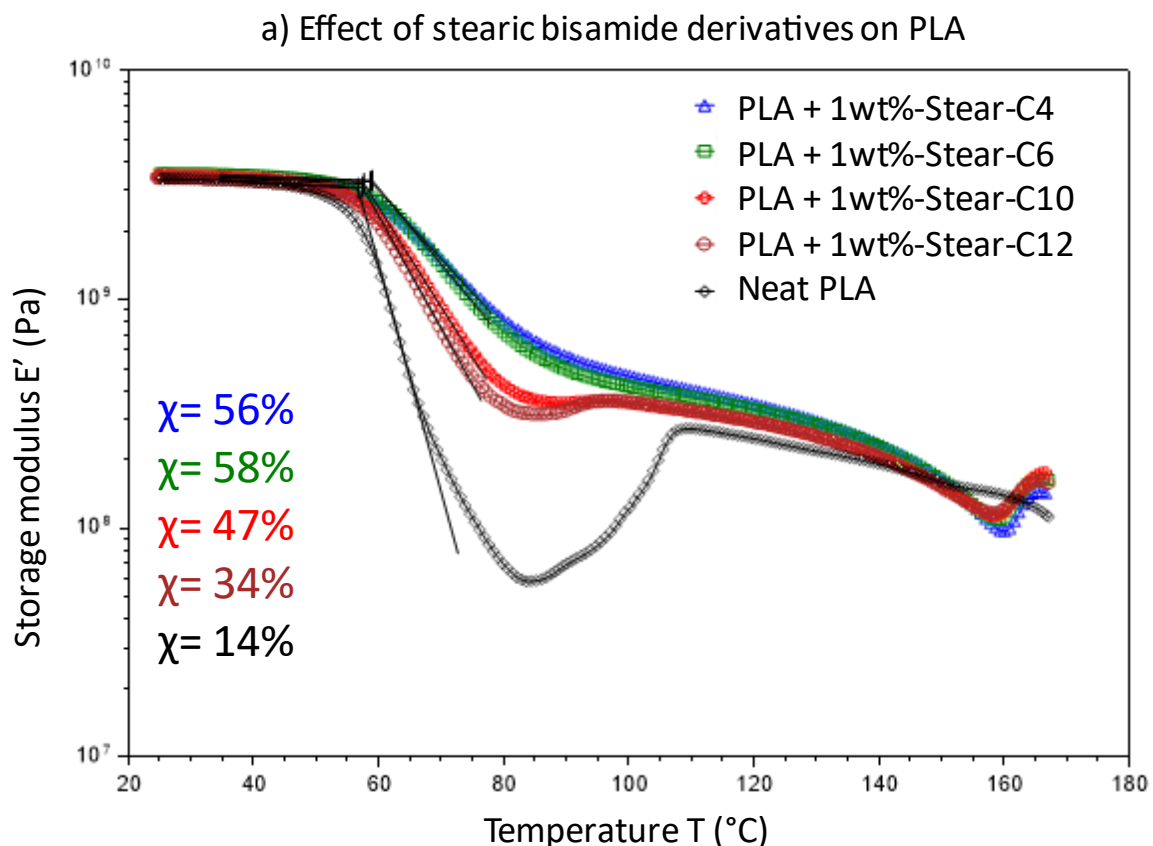
Fatty acid	Diamine	Temperature (°C)	Onset E' (°C) ^a	Max tan δ (°C) ^a	HDT (°C) ^a	$\chi_{c,c}$ (%) ^b	T _g (°C) ^b	T _m (°C) ^b
Stearic	C4	95	57.9	73.0	96	48	51	173
		100	58.1	73.8	102	48	51	172
		110	58.3	73.2	119	57	57	174
	C6	95	56.7	73.4	93	48	56	173
		100	57.2	72.5	103	47	51	173
		110	58.5	73.3	115	58	53	173
	C10	95	57.2	64.8	66	19	56	173
		100	58.1	67.2	78	35	55	172
		110	57.3	71.0	102	47	54	173
	C12	95	56.6	63.7	63	21	55	172
		100	57.7	65.9	73	24	61	173
		110	57.4	70.1	81	34	53	173
12-hydroxystearic	C4	95	58.0	65.6	65	20	55	172
		100	56.8	66.4	72	35	55	173
		110	58.7	73.5	107	51	53	174
	C6	95	56.3	64.3	66	28	53	173
		100	56.0	69.9	81	34	54	173
		110	57.4	72.7	105	51	54	174
	C10	95	56.7	63.4	63	20	55	172
		100	56.7	64.9	68	23	55	166
		110	56.8	66.0	73	28	55	173
	C12	95	57.1	63.5	63	27	56	173
		100	57.3	64.2	67	28	56	173
		110	56.0	68.8	79	47	52	173

a) DMA from 25°C to 170°C, 1Hz, 0.1% strain b) DSC 1st heating 20°C to 190°C, 10°C/min

The first observation that can be made is that the best moulding temperature is 110°C. Indeed, whatever the considered formulation, the highest crystallinity ratios were always measured when the sample had been made at 110°C. Along with the crystallinity ratio, the highest HDTs are obtained using the mould at that temperature for the different samples. More particularly, the best performance in terms of crystallisation rate were obtained with the shorter diamines, as expected from the DSC preliminary results. This is further confirmed by the values of HDT measured through the different samples. Samples with high crystallinity ratios gave high HDTs, which is consistent with the behaviour of a semi-crystalline polymer. The HDT is improved from 63°C for an amorphous PLA to 119°C in the best-case scenario (1wt% C4-Stear at 110°C), closely followed by the sample with 1wt% C6-Stear at 110°C, both samples respectively having crystallinity ratios of 57% and 58%. The trend with the other samples was expected: the lower the crystallinity ratio, the lower the HDT.

The importance of the melting point and crystallisation temperature of our nucleating agents was also shown. Globally, for the same fatty acid precursor of a bis-amide, the lower

the crystallisation temperature, the less efficient it will be regarding the nucleation efficiency. This is particularly verified in the case of the 12-hydroxystearic acid derivatives where the C12-12-HSA bis-amide exhibited a higher crystallisation point (136°C) than the C10-12-HSA bis-amide (125°C) and consequently gave samples with higher crystallinity ratios. Regarding the performance achieved by neat PLA, the onset temperatures for the storage moduli were slightly higher when high crystallinity ratios were achieved, around 59°C-60°C. More importantly, the temperature corresponding to the maximum value of the $\tan \delta$ curve shifted more significantly, now reaching values above 70°C compared to 65°C previously measured. Also, a slight shift of the T_g could be measured towards higher values in some cases but was not consistent with the measured crystallinity ratios. This was attributed to the bad thermal contact of the PLA sample in the DSC pan, which led to less pronounced thermal transitions during the first heating upon which the transitions were measured.



b) Effect of 12-HSA bisamide derivatives on PLA

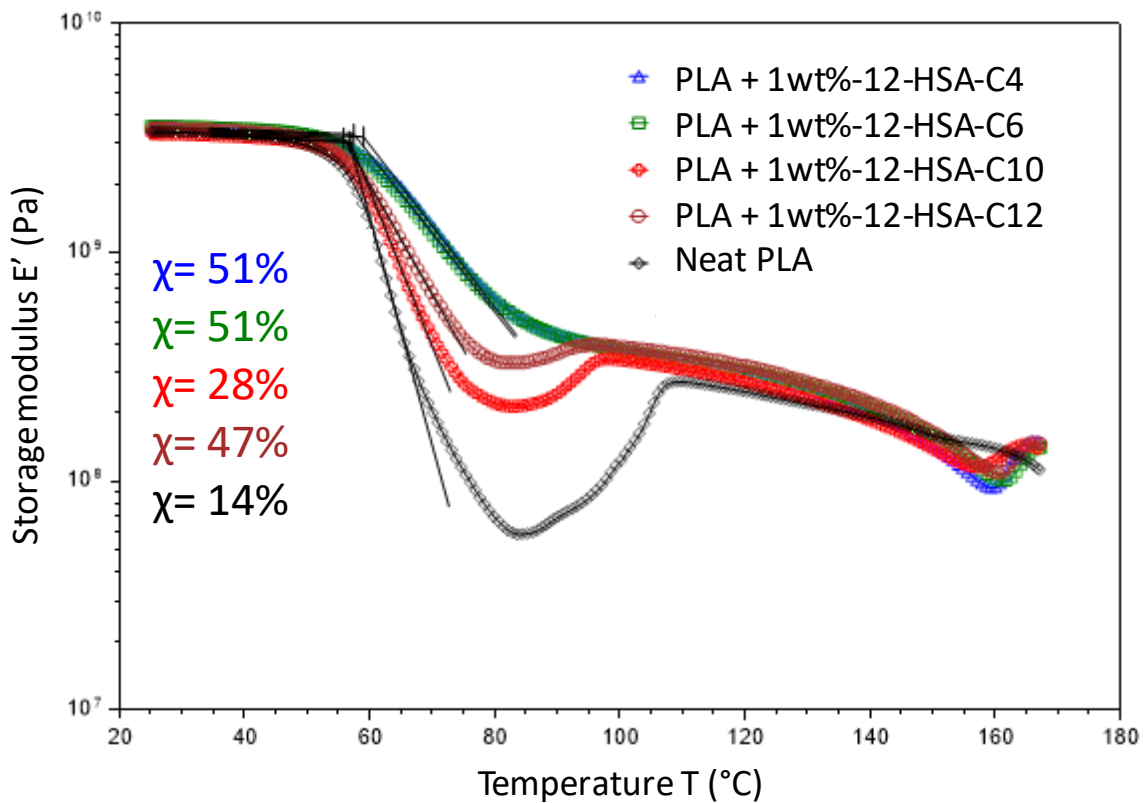


Fig. II. 17: Storage modulus vs temperature ($3^{\circ}\text{C}/\text{min}$ (heating rate) for injection-moulded samples at 110°C for 1min 15s of PLA mixed with 1wt% of: a) stearic acid derived bis-amides, b) 12-hydroxystearic derived bis-amides

Two DMA plots in Fig. II. 17 illustrate the performance of the 8 nucleating agents on the storage modulus of the samples *versus* the temperature. It is interesting to notice the effect of the crystallinity ratios on the thermo-mechanical behaviour of the samples at temperatures higher than the T_g of PLA. Compared to the PLA reference also moulded at 110°C , the fall of modulus is indeed being reduced thanks the crystalline zones within our PLA samples. Another noticeable behaviour is the higher the crystallinity ratio, the less the drop of the storage modulus. In the case of samples reaching over 50% crystallinity ratios, there was no pit shaped fall of storage modulus, accounting for a much better thermal resistance behaviour.

c. Optimisation: effect of time and loading

To further discriminate our nucleating agents, the composition of the samples was changed, namely, to diminish the amount of nucleating agent used to see whether there would be an effect on the crystallisation performance. Here, the focus was narrowed to the most efficient nucleating agents which are the four ones made from the C4- and the C6-diamines with either stearic acid or 12-hydroxystearic acid. Three new loadings, 0.1wt%, 0.5wt

and 0.8wt%, were tested, having already the data for a 1wt% loading. At the same time, a final optimisation was conducted by trying to reduce the moulding time. We tried to reduce as much as it was possible the amount of time the sample would be held in the mould at 110°C. Unfortunately, the fastest possible cycle was 25s since the samples had to be injected and removed by hand with no possibility of going any faster. The measured crystallinity ratios are displayed in Fig. II. 18.

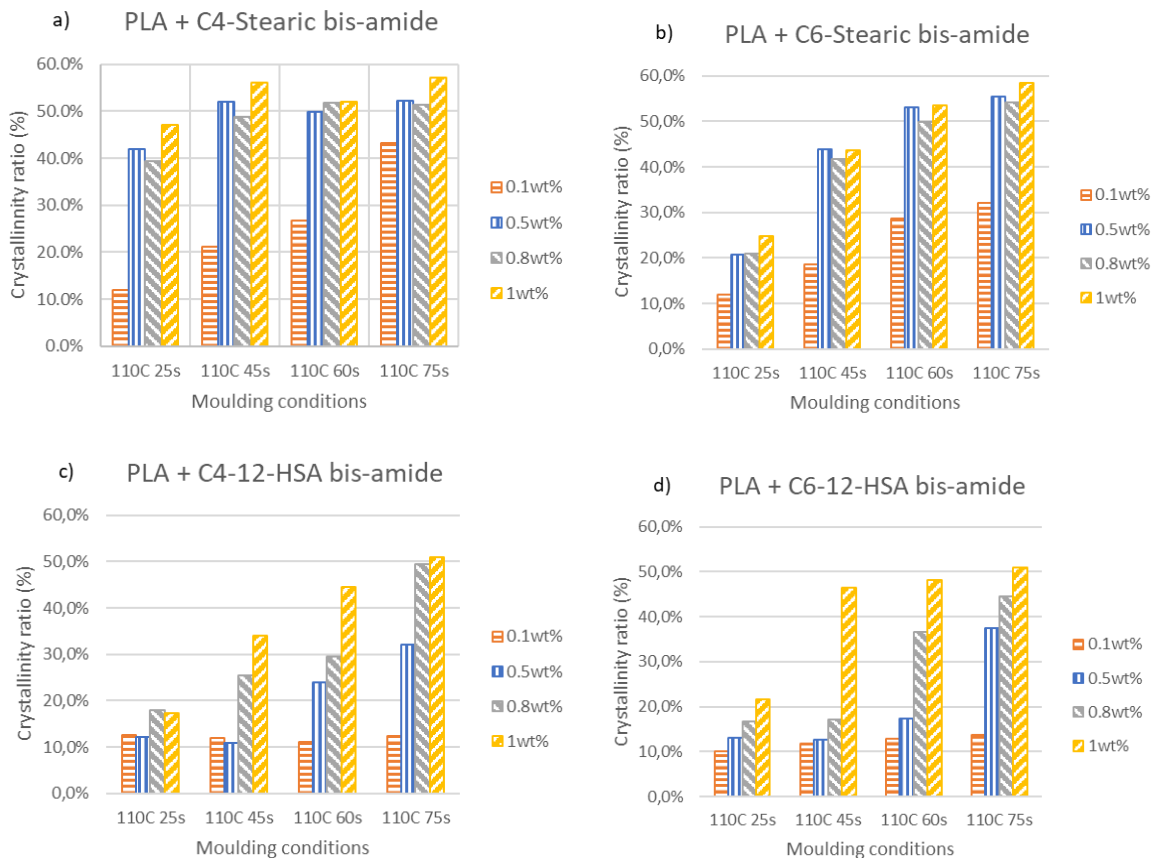


Fig. II. 18: Crystallinity ratios in the DSC at 10°C/min (1st heating) for 4 moulding times at 110°C and 4 sample compositions with a) C4-stearic bis-amides, b) C6-stearic bis-amides, c) C4-12-HSA bis-amides, d) C6-12-HSA bis-amides

For the C4-stearic bis-amide loaded samples, reducing the amount of nucleating agent had very little effect. Indeed, high crystallinity ratios near or above 50% were still obtained at loadings from 0.5wt% and over. This was also observed when the moulding time was reduced, namely, going down to 45s, the crystallisation rates were still nearing 50%. In the case of the shortest moulding time, 25s, there was a decrease in crystallinity ratio, this time averaging 40-45% depending on the loading. It is interesting to note that three loadings achieved rather similar performances, meaning this particular nucleating agent was indeed very efficient. In the case of a very small loading, 0.1wt%, a significant difference could be noticed in the

Chapter 2

crystallisation rate. Although it did increase with the moulding time, the crystallinity ratio still remained below 30% up to 60s. However, crystallinity ratios over 40% at 1min 15s of moulding time could be obtained, also showing that the C4-stearic bis-amide nucleating agent is indeed very efficient in promoting the crystallisation of PLA. Such performance was not achieved with the other considered nucleating agents. The second-best performing nucleating agent is the other stearic acid derived bis-amide molecule. Crystallinity ratios near and over 50% were achieved for loadings from 0.5wt% to 1wt% but at moulding time of 1min and over. In the case of a 45s moulding time, the crystallisation rate came down to 40% for these three loadings, again showing very little difference in behaviour between them. At the shortest moulding time however, the crystallinity ratio dropped to 20-25% for these three loadings, clearly indicating that such a short moulding time is insufficient using this nucleating agent. Considering the 0.1wt% loading samples, the maximum crystallisation rate was 32% during the longest moulding time and quickly decreased with the decrease in moulding time, showing this loading is too low for this nucleating agent.

Regarding the 12-HSA bis-amide samples, they achieved the lowest performances. At a 1wt% loading and long moulding times, high crystallinity ratios were obtained, however, they decreased rather quickly below 40% once the moulding time was shortened along with the loadings. Apart from the 1wt% loading, the crystallinity ratios quickly fell below 20% in the case of the C6-12-HSA bis-amide compound. A similar trend can be noticed for the C4-12-HSA bis-amide. Therefore, these nucleating agents really need to be used at high loadings and remain at 110°C for longer than the stearic based nucleating agents which was there considered as the best nucleating agents.

Table II. 6: HDTs and crystallinity ratios for samples moulded at 110°C for a) 25s, b) 45s, c) 60s & d) 75s

a)

Fatty acid	Diamine	Weight ratio	HDT (°C) ^a	$\chi_{c,c}$ (%) ^b
Stearic	C4	0.1	63	12
		0.5	104	42
		0.8	102	39
		1	111	47
	C6	0.1	62	12
		0.5	65	21
		0.8	66	21
		1	71	25
12-hydroxystearic	C4	0.1	62	13
		0.5	63	12
		0.8	63	18
		1	64	17
	C6	0.1	63	10
		0.5	64	13
		0.8	64	17
		1	64	22

b)

Fatty acid	Diamine	Weight ratio	HDT (°C) ^a	$\chi_{c,c}$ (%) ^b
Stearic	C4	0.1	68	21
		0.5	111	52
		0.8	110	49
		1	109	56
	C6	0.1	64	19
		0.5	98	44
		0.8	101	42
		1	104	44
12-hydroxystearic	C4	0.1	63	12
		0.5	63	11
		0.8	71	25
		1	77	34
	C6	0.1	64	12
		0.5	68	13
		0.8	66	17
		1	104	47

c)

Fatty acid	Diamine	Weight ratio	HDT (°C) ^a	$\chi_{c,c}$ (%) ^b
Stearic	C4	0.1	74	27
		0.5	114	50
		0.8	103	52
		1	123	52
	C6	0.1	71	29
		0.5	109	53
		0.8	106	50
		1	113	54
12-hydroxystearic	C4	0.1	64	11
		0.5	75	24
		0.8	78	29
		1	104	44
	C6	0.1	64	13
		0.5	69	17
		0.8	84	37
		1	99	48

d)

Fatty acid	Diamine	Weight ratio	HDT (°C) ^a	$\chi_{c,c}$ (%) ^b
Stearic	C4	0.1	94	43
		0.5	112	52
		0.8	110	51
		1	119	57
	C6	0.1	76	32
		0.5	106	56
		0.8	108	54
		1	115	58
12-hydroxystearic	C4	0.1	66	12
		0.5	80	32
		0.8	96	49
		1	107	51
	C6	0.1	66	14
		0.5	87	38
		0.8	96	45
		1	105	51

a) DMA from 25°C to 170°C, 1Hz, 0.1% strain b) DSC 1st heating 20°C to 190°C, 10°C/min

To further illustrate a direct consequence of a higher crystallinity ratio of PLA samples, DMA measurements were also made along with the DSC analysis and the results are reported in Table II. 6. Here, the interest is to see the evolution of the storage modulus curve and more importantly whether a big loss after the T_g of PLA could be noticed. This is reported through the HDT values, HDT values below 80°C account for a rather bad heat resistance of the sample. All these observations made previously are confirmed by the measured HDT criterion and whose values reported in Table II. 6. Here again, as previously observed, the higher the crystallinity ratio, the higher the HDT. HDTs near or above 100°C could be achieved with crystallinity ratios approaching or above 40-45%.

In Fig. II. 19, an illustration of the performance of the C4-stearic bis-amide nucleating agent is shown, regarding both the loading of the PLA sample and the moulding time. First, the effect of different moulding times using a very low loading of nucleating agent, 0.1wt% is displayed. The longer the sample stayed in the mould, the higher the crystallinity (shown using the DSC) but also the better its thermal behaviour. Directly linked to the crystallinity ratio, different behaviours are observed, namely, how the fall of modulus becomes less and less appearing when the crystallinity ratio increases. In the best-case scenario, a rather smooth profile is obtained for the most crystalline sample. On the second plot, the effect of the amount of this particular nucleating agent in PLA is shown. The shortest moulding time (25s) was tested on purpose, hoping the achieved thermal performance would remain at its best. As previously shown using DSC analysis, there is indeed very little difference between the highest loadings. Although the crystallinity ratios are slightly different (39% to 47%), the thermal behaviours are actually rather similar when looking at the graph. Logic is respected since a very small difference can be noticed as the more crystallised samples have slightly higher storage modulus values around 90°C . However, such a difference is not significant compared to the behaviour obtained with neat PLA, which could not be injection-moulded in such conditions.

The efficiency of the C4-Stear nucleating agent at very low loadings such as 0.1wt% is confirmed, since the HDT was significantly increased at moulding times of 1min15. Such performance could not be achieved with the other nucleating agents. Along this, at short moulding times, *e.g.* 25s, only the samples made with C4-Stearic bis-amide at more than 0.5wt% loading exhibit high HDTs above 100°C along with crystallinity ratios above 40%. Samples with C6-Stearic bis-amide display the same behaviour from 45s of moulding time

onwards. In the case of 12-hydroxystearic based bis-amides, HDT values above 100°C could only be achieved at high loadings (1wt%) and at moulding times over 1min, accounting for the lesser performance of such nucleating agents.

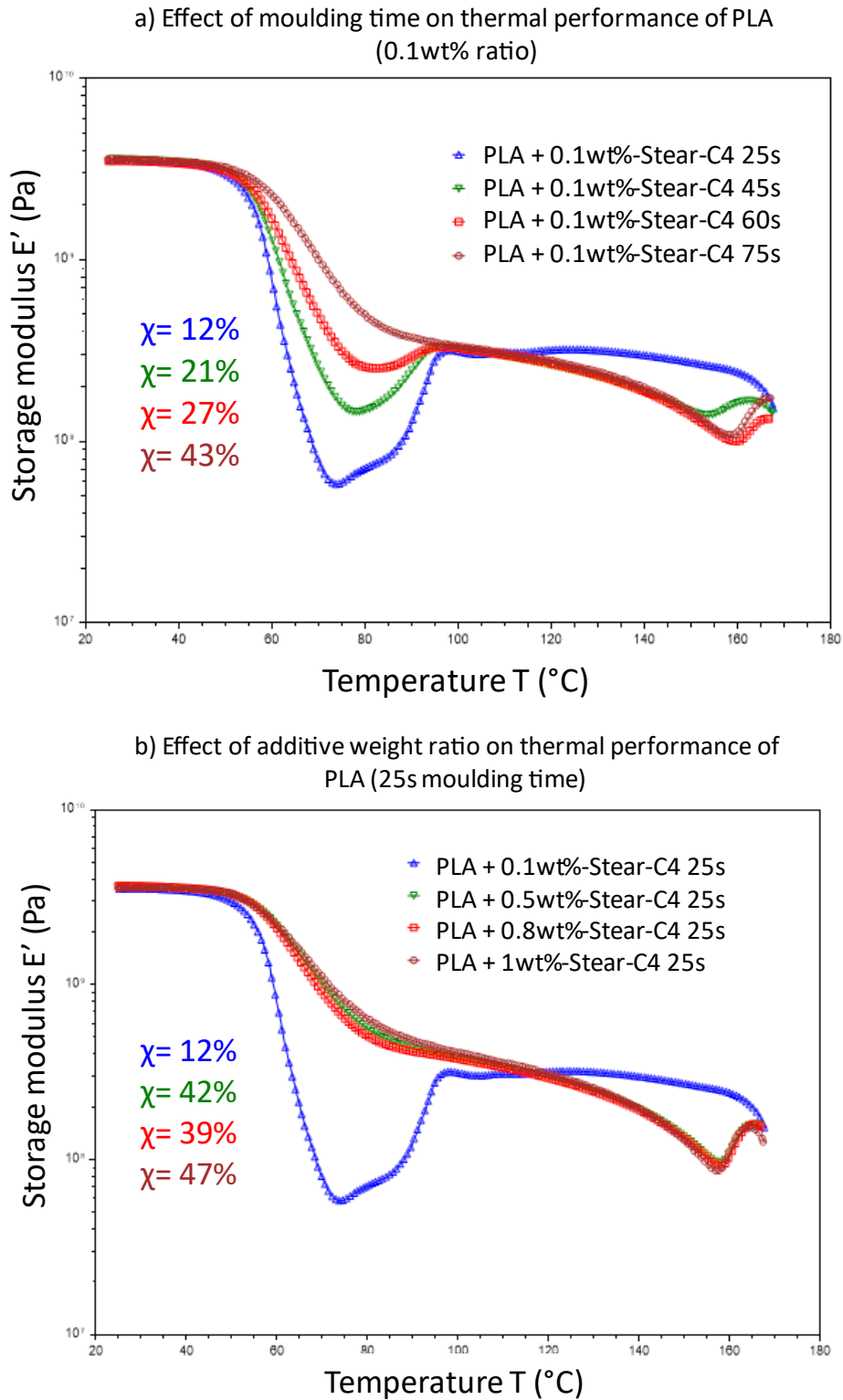


Fig. II. 19: Storage modulus vs temperature of PLA samples loaded with C4-stearic bis-amide. a) Effect of the moulding time on the thermal behaviour of the PLA samples, b) Effect of the nucleating agent loading

Regarding the aspect of the curves after the fall of modulus, two behaviours can be noticed, one regarding the 0.1wt% loaded samples and the other samples. The storage modulus for the 0.1wt% loaded samples increases strongly due to the cold crystallisation and then reaches a plateau which lasts until the melting point of PLLA near 170°C. In the case of the other samples, this plateau does not really exist, and the storage modulus continues to decrease until 160°C, then increases sharply and then starts to decrease again. This is due to the fact that the 0.1wt% loaded sample will form preferentially the α phase of PLLA during the cold crystallisation. In the case of the other samples, the α' of PLLA has been preferentially formed. This phase has a lower melting point than the α phase, therefore explaining the decrease of storage modulus. The sharp increase at 160°C corresponds to the α' to α transition which results in more material remaining crystallised. Eventually, the storage modulus starts to drop around 170°C as the melting point of the α phase is reached.

d. Crystallographic structure

The PLA samples with 1wt% of nucleating agent made from either stearic acid or 12-hydroxystearic acid based nucleating agents and injection moulded at 110°C for 75s were put through a wide-angle X-ray scattering (WAXS) analysis to confirm the preferential PLA crystalline form obtained. As a reference, a neat PLA sample moulded in the same conditions (but with a very low crystallinity ratio) and a neat PLA sample which was kept at 110°C for 10min were also analysed in the same way.

The corresponding diffractograms are reported in Fig. II. 20 and Fig. II. 21. All PLA samples show reflections corresponding to the α' phase (200/110) and (203) with no or very small (010) or (210) reflection corresponding to the α crystalline structure of PLA³⁴⁻³⁶. The latter was only noticed in the neat PLA sample held for 10 mins at 110°C and very slightly for PLA+1wt%-C4-Stear. This is expected since PLA preferentially crystallises in the α' form at 110°C when cooled from the melt, although it is reported that the α form may also be conjointly formed at this temperature^{6,35}. This is also in accordance with the small exotherm observed on DSC thermograms before the melting endotherm (Fig. II. 16). Indeed, this exotherm is characteristic of an α' to α transition upon heating and further emphasises the presence of the α' crystalline form into our crystallised samples^{34,35,37}. Moreover, using the Debye-Scherrer equation on the (200/110) peaks, it was possible to calculate the average size of the crystallites using the full width at half-maximum (Table II. 7).

$$\tau = \frac{K \times \lambda}{\beta \times \cos(\theta)}$$

With:

- K = the Scherrer constant , 0.89
- λ = X-ray source wavelength, 1.5418 Å
- β = the full width at height maximum (rad)
- θ = the Bragg peak angle (rad)

Table II. 7: Crystallite size of crystallised PLA samples using the (200/110) peak in XRD

Fatty acid	Diamine	Bragg angle (2 θ)	FWHM	Crystallite size (nm)
PLA 75 secs	-	16.5384	0.32807	24.2
PLA 10 mins	-	16.6770	0.3374	23.6
Stearic	C4	16.6308	0.33001	24.1
	C6	16.6308	0.32866	24.2
	C10	16.5846	0.3239	24.5
	C12	16.6308	0.3325	23.4
12-hydroxystearic	C4	16.5384	0.35123	22.6
	C6	16.5846	0.32121	24.7
	C10	16.6308	0.32619	24.4
	C12	16.6308	0.32646	24.3

The calculated crystallite size shows no great difference between the samples, which was not expected since the use of nucleating agents would have been thought to diminish the crystallite size.

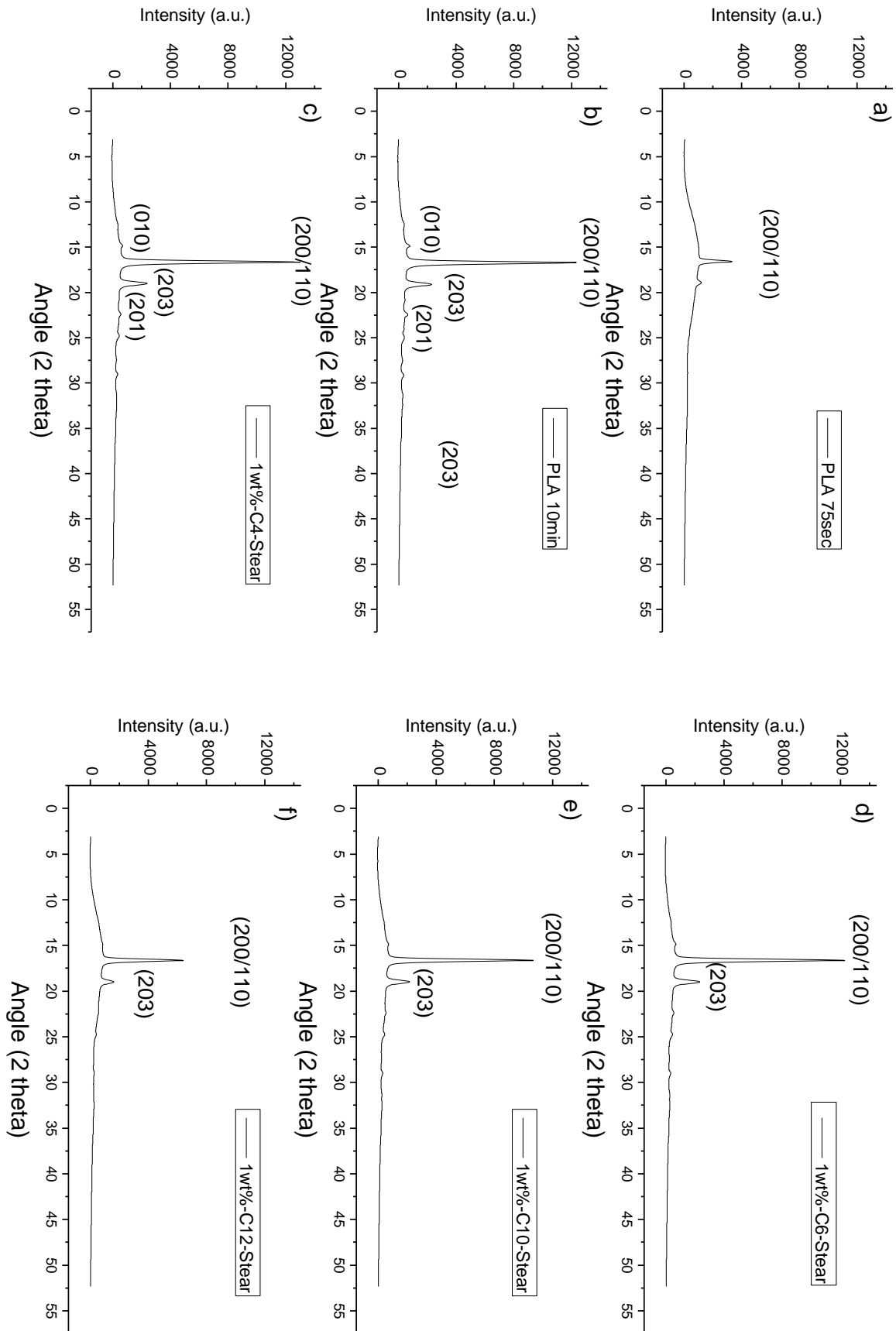


Fig. II. 20: WAXD traces of injection moulded samples at 110°C: a) PLA 75sec, b) PLA 10mins, c) PLA+1wt%-C4-Stear, d) PLA+1wt%-C6-Stear, e) PLA+1wt%-C10-Stear & f) PLA+1wt%-C12-Stear

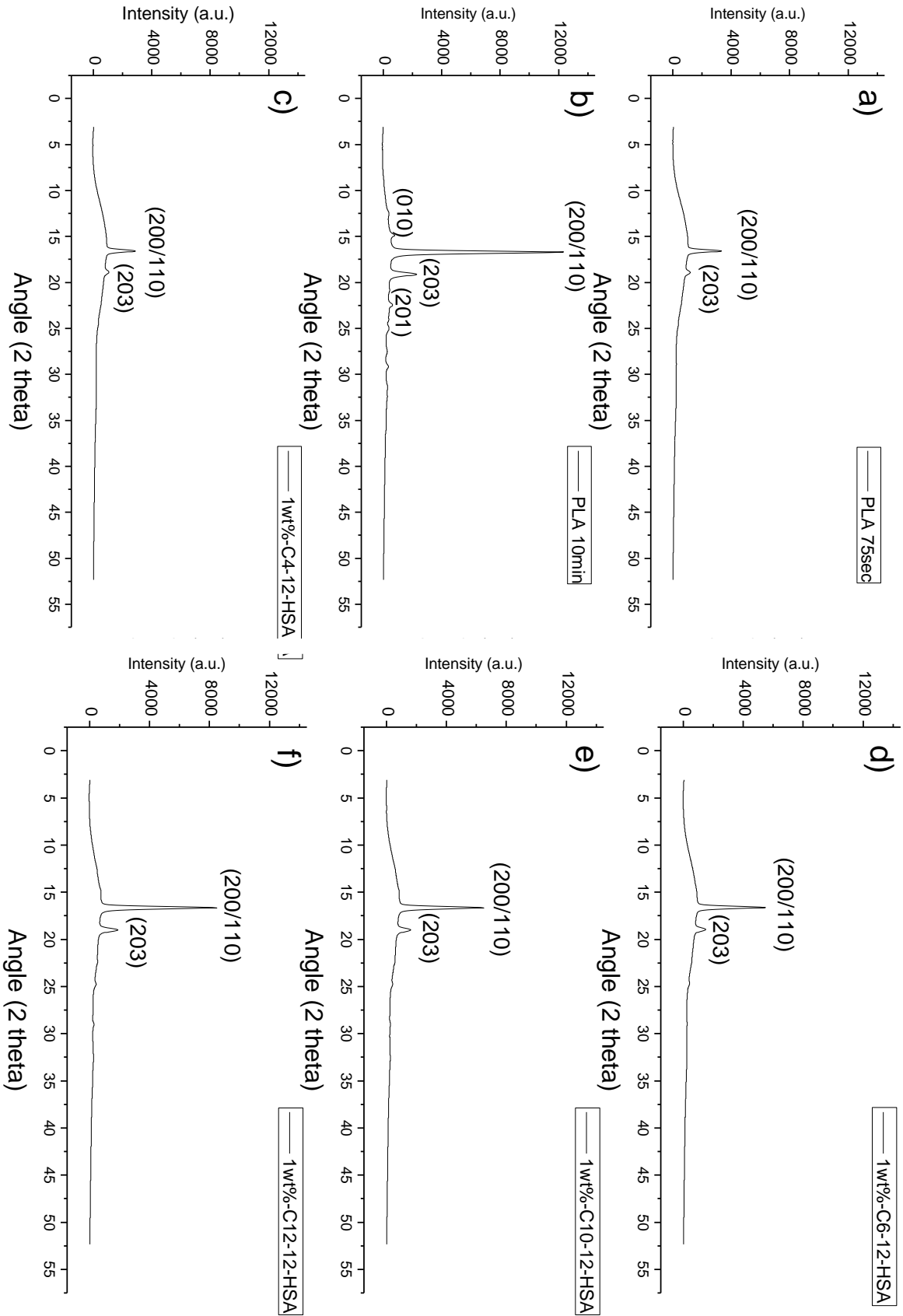


Fig. II. 21: WAXD traces of injection moulded samples at 110°C: a) PLA 75sec, b) PLA 10mins, c) PLA+1wt%-C4-12-HSA, d) PLA+1wt%-C6-12-HSA, e) PLA+1wt%-C10-12-HSA & f) PLA+1wt%-C12-12-HSA

4. Conclusion and perspectives

In this part, we developed and used different nucleating agents derived from C18 fatty acids and linear aliphatic diamines. Using a thermal process, the corresponding bis-amide compounds were synthesised and through DSC analysis, discriminated the different compounds regarding their ability to enhance the crystallisation kinetics of PLA.

The most efficient bis-amides are the ones obtained from stearic acid or 12-hydroxystearic acid using 1,4-diaminobutane or 1,6-diaminohexane which showed the highest melting and crystallisation points. In particular, the C4-Stear bis-amide exhibited the best performance when mixed with PLA. Using it, the highest crystallisation ratios over 50% were achieved along with the highest heat deflection temperature nearing 120°C (as previously defined per our standards). Considering these facts, it has been decided to use the four most efficient nucleating agents to produce PLA cups, through a mini-industrial injection moulding process, to measure macroscopic properties. Namely, the primary focus will be on the gas barrier properties of the obtained cups along with their resistance to vertical compression.

The production part will be further developed in the upcoming chapters, however, for the sake of understanding, it will be briefly described here. To produce our PLA cups in the shape of a small cup, a master batch with the designated nucleating agent at a 6wt% loading in neat PLA was first made using a twin-screw extruder. This master batch was then diluted with neat PLA to obtain the three targeted compositions: 0.5wt%, 0.75% and 1wt%. The compounds were obtained under the form of small pellets. These pellets were dried and then put in a Babyplast mini-injection moulding machine equipped with a specifically designed mould to obtain our cups. The mould is divided into two parts: a mobile part cooled by a cold-water circulation and a still part which can be heated to a set temperature. Our idea was to find injection moulding conditions to produce PLA samples with high crystallinity ratios straight away. Unfortunately, it turned out that the temperature differential in the mould would make it impossible to achieve. The mobile part of the mould would always remain too cold to allow the compounds to crystallise. When the temperature of the still part was increased, we observed a discrepancy on the cups. Indeed, the bottom part of the sample exposed to the hotter part of the mould would crystallise whereas on the other hand, the top part of the containers would remain amorphous as they would be exposed to the colder part of the

Chapter 2

mould. Increasing the moulding time and the temperature only led to samples which would not be ejected or worse, would start melting again due to the high temperatures used.

Unfortunately, to still be able to go on with our initial project, it has been decided to produce these cups using so-called “cold moulding conditions” *i.e.*, to make amorphous cups, which will be thermally annealed later to obtain samples with different crystallinity ratios only due to the nucleating agent used. Again, while performing the thermal annealing, it was not possible to find conditions in the oven which would be both reproducible and discriminatory between the different samples. Thanks to the nucleating agents, the crystallisation happens in a very narrow temperature range and rather sharply, which meant the annealing time would depend on how long the oven would take to equilibrate once the samples had been loaded (which could not be anticipated) rather than imposing a defined annealing time from the start. Therefore, the temperature exposure of the samples could not be controlled and led to annealed samples which did suffer the same thermal treatment.

As a general perspective, it would be interesting to test these formulations in an injection moulding machine in which it is possible to better control the mould temperature. This would allow to get suitable temperatures to trigger the crystallisation of the samples and evaluate the performance of these nucleating agents in industrial production processes.

5. Experimental & SI

5.1. Materials

PLA was purchased from Natureplast (Caen, FR) under the tradename PLI 005 (D-lactide<0.5%, MFI=25-35g/10min at 190°C). 1,6-diaminohexane, 1,5,7-triazabicyclo[4,4,0]dec-5-ene and stearic acid were purchased from Sigma-Aldrich. 12-hydroxystearic acid and 1,4-diaminobutane were purchased from Alfa Aesar. 1,10-diaminododecane, 1,12-diaminododecane and oleyl chloride (70%) were purchased from TCI used without purification. Methyl ricinoleate was purchased from Nu-Chek-Prep (MN, USA) with a purity over 99% and were used without any further purification.

5.2. Purification

1,6-diaminohexane was recrystallised in cyclohexane prior to use for synthesis. An insoluble white solid could be found, in which case it was removed by filtration of the hot cyclohexane. The purified product was dried under slight reduced pressure for 12h.

5.3. Synthesis of bis-amides from acyl chlorides – Schotten-Baumann procedure

C4-Oleic: 146.5mg of 1,4-diaminobutane (1.66mmol) were put in 10mL of dichloromethane upon which 10mL of an aqueous solution of NaOH(aq) at 1mol/L were added under low stirring. 1.176g (3.35mmol) of oleyl chloride (85% pure) were slowly added using a syringe directly into the organic phase at room temperature and left for 2h. The obtained white powder was washed with dichloromethane, water and diethyl ether and left to dry under reduced pressure for 12h at 80°C. Yield=32%.

C6-Oleic: 193.1mg of 1,6-diaminohexane (1.66mmol) were put in 10mL of dichloromethane upon which 10mL of an aqueous solution of NaOH(aq) at 1mol/L were added under low stirring. 1.176g (3.35mmol) of oleyl chloride (85% pure) were slowly added using a syringe directly into the organic phase at room temperature at left for 2h. The obtained white powder was washed with dichloromethane, water and diethyl ether and left to dry under reduced pressure for 12h at 80°C. Yield=37%.

C10-Oleic: 286.3mg of 1,10-diaminododecane (1.66mmol) were put in 10mL of dichloromethane upon which 10mL of an aqueous solution of NaOH(aq) at 1mol/L were added under low stirring. 1.176g (3.35mmol) of oleyl chloride (85% pure) were slowly added using a syringe directly into the organic phase at room temperature at left for 2h. The obtained white

Chapter 2

powder was washed with dichloromethane, water and diethyl ether and left to dry under reduced pressure for 12h at 80°C. Yield=67%.

C12-Oleic: 332.9mg of 1,12-diaminododecane (1.66mmol) were put in 10mL of dichloromethane upon which 10mL of an aqueous solution of NaOH(aq) at 1mol/L were added under low stirring. 1.176g (3.35mmol) of oleyl chloride (85% pure) were slowly added using a syringe directly into the organic phase at room temperature and left for 2h. The obtained white powder was washed with dichloromethane, water and diethyl ether and left to dry under reduced pressure for 12h at 80°C. Yield=66%.

5.4. Synthesis of bis-amides from carboxylic acids

C4-Stearic: 7.901g of 1,4-diaminobutane (89.6mmol) and 51g (179.3mmol) of stearic acid were put in a 500mL round bottom flask with magnetic stirring at 150°C for 24h. The obtained brown solid was ground into a powder and washed 5 times with 400mL of ethanol and left to dry under reduced pressure for 12h at 80°C to give a white slightly brown powder. Yield=92%.

C6-Stearic: 5.106g of 1,6-diaminohexane (43.94mmol) and 25g (87.88mmol) of stearic acid were put in a 250mL round bottom flask with magnetic stirring at 150°C for 24h. The obtained brown solid was ground into a powder and washed 3 times with 400mL of ethanol and left to dry under reduced pressure for 12h at 80°C. Yield=88%.

C10-Stearic: 302.94mg of 1,10-diaminododecane (1.758mmol) and 1g (3.515mmol) of stearic acid were put in a 25mL round bottom flask with magnetic stirring at 150°C for 6h under vacuum. The obtained brown solid was ground into a powder and washed 3 times with 20mL of tetrahydrofuran and left to dry under reduced pressure for 12h at 80°C to give a white slightly brown powder. Yield=69%.

C12-Stearic: 352.15mg of 1,12-diaminododecane (3.515mmol) and 1g (1.758mmol) of stearic acid were put in a 500mL round bottom flask with magnetic stirring at 150°C for 6h under vacuum. The obtained brown solid was ground into a powder and washed 3 times with 20mL of tetrahydrofuran and left to dry under reduced pressure for 12h at 80°C to give a white slightly brown powder. Yield=53%.

C4-12-HSA: 2.567g of 1,4-diaminobutane (29.12mmol) and 17.5g (58.24mmol) of 12-hydroxystearic acid were put in a 100mL round bottom flask with magnetic stirring at 150°C for 24h. The obtained brown solid was ground into a powder and washed 5 times with 200mL

of ethanol and left to dry under reduced pressure for 12h at 80°C to give a white slightly brown powder. Yield=75%.

C6-12-HSA: 3.38g of 1,6-diaminohexane (29.12mmol) and 17.5g (58.24mmol) of 12-hydroxystearic acid were put in a 100mL round bottom flask with magnetic stirring at 150°C for 24h. The obtained brown solid was ground into a powder and washed 3 times with 200mL of ethanol and left to dry under reduced pressure for 12h at 80°C to give a white slightly brown powder. Yield=77%.

C10-12-HSA: 286.7mg of 1,10-diaminodecane (1.664mmol) and 1g (3.328mmol) of 12-hydroxystearic acid were put in a 25mL round bottom flask with magnetic stirring at 150°C for 24h under vacuum. The obtained brown solid was ground into a powder and washed 3 times with 20mL of ethanol and twice with 20mL of tetrahydrofuran and left to dry under reduced pressure for 12h at 80°C to give a white slightly brown powder. Yield=59%.

C12-12-HSA: 333.4mg of 1,12-diaminododecane (1.664mmol) and 1g (3.328mmol) of 12-hydroxystearic acid were put in a 25mL round bottom flask with magnetic stirring at 150°C for 31h under vacuum. The obtained brown solid was ground into a powder and washed 3 times with 20mL of ethanol and twice with 20mL of tetrahydrofuran and left to dry under reduced pressure for 12h at 80°C to give a white slightly brown powder. Yield=65%.

5.5. Synthesis of bis-amides from methyl esters

C4-Ricinoleic: 500 mg of methyl ricinoleate, 93.0mg of 1,4-diaminobutane and 44.6mg of TBD (1:0.5:0.2, molar ratios) were put in a Schlenk tube with a condenser and a magnetic stirrer at 120°C for 3h then under vacuum for 1h at 120°C. The white solid was recuperated and washed with 50mL of water and 15mL of cold ethanol. Yield=30%.

C6-Ricinoleic: 1g of methyl ricinoleate, 185.9mg of 1,6-diaminohexane and 89.1mg of TBD (1:0.5:0.2, molar ratios) were put in a Schlenk tube with a condenser and a magnetic stirrer at 120°C for 3h then under vacuum for 1h at 120°C. The solid was recuperated and washed with 50mL of water and 15mL of cold ethanol. Yield=25%.

C10-Ricinoleic: 1g of methyl ricinoleate, 275.3mg of 1,10-diaminodecane and 89.1mg of TBD (1:0.5:0.2, molar ratios) were put in a Schlenk tube with a condenser and a magnetic

Chapter 2

stirrer at 120°C for 3h then under vacuum for 1h at 120°C. The solid was recuperated and washed with 15mL of cold ethanol. Yield=29%.

C12-Ricinoleic: 1g of methyl ricinoleate, 320.6mg of 1,12-diaminododecane and 89.1 mg of TBD (1:0.5:0.2, molar ratios) were put in a Schlenk tube with a condenser and a magnetic stirrer at 120°C for 3h then under vacuum for 1h at 120°C. The solid was recuperated and washed with 15mL of cold ethanol. Yield=35%.

5.6. Sample preparation PLA + nucleating agent for DSC

PLA pellets were dried for at least 12h under reduced pressure at 80°C. For the DSC preliminary study, the pellets and the nucleating agent were put together in a small aluminium container on hot plate set at 200°C. Once the two compounds had melted, they were stirred together using a metal spatula until the mixture looked smooth. The aluminium container was then put on the cold practice bench to cool. The total mixing time did not exceed 3 mins in order to limit the degradation of the PLA. A small sample of about 6mg was then cut from the obtained compound to be used for DSC analysis.

5.7. Sample preparation of PLA with nucleating agents for the DMA

PLA pellets were dried for at least 12h under reduced pressure at 80°C. About 7g of total compound was introduced in the Thermoscientific Minilab II HAAKE Rheomex CTW5 twin screw mini compounder with a recirculating canal. The mixing speed was set to 100RPM in corotation mode and the mixing time of about 5 min at 183°C. The mixture was then transferred into a hot cylinder and injected under 400bars into a mould warmed to the desired temperature using a Thermoscientific HAAKE MiniJet Pro apparatus.

References

1. Kalb, B. & Pennings, A. J. General crystallization behaviour of poly(l-lactic acid). *Polymer* **21**, 607–612 (1980).
2. Miyata, T. & Masuko, T. Crystallization behaviour of poly(l-lactide). *Polymer* **39**, 5515–5521 (1998).
3. Saeidlou, S., Huneault, M. A., Li, H. & Park, C. B. Poly(lactic acid) crystallization. *Prog. Polym. Sci.* **37**, 1657–1677 (2012).
4. Lehermeier, H. J., Dorgan, J. R. & Way, J. D. Gas permeation properties of poly(lactic acid). *J. Membr. Sci.* **190**, 243–251 (2001).
5. Drieskens, M. *et al.* Structure versus properties relationship of poly(lactic acid). I. Effect of crystallinity on barrier properties. *J. Polym. Sci. Part B Polym. Phys.* **47**, 2247–2258 (2009).
6. Cocca, M., Lorenzo, M. L. D., Malinconico, M. & Frezza, V. Influence of crystal polymorphism on mechanical and barrier properties of poly(l-lactic acid). *Eur. Polym. J.* **47**, 1073–1080 (2011).
7. Guinault, A., Sollogoub, C., Ducruet, V. & Domenek, S. Impact of crystallinity of poly(lactide) on helium and oxygen barrier properties. *Eur. Polym. J.* **48**, 779–788 (2012).
8. Fernandes Nassar, S. *et al.* Multi-scale analysis of the impact of polylactide morphology on gas barrier properties. *Polymer* **108**, 163–172 (2017).
9. Nam, J. Y. *et al.* Morphology and crystallization kinetics in a mixture of low-molecular weight aliphatic amide and polylactide. *Polymer* **47**, 1340–1347 (2006).
10. Xing, Q., Zhang, X., Dong, X., Liu, G. & Wang, D. Low-molecular weight aliphatic amides as nucleating agents for poly (L-lactic acid): Conformation variation induced crystallization enhancement. *Polymer* **53**, 2306–2314 (2012).
11. Xing, Q. *et al.* Tailoring crystallization behavior of poly (l-lactide) with a low molecular weight aliphatic amide. *Colloid Polym. Sci.* **293**, 3573–3583 (2015).
12. Chen, L. & Dou, Q. Influence of the combination of nucleating agent and plasticizer on the non-isothermal crystallization kinetics and activation energies of poly(lactic acid). *J. Therm. Anal. Calorim.* **139**, 1069–1090 (2020).
13. Saitou, K. & Yamaguchi, M. Transparent poly(lactic acid) film crystallized by annealing beyond glass transition temperature. *J. Polym. Res.* **27**, 104 (2020).
14. Takenaka, A. *et al.* Manufacturing method of biodegradable resin molding. (2007).
15. Onishi, H. & Morishita, K. Polylactic acid resin composition and resin molded article thereof. (2016).
16. Hill, R. & Walker, E. E. Polymer constitution and fiber properties. *J. Polym. Sci.* **3**, 609–630 (1948).
17. Stempfle, F., Ortman, P. & Mecking, S. Long-Chain Aliphatic Polymers To Bridge the Gap between Semicrystalline Polyolefins and Traditional Polycondensates. *Chem. Rev.* **116**, 4597–4641 (2016).
18. Hendel, S. *Organic Chemistry, 6th Edition [Prentice Hall: Sixth edition]*.
19. Bennett, C. & Mathias, L. J. Linear Unsaturated Polyamides: Nylons 6 u18 and 18 u18. *Macromol. Chem. Phys.* **205**, 2438–2442 (2004).
20. Pardal, F. *et al.* Unsaturated Polyamides from Bio-Based Z-octadec-9-enedioic Acid. *Macromol. Chem. Phys.* **209**, 64–74 (2008).
21. Desroches, M., Caillol, S., Auvergne, R., Boutevin, B. & David, G. Biobased cross-linked polyurethanes obtained from ester / amide pseudo- diols of fatty acid derivatives synthesized by thiol –ene coupling. *Polym. Chem.* **3**, 450–457 (2012).
22. Allen, C. L., Chhatwal, A. R. & Williams, J. M. J. Direct amide formation from unactivated carboxylic acids and amines. *Chem. Commun.* **48**, 666–668 (2011).
23. Lanigan, R. M. & Sheppard, T. D. Recent Developments in Amide Synthesis: Direct Amidation of Carboxylic Acids and Transamidation Reactions: Recent Developments in Amide Synthesis. *Eur. J. Org. Chem.* **2013**, 7453–7465 (2013).
24. Piazza, G. J., Bistline, R. G., Bilyk, A., Fearheller, S. H. & Haas, M. J. A novel technique for the preparation of secondary fatty amides II: The preparation of ricinoleamide from castor oil. *J. Am. Oil Chem. Soc.* **70**, 727–729 (1993).
25. Sabot, C., Kumar, K. A., Meunier, S. & Mioskowski, C. A convenient aminolysis of esters catalyzed by 1,5,7-triazabicyclo[4.4.0]dec-5-ene (TBD) under solvent-free conditions. *Tetrahedron Lett.* **48**, 3863–3866 (2007).
26. Pramanik, S., Sagar, K., Konwar, B. K. & Karak, N. Synthesis, characterization and properties of a castor oil modified biodegradable poly(ester amide) resin. *Prog. Org. Coat.* **75**, 569–578 (2012).

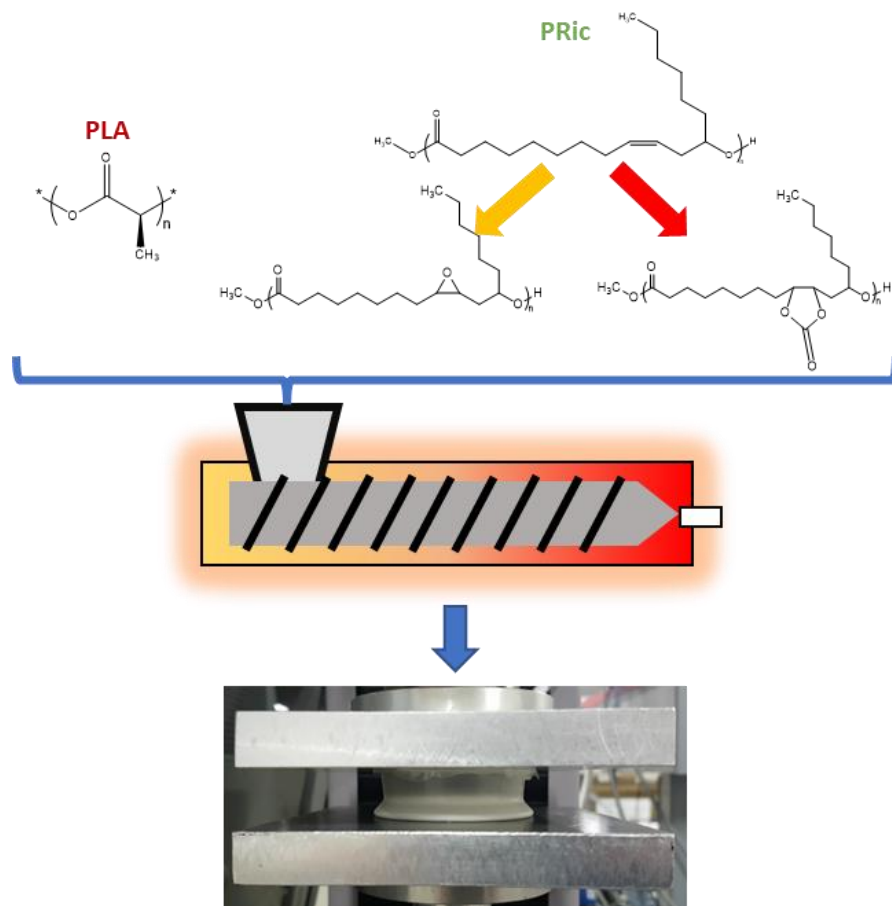
Chapter 2

27. Lebarbé, T., Grau, E., Alfos, C. & Cramail, H. Fatty acid-based thermoplastic poly(ester-amide) as toughening and crystallization improver of poly(l-lactide). *Eur. Polym. J.* **65**, 276–285 (2015).
28. Zhang, R. *et al.* A practical and sustainable protocol for direct amidation of unactivated esters under transition-metal-free and solvent-free conditions. *Green Chem.* (2021) doi:10.1039/D1GC00720C.
29. Sato, K. Crystallization behaviour of fats and lipids — a review. *Chem. Eng. Sci.* **56**, 2255–2265 (2001).
30. Himawan, C., Starov, V. M. & Stapley, A. G. F. Thermodynamic and kinetic aspects of fat crystallization. *Adv. Colloid Interface Sci.* **122**, 3–33 (2006).
31. Poopalam, K. D., Raghunanan, L., Bouzidi, L., Yeong, S. K. & Narine, S. S. The anomalous behaviour of aliphatic fatty diamides: Chain length and hydrogen bonding interactions. *Sol. Energy Mater. Sol. Cells* **201**, 110056 (2019).
32. Vasanthakumari, R. & Pennings, A. J. Crystallization kinetics of poly(l-lactic acid). *Polymer* **24**, 175–178 (1983).
33. De Santis, F., Pantani, R. & Titomanlio, G. Nucleation and crystallization kinetics of poly(lactic acid). *Thermochim. Acta* **522**, 128–134 (2011).
34. Wasanasuk, K. & Tashiro, K. Crystal structure and disorder in Poly(l-lactic acid) δ form (α' form) and the phase transition mechanism to the ordered α form. *Polymer* **52**, 6097–6109 (2011).
35. Zhang, J., Tashiro, K., Tsuji, H. & Domb, A. J. Disorder-to-Order Phase Transition and Multiple Melting Behavior of Poly(L-lactide) Investigated by Simultaneous Measurements of WAXD and DSC. *Macromolecules* **41**, 1352–1357 (2008).
36. Zhu, R., Zheng, R., Fu, L., Li, Z. & Yan, C. Thermal stability of poly(l-lactide) α' crystals and its blocking effect on perfection of α crystals. *Mater. Today Commun.* **23**, 100900 (2020).
37. Zhang, J. *et al.* Crystal Modifications and Thermal Behavior of Poly(l-lactic acid) Revealed by Infrared Spectroscopy. *Macromolecules* **38**, 8012–8021 (2005).

Chapter III:

Use of poly(methyl ricinoleate) (PRic) and its derivatives as additives for PLA

Toughening effect and modification of gas barrier properties



Contents

Global Introduction	150
Part A: Synthesis of a well-controlled and defined PRic from a 99% pure monomer	155
1. PRIC-LCPO and its derivatives as additives for PLA	155
1.1. Synthesis and characterisation	155
a. Synthesis.....	155
b. Characterisation	156
1.2. Chemical modification: epoxidation of the alkene function.....	159
a. Synthesis.....	159
b. Characterisation	160
2. Melt-blending with PLA: towards improved mechanical and gas barrier properties.	166
2.1. Melt-blending and injection moulding process	166
2.2. Structural characterisation.....	167
2.3. Thermal characterisation	169
2.4. Morphology through SEM.....	170
2.5. Vertical compression testing.....	173
2.6. Oxygen barrier properties.....	180
3. Discussion and conclusion	183
4. Experimental & SI	184
4.1. Synthesis of PRic-LCPO	184
4.2. Synthesis and purification of PRic-LCPO-EXX.....	184
4.3. SEM analysis	184
4.4. Vertical compression testing.....	185
4.5. Oxygen permeability measurement.....	185

Part B: Use of the industrial PRic grade	187
1. PRIC-100 and its derivatives as additives for PLA	187
1.1. Characterisation of PRic-100	187
a. Structure	187
b. Thermal analysis	190
1.2. Epoxidation of PRic-100	190
a. Synthesis	190
b. Characterisation	190
1.3. Carbonatation of epoxidized PRic-100	194
a. Synthesis	194
b. Characterisation	195
2. Melt-blending with PLA: study of the mechanical and gas barrier properties	200
2.1. Structural characterisation	200
2.2. Thermal characterisation	202
2.3. Morphology through SEM	203
2.4. Vertical compression testing	207
a. PLA + PRic-100	208
b. PLA + PRic-100-EXX	209
c. PLA + PRic-100-Carbonate	212
2.5. Oxygen barrier properties	215
3. Discussion and conclusions	219
4. Experimental & SI	221
Comparison between both PRic grades	223
General conclusion and perspectives	225
References	227

Global Introduction

In the previous chapter, the focus was put on one major drawback of PLA, which is its low crystallisation kinetics. The use of nucleating agents allowed this issue to be overcome and therefore gain a better thermal resistance for PLA materials.

Here, another inherent problem of PLA, its brittleness at room temperature is addressed. Since the T_g of PLA is reported around 55°C, PLA is in its glassy state at room temperature, which is characterised by its high brittleness. In order to make PLA suitable for uses at room temperature, many different strategies have been imagined and reported such as the use of plasticisers, blending with a ductile polymer or copolymerisation¹⁻⁶. One common toughening strategy is typically to mix a “soft”, low T_g polymer with the “hard” brittle polymer, in our case the PLA. Previous work from the LCPO and ITERG by Lebarbé *et al.* showed the high efficiency of a bio-based polymer toughening agent that is the poly(methyl ricinoleate) or PRic. Such polymer is a fatty polyester bearing an alkene function in the 9-10 position, in the *cis* configuration and a six-carbon atom dangling chain on the twelfth carbon atom. Such structure is responsible for PRic being a low T_g amorphous polymer, opposite to its hydrogenated counterpart the poly(12-hydroxystearate) which is semi-crystalline due to the absence of the alkene moiety^{7,8}. Their first strategy was to synthesise novel PLLA-*b*-PRic-*b*-PLLA copolymers, which showed highly improved mechanical properties. The tensile strain at break would improve from 5% to nearly 100% by including 13wt% of PRic in the block copolymer and would therefore give a ductile material⁵. They later discovered that directly mixing pure PRic with PLA through a melt-blending process would be sufficient at loadings such as 10wt%⁹. Here, not only would the samples display a tensile strain at break of nearly 200%, the PRic would also act as a crystallisation booster with reported crystallinity ratios above 40% with a subsequent improvement of its thermal behaviour.

In this chapter, the focus is put on the use of PRic as an additive for PLA with regard to macroscopic properties such as the mechanical and the gas barrier properties, more particularly the O₂ barrier behaviour. PRic is a bio-based polymer obtained from the polycondensation of ricinoleic acid (*i.e.* 12-hydroxy-9-*cis*-octadecenoic acid) or methyl ricinoleate (*i.e.* methyl 12-hydroxy-9-*cis*-octadecenoate)⁷, derived from castor oil either

through its hydrolysis or methanolysis, respectively. A possible composition of the fatty derivatives found in castor oil is reported in Table III. 1.

Table III. 1: Castor oil fatty acid composition

Fatty acid	Molecular formula	Percentage (%)
Palmitic acid	$C_{16}H_{32}O_2$	0.8 - 1.1
Stearic acid	$C_{18}H_{36}O_2$	0.7 – 1.0
Oleic acid	$C_{18}H_{34}O_2$	2.2 – 3.3
Linoleic acid	$C_{18}H_{32}O_2$	4.1 – 4.7
Linolenic acid	$C_{18}H_{30}O_2$	0.5 – 0.7
Ricinoleic acid	$C_{18}H_{34}O_3$	87.7 – 90.4

Thankfully, the content of ricinoleic acid in castor oil is very high and rather constant^{10,11}, therefore allowing the easy purification of ricinoleic acid as the starting material for polycondensation. The particularity of ricinoleic acid is to bear an alkene function on its main chain along with a dangling chain of five methylene groups and one terminal methyl group and a hydroxyl group (Fig III. 1). Such structure allows this monomer or its methyl ester derivative to polymerise through polycondensation, giving the PRic, a polyester with an alkene group and a dangling chain on every repeat unit giving a “comb-shaped” structure (Fig III. 2).

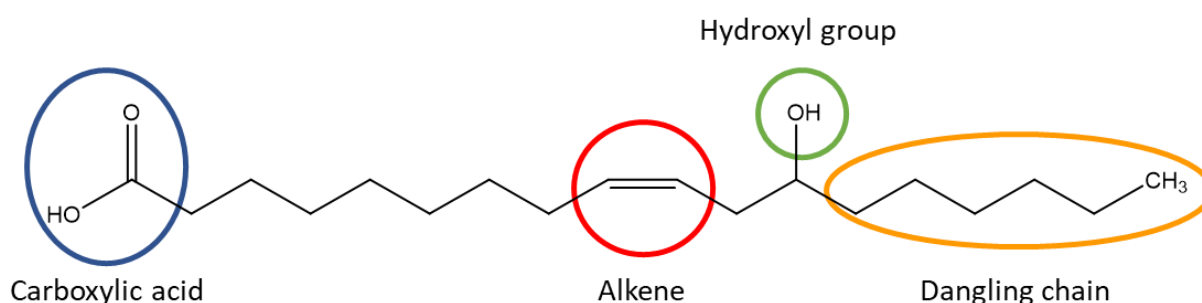


Fig III. 1: Structure of ricinoleic acid with its chemical features

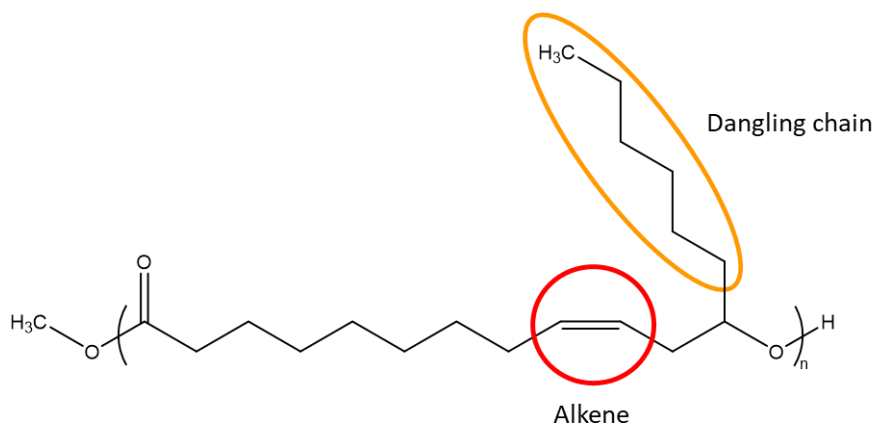


Fig III. 2: Structure of poly(methyl ricinoleate)

The strategy of this study has been to start from a neat PRic as an additive for PLA and then assess the mechanical and gas barrier properties of the obtained material. Then, taking advantage of the available alkene function, the PRic was chemically modified. Again, the mechanical and gas barrier properties were evaluated, hoping the new chemical functions such as epoxides and cyclic carbonates would have an effect on the gas barrier properties without affecting the toughening effect observed with the addition of neat PRic in PLA.

This work has been done using two different grades of PRic and therefore the following chapter was divided into two parts. First, a homemade PRic from an over 99% pure methyl ricinoleate monomer which allowed attaining 5-digit molar masses, Mw around 20,000g/mol. Second, an industrially available PRic, synthesised, purified and supplied by the ITERG, based on methyl ricinoleate that was only 85% pure. The molar mass of this grade is subsequently lower, Mw around 5200g/mol, due to the presence of multiple other fatty acid methyl esters bearing no hydroxyl group and therefore acting as chain stoppers of the polycondensation (Fig III. 3 and Table III. 2). In the case of this particular grade, smaller chains are present which can have an effect on the interfacial compatibility as their lower molar mass can render them more soluble in PLA and therefore allow them to act as compatibilizers.

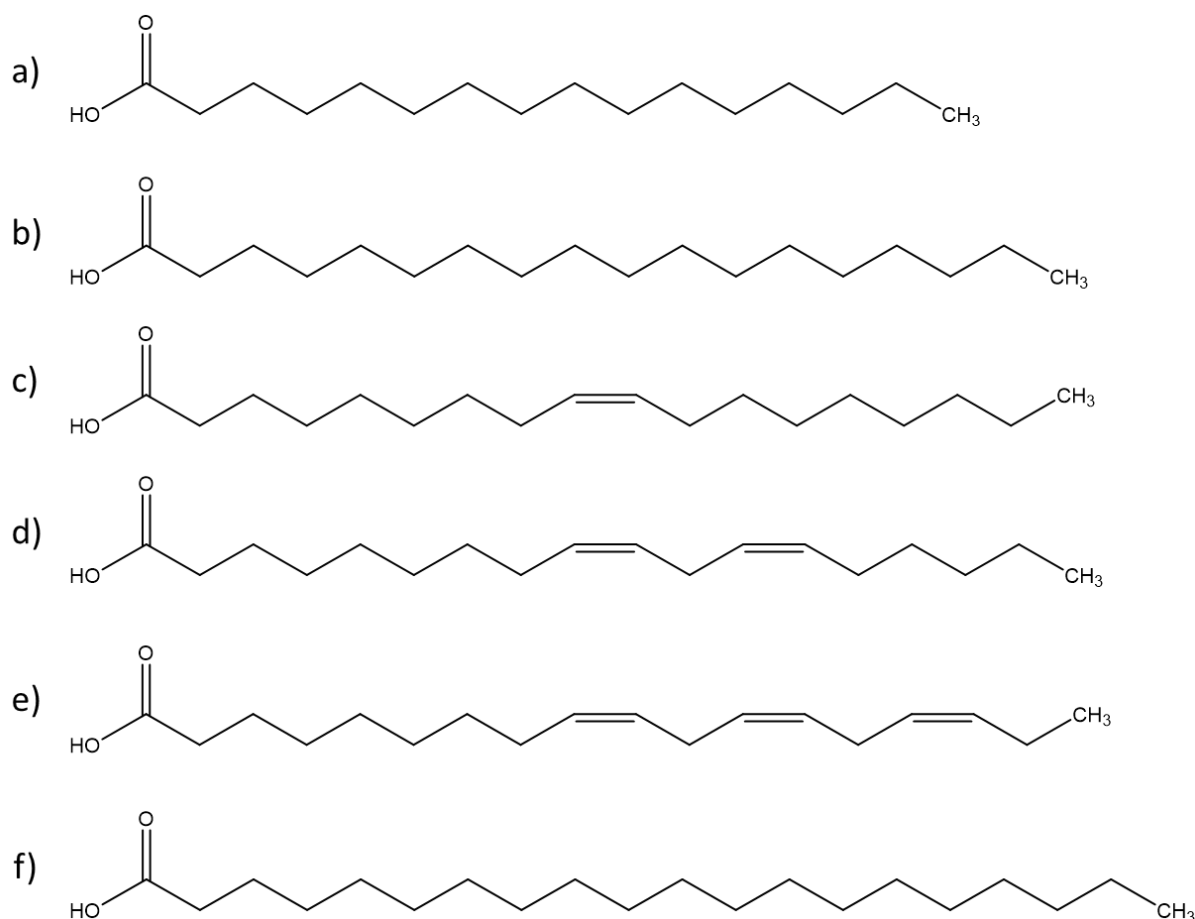


Fig III. 3: Possible fatty acids in castor oil: a) Palmitic acid, b) Stearic acid, c) Oleic acid, d) Linoleic acid, e) Linolenic acid and f) Arachidic acid

Table III. 2: Composition of the refined castor oil used at ITERG for the synthesis of PRic

Fatty acid	Molecular formula	Percentage (%)
Palmitic acid	$C_{16}H_{32}O_2$	1.1
Stearic acid	$C_{18}H_{36}O_2$	10.1
Oleic acid	$C_{18}H_{34}O_2$	
Ricinoleic acid	$C_{18}H_{34}O_3$	86.3
Arachidic acid	$C_{20}H_{40}O_2$	0.9

Since the efficiency of the PRic from the ITERG is already known to greatly toughen PLA⁹, the study will not only compare the difference in mechanical performance of the PRic produced by the ITERG and the PRic produced in the lab, but also look at the O₂ permeability properties of the obtained samples.

Also, since PRic bears an alkene group on every repeat unit, the idea is to take advantage of that chemical function and, through alkene chemistry, bring new chemical moieties to the

Chapter 3

PRic and assess the effect of these chemical moieties. As described by Mutlu and Meier, there are several possibilities available to modify PRic using alkene chemistry such as oxidation, hydrogenation, epoxidation, halogenation, sulfonation or metathesis¹². Here, the first considered reaction is the epoxidation since it can allow multiple other reactions afterwards such as carbonatation, hydrogenation, hydration, amine addition etc. Once the epoxidized derivatives were obtained, many reactions were attempted to take advantage of the epoxide group's chemistry. However, most of these tests were unsuccessful, the only reaction working without any trouble being the carbonatation reaction yielding cyclic carbonates. Again, the presence of cyclic carbonate groups might also have an effect of the O₂ permeability of the material. Furthermore, as shown by Ren *et al.*, this can open the path towards novel cross-linked materials such as NIPUs though the reaction of a primary amine with the formed cyclic carbonate to yield a hydroxyurethane group¹⁴.

Part A: Synthesis of a well-controlled and defined PRic from a 99% pure monomer

In this first part, a highly pure monomer was used to synthesise the PRic thereafter called PRic-LCPO. This was decided in order to aim for higher molar masses than the ones that are obtained with the commercial PRic from ITERG and therefore compare the effect of having a PRic with higher molar masses and also a higher degree of purity.

1. PRIC-LCPO and its derivatives as additives for PLA

1.1. Synthesis and characterisation

a. Synthesis

The synthesis of PRic was inspired from the one reported by Dworakowska *et al.*⁷ and Méheust *et al.*⁸ from works conducted at the LCPO. They chose the synthetic path using methyl ricinoleate (>99%, Nu-chek Prep.) as the starting monomer and titanium (IV) isopropoxide as the catalyst of the transesterification reaction (Fig III. 4). Through this path, methanol is produced and can be removed by the use of vacuum to shift the equilibrium towards the formation of the polymer. The reaction was monitored by means of ¹H NMR and SEC to follow both the conversion of the methyl ester groups and the hydroxyl groups and the evolution of the molar mass of the synthesised polymer. Using 1wt% of catalyst, Mw values above 20,000 g/mol could be obtained in 8 hours at 180°C but with a dispersity of 3.1 due to the occurrence of side reactions.

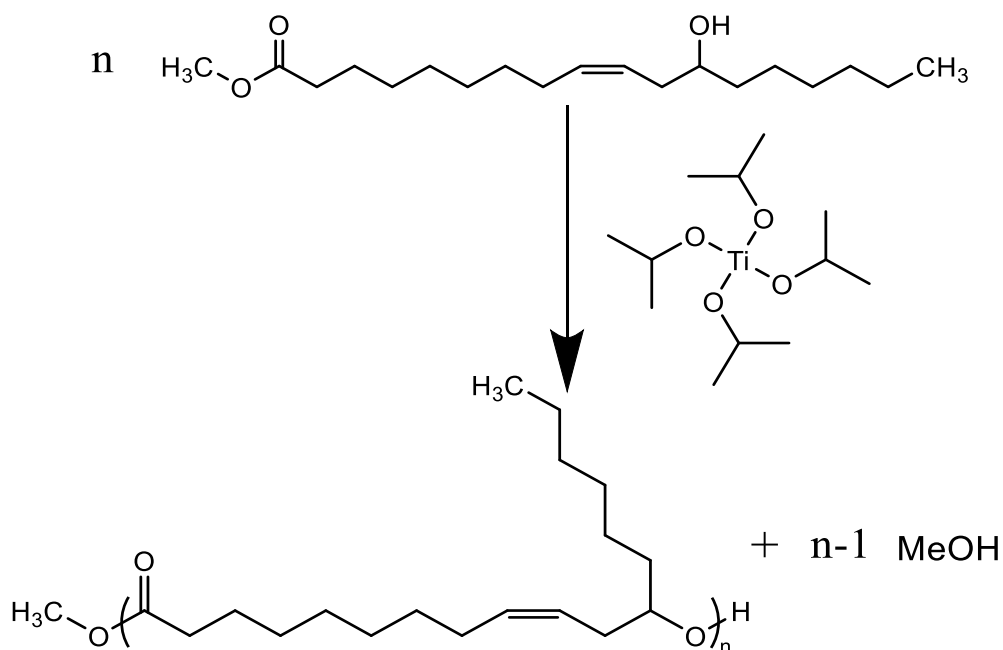


Fig III. 4: Synthetic path to PRic from methyl ricinoleate

In this case, the same procedure was used, with the exception that the quantity of catalyst was diminished down to 0.5wt%. This was due to the fact that during preliminary experiments, side reactions would occur too much, as mentioned previously, and an effort was made to try to limit them. The reaction time subsequently increased to reach the same target Mw around 20,000 g/mol. No purification was conducted following the synthesis.

b. Characterisation

The synthesised polymer was analysed by means of the ^1H NMR, the SEC in THF and the DSC. ^1H NMR allowed the monitoring of the conversion of the methyl ester functions along with the hydroxyl groups using the H_a protons as the reference ($-\text{CH}_3$, t, 0.8ppm). The ^1H NMR spectra of the monomer and the synthesised PRic are given in Fig III. 5. Among the things that can be noticed, first, the signal for the protons H_h shift from 3.6 ppm to 4.9 ppm (denoted H_h') as a result of the formation of an ester bond. The signal for the protons H_i corresponding to the methyl ester protons, also diminishes thanks to the transesterification and the release of methanol. Finally, the signal for the protons denoted H_e and H_f overlap due to the formation of the new ester function. The alkene protons H_j and H_k also shift from respectively from 5.4 ppm and 5.6 ppm to 5.3 and 5.5 ppm as result of the change of the electronic environment.

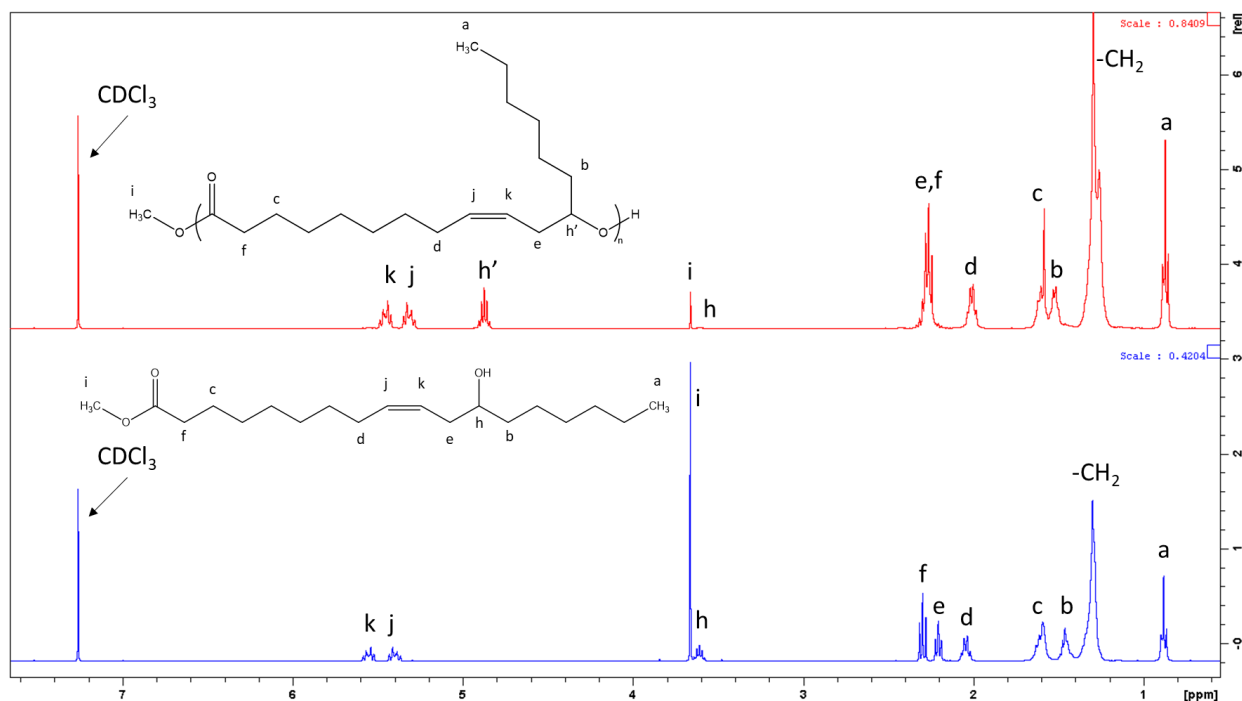


Fig III. 5: ^1H NMR spectra of Me-Ric (blue, bottom) and PRic-LCPO (red, top)

The integration values also allow to approximate a theoretical M_n using Carothers' equation¹⁵ which goes as such:

$$M_n = M_0 * \frac{1}{1 - p}$$

With M_0 the molar mass of the repeat unit (280.4 g/mol) and p the conversion.

Here, to evaluate p , three different integration values can be chosen from the peaks corresponding to the protons H_h , H_i or $H_{h'}$. The values of these integrals and the calculated M_n using Carothers' equation are reported in Table III. 3.

Table III. 3: Calculation of the theoretical M_n of PRic-LCPO using ^1H NMR in CDCl_3

Proton Peak	Start	End	% change	M_n theory (g/mol)	\bar{D} theory
H_i	2.8636	0.1607	94.4	5000	1.94
H_h	0.9689	0.0338	96.5	8000	1.97
$H_{h'}$	0	0.9271	92.7	3900	1.93

The calculation of the theoretical M_n through this method gives a relatively wide range of molar mass from 4,000 g/mol to 8,000 g/mol. The dispersity is also supposed to be strictly inferior to 2, as $D=1+p$. Also, it is necessary to take into account that the integration values of

H_h and H_i include the chain ends and the residual monomer, therefore, using the H_h integration value would be more accurate. The average molar mass (M_n and M_w) values obtained by the SEC in THF against a PS standard are reported in Table III. 4 along with the chromatogram in Fig III. 6.

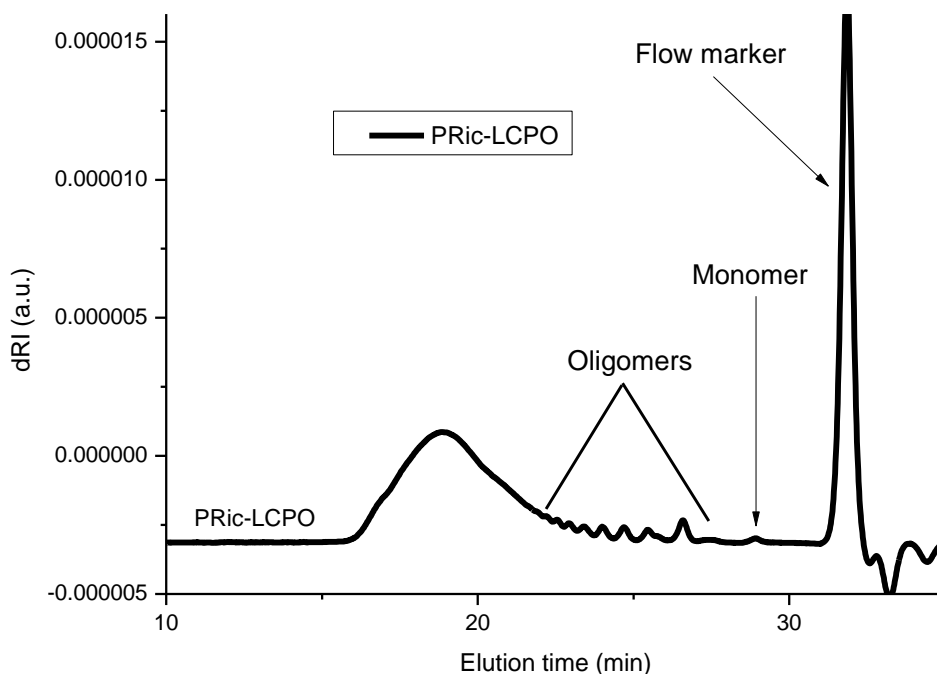


Fig III. 6: SEC chromatogram of PRic-LCPO, THF, PS standard

Table III. 4: Calculated average molar masses of PRic-LCPO using the SEC, THF, PS standard

PRic grade	M_n (g/mol)	M_w (g/mol)	\bar{D}
LCPO	5900	24000	4.1

First, the SEC chromatogram reveals very little residual monomer, which proves the efficiency of the polymerisation. However, the molar masses are higher than the ones expected using the ^1H NMR. Indeed, first the M_n is up nearly 6,000 g/mol and more importantly, the M_w is up to 24,000 g/mol with a dispersity over 4. This clearly indicates the presence of side reactions as reported by Dworakowska *et al.*⁷ even when trying to diminish them using less catalyst. This could be due to the increased reaction time (15h vs 8h). Finally, the thermal properties of PRic-LCPO were assessed using the DSC. The thermal signature of

an amorphous polymer is observed with no melting endotherm or crystallisation exotherm, the T_g is measured at -72°C , which is in accordance with the literature^{7,8}.

1.2. Chemical modification: epoxidation of the alkene function

a. Synthesis

Taking advantage of the alkene function on every repeat unit of PRic, a post-functionalisation was conducted to form a secondary epoxy group. The synthesis was first inspired from the procedure used by Bertho *et al*¹⁶ for their epoxidation procedure of *cis*-1,4-polybutadiene using *meta*-chloroperoxybenzoic acid (*m*-CPBA). Other procedures involving *m*-CPBA are reported for the epoxidation of unsaturated polyesters¹⁷, but the study by Ren *et al.* was of particular interest. In this study, the authors synthesised PRic with M_n values between 2,100 g/mol and 3,200 g/mol with low dispersity values between 1.5 and 1.8. They then used *m*-CPBA to epoxidize their PRic and then convert them into cyclic carbonates and then used a diamine to synthesise cross-linked polyhydroxyurethanes (PHUs)¹⁴. It was decided to use the same procedure corresponding to the reaction scheme in Fig III. 7.

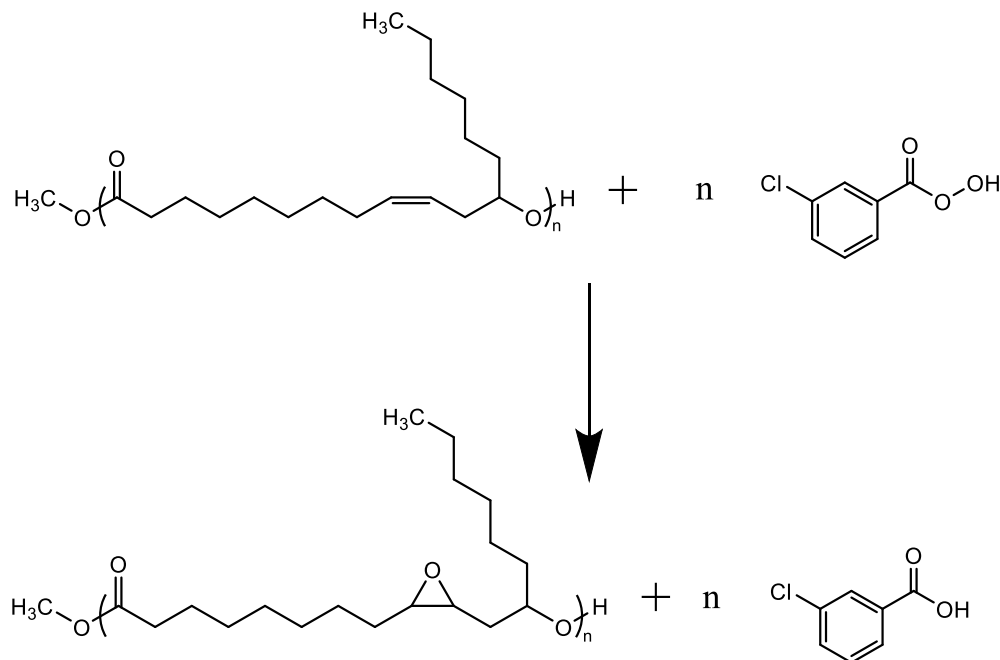


Fig III. 7: Synthetic path from PRic to epoxidized PRic using *m*-CPBA

In this case, it was not possible to obtain an epoxidized PRic in which 100% of the alkene functions had been consumed for the reaction, the maximum amount being of 85%.

Therefore, different amounts of *m*-CPBA were used to synthesise PRics which had a 25%, 50% or 85% conversion of their alkene functions (see Table III. 5). The targeted conversion values were determined through a preliminary study using a previously synthesised PRic at the LCPO with similar molar masses. This preliminary study was also used to define the conditions in which the syntheses should be conducted.

Table III. 5: Amounts of *m*-CPBA used to synthesise epoxidized PRics

PRic grade obtained	<i>m</i> -CPBA amount (eq)	Targeted alkene conversion (%)
PRic-LCPO-E25	0.5	25
PRic-LCPO-E50	1	50
PRic-LCPO-E85	1.5	85

The syntheses were conducted at room temperature using THF as the solvent as all the reactants and products are soluble in it. To purify and recuperate the epoxidized PRics, the latter were precipitated in cold methanol, leaving the remaining *m*-CPBA and the formed 3-chlorobenzoic acid in the solvent phase. The amount of remaining 3-chlorobenzoic acid was checked by ¹H NMR and if needed, other precipitations were conducted to further purify the epoxidized PRics until the remaining by-products would account for less than 5mol%. Indeed, at such level, it was found that further purification through precipitation would be inefficient. Purification through washing, using chloroform as the organic phase and a saturated aqueous metabisulfite solution, was also tested but led to a very stable emulsion which lasted for days and therefore was inappropriate for this study.

b. Characterisation

First, the structure and purity of the synthesised PRics was checked using the ¹H NMR and the H_a protons as the reference (-CH₃, t, 0.8ppm) (spectra in Fig III. 8). The peaks corresponding to the alkene protons of PRic-LCPO (5.3 and 5.5 ppm, H_j and H_k) show a lower intensity accounting for a disappearance of the corresponding protons. At the same time, new signals appeared at 2.9 and 3.0 ppm corresponding to the protons of the newly formed epoxides. As such, the signal at 4.9 ppm corresponding to proton H_{h'} decreased and another signal appeared at 5.0 ppm corresponding to the same proton (denoted H_{h''}) but in the vicinity of an

epoxide instead of an alkene group. Also, the more *m*-CPBA was used, the more important the decrease of the existing peaks and the increase of the newly formed peaks. Also, a shift of the H_d and H_e protons was noticed towards lower chemical shifts (denoted H_d' and H_e') due to the change from an alkene to an epoxide. The characteristics of the synthesised PRics are reported in Table III. 6. The first thing that can be observed is the difference through the NMR between the amount of consumed alkene function and the amount of formed epoxide. For PRic-LCPO-E25 and PRic-LCPO-E50, about 10% of the converted alkenes do not appear as epoxides on the ¹H NMR spectra. In the case of PRic-LCPO-E85, this goes up to 15%. No signal on the NMR spectra seems to correspond to the formation hydroxyl groups through the opening of the epoxides, which could be expected since the used solvent is not dry and the synthesised 3-chlorobenzoic acid could act as an acidic catalyst favouring the opening of the epoxide. Therefore, our hypothesis would be that some of the epoxides have self-reacted to form ether bonds between themselves, which would be confirmed through the SEC.

Table III. 6: ¹H NMR integration values of a) PRic-LCPO-E25, b) PRic-LCPO-E50 and c) PRic-LCPO-E85

a)	Proton Peak	Start	End	% change
	H _h '	0.9271	0.7049	24
	H _h ''	0	0.2185	24
	H _j '	0.9295	0.7021	24
	H _j ''	0	0.1970	21
	H _k '	0.9407	0.7182	24
	H _k ''	0	0.2061	22

b)	Proton Peak	Start	End	% change
	H _{h'}	0.9271	0.4182	55
	H _{h''}	0	0.4724	51
	H _{j'}	0.9295	0.4064	56
	H _{j''}	0	0.4667	50
	H _{k'}	0.9407	0.4148	56
	H _{k''}	0	0.4776	51

c)	Proton Peak	Start	End	% change
	H _{h'}	0.9271	0.1592	83
	H _{h''}	0	0.7495	81
	H _{j'}	0.9295	0.1300	86
	H _{j''}	0	0.7007	75
	H _{k'}	0.9407	0.1361	86
	H _{k''}	0	0.6902	73

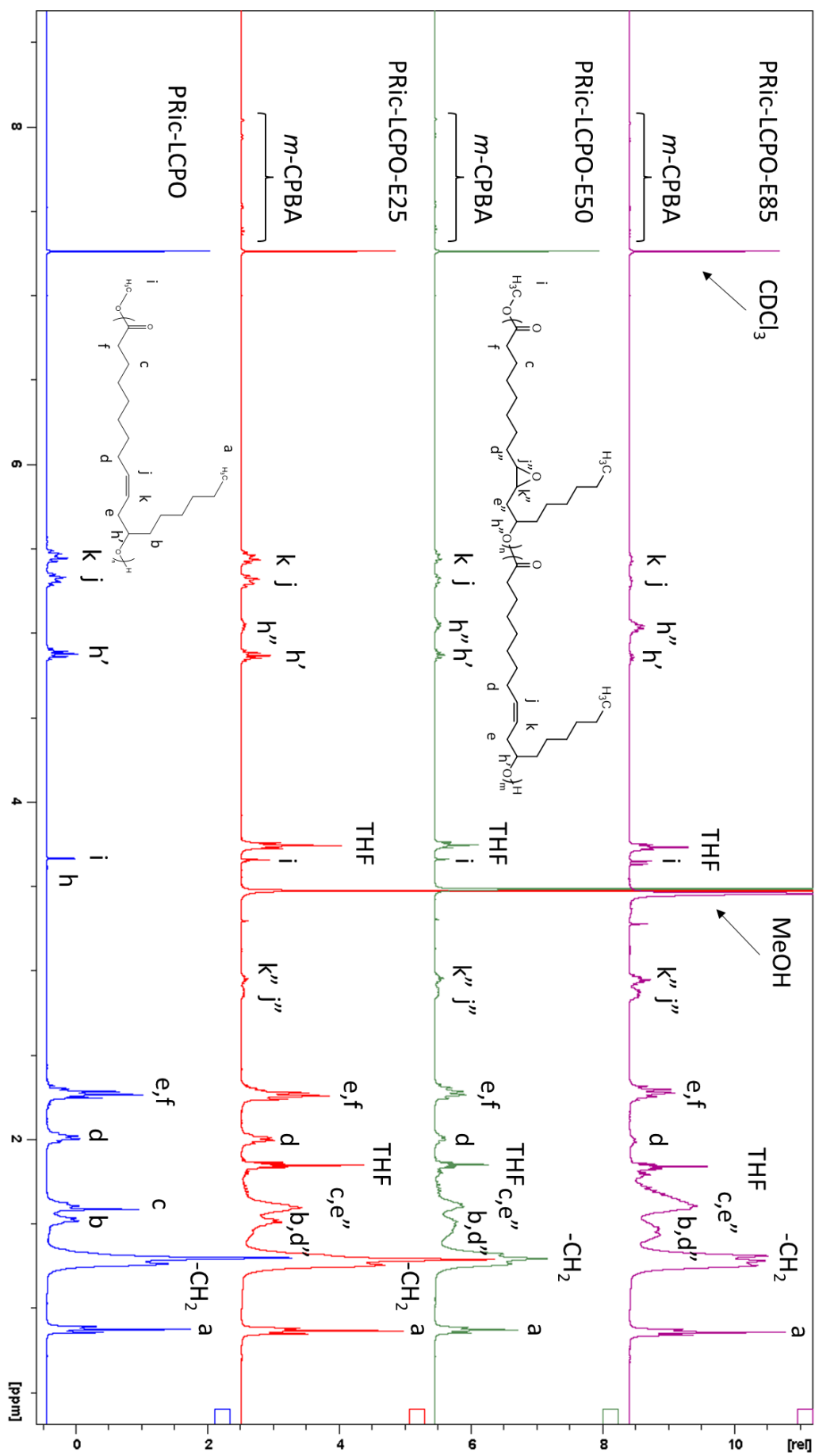


Fig III. 8: ^1H NMR spectra of the three epoxidized PRic-LCPO

Subsequently, the molar mass of the synthesised PRics was determined using the SEC in THF. The chromatograms are shown in Fig III. 9 and the calculated mass in Table III. 7.

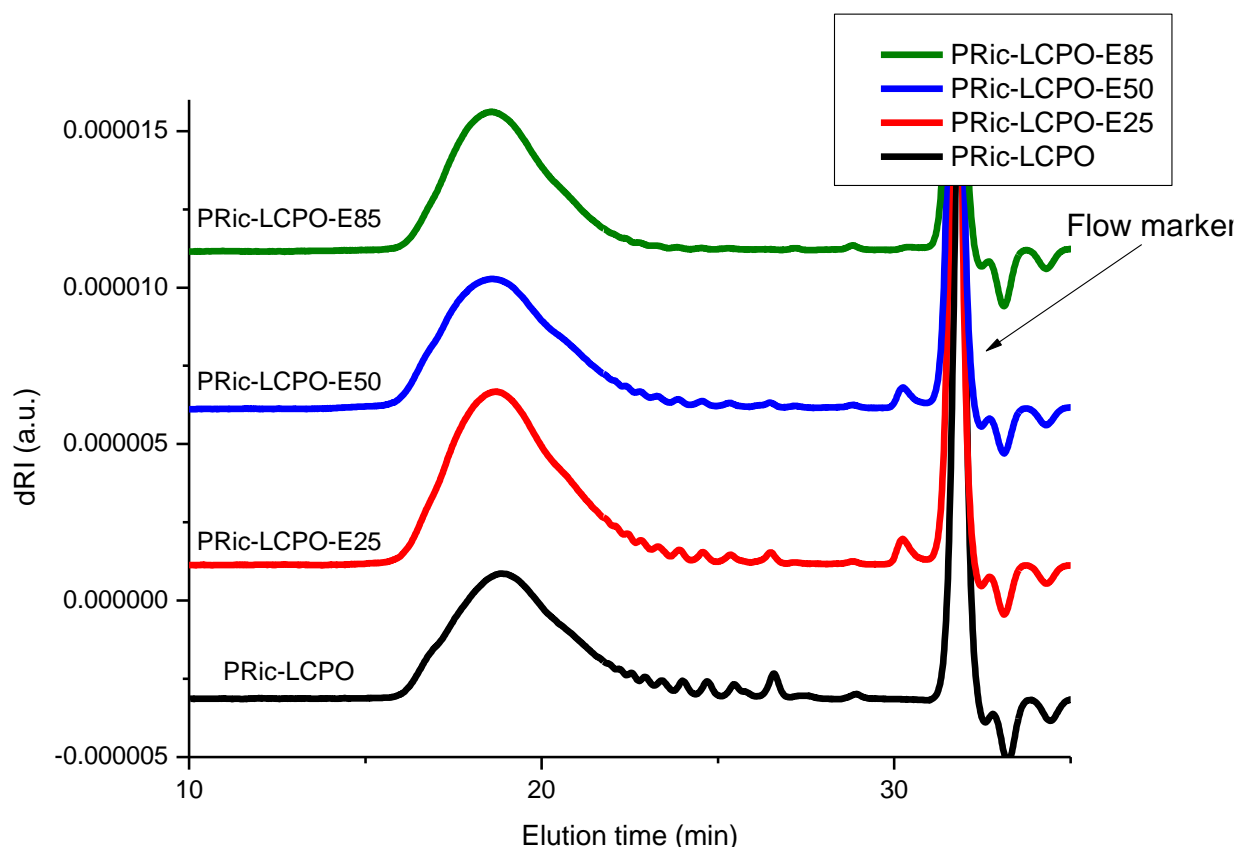


Fig III. 9: SEC traces of PRic-LCPO and the synthesised PRic-LCPO-EXX, THF, PS standard

Table III. 7: Molar masses of PRic-LCPO-EXX using the SEC in THF, PS standard

PRic grade	Mn (g/mol)	Mw (g/mol)	\bar{D}
LCPO	5900	24000	4.1
LCPO-E25	7200	27000	3.7
LCPO-E50	8700	29000	3.3
LCPO-E85	12000	28000	2.3

Looking at both the chromatograms and the calculated values, no significant weight average molar mass (M_w) increase could be noticed. However, looking at the M_n , an increase could be noticed due to the fact that the oligomers were eliminated through the precipitation process as confirmed by the chromatograms in which the peaks corresponding to such

oligomers disappear in the epoxidized PRics (Fig III. 9). This trend increases with the amount of epoxy, therefore showing that the more epoxides borne by PRic, the more it is going to be soluble in methanol. Such increase in M_n narrows the dispersity of the polymers dropping from 4.1 to 2.3 in the best-case scenario. Also, correlating these observations with the ^1H NMR, the increase of M_n is also a sign the smaller epoxidized have reacted upon themselves to form longer chains through ether bonds.

Finally, the thermal properties of these polymers were assessed using the DSC. For this, two different cycles were used, the first one would not go above 120°C to measure the T_g of the additive as such. The second cycle would go up to 150°C and stay at that temperature for 10 mins in order to cure the epoxidized PRics. Such curing would occur through the self-reaction of the epoxides upon themselves to form a crosslinked polymer. The measured values are reported in Table III. 8.

*Table III. 8: T_g values of PRic-LCPO and its epoxidized forms before and after curing in the DSC, *obtained from preliminary study*

PRic grade	T_g no curing ($^\circ\text{C}$)	T_g after curing ($^\circ\text{C}$)
LCPO	-72	-
LCPO-E25	-64	-63
LCPO-E50	-54	-49
LCPO-E85	-53*	-40

The measured T_g s show an increase of the T_g value with the amount of epoxides. Typically, the more epoxides borne by PRic, the higher the T_g . The change in T_g after the curing cycle also shows these epoxides can self-react through the formation of ether bonds. This shows by the increase of the T_g for PRic-LCPO-E25 and PRic-LCPO-E50. In the case of PRic-LCPO-E85, the reported value without curing was taken from the polymer synthesised during preliminary which holds the same characteristics. Indeed, for the PRic-LCPO-E85 which was used for this study, the DSC measure was performed more than 4 months after the synthesis of this product which was kept around 20°C . The measured values were identical (-40°C before and after curing) due to the fact that epoxides had already reacted at room temperature and therefore have partially cross-linked this additive. This was confirmed through ^1H NMR in which the

epoxide proton signals have diminished as a proof they have reacted over time. This is of particular importance since it means the PRic-LCPO-E85 that was incorporated into PLA may not have had all of its original epoxide functions.

2. Melt-blending with PLA: towards improved mechanical and gas barrier properties

The aim of the study is to test the effect of the previously synthesised PRics when used as additives for PLA.

From previous works⁹, it is known that neat PRic has a toughening effect on PLA. Here, the aim is to assess macroscopic properties of injection-moulded PLA cups such as the vertical compression resistance and the O₂ gas barrier properties and correlate them with the microstructure of the PLA+PRic formulations.

2.1. Melt-blending and injection moulding process

In order to study the macroscopic properties of PLA+PRic formulations, mini-industrial processes were used to mimic real industrial conditions. To mix the PLA with the considered additives, the melt-blending method using a twin-screw extruder was chosen. The PLA pellets were dried before processing to eliminate the moisture. First, a master batch was produced holding 6wt% of additive (for 94wt% of PLA) and was processed twice to ensure its homogeneity. Second, this master batch was diluted using neat PLA (processed once to obtain similar size pellets to the master batch) in order to obtain the targeted compositions for our different formulations. In the case of PRic-like additives, weight loadings were chosen at 2wt%, 4wt% and 6wt% (for respectively, 98wt%, 96wt% and 94wt% of PLA). The formulations were obtained under the form of small pellets which were then put in a Babyplast mini-injection moulding machine with a specifically designed mould (Fig III. 10). The idea was to find optimal processing conditions to make cups in an automated mode, namely, in a continuous manner until the number of desired cups was reached or the machine ran out of pellets to feed on. This is also crucial since, during the production process, parts of the mould will warm up until they reach stationary conditions which are more representative and reproduceable. Neat PLA

was used as a reference for setting the injection moulding parameters and also to produce cups which would be used to measure thermal, mechanical and permeability reference properties. The total injection moulding cycle time was 23 seconds. The produced cups are small size cups of approximately 51mm of inside diameter, 25mm height and 1.23mm thickness designed to mimic potential food containers used in the food packaging industry (see Fig III. 11).

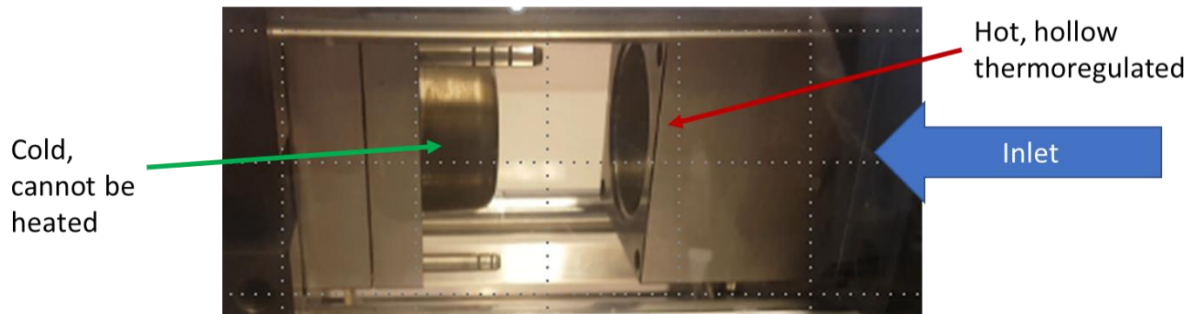


Fig III. 10: Picture and comments on the mould used in the Babyplast machine



Fig III. 11: Picture of an injection moulded neat PLA cup

2.2. Structural characterisation

To evaluate the influence of the extrusion process along with the injection moulding process, SEC analyses were made on samples taken from the injection moulded cups. The results are reported in Table III. 9.

Table III. 9: SEC results of PLA + PRic-LCPO and derivatives samples, THF, PS standard

Additive	Loading (wt%)	Mn (g/mol)	Mw (g/mol)	Đ
Neat PLA	0	39000	81000	2.1
PRic-LCPO	2	60000	97000	1.6
	4	30000	84000	2.8
	6	27000	86000	3.1
PRic-LCPO- E25	2	58000	96000	1.6
	4	31000	89000	2.8
	6	40000	96000	2.4
PRic-LCPO- E50	2	37000	89000	2.4
	4	56000	97000	1.7
	6	40000	95000	2.4
PRic-LCPO- E85	2	22000	44000	2.0
	4	26000	52000	2.0
	6	29000	62000	2.1

The SEC results are rather unexpected. Higher molar masses are measured for samples containing PRic-LCPO, PRic-LCPO-E25 or PRic-LCPO-E50 than the neat PLA sample. This indicates a stabilising effect from these additives on processed PLA since the process using the extrusion can greatly damage the polyester chains. On the contrary, PLA samples mixed with PRic-LCPO-E85 show a decrease in terms of molar mass, nearly twice as low that of neat PLA. This is a bias that can have an effect on further measured properties such as the thermal properties or the mechanical properties of the sample.

2.3. Thermal characterisation

First, a DSC analysis was conducted to check the crystallinity ratios of the injection moulded samples and see whether the injection moulding process had an effect depending on the used additive. The results are reported in Table III. 10.

Table III. 10: DSC results of PLA + PRic-LCPO and derivatives, 1st heating, 10°C/min

Additive	Loading (wt%)	ΔH_{cc} (J/g)	ΔH_m (J/g)	$\Delta H_{\alpha' \rightarrow \alpha}$ (J/g)	$\chi_{c, c}$ (%)	T_g (°C)	T_m (°C)
Neat PLA	0	41.3	45.6	2.1	2	58	173
PRic-LCPO	2	38.8	50.6	5.7	7	58	172
	4	35.9	50.0	5.6	10	58	172
	6	32.7	47.1	5.4	10	58	173
PRic-LCPO-E25	2	38.6	48.9	5.3	6	59	172
	4	39.4	50.3	5.2	7	58	172
	6	33.9	48.6	5.1	10	57	172
PRic-LCPO-E50	2	40.7	50.6	4.7	6	58	172
	4	35.8	49.0	5.7	9	58	172
	6	34.2	47.8	5.5	9	58	172
PRic-LCPO-E85	2	41.3	50.7	-	10	52	171
	4	38.3	50.6	-	14	53	172
	6	40.6	48.9	2.9	6	54	172

The addition of additives in PLA has a slight effect on the crystallinity ratios. Neat PLA samples had a crystallinity ratio of 2% in these processing conditions whereas, depending on the additive and its loading, slightly higher ratios were achieved from 6% to 14%, accounting for a little effect of the additives on the crystallisation kinetics of PLA. Most crystallinity ratio values for one additive span over 3-4% which is not a significant difference. In the case of PRic-LCPO-E85, there is more than double the difference between the lowest and the highest value. Also, for this particular set of additives, the T_g value is lower than for every other sample with relatively stable melting points. This might be due to a partial solubility of this particular additive in the PLA matrix which would shift the measured T_g towards lower values according to Fox's equation¹⁸. Given the T_g values of the additives, the calculated T_g s through Fox's equation correspond with the measured T_g s on the DSC.

2.4. Morphology through SEM

Cryo-fractured samples prepared from the injection-moulded cups were put through the SEM to analyse the morphology of the mixtures. The observed surface is perpendicular to the injection flow. As a reference, a surface from a neat PLA sample was observed to show the absence of any nodule at the fractured surface (Fig III. 12).

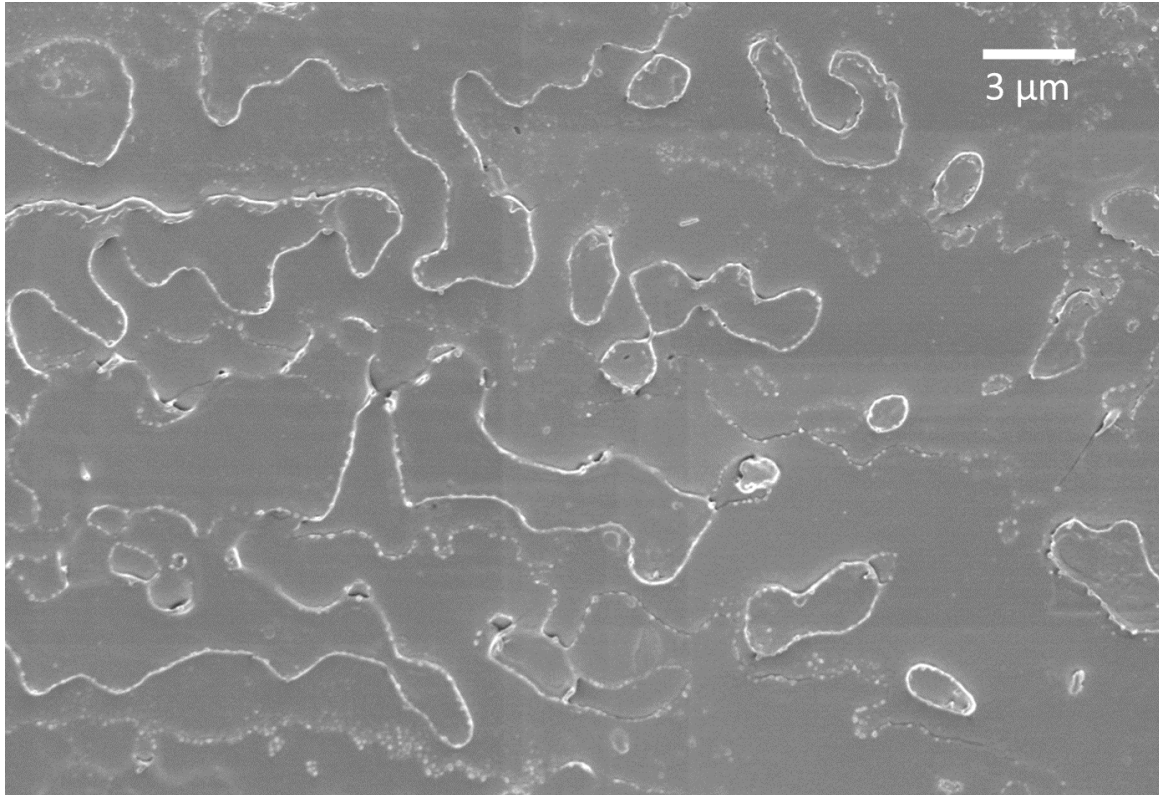


Fig III. 12: SEM picture neat PLA

PRic is not expected to be soluble in PLA as reported in the literature^{5,9} and therefore nodules of PRic and PRic-like additives are expected to be found in the PLA matrix. This was indeed observed in all the fractured samples (Fig III. 14) The mean average size of the nodules was measured using the ImageJ software (Table III. 11). Since the observed nodules had an elliptical shape, the reported values are the major axis, the minor axis along with the associated dispersity index. Such was calculated as such:

$$PDI = \left(\frac{\sigma}{a}\right)^2$$

With:

- σ = the standard deviation (nm)

- a = the major or minor axis length (nm)

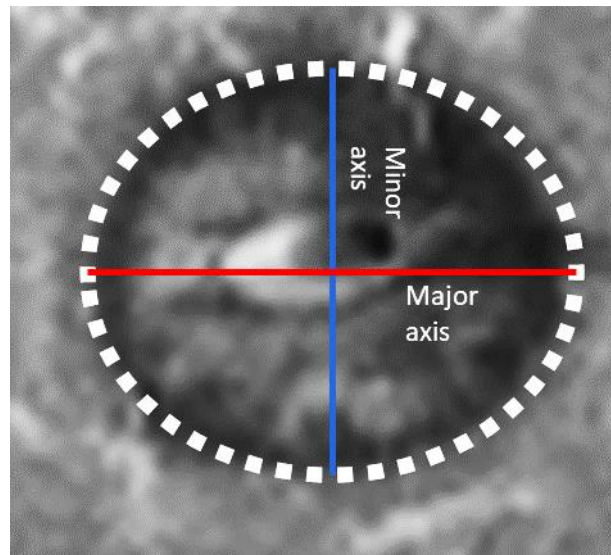


Fig III. 13: Size measurement of a nodule inside PLA

Table III. 11: Nodule size and dispersity for PLA with PRic-LCPO and its derivatives

Additive	Loading (wt%)	Ellipse major (nm)	SD	PDI	Ellipse minor (nm)	SD	PDI
PRic-LCPO	2	837	341	0.17	570	207	0.13
	4	944	274	0.08	804	228	0.08
	6	736	454	0.38	479	276	0.33
PRic-LCPO-E25	2	2012	1247	0.38	1594	1024	0.41
	4	810	235	0.08	684	221	0.10
	6	473	138	0.09	366	90	0.06
PRic-LCPO-E50	2	842	589	0.49	547	337	0.38
	4	788	565	0.51	601	385	0.41
	6	695	381	0.30	543	287	0.28
PRic-LCPO-E85	2	1030	1054	1.05	687	507	0.54
	4	942	485	0.26	709	398	0.31
	6	839	768	0.84	648	430	0.44

When PRic-LCPO is used as an additive, the size of the nodules remains relatively the same, even when higher loadings were considered. As PRic-LCPO was epoxidized at 25%, the size of

the nodules diminished with increasing amounts of additive. The reduction in size of the nodules is also correlated to a higher amount of nodules in the PLA matrix as can be seen in Fig III. 14. Therefore, the change in the nodules' size was attributed to a better mixing of these additives at the concerned loadings. It is interesting to notice high PDI values for samples containing PRic-LCPO-E50 and PRic-LCPO-E85 (above 0.5) showing a relatively high size distribution of the nodules in these cases. This could be observed in the MEB pictures (Fig III. 14) of the associated samples. In the case of PRic-LCPO-E85, the density of nodules is much lower than with the other additives and the SEM images show big unresolved patches not corresponding to a nodule. These observations lead to suppose a better solubility of PRic-LCPO-E85 in PLA. More interestingly, it can be noted that the interfaces between the nodules and the PLA matrix do not show any defect.

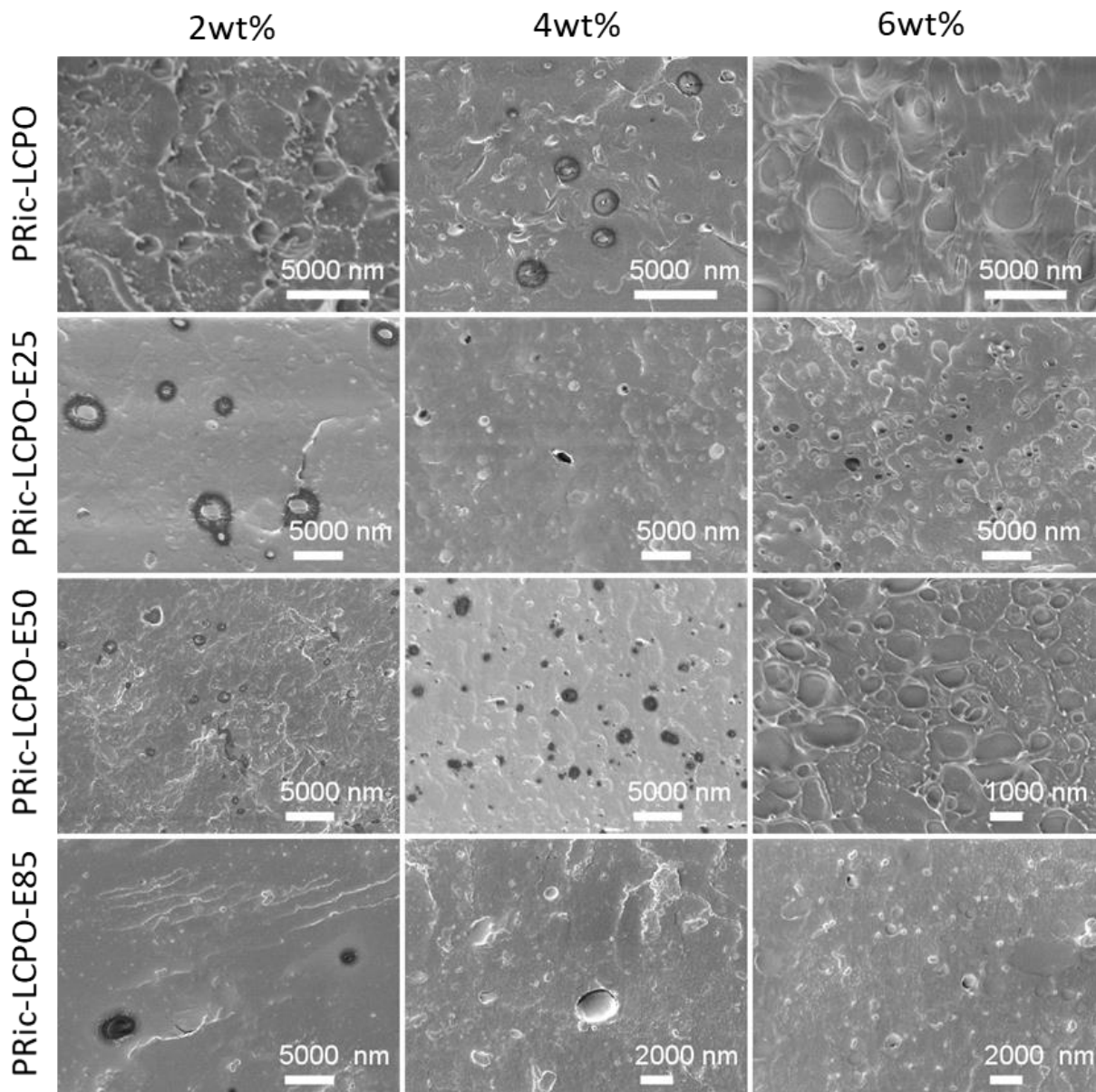


Fig III. 14: SEM images of PLA+PRic-LCPO and its derivatives

2.5. Vertical compression testing

The mechanical properties of the PLA samples were assessed using the vertical compression resistance test. Due to the complexity of the shape of our cups, no section area could be calculated, therefore all measurements are reported as a force in Newtons vs the compressive strain. Neat PLA cups were used as a reference and gave the characteristics reported in Fig III. 15 and Table III. 12.

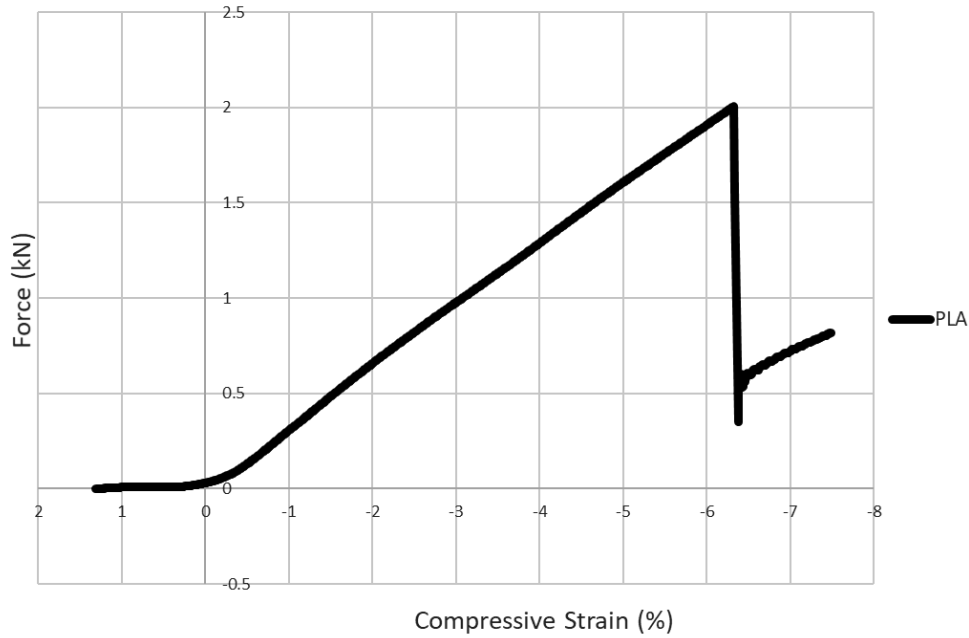


Fig III. 15: Force vs strain of a neat PLA sample, -10mm/min

Table III. 12: Results of the mechanical testing of neat PLA using ten replicas

Sample	Slope (N)	Force at break (kN)	Strain at break (%)
PLA	351±13	2.0±0.1	-6.3±0.1

PLA displays its typical brittle behaviour, the fracture occurs in the elastic domain, at a low strain (-6%) and no plastic deformation can be observed. The force at break, which corresponds to the maximum force in this case, is 2 kN with a slope at origin of 351 N (this slope is directly proportional to the compression modulus of the material through the use of the section area, which could not be calculated in this case).

When the strain exceeded -25%, the sample was considered as not broken since such deformation under a compression corresponds to a non-linear behaviour of the material. The results for PRic-LCPO, PRic-LCPO-E25, PRic-LCPO-E50 and PRic-LCPO-E85 are reported in Fig III. 16 to Fig III. 19 and Table III. 13 to Table III. 16 with neat PLA as the reference.

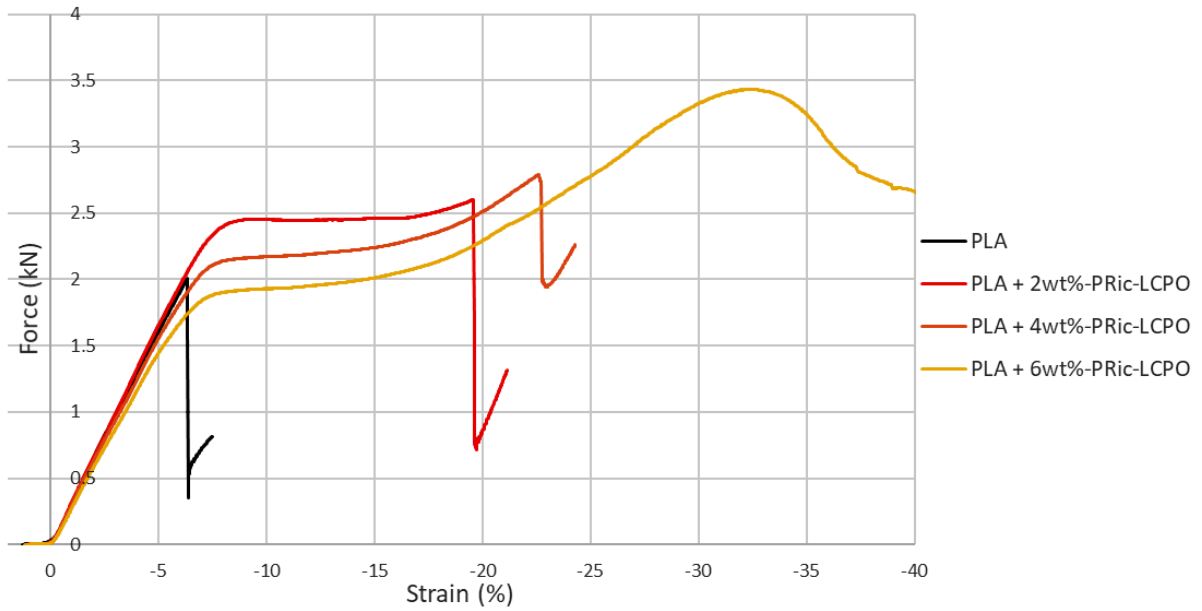


Fig III. 16: Force vs strain of PLA+PRic-LCPO

Table III. 13: Results of the mechanical testing of PLA+PRic-LCPO, using ten replicas

Sample	Slope (N)	Force Plateau (kN)	Yield point (%)	Force at break (kN)	Strain at break (%)
PLA	351 ±13	2.0 ±0.1	-6.3 ±0.1	2.0 ±0.1	-6.3 ±0.1
PLA+2wt%-PRic-LCPO	360 ±16	2.5 ±0.1	#	2.7 ±0.2	-19.7 ±2.1
PLA+4wt%-PRic-LCPO	335 ±13	2.2 ±0.1	#	2.7 ±0.1	-22.7 ±0.2
PLA+6wt%-PRic-LCPO	326 ±8	1.9 ±0.1	#	#	>-25%

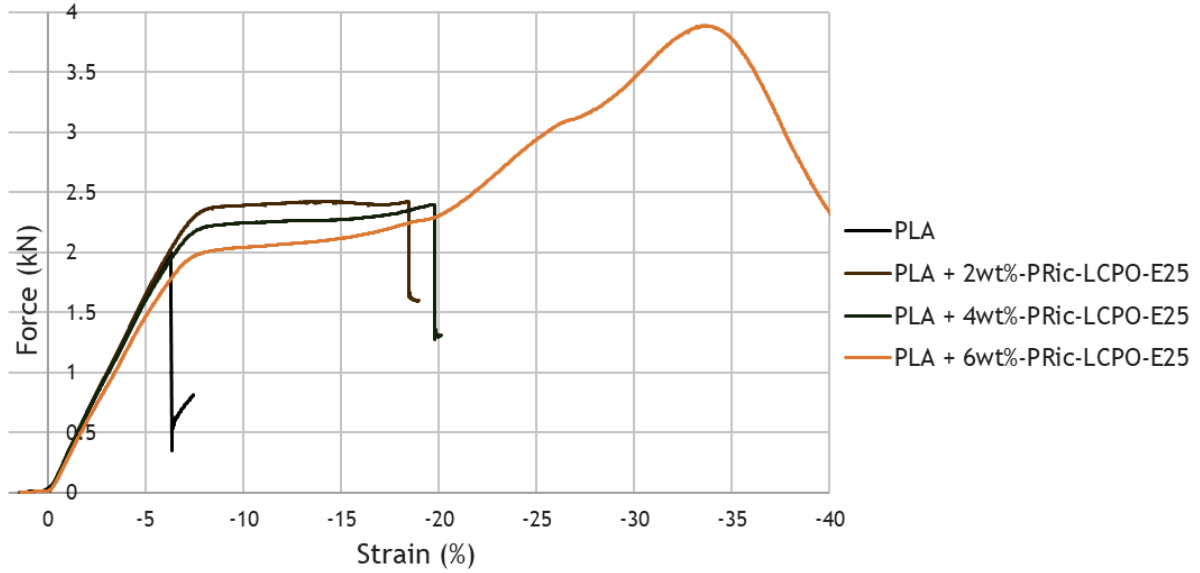


Fig III. 17: Force vs strain of PLA+PRic-LCPO-E25

Table III. 14: Results of the mechanical testing of PLA+PRic-LCPO-E25 using ten replicas

Sample	Slope (N)	Force Plateau (kN)	Yield point (%)	Force at break (kN)	Strain at break (%)
PLA	351 ±13	2.0 ±0.1	-6.3 ±0.1	2.0 ±0.1	-6.3 ±0.1
PLA+2wt%-PRic-LCPO-E25	353 ±10	2.4 ±0.1	#	2.5 ±0.1	-18.4 ±1.0
PLA+4wt%-PRic-LCPO-E25	340 ±15	2.2 ±0.1	#	2.4 ±0.1	-19.5 ±0.6
PLA+6wt%-PRic-LCPO-E25	327 ±6	2.1 ±0.1	#	#	>25

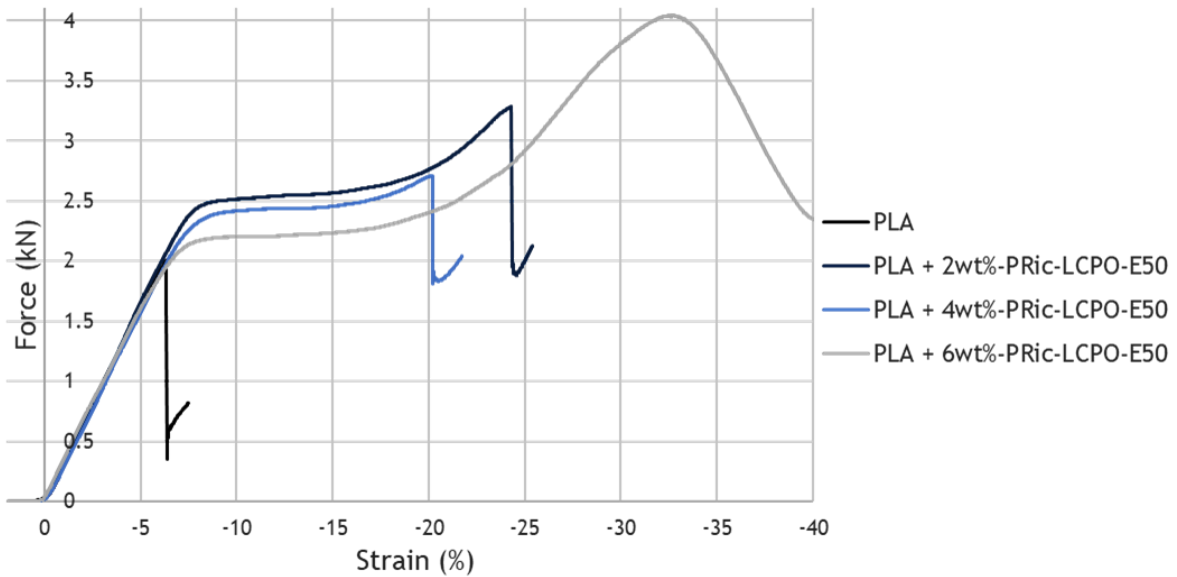


Fig III. 18: Force vs strain PLA+PRic-LCPO-E50

Table III. 15: Results of the mechanical testing of PLA+PRic-LCPO-E50 using ten replicas

Sample	Slope (N)	Force Plateau (kN)	Yield point (%)	Force at break (kN)	Strain at break (%)
PLA	351 ± 13	2.0 ± 0.1	-6.3 ± 0.1	2.0 ± 0.1	-6.3 ± 0.1
PLA+2wt%-PRic-LCPO-E50	352 ± 22	2.5 ± 0.1	#	3.2 ± 0.2	-23.8 ± 1.4
PLA+4wt%-PRic-LCPO-E50	347 ± 16	2.5 ± 0.1	#	2.7 ± 0.2	-20.9 ± 1.4
PLA+6wt%-PRic-LCPO-E50	336 ± 7	2.2 ± 0.1	#	#	>25

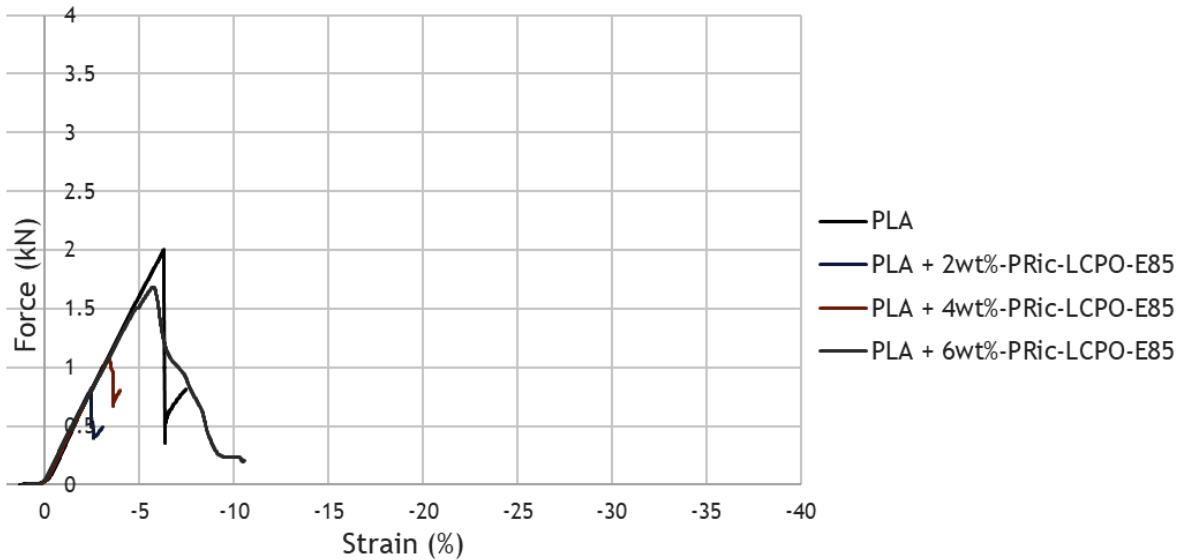


Fig III. 19: Force vs strain PLA+PRic-LCPO-E85

Table III. 16: Results of the mechanical testing of PLA+PRic-LCPO-E85 using ten replicas

Sample	Slope (N)	Force Plateau (kN)	Yield point (%)	Force at break (kN)	Strain at break (%)
PLA	351 ±13	2.0 ±0.1	-6.3 ±0.1	2.0 ±0.1	-6.3 ±0.1
PLA+2wt%-PRic-LCPO-E85	353 ±8	0.8 ±0.1	-2.5 ±0.1	0.8 ±0.1	-2.5 ±0.1
PLA+4wt%-PRic-LCPO-E85	344 ±5	1.1 ±0.1	-3.5 ±0.1	1.1 ±0.1	-3.5 ±0.1
PLA+6wt%-PRic-LCPO-E85	333 ±5	1.7 ±0.1	-5.7 ±0.1	1.7 ±0.1	-5.7 ±0.1

The mechanical properties are promising. Compared with neat PLA, there is an improvement in terms of mechanical behaviour observed with all the additives excepting PRic-LCPO-E85, which will be discussed later. The first noticeable feature is the improvement of the strain at break from -6% to at least -18% and over. At the highest loadings, 6wt%, no brittle fracture would be noticed, and the sample could be compressed to the very high strains without suddenly breaking as observed with all the other samples as illustrated in Fig III. 20. Individually, for PRic-LCPO and PRic-LCPO-E25, the higher the loading, the higher the strain at break. This was not observed with PRic-LCPO-E50 since the samples at a loading of 4wt% display the lowest strain at break values for this additive (-21%). Another major difference with neat PLA is the apparition of a ductile plateau in all the samples. Such feature accounts

for a plastic deformation of the samples. This behaviour is not present with neat PLA as, due to their brittleness, neat PLA samples break in the elastic deformation zone and display no plastic behaviour. A trend can be noticed regarding the force value of these plateaux. The more additive in the PLA matrix, the lower the ductile plateau value will be. This is expected since it is a well-known phenomenon for polymers holding additives. More particularly, the values of the force plateau increase at similar loadings with the number of epoxides on the PRic chains. This is explained by the intrinsic properties of these additives: the more epoxides, the higher the T_g . In other words, the more epoxides are created on a PRic, the “harder” it becomes; therefore, the observed global behaviour of the materials translates into a lesser softening characterised by a smaller decrease of the ductile plateau value. Regarding the slope values, again, there is an expected behaviour as they decrease slightly with the increasing amount of additive. This is also typical as moduli tend to follow a similar trend for polymers loaded with additives.

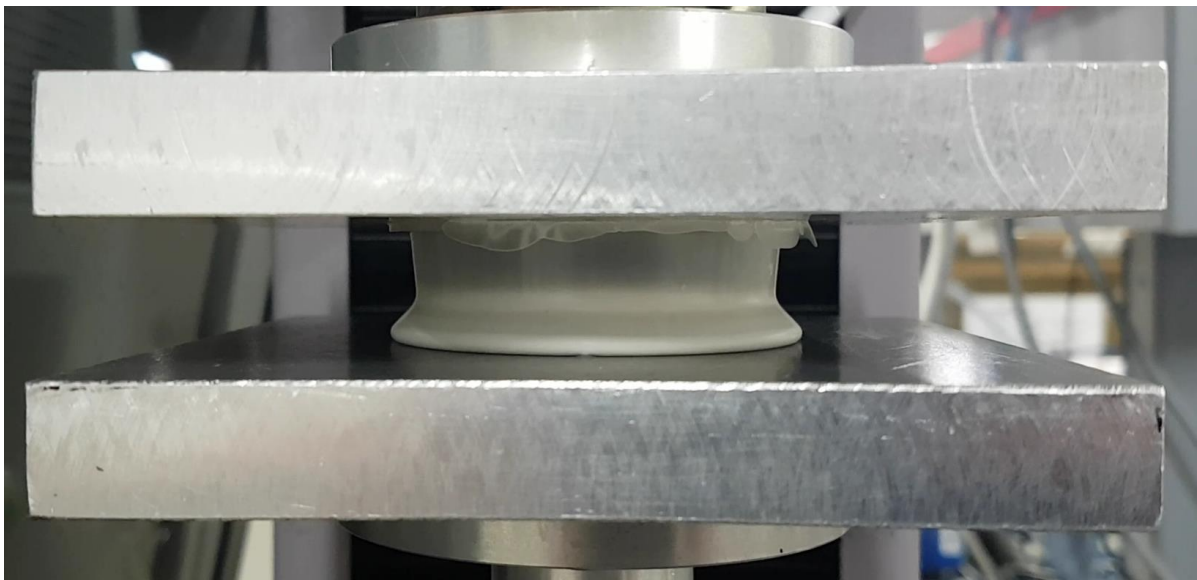


Fig III. 20: Picture of a cup during a compression test displaying a ductile behaviour and no brittle fracture

The case of PLA samples loaded with PRic-LCPO-E85 is very particular. The mechanical properties are worse than the ones for neat PLA samples. Three main assumptions can be made: first, the strong decrease in molar mass of the PLA matrix observed by the SEC for this set of samples plays an effect as it leads to lower mechanical properties as reported in the literature^{19,20}. Second, the high amount of epoxides on the additive could make it more soluble in PLA, as such solubility would be increased thanks to a PLA of a lower molar mass. Third, and

correlated to the latter, the SEM images of the samples showed less and smaller nodules and big patches with a stronger contrast which could be zones in which the PLA and the PRic-LCPO-E85 are actually homogeneously mixed together and therefore display mechanical properties in between the ones of PRic-LCPO-E85 (which correspond to a viscous liquid) and the ones of PLA at room temperature.

2.6. Oxygen barrier properties

Finally, the O₂ barrier properties of the samples were assessed. Two samples per formulation were analysed at the same time to check for any discrepancy. To do so, the injection moulded cups were sealed under a N₂ atmosphere on a glass panel with a Presens O₂ sensor to instantly measure the amount of O₂ in sealed-off atmosphere inside the cup. The measures were conducted at 23°C and 50% RH and the results are reported in Fig III. 21 and Table III. 17.

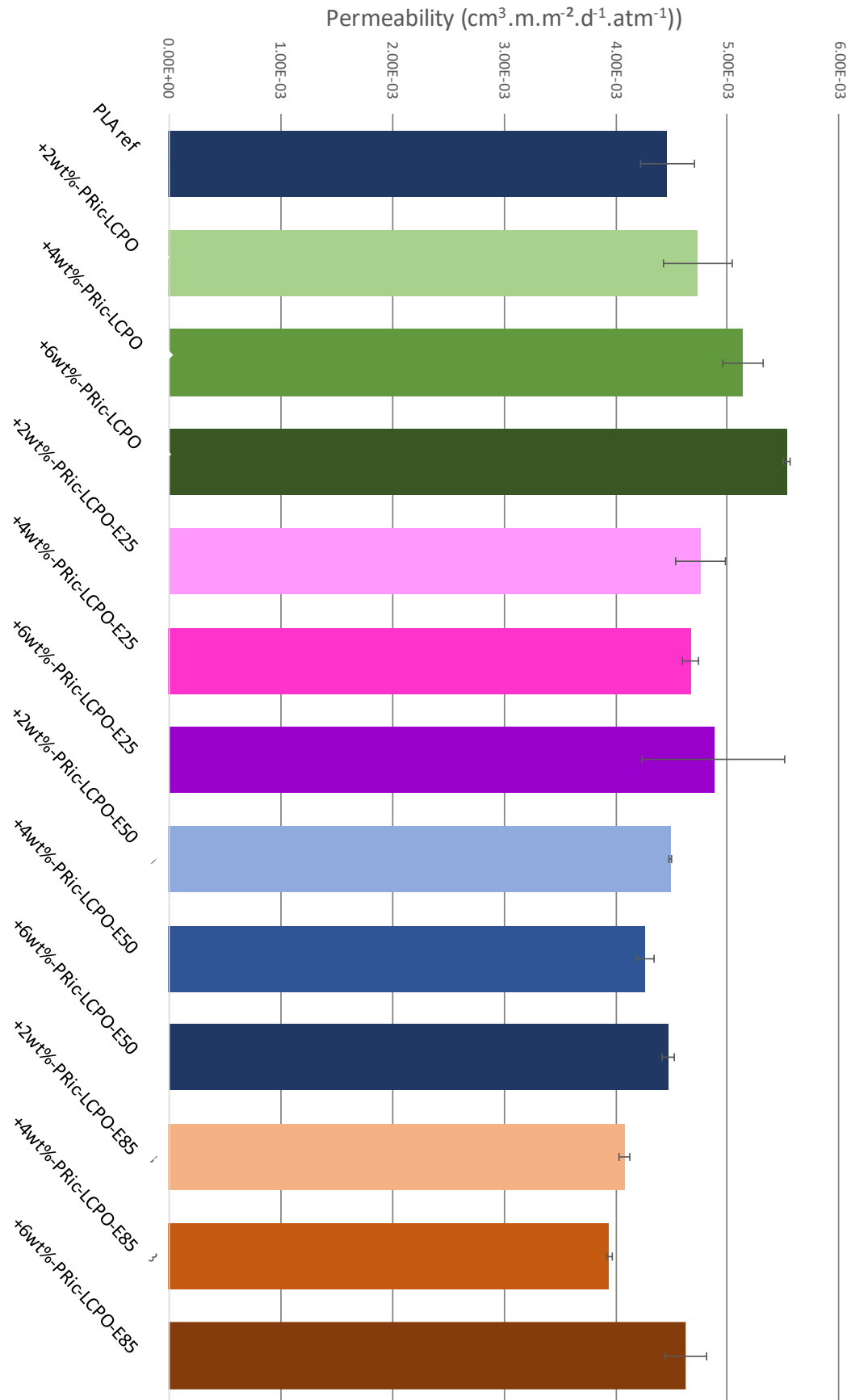


Fig III. 21: O_2 average permeability values (2 samples) of PLA samples with Pric-LCPO and its derivatives as additives - 23°C , 50 % RH

Table III. 17: O₂ permeability results of PLA + PRic-LCPO and its derivatives

Samples	O₂ Permeability (10⁻³.cm³.m.m⁻².d⁻¹.atm⁻¹)
PLA ref	4.5 ± 0.2
+2wt%-PRic-LCPO	4.7 ± 0.3
+4wt%-PRic-LCPO	5.1 ± 0.2
+6wt%-PRic-LCPO	5.5 ± 0.1
+2wt%-PRic-LCPO-E25	4.8 ± 0.2
+4wt%-PRic-LCPO-E25	4.7 ± 0.1
+6wt%-PRic-LCPO-E25	4.9 ± 0.6
+2wt%-PRic-LCPO-E50	4.5 ± 0.1
+4wt%-PRic-LCPO-E50	4.3 ± 0.1
+6wt%-PRic-LCPO-E50	4.5 ± 0.1
+2wt%-PRic-LCPO-E85	4.1 ± 0.1
+4wt%-PRic-LCPO-E85	3.9 ± 0.1
+6wt%-PRic-LCPO-E85	4.6 ± 0.2

The measured O₂ permeability values are all close to the value measured with neat PLA. Here, a small increase can be noticed when PRic-LCPO is added to PLA, the increase becoming more important when more PRic-LCPO was added. This is due to the free volume created in the PLA matrix by adding an immiscible polymer inside it. Regarding the epoxidized PRic-LCPO samples, the O₂ permeability values slightly diminish at 2wt% and 4wt% loadings and even further with an increasing amount of epoxides, however these values increase back at high loadings (6wt%). Regarding the reference value for neat PLA, these values are satisfactory

since the O₂ permeability does not increase too much with the addition of PRic-LCPO and is even stabilised with the addition of epoxides.

3. Discussion and conclusion

The addition of PRic-LCPO and its epoxy derivatives did not have a clear effect on the crystallisation kinetics of PLA in these processing conditions. The studied samples were amorphous and the small difference in terms of crystallinity ratio could not lead to differences of macroscopic properties. Regarding the mechanical properties, they were enhanced thanks to the addition of PRic-LCPO, PRic-LCPO-E25 and PRic-LCPO-E50. At the highest loadings, the brittle behaviour typical of PLA could no longer be observed, high strains at break were achieved without greatly compromising the modulus. Observations through the SEM showed the presence of nodules which prove the incompatibility of these additives with PLA. Such morphology explains the toughening effect observed during the vertical compression testing. In the case of PRic-LCPO-E85, lower molar masses were measured on the samples after processing. Moreover, the mechanical properties revealed to be less than those of neat PLA. The SEM images gave a good explanation: along with a lower molar mass, there were no or very few nodules that could be observed. Instead, darker patches along the surface suggested this additive was more miscible in PLA and therefore deeply modified its properties such as its T_g or its mechanical properties. The measured T_gs were indeed lower than of neat PLA or the other formulations which do not display a shift of the T_g towards lower values. In the end, the O₂ permeability was measured and revealed only minor modifications depending on the additive. Neat PRic-LCPO increased the permeability thanks to an increase of free volume while the increase of epoxides on PRic seemed to slightly diminish the O₂ permeability. All in all, the use of a highly pure grade of PRic did enhance the mechanical properties of PLA but not to the extent as reported in the literature. Also, there was no clear effect on the crystallisation kinetics. Regarding the O₂ permeability properties, the reported values are quite close to the one for neat PLA and therefore do not constitute a real improvement in terms of a more barrier material or a more permeant material.

4. Experimental & SI

4.1. Synthesis of PRic-LCPO

Methyl ricinoleate (>99%, Nu-Chek Prep., USA) was put in a 1l reactor equipped with a mechanical stirrer and with an air inlet/outlet. First, the monomer was left for at least 12h at 70°C under vacuum prior to starting the polymerisation. 0.5wt% of titanium isopropoxide were added upon return to room temperature under a nitrogen atmosphere thanks to a 5wt% solution in dichloromethane. The mixture was left to stir under nitrogen atmosphere at room temperature for 30 mins then heated to 70°C while slowly reducing the pressure inside the vessel. After 30 mins, the reactor was heated to 120°C for 1 hour, then 140°C for 1 hour and finally to 180°C for 15 hours.

4.2. Synthesis and purification of PRic-LCPO-EXX

PRic-LCPO was solubilised in THF (0.167g/ml) in a round-bottomed flask under a mechanical stirrer. Once the polymer was solubilised, the solution was cooled to 0°C using an ice-bath. A solution containing THF and *m*-CPBA (0.667g/ml) was prepared on the side. Once the polymer solution was cooled to 0°C, the THF solution containing *m*-CPBA was injected dropwise using a syringe and a needle with the polymer solution still kept in an ice-bath. After one hour, the ice-bath was removed to allow the reaction to proceed at room temperature for 20 hours. The epoxidized polymer was precipitated in cold methanol (-50°C) to eliminate the unreacted *m*-CPBA and eliminate the formed 3-chlorobenzoic acid. The volume of methanol used for precipitation was at least 10:1 compared to the THF solution containing the polymer. The process was repeated until the residual *m*-CPBA/3-chlorobenzoic acid was lower than 5mol%. The precipitated polymer was then collected and dried under vacuum at 50°C for 12 hours.

4.3. SEM analysis

SEM samples were prepared by freeze-fracturing. The observed surfaces were taken on the side of the cups and perpendicularly to the injection flow. This was of outright importance since it was noticed that the observed morphology of surfaces taken on the same direction as the injection flow showed highly elongated ellipses. This proved that the injection moulding technique had a deep effect on the morphology of the samples. The SEM pictures were then analysed using the ImageJ software. Machine learning was used to recognise the nodules in

the PLA matrix and isolate them. A macro was then developed by Quentin Jaussaud to measure the size of these elliptical shaped nodules. The perimeter, major axis and minor axis were measured along with the polydispersity index instead of the standard deviation.

4.4. Vertical compression testing

Vertical compression testing was conducted in an INSTRON apparatus using parallel plates. Tests were conducted at a -10mm/min speed using 10 replicas for each compound. Due to the complexity of the object, no definite section could be calculated, therefore values are reported as a force (N) vs displacement (mm). The values for the slope at origin, yield force, force plateau, strain at break were reported.

4.5. Oxygen permeability measurement

Two cups were used per formulation for this test. These were sealed off in a glove box using pure N₂ and a small container with a saturated solution of magnesium nitrate hexahydrate to compensate the global relative humidity to 53% RH at 23°C. The glass panels used to seal the cups were equipped with a Pst6 Presens sensor to measure the activity of O₂ inside the sealed atmosphere (Fig III. 22). The evolution of the amount of oxygen was monitored at least once a day until the increase followed a linear trend. The permeability was calculated using the following formula:

$$Perm = \frac{Slope \times volume \times thickness}{a \times \Delta P}$$

- Perm = the permeability in cm³ (O₂).m.m⁻².day.atm
- Volume in cm³, 49.2 cm³
- Thickness in m, 0.001225 m
- a = area in m², 0.000556 m²
- ΔP = O₂ pressure differential in atm, 0.21 atm

Chapter 3

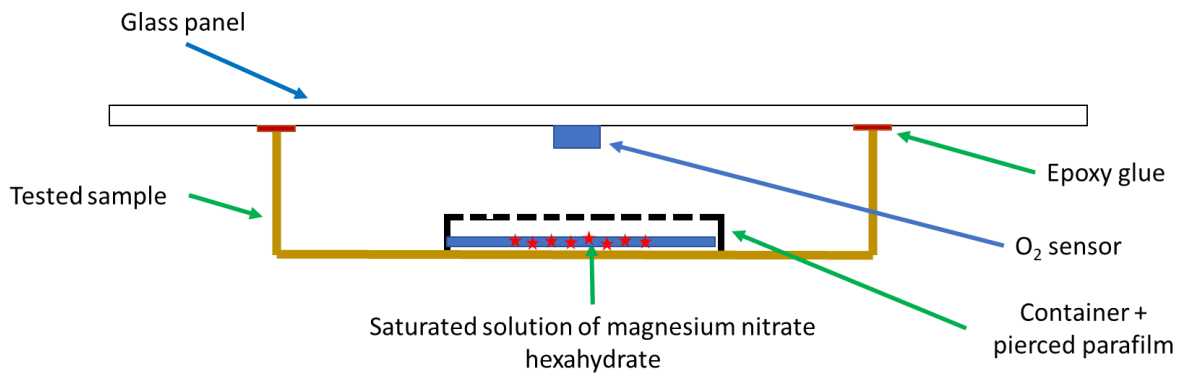


Fig III. 22: Schematic representation of the system used to measure the O₂ permeability of a sample

Part B: Use of the industrial PRic grade

1. PRIC-100 and its derivatives as additives for PLA

In this part, the industrially available PRic was used to conduct this study. This particular grade has already shown to have a very strong toughening effect on PLA as discussed in the introduction to this chapter⁹. Here, the idea will be to assess the performance of the PLA materials made with PRic from ITERG (thereafter named PRic-100) and thanks to the higher available quantities, do an extra step of chemistry by converting the epoxide moieties. First, the alkene functions were exploited to synthesise a PRic containing epoxy groups, then, going a step further, the formed epoxy groups were converted into cyclic carbonate groups thanks to a pressurised CO₂ reaction vessel.

1.1. Characterisation of PRic-100

a. Structure

As mentioned in the introduction, PRic-100 is synthesised from methyl ricinoleate with a lower purity than the one used for PRic-LCPO, therefore allowing other fatty derivatives to act as chain stoppers of the polycondensation. This can be noticed through the ¹H NMR in which proton signals not corresponding to methyl ricinoleate or PRic can be noticed (Fig III. 23).

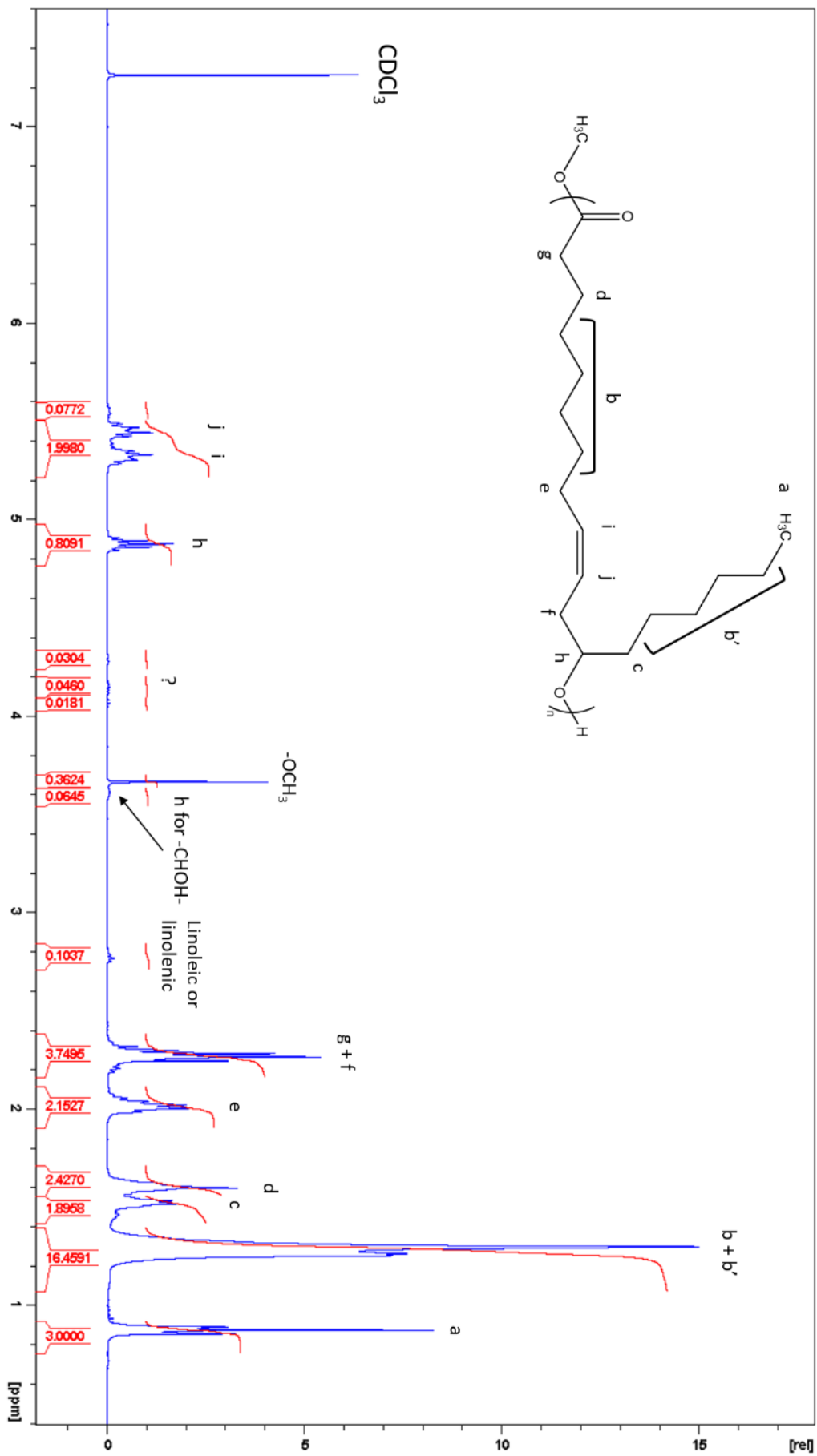


Fig III. 23: ^1H NMR spectrum of PRic-100

Along with the peaks, which do clearly not correspond to PRic-100 such as around 2.7-2.8 ppm and also between 4.0 and 4.4 ppm, some other proton signals overlap with proton signals corresponding to PRic-100. This can be seen through the integrals' values which are higher than the number of corresponding PRic-100 protons in those cases. Also, using the $-CH_3$ signal at 0.9 ppm as a reference accounting for three protons, 0.0645 protons remain at 3.6 ppm accounting for the protons in alpha of the $-OH$ group of the ricinoleic acid, whereas 0.3643 protons corresponding to the methyl ester group remain. That is to say, considering these protons as chain end markers, there is twice the amount of ester groups than hydroxyl groups, showing that half of the polymer chains were terminated by a motive bearing no hydroxyl group. It can be easily understood since the starting material contains "regular" FAME.

The SEC was used to assess the molar masses and their distribution. The SEC trace is reported in Fig III. 24 and the values are reported in Table III. 18.

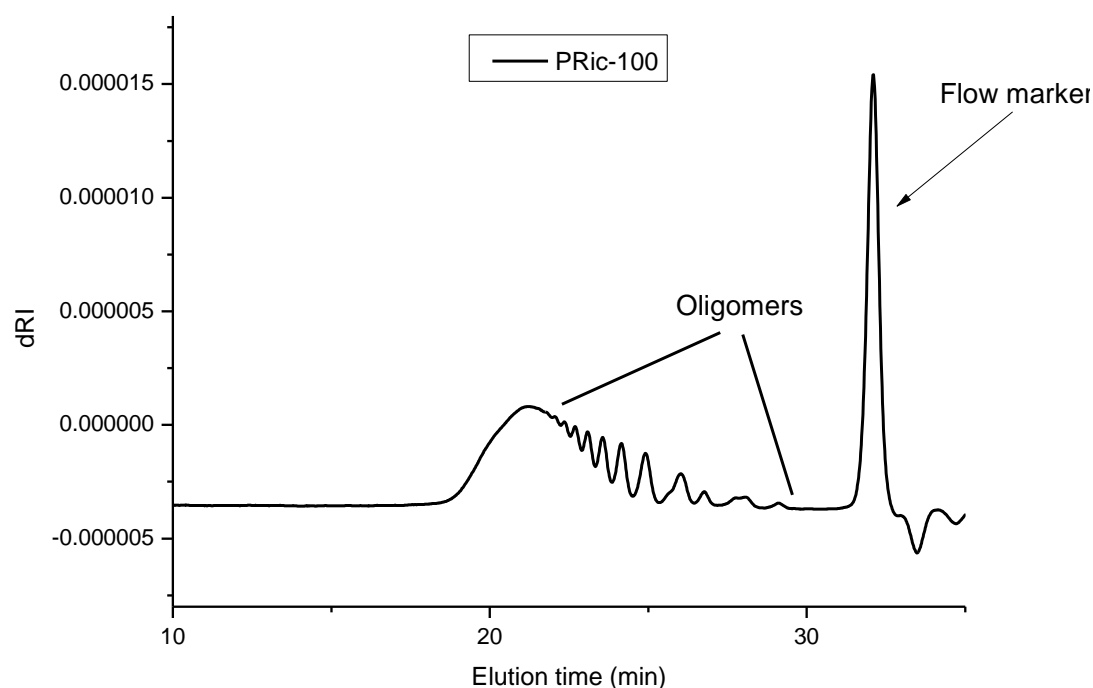


Fig III. 24: SEC trace of PRic-100, THF, PS standard

Table III. 18: Molar masses of PRic-100 measured by SEC in THF (PS standard)

Polymer	Mn (g/mol)	Mw (g/mol)	\bar{D}
PRic-100	2500	5200	2.1

The first observations to be made concern the clear lower molar masses compared to PRic-LCPO. Here, the Mw does not exceed 6000 g/mol with a relatively controlled dispersity of 2.1,

which is still higher than the theoretical maximum dispersity expected for a polycondensation (maximum of 2 according to Carothers' equation¹⁵). In comparison, an M_w over 20,000 g/mol and a dispersity of 4.1 for PRic-LCPO were obtained. Such lower mass is due to the presence of many oligomers which clearly appear on the SEC chromatogram.

b. Thermal analysis

PRic-100 was also analysed using the DSC. The thermal analysis revealed a T_g at -81°C and no endotherm or exotherm. This is lower than the measured T_g for PRic-LCPO which was -72°C . This is explained mainly by the difference in terms of molar masses with PRic-LCPO being between 3 to 4 four times higher than PRic-100 and also by the absence of small oligomers which could act as plasticisers in the case of PRic-100.

1.2. Epoxidation of PRic-100

a. Synthesis

The epoxidation step of PRic-100 is similar to the one developed in Part A of this chapter. PRic-100 was solubilised in THF and *m*-CPBA was used to convert the alkene groups to epoxide groups. The synthesised product was precipitated in cold methanol to eliminate the residual *m*-CPBA and the formed 3-chlorobenzoic acid. Again, two or three precipitations were necessary to obtain less than 5mol% of residual side-products which can be either *m*-CPBA or 3-chlorobenzoic acid. The synthesised polymers are denoted as such: PRic-100-EXX, XX corresponding to the targeted ratio of converted alkenes.

b. Characterisation

The epoxidized PRics were characterised by means of ^1H NMR, the SEC in THF and the DSC. As for the epoxidation of PRic-LCPO, ^1H NMR was used to measure the consumption of the alkene groups (protons H_i and H_j) and the appearance of the epoxide groups (protons H_r and H_r') by following the evolution of the corresponding proton signals (Fig III. 25). Also, the evolution of the H_h protons into H_h' protons gave a quantitative indication of the amount of consumed alkenes and formed epoxide (Table III. 19). Protons accounting for the apparition of epoxide groups have indeed appeared (2.8 and 2.9ppm), while a shift of H_h protons to H_h' protons also happens from 4.9ppm to 5.1ppm.

Table III. 19: ^1H NMR proton integration to follow the alkene conversion in CDCl_3 , a) PRic-100-E25, b) PRic-100-E50, c) PRic-100-E85

a)	Proton Peak	Start	End	% change
	H_h	0.8736	0.6510	22.9
	$\text{H}_{h'}$	0	0.1730	19.8
	H_i	0.958	0.712	25.7
	$\text{H}_{i'}$	0	0.2108	22.0
	H_j	0.958	0.712	25.7
	$\text{H}_{j'}$	0	0.2124	22.2

b)	Proton Peak	Start	End	% change
	H_h	0.8736	0.4258	51.3
	$\text{H}_{h'}$	0	0.4018	46.0
	H_i	0.958	0.4538	52.6
	$\text{H}_{i'}$	0	0.4221	44.1
	H_j	0.958	0.4428	53.8
	$\text{H}_{j'}$	0	0.4452	46.5

c)	Proton Peak	Start	End	% change
	H_h	0.8736	0.0777	88.9
	$\text{H}_{h'}$	0	0.7218	82.6
	H_i	0.958	0.0572	94.0
	$\text{H}_{i'}$	0	0.7593	79.3
	H_j	0.958	0.0567	94.1
	$\text{H}_{j'}$	0	0.7731	80.7

Regarding the peak integrations measured by ^1H NMR, the structure of the epoxidized PRic-100 was confirmed and showed little ring opening of the formed epoxides or any other side reactions. To further confirm the structure, SEC measurements were conducted. The according results are reported in Fig III. 26 and Table III. 20.

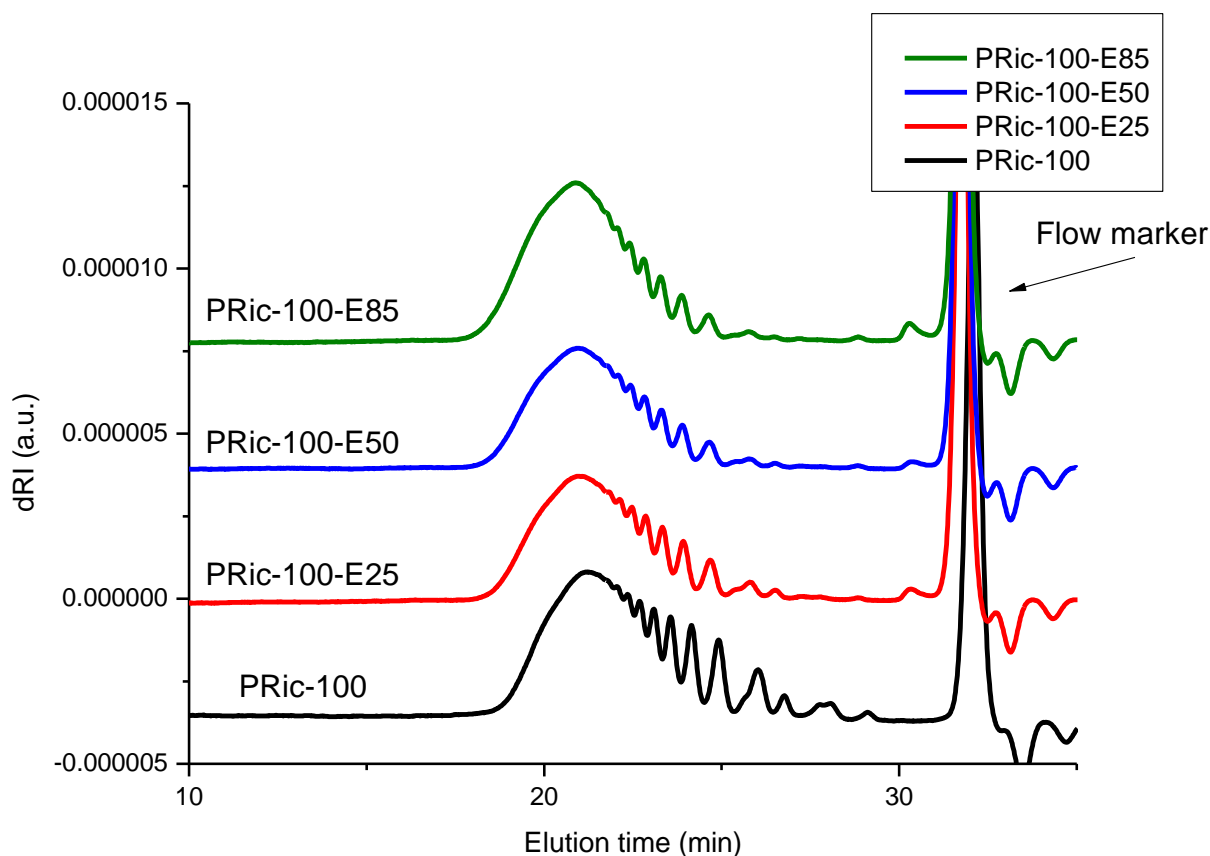


Fig III. 26: SEC traces of PRic-100 and its epoxidized derivatives

Table III. 20: SEC results for PRic-100 and its epoxidized derivatives, THF, PS standard

PRic grade	Mn (g/mol)	Mw (g/mol)	\bar{D}
100	2500	5200	2.0
E25	3100	5800	1.8
E50	3800	6000	1.6
E85	4100	6700	1.6

Here again, like the epoxidized PRic-LCPO compounds from Part A, the epoxidized PRic-100 polymers show an increase in the molar masses along with a decrease of the dispersity. As it can be seen in Fig III. 26, the amount of low mass oligomers has diminished due to the

purification step. Indeed, oligomers are less prone to precipitate and will therefore remain in solubilised leading to polymers with an increased molar mass.

The thermal characteristics of these polymers were finally determined using the DSC. Two different cycles were used, the first one would not go above 120°C to measure the Tg of the additive as such upon the second heating. The second cycle would go up to 150°C and stay at that temperature for 10 mins in order to cure the epoxidized PRics. The measured values are reported in Table III. 21.

Table III. 21: Measured Tgs of PRic-100 and its epoxidized derivatives, 10°C/min

PRic grade	Tg no curing (°C)	Tg after curing (°C)
100	-81	-
100-E25	-70	-68
100-E50	-61	-57
100-E85	-52	-42

The measured Tgs are all higher than neat PRic-100. The more epoxides, the higher the Tg value. Most noticeably, PRic-100-E85 displayed a Tg which was 30°C higher than PRic-100. Also, proving their ability to further react, the Tgs measured after curing were higher than before curing. This is due to the self-reaction of the epoxides upon themselves, therefore creating crosslinks between the polymer chains through the creation of ether bonds. Such network creation limits the mobility of the polymer chains and therefore results in a higher Tg.

1.3. Carbonatation of epoxidized PRic-100

a. Synthesis

Due to the ability of the epoxides to react, the choice was made to conduct another synthetic step and convert the epoxides on the epoxidized PRic-100 polymers into cyclic carbonates as Ren *et al.* did in their work¹⁴. The synthesis was conducted following a reported route by Alves *et al.* which is also close to the one used by Ren *et al.*^{14,21} (Fig III. 27). An autoclave was used to conduct the synthesis. At room temperature, the polymer was loaded with 3wt% of tetrabutylammonium bromide as the catalyst and once sealed, 40 bars of CO₂

were injected. The reactor would then be heated to 150°C for 24h. Upon heating to 150°C, the pressure inside the vessel increased to approximately 80 bars before stabilising at this value. No purification was conducted after the synthesis, therefore leaving the catalyst inside the synthesised product.

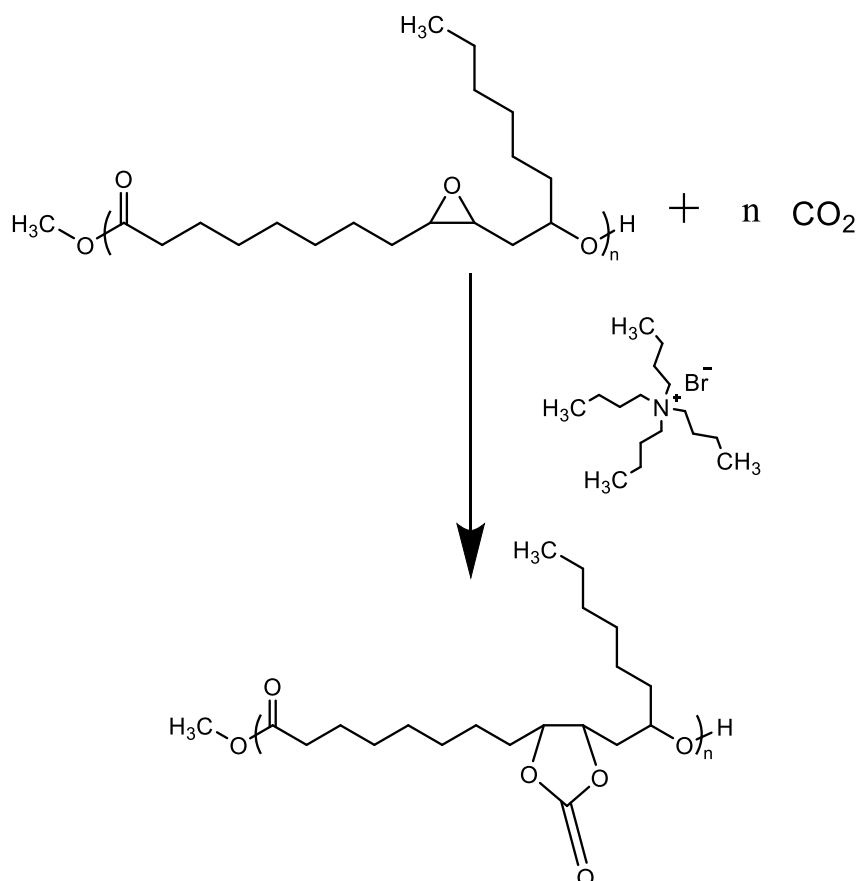


Fig III. 27: Reaction scheme to obtain carbonated PRic-100

b. Characterisation

The carbonated PRics were first characterised by ^1H NMR to follow the consumption of the epoxides and the formation of the cyclic carbonate groups (Fig III. 28). What can be first noticed is the total disappearance of the peaks at 2.8ppm and 2.9ppm which corresponded to the protons of the epoxide group (blue circle). This means that the epoxides have all been consumed during the reaction. Moreover, new peaks appeared in the range 4.2 to 4.7 ppm (green circle) which are reported to correspond to protons linked to a carbonate group¹⁴.

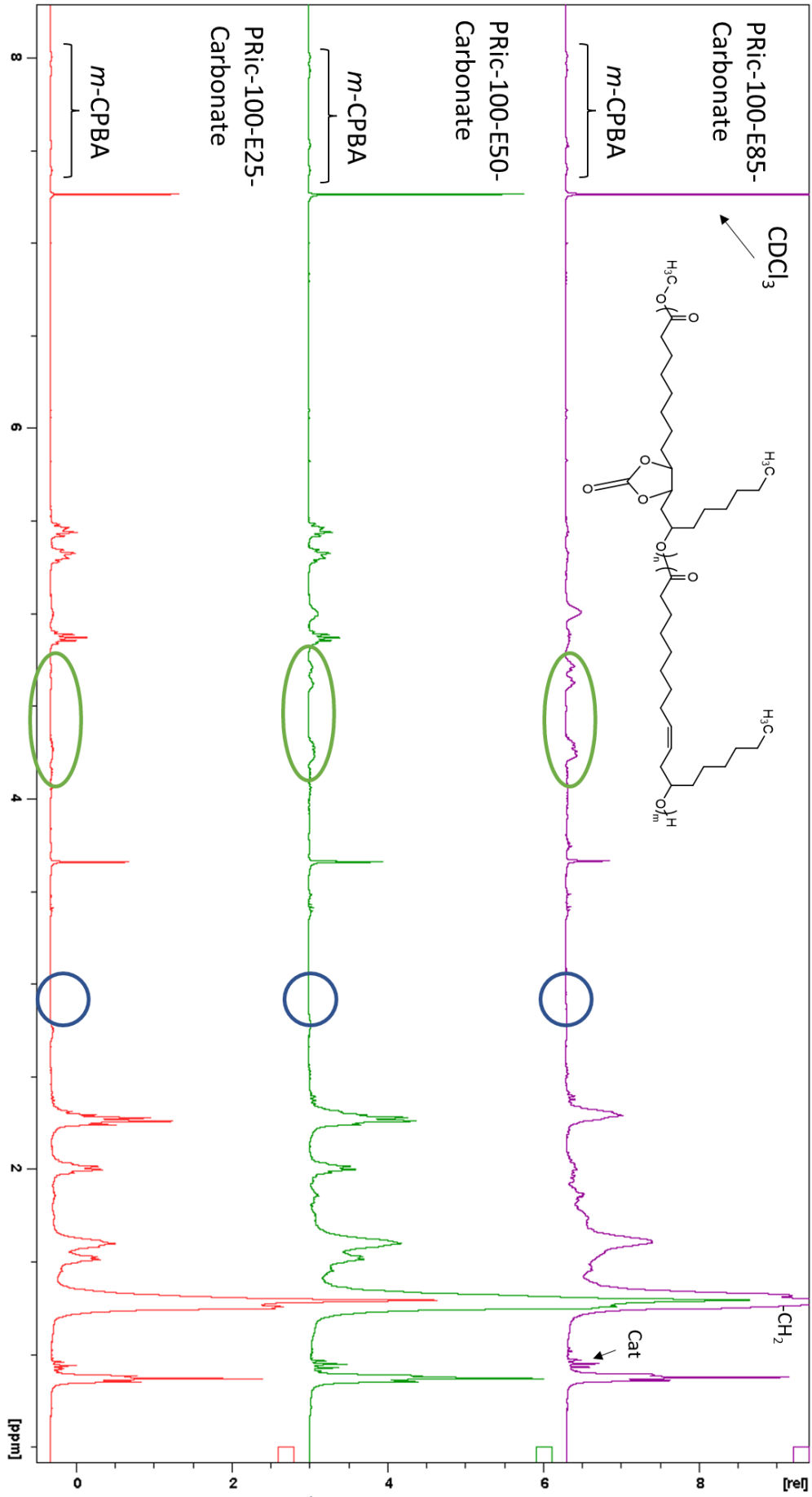


Fig III. 28: Stacked ^1H NMR spectra of carbonated PRic-100

As a complement to the ^1H NMR, FTIR spectra were acquired to confirm the apparition of carbonate groups (Fig III. 29, Fig III. 30 and Fig III. 31). For every targeted amount of carbonate groups, a characteristic peak of carbonate groups appeared around $1800\text{-}1810\text{cm}^{-1}$, therefore proving their synthesis. In the case our PRic-100-E85-Carbonate, two extra peaks, also accounting for carbonated groups, clearly appeared around 1040cm^{-1} and 1170cm^{-1} . The transmission intensity of this peak would also increase with an increasing amount of carbonate groups, further proving the correct result of this synthesis.

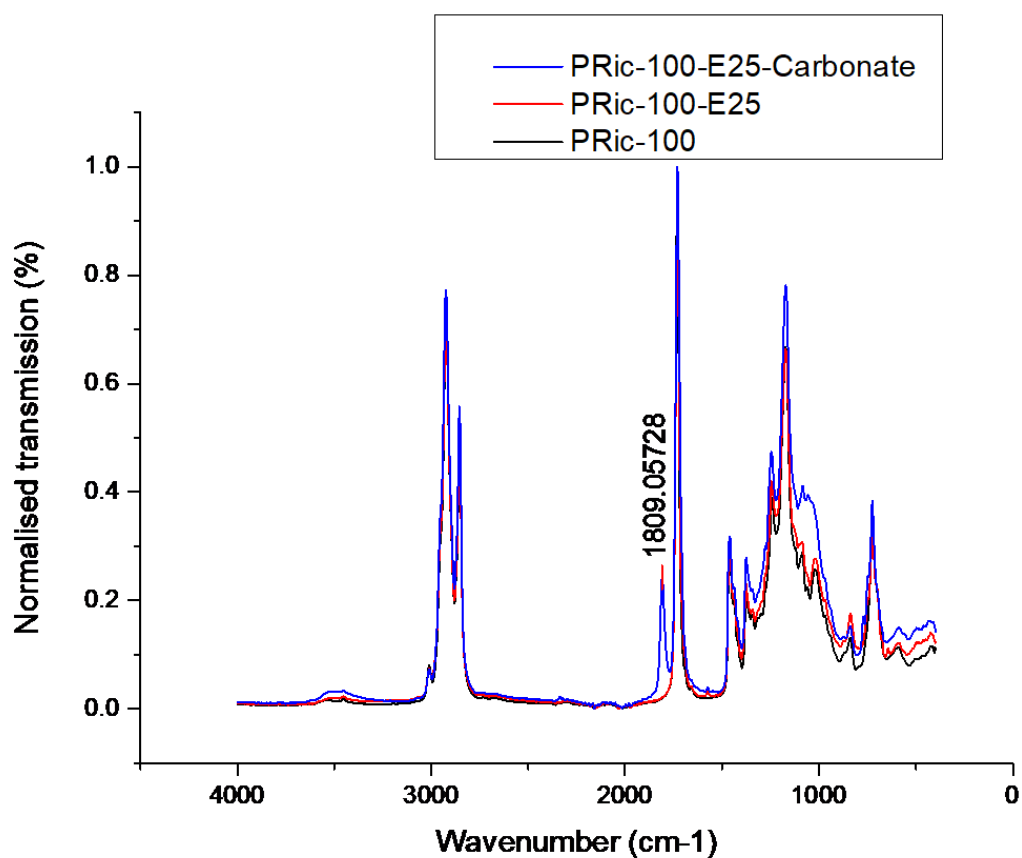


Fig III. 29: FTIR transmission spectra of PRic-100, PRic-100-E25 and PRic-100-E25-Carbonate

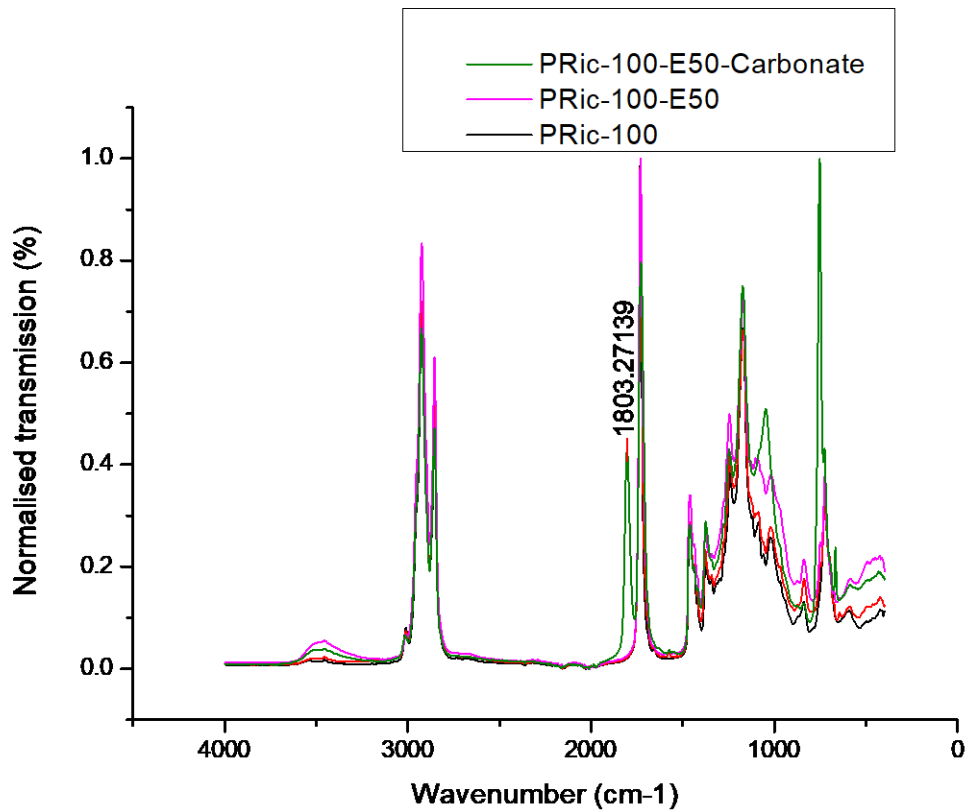


Fig III. 30: FTIR transmission spectra of PRic-100, PRic-100-E50 and PRic-100-E50-Carbonate

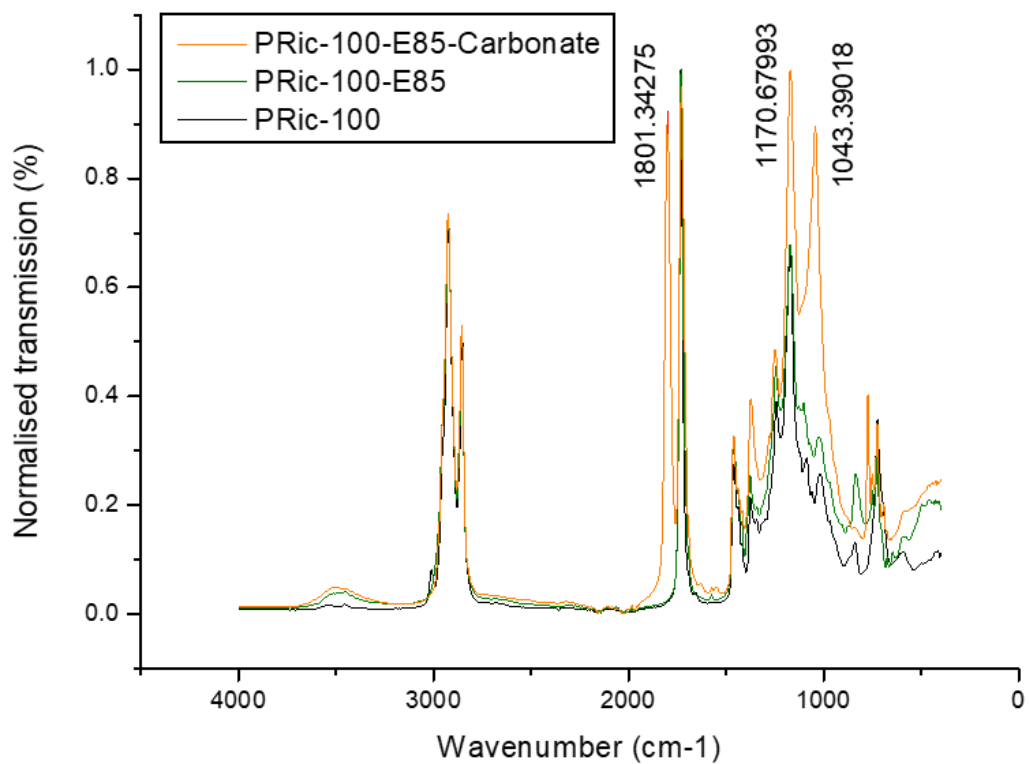


Fig III. 31: FTIR transmission spectra of PRic-100, PRic-100-E85 and PRic-100-E85-Carbonate

The SEC was then used to check the evolution of the molar mass of the different polymers. The results and chromatograms are displayed in Fig III. 32 and Table III. 22.

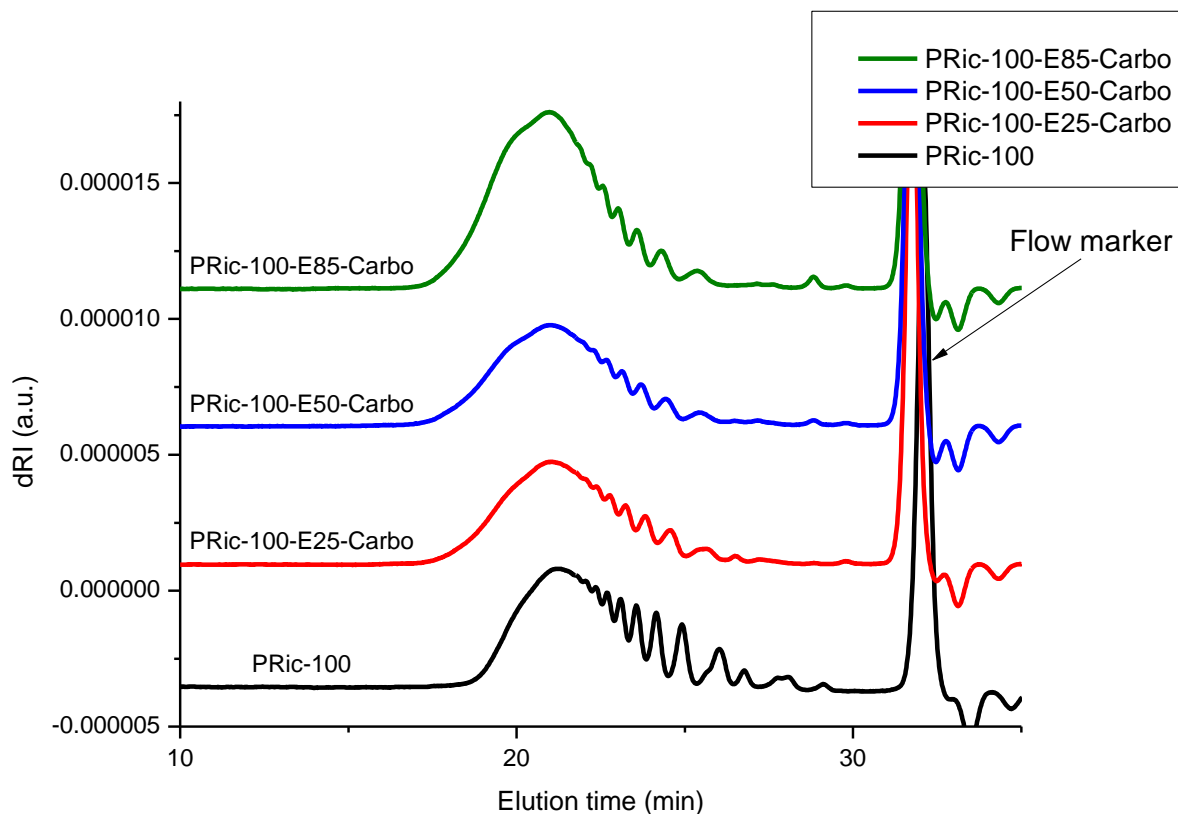


Fig III. 32: SEC traces of PRic-100 and its carbonated derivatives, THF, PS standard

Table III. 22: SEC results for PRic-100 and its carbonated derivatives, THF, PS standard

PRic grade	Mn (g/mol)	Mw (g/mol)	\bar{D}
100	2500	5200	2.1
100-E25-Carbonate	3200	6600	2.0
100-E50-Carbonate	3800	7500	2.0
100-E85-Carbonate	4250	7800	1.8

The SEC measurements show a further increase of the molar mass of the functionalised polymers. As observed before with the epoxidized PRic-100, this is due to the elimination of the low molar mass oligomers during the precipitation step. The slight change of molar mass compared to the epoxidized PRics can be attributed to the formation of the cyclic carbonate groups. Finally, the thermal properties of the carbonated PRic-100 were assessed using the

DSC. The T_gs were measured upon the second heating cycle, the values are reported in Table III. 23.

Table III. 23: T_g values of the carbonated derivatives of PRic-100, 2nd heating ramp, 10°C/min

PRic grade	T _g (°C)
100	-81
100-E25-Carbonate	-67
100-E50-Carbonate	-52
100-E85-Carbonate	-30

Again, the T_g values further increase with the conversion of the epoxides into cyclic carbonates. The highest T_g is now up to -30°C for PRic-100-E85-Carbo which bears the highest amount of cyclic carbonate groups. This accounts for polymer chains, which are less mobile and therefore require more energy to be able to move between themselves. Such feature might act as lower toughening properties for PLA.

2. Melt-blending with PLA: study of the mechanical and gas barrier properties

As described in Part A, the synthesised additives were melt-blended with PLA using a twin-screw extrusion device. A master batch holding 6wt% of additives was first made then diluted using neat PLA to obtain the other desired loadings (2wt% and 4wt%). After mixing and palletisation, small cups were injection-moulded using a Babyplast injection moulding machine and a specifically designed mould. The obtained cups were analysed and used to measure the mechanical and O₂ gas barrier properties of the considered formulation.

2.1. Structural characterisation

First, the samples were analysed using the SEC in THF to see whether the processing had any effect on the chain structure of the polymers. The results of the SEC are given in Table III. 25.

Table III. 24: Molar masses of PLA+PRic-100-EXX, SEC in THF, PS standard

Additive	Loading (wt%)	Mn (g/mol)	Mw (g/mol)	Đ
Neat PLA	0	39000	81000	2.1
	2	39000	92000	2.4
PRic-100	4	41000	88000	2.1
	6	35000	90000	2.6
PRic-100-E25	2	40000	93000	2.3
	4	53000	97000	1.8
	6	39000	93,000	2.4
PRic-100-E50	2	47000	92000	2.0
	4	28000	86000	3.0
	6	52000	92000	1.8
PRic-100-E85	2	33000	91000	2.8
	4	49000	93000	1.9
	6	37000	88000	2.4

Table III. 25: Molar masses of PLA+PRic-100-EXX-Carbonate, SEC in THF, PS standard

Additive	Loading (wt%)	Mn (g/mol)	Mw (g/mol)	Đ
Neat PLA	0	39000	81000	2.1
	2	39000	92000	2.4
PRic-100	4	41000	88000	2.1
	6	35000	90000	2.6
PRic-100-E25-Carbonate	2	14000	51000	3.5
	4	19000	48000	2.5
	6	16000	57000	3.6
PRic-100-E50-Carbonate	2	23000	61000	2.6
	4	23000	53000	2.3
	6	21000	57000	2.7
PRic-100-E85-Carbonate	2	43000	86000	2.0
	4	29000	78000	2.7
	6	37000	84000	2.2

As observed with PRic-LCPO, the measured molar masses are stable and similar when PRic-100 and its epoxidized derivatives were used as additives in PLA. This was also the case with PRic-100-E85-Carbonate. However, in the case of the two remaining carbonated additives, the M_n was divided by two and the M_w reduced by about 30%. This is concerning since it can induce a strong bias when properties of these samples will be assessed such as the thermal properties or the mechanical properties.

2.2. Thermal characterisation

The samples were put in the DSC to check their crystallinity ratio and see whether the injection moulding process had an effect of allowing the samples to partially crystallise. The results are reported in Table III. 26 for the PRic-100 bearing epoxides and in Table III. 27 for the PRic-100 bearing carbonate groups.

Table III. 26: DSC results PLA+PRic-100 and its epoxide derivatives

Additive	Loading (wt%)	ΔH_{cc} (J/g)	ΔH_m (J/g)	$\Delta H_{\alpha' \rightarrow \alpha}$ (J/g)	$\chi_{c,c}$ (%)	T_g (°C)	T_m (°C)
Neat PLA	0	41.3	45.6	2.1	2	58	173
PRic-100	2	38.0	50.4	6.0	7	57	172
	4	35.7	47.5	5.1	7	58	172
	6	34.4	50.8	5.6	11	57	171
PRic-100-E25	2	38.2	49.9	5.5	8	56	172
	4	37.3	47.1	5.0	6	56	172
	6	35.2	46.2	5.6	6	56	172
PRic-100-E50	2	37.7	50.2	5.2	8	57	172
	4	36.4	49.1	5.0	8	57	172
	6	35.0	48.6	5.5	9	56	172
PRic-100-E85	2	37.7	50.1	5.6	8	57	172
	4	36.3	48.4	5.6	8	56	172
	6	35.1	48.0	5.8	9	57	172

Table III. 27: DSC results PLA+PRic-100 and its carbonated derivatives

Additive	Loading (wt%)	ΔH_{cc} (J/g)	ΔH_m (J/g)	$\Delta H_{\alpha' \rightarrow \alpha}$ (J/g)	$\chi_{c, c}$ (%)	T_g (°C)	T_m (°C)
Neat PLA	0	41.3	45.6	2.1	2	58	173
PRic-100	2	38.0	50.4	6.0	7	57	172
	4	35.7	47.5	5.1	7	58	172
	6	34.4	50.8	5.6	11	57	171
PRic-100-E25-Carbonate	2	39.5	50.7	2.9	9	55	172
	4	39.5	49.3	2.0	10	53	171
	6	41.0	50.1	3.7	6	54	172
PRic-100-E50-Carbonate	2	38.1	45.6	2.5	5	53	171
	4	38.2	47.0	0.3	10	53	171
	6	39.3	48.6	3.2	7	55	172
PRic-100-E85-Carbonate	2	39.3	47.5	3.9	5	58	173
	4	37.0	49.1	5.0	8	57	172
	6	36.7	49.5	5.1	9	57	171

The DSC does not reveal any significant difference between the samples in terms of crystallinity ratios, meaning the measured mechanical properties or the gas barrier properties of the different sets of samples should not be influenced by a different crystalline state between one another. Also, the melting points of the samples were rather stable (171-173°C) showing a relatively good thermal stability after processing. One discrepancy that could be noticed was the slightly lower T_g s measured when PRic-100-E25-Carbonate and PRic-100-E50-Carbonate were used. This could be due to a partial solubility of these additives inside the PLA matrix, therefore resulting in that T_g decrease according to Fox's equation¹⁸ along with the lower molar mass measured in the SEC.

2.3. Morphology through SEM

Surfaces of the injection moulded samples were observed using the SEM. Here, the idea was to observe the morphology obtained with the different blends and therefore offer extra information regarding the later observed mechanical and gas barrier properties. The observed surfaces were obtained through freeze-fracturing the side of the cups in order to be perpendicular to the injection flow. As said before, reports from the literature mention

nodules dispersed in the PLA matrix due to the low solubility of PRic in PLA^{5,9}, therefore, such nodules are expected to be observed using the considered additives.

The immiscibility of PLA and PRic-100 is verified since nodules can be observed whatever the considered loading. The same can be observed for PRic-100-E25, -E50 and -E85 and their carbonated derivatives showing the chemical modification of PRic-100 with more polar groups did not fundamentally change the morphology of the blends (Fig III. 33 and Fig III. 34).

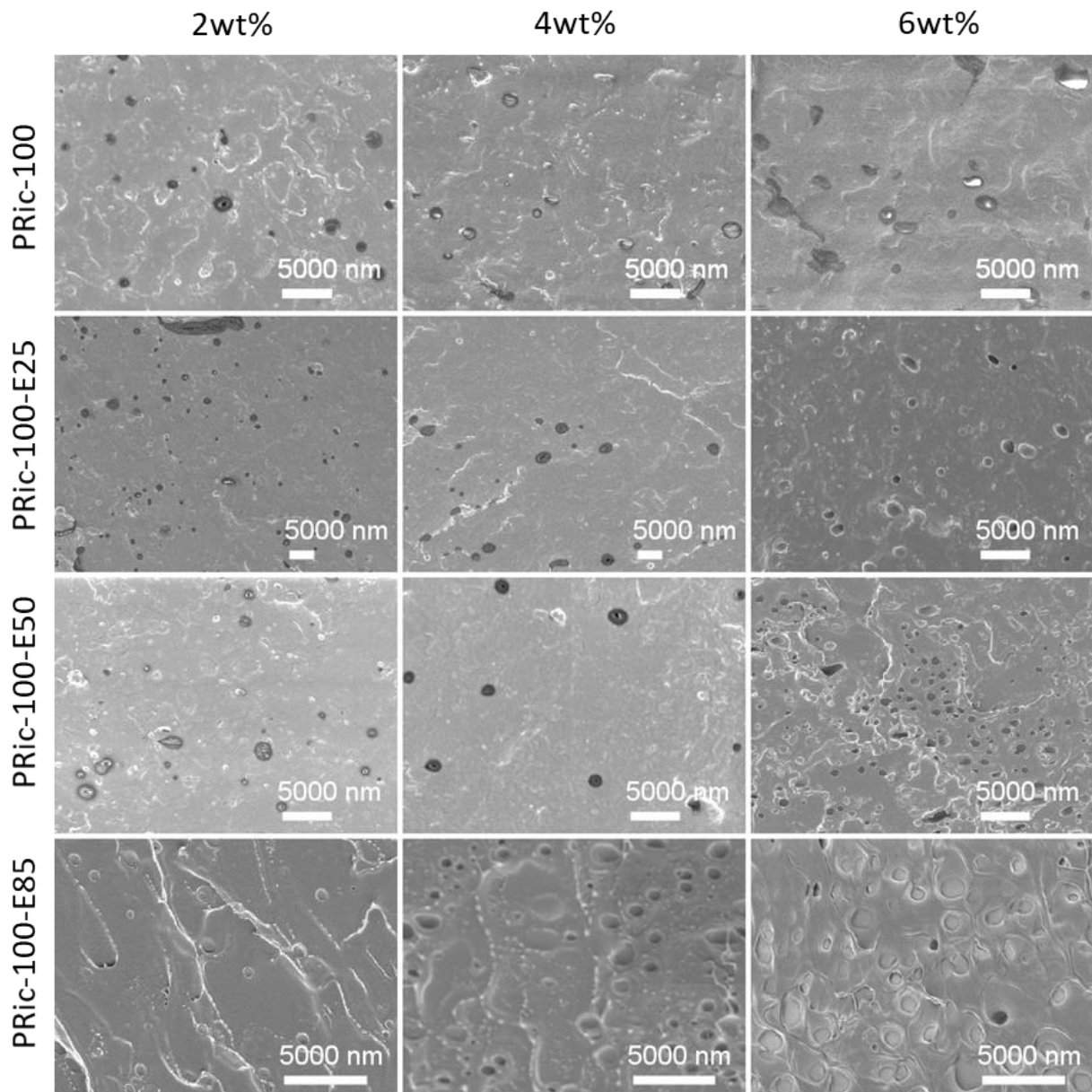


Fig III. 33: SEM pictures of PLA+PRic-100 and its epoxidized derivatives

Table III. 28: Nodule size PLA+PRic-100 and its epoxidized derivatives

Additive	Loading (wt%)	Ellipse major (nm)	SD	PDI	Ellipse minor (nm)	SD	PDI
PRic-100	2	737	423	0.33	568	353	0.39
	4	1471	938	0.41	1004	593	0.35
	6	2755	1623	0.35	1447	518	0.13
PRic-100-E25	2	1570	1706	1.18	977	682	0.49
	4	1211	886	0.54	897	641	0.51
	6	819	400	0.24	689	280	0.17
PRic-100-E50	2	1161	640	0.30	916	536	0.34
	4	1238	732	0.35	884	421	0.23
	6	789	263	0.11	574	179	0.10
PRic-100-E85	2	805	367	0.21	651	297	0.21
	4	484	238	0.24	340	152	0.20
	6	862	337	0.15	650	293	0.20

When PRic-100 is used as an additive, the nodules' size increases with the amount of additive, showing the immiscibility of PRic-100 with PLA. However, when PRic-100 was epoxidized at 25% and 50%, the size of the nodules diminished with an increasing amount of additive. In the case of the 85% epoxidized PRic-100, the size of the nodules first diminished from 2wt% to 4wt% and then increased at 6wt%. However, this variation in size was mainly attributed to the change in the amount of nodules present in the different samples. As it can be seen in the SEM pictures (Fig III. 33), the distribution of nodules is not the same for every additive, therefore leading to smaller nodules but better dispersed in some cases and bigger nodules but less dispersed in other cases. Interestingly, the interface between the nodules and the PLA matrix did not display any defect.

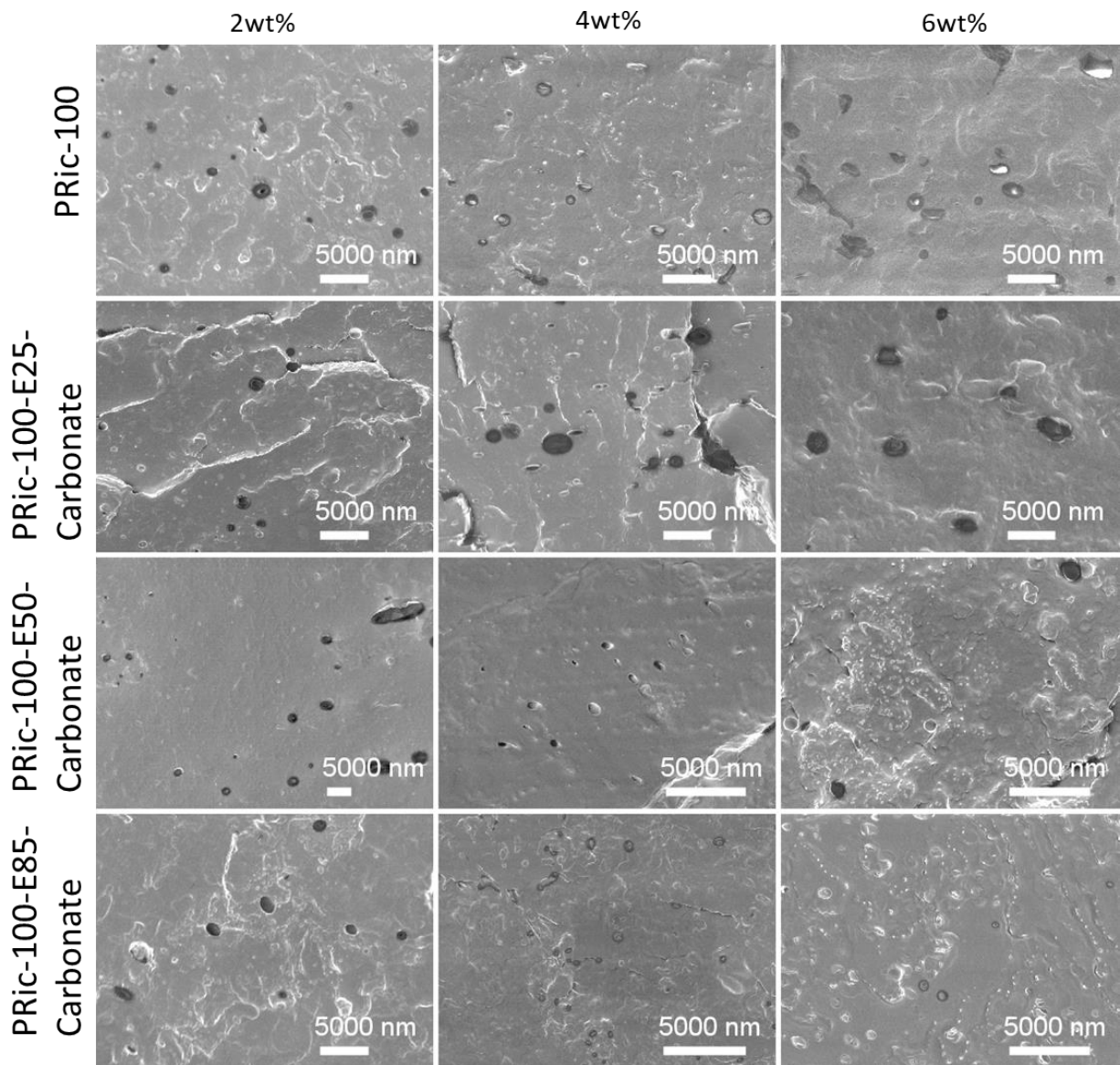


Fig III. 34: SEM pictures of PLA+PRic-100 and its carbonated derivatives

Table III. 29: Nodule size PLA+PRic-100 and its carbonated derivatives

Additive	Loading (wt%)	Ellipse major (nm)	SD	PDI	Ellipse minor (nm)	SD	PDI
PRic-100	2	737	423	0.33	568	353	0.39
	4	1471	938	0.41	1004	593	0.35
	6	2755	1623	0.35	1447	518	0.13
PRic-100-E25-Carbonate	2	888	278	0.10	707	218	0.10
	4	1564	1744	1.24	786	611	0.60
	6	2796	1259	0.20	2107	771	0.13
PRic-100-E50-Carbonate	2	2338	1893	0.66	1745	1030	0.35
	4	714	175	0.06	443	83	0.03
	6	629	318	0.26	587	267	0.21
PRic-100-E85-Carbonate	2	1350	624	0.21	1024	485	0.22
	4	448	314	0.49	313	213	0.46
	6	596	226	0.14	430	139	0.11

Here, the nodules' size increases with the amount of additive when PRic-100 was carbonated at 25% and follows the trend observed for neat PRic-100. However, when PRic-100 was carbonated at 50% and 85%, the size of the nodules diminished with an increasing amount of additive, as observed previously for PRic-100-E25 and PRic-100-E50. This was also attributed to a better dispersion of the additive at high quantities. As previously observed, the interface between the nodule and the matrix did not show any defect.

2.4. Vertical compression testing

The mechanical properties of the materials were assessed using the vertical compression testing at 10mm/min. Due to the complexity of the injection moulded cups, no section could be calculated, therefore all the results will be given as force vs strain curves which were obtained using ten replicas for each set of samples. Beneath the curves (Fig III. 35 to Fig III. 41: Force vs strain curves PLA+PRic-100-E85-Carbonate), a table recapping the measured mechanical characteristics of the samples is given (Table III. 30 to Table III. 36).

a. PLA + PRic-100

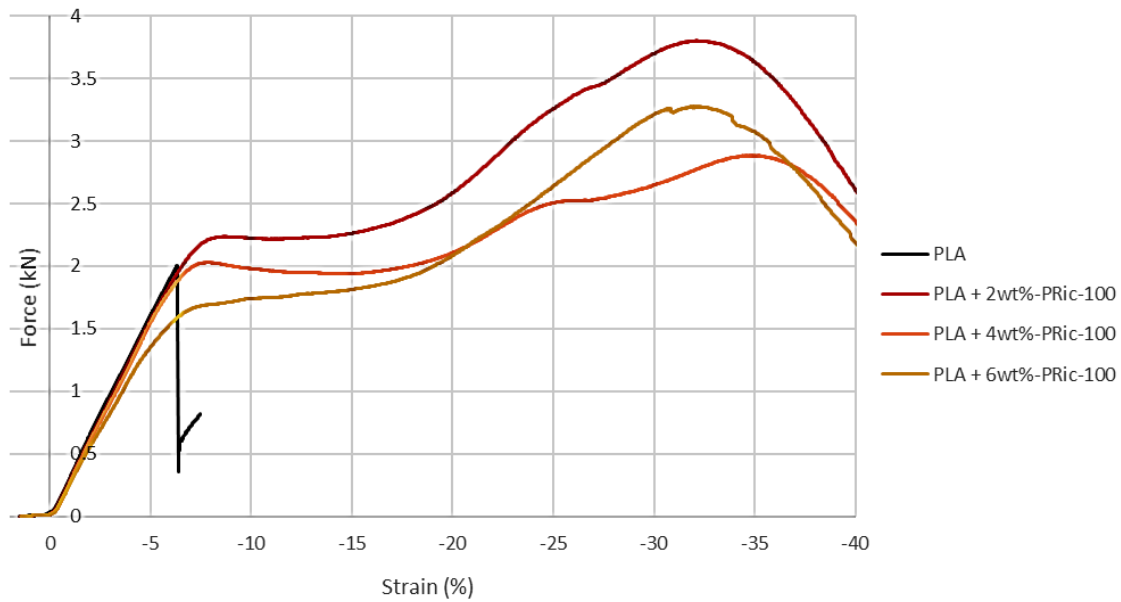


Fig III. 35: Force vs strain curve of PLA+PRic-100

Table III. 30: Mechanical results PLA+PRic-100 using ten replicas

Sample	Slope (N)	Force Plateau (kN)	Yield point (%)	Force at break (kN)	Strain at break (%)
PLA	351 ±13	2.0 ±0.1	-6.3 ±0.1	2.0 ±0.1	-6.3 ±0.1
PLA+2wt%-PRic-100	345 ±10	2.2 ±0.1	-8.7 ±0.1	#	>-25
PLA+4wt%-PRic-100	346 ±10	2.0 ±0.1	-7.9 ±0.1	#	>-25
PLA+6wt%-PRic-100	322 ±8	1.7 ±0.1	#	#	>-25

First, neat PRic-100 was tested as an additive for PLA. From Fig III. 35, it can be seen a clear improvement of mechanical behaviour. As summarised in Table III. 30, for every considered loading, there would not be any sudden and brittle fracture of the samples. The compression strain could go over -40% (not shown) without the sample breaking. Regarding the other data, the measured slope at origin decreases with the addition of PRic-100 which is expected. At 2wt%, the force plateau is measured 2.21kN which is higher than the maximum that could be obtained with neat PLA (which breaks at a force of about 2kN). This plateau value would then decrease with an increasing amount of additive, which again is an expected behaviour.

Overall, the addition of PRic-100 in PLA even at low loadings, greatly improved its mechanical behaviour in terms of strain at break without decreasing the modulus too much.

b. PLA + PRic-100-EXX

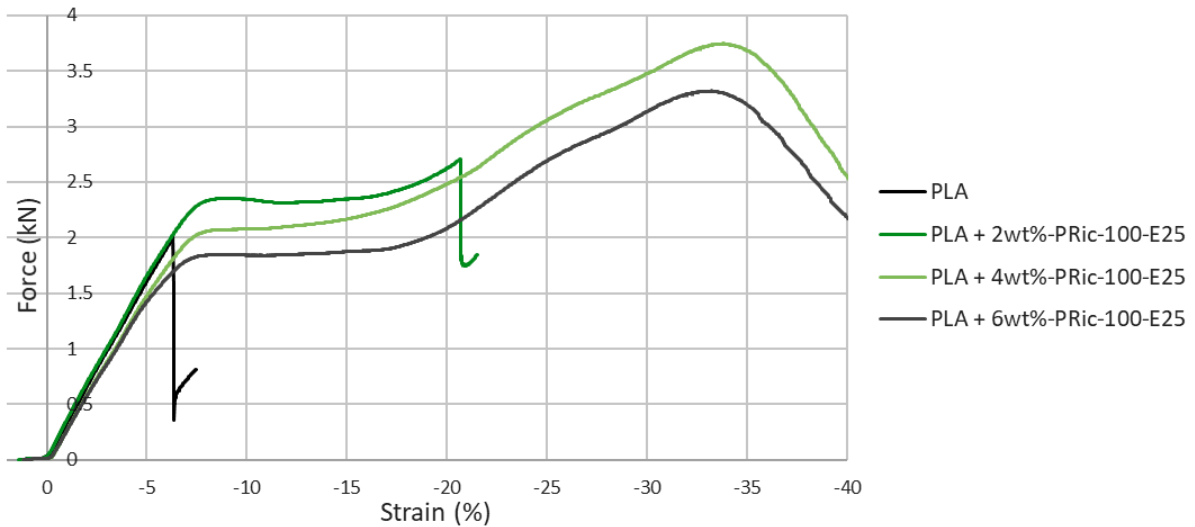


Fig III. 36: Force vs strain curves of PLA+PRic-100-E25, 10mm/min

Table III. 31: Mechanical results PLA+PRic-100-E25 using ten replicas

Sample	Slope (N)	Force Plateau (kN)	Yield point (%)	Force at break (kN)	Strain at break (%)
PLA	351 ±13	2.0 ±0.1	-6.3 ±0.1	2.0 ±0.1	-6.3 ±0.1
PLA+2wt%-PRic-100-E25	364 ±19	2.4 ±0.1	#	2.7 ±0.1	-20.8 ±0.8
PLA+4wt%-PRic-100-E25	331 ±8	2.1 ±0.1	#	#	>-25
PLA+6wt%-PRic-100-E25	319 ±7	1.9 ±0.1	#	#	>-25

In the case of PRic-100-E25 used an additive, it can be noticed that at low loadings (2wt%), the samples would actually break in a brittle manner and that higher loadings are required to stop observing this behaviour. However, the strain at break is over -20%, which is already a solid improvement compared to neat PLA. Interestingly, the slope value for that sample is actually higher than the one of neat PLA, meaning this set of samples is stiffer than neat PLA while showing a better resistance to deformation. Also, the force at break is up to 2.7kN, which is a 35% improvement compared to neat PLA. Here, the force plateaux are also higher than

with neat PRic-100, and still decrease with an increasing amount of additive, with a maximum reached at 2.4kN and a minimum at 1.9kN.

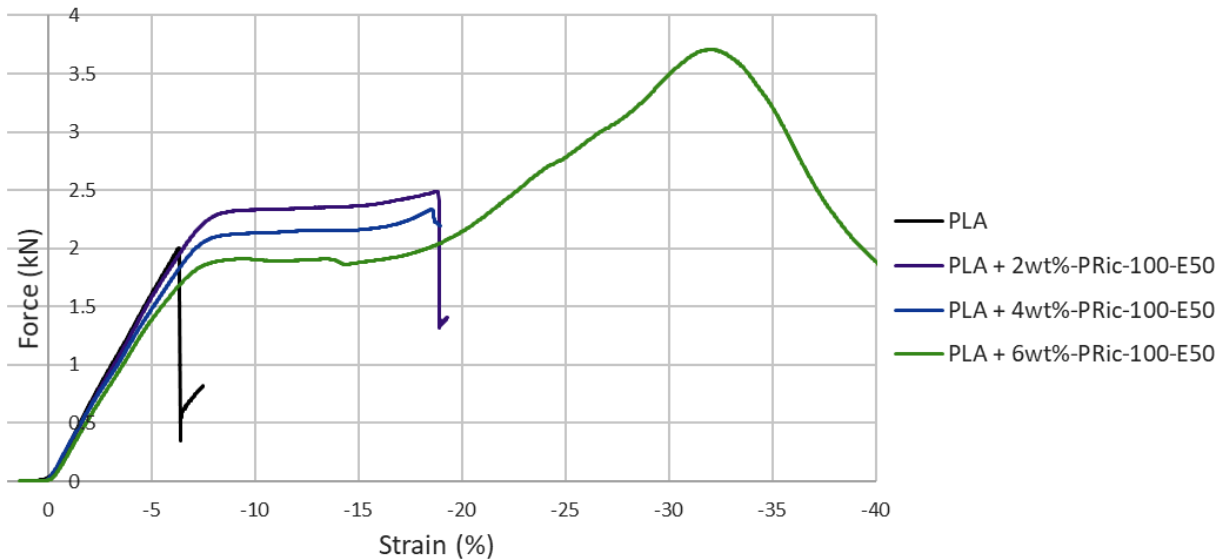


Fig III. 37: Force vs strain curves of PLA+PRic-100-E50 samples

Table III. 32: Mechanical results PLA+PRic-100-E50 using ten replicas

Sample	Slope (N)	Force Plateau (kN)	Yield point (%)	Force at break (kN)	Strain at break (%)
PLA	351 ±13	2.0 ±0.1	-6.3 ±0.1	2.0 ±0.1	-6.3 ±0.1
PLA+2wt%-PRic-100-E50	331 ±6	2.3 ±0.1	#	2.6 ±0.1	-19.6 ±1.2
PLA+4wt%-PRic-100-E50	334 ±6	2.2 ±0.1	#	2.2 ±0.2	-18.6 ±0.9
PLA+6wt%-PRic-100-E50	310 ±7	1.9 ±0.1	#	#	>-25

Here, the mechanical improvement of PLA is even more reduced. Only samples loaded with 6wt% of PRic-100-E50 would not break in a brittle manner under the compression test. The strains at break were still however rather high (-20% and -19%) compared to neat PLA. Here though, the force at break values are smaller than using PRic-100-E25, 2.6kN and 2.2kN, showing a lesser efficiency of the additive for the mechanical reinforcement of PLA. However, the resistance to the applied force and the applied strain was still improved compared to the performance of neat PLA.

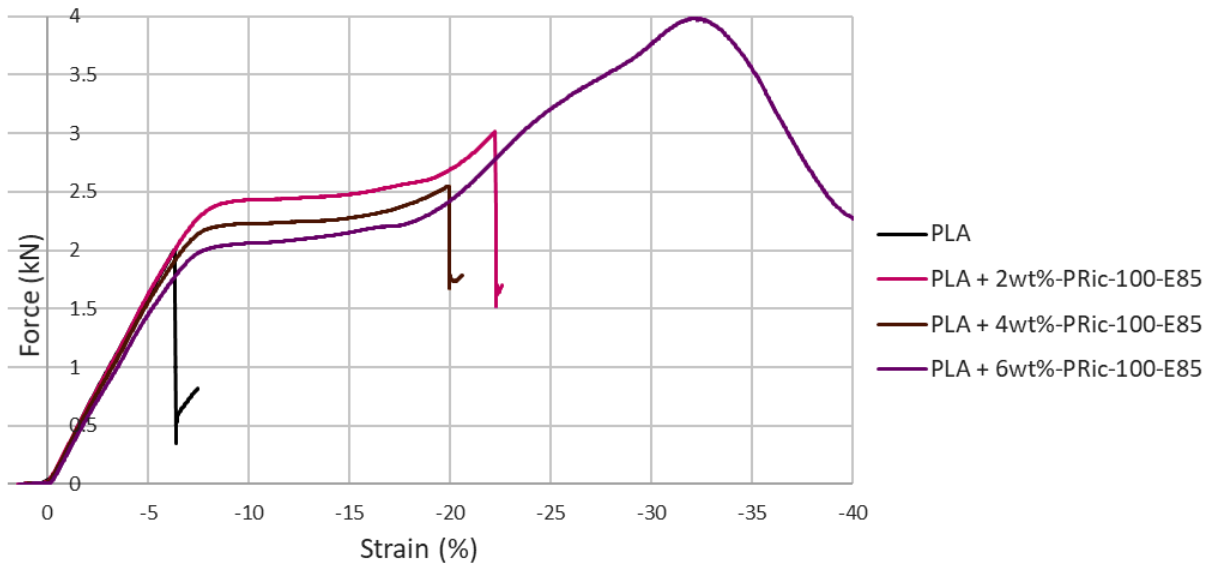


Fig III. 38: Force vs strain curves of PLA+PRic-100-E85 samples

Table III. 33: Mechanical results PLA+PRic-100-E85 using ten replicas

Sample	Slope (N)	Force Plateau (kN)	Yield point (%)	Force at break (kN)	Strain at break (%)
PLA	351 ±13	2.0 ±0.1	-6.3 ±0.1	2.0 ±0.1	-6.3 ±0.1
PLA+2wt%-PRic-100-E85	338 ±26	2.4 ±0.1	#	3.1 ±0.1	-22.1 ±0.6
PLA+4wt%-PRic-100-E85	334 ±8	2.2 ±0.1	#	2.7 ±0.2	-20.3 ±0.9
PLA+6wt%-PRic-100-E85	316 ±7	2.1 ±0.1	#	#	>-25

Here again, only the samples the most loaded with the additive showed the best mechanical behaviour regarding breaking. Both samples at 2wt% and 4wt% would break eventually, still at rather high strains (-22% and -20%). It is interesting to notice though, the better performance of the 2wt% loaded sample compared to the 4wt% loaded sample. Both the strain at break and the force at break were higher for the 2wt% sample than the 4wt% sample. Also, it can be noticed that among all samples, the highest force plateau values were obtained with this additive. This was attributed to the higher T_g for PRic-100-E85 compared to the other epoxidized PRic-100 additives, therefore leading to a “harder” additive which would less hamper the stiffness of the PLA material.

c. PLA + PRic-100-Carbonate

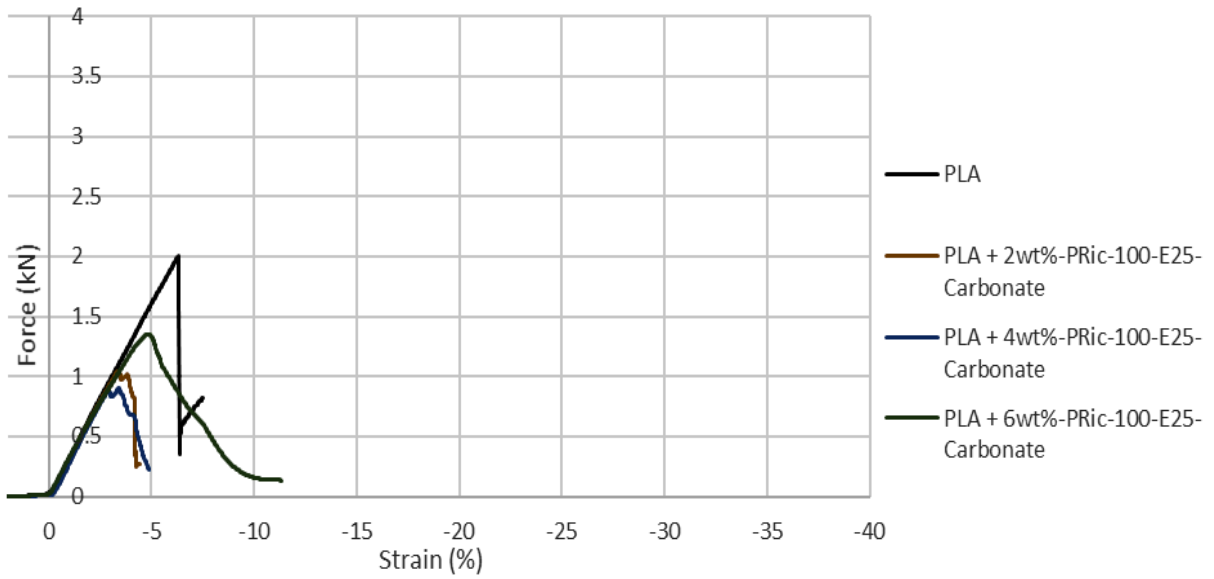


Fig III. 39: Force vs strain curves PLA+PRic-100-E25-Carbonate

Table III. 34: Mechanical results PLA+PRic-100-E25-Carbonate using ten replicas

Sample	Slope (N)	Force Plateau (kN)	Yield point (%)	Force at break (kN)	Strain at break (%)
PLA	351 ±13	2.0 ±0.1	-6.3 ±0.1	2.0 ±0.1	-6.3 ±0.1
PLA+2wt%-PRic-100-E25-Carbonate	349 ±11	1.1 ±0.1	-3.4 ±0.1	1.1 ±0.1	-3.4 ±0.1
PLA+4wt%-PRic-100-E25-Carbonate	343 ±12	0.9 ±0.1	-3.0 ±0.1	0.9 ±0.1	-3.0 ±0.1
PLA+6wt%-PRic-100-E25-Carbonate	336 ±7	1.4 ±0.1	-4.8 ±0.1	1.4 ±0.1	-4.8 ±0.1

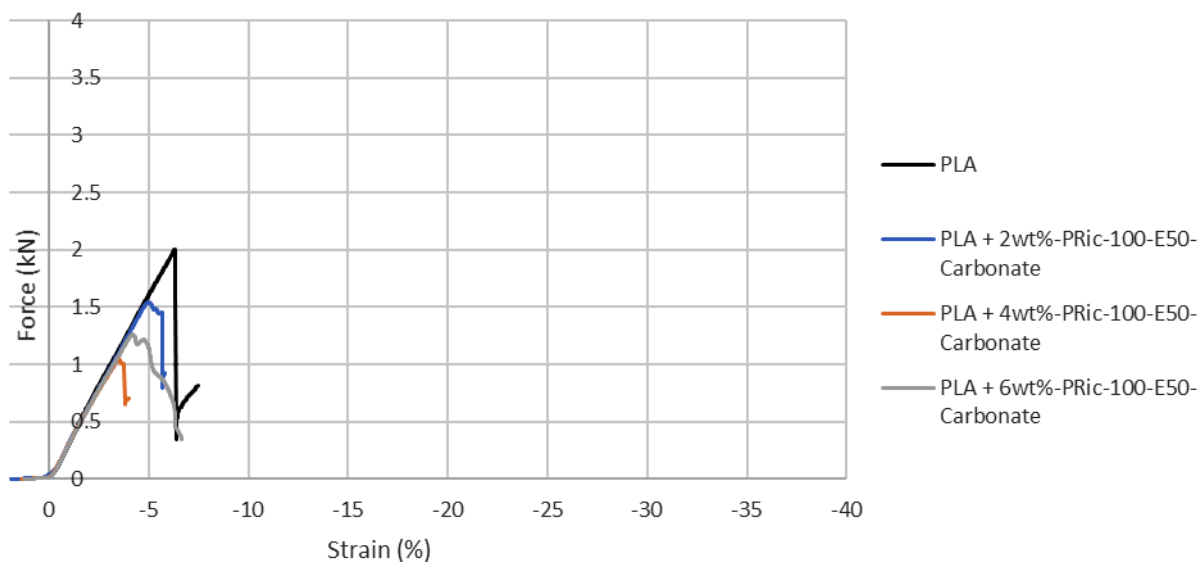


Fig III. 40: Force vs strain curves PLA+PRic-100-E50-Carbonate

Table III. 35: Mechanical results PLA+PRic-100-E50-Carbonate using ten replicas

Sample	Slope (N)	Force Plateau (kN)	Yield point (%)	Force at break (kN)	Strain at break (%)
PLA	351 ±13	2.0 ±0.1	-6.3 ±0.1	2.0 ±0.1	-6.3 ±0.1
PLA+2wt%-PRic-100-E50-Carbonate	352 ±6	1.6 ±0.1	-5.0 ±0.1	1.6 ±0.1	-5.0 ±0.1
PLA+4wt%-PRic-100-E50-Carbonate	342 ±11	1.1 ±0.1	-3.5 ±0.1	1.1 ±0.1	-3.5 ±0.1
PLA+6wt%-PRic-100-E50-Carbonate	344 ±4	1.3 ±0.1	-4.2 ±0.1	1.3 ±0.1	-4.2 ±0.1

The measured mechanical performance of PLA with PRic-100-E25-Carbonate and PRic-100-E50-Carbonate was not expected. The samples showed a much lower mechanical resistance than neat PLA, all breaking at very low strains and at low forces. Visually, the samples broke in a brittle manner, with cracks appearing very early during the test. Such behaviour was mainly attributed to the huge decrease of molar mass that was measured through the SEC. It has been reported that PLA with a lower molar mass exhibits lower mechanical properties^{19,20} therefore explaining such poor performance.

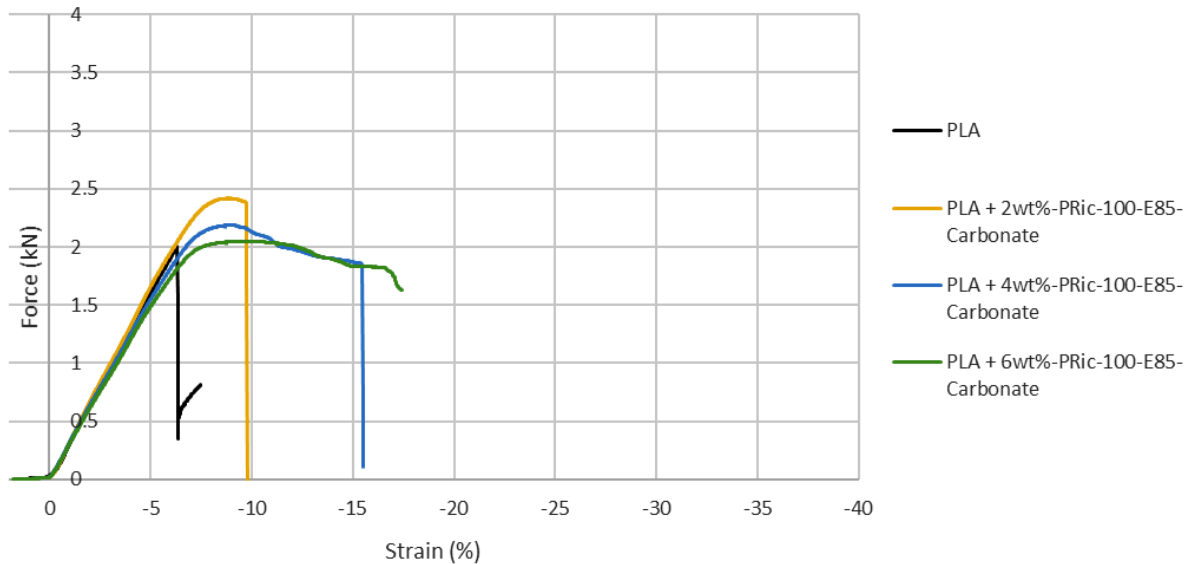


Fig III. 41: Force vs strain curves PLA+PRic-100-E85-Carbonate

Table III. 36: Mechanical results PLA+PRic-100-E85-Carbonate using ten replicas

Sample	Slope (N)	Force Plateau (kN)	Yield point (%)	Force at break (kN)	Strain at break (%)
PLA	351 ±13	2.0 ±0.1	-6.3 ±0.1	2.0 ±0.1	-6.3 ±0.1
PLA+2wt%-PRic-100-E85-Carbonate	367 ±16	2.4 ±0.1	-9.3 ±0.6	2.4 ±0.1	-9.4 ±0.6
PLA+4wt%-PRic-100-E85-Carbonate	339 ±20	2.2 ±0.1	-9.1 ±0.2	1.9 ±0.1	-15.0 ±1.4
PLA+6wt%-PRic-100-E85-Carbonate	319 ±9	2.1 ±0.1	-9.9 ±0.3	1.9 ±0.1	-17.3 ±0.8

Eventually, PRic-100-E85-Carbonate was tested as an additive. Contrary to the two latest considered additives, no catastrophic mechanical performance could be observed. There was an improvement in the mechanical properties of PLA with the use of PRic-100-E85-Carbonate. The strain at break was improved, reaching -17% in the best-case scenario. The force plateau was also improved for every loading, however, once the yielding point was reached, there was no recovery from the sample. The 2wt% loaded sample showed a very sudden and brittle fracture behaviour almost as the 4wt% loaded sample. In the case of the 6wt% loaded sample, the fracture was more gradual however still led to a final breakage around a -17% strain. It is interesting to notice the three sets of samples showed a rather similar yielding point in terms

of strain, with the corresponding force following the trend already observed before: the more additive, the lower the force plateau.

2.5. Oxygen barrier properties

The results of O₂ permeability are presented in Fig III. 42 and Table III. 37. As a reference, the values obtained for neat PLA cups in Part A were used here. The calculated PLA O₂ permeability was of $4.5 \times 10^{-3} \text{ cm}^3 \cdot \text{m} \cdot \text{m}^{-2} \cdot \text{d}^{-1} \cdot \text{atm}^{-1}$. First, the performance achieved by the samples containing neat PRic-100 was observed. The addition of PRic-100 increases slightly the O₂ permeability, going up to $5.8 \times 10^{-3} \text{ cm}^3 \cdot \text{m} \cdot \text{m}^{-2} \cdot \text{d}^{-1} \cdot \text{atm}^{-1}$ in the case of a 6wt% loading. As well, the more additive, the higher the permeability. This is typically explained by the increase of free volume inside the PLA matrix due to the addition of an immiscible polymer²². In the case of the addition of PRic-100-E25, the low loading showed a slightly lower O₂ permeability however with a high standard deviation. The same trend as before seems to appear: the more additive, the higher the permeability, however, due to the high standard deviation, the measured values can be considered as similar and similar to the one of neat PLA. For PRic-100-E50 loaded samples, the same trend is present, and the permeability values are higher than the ones of neat PLA. The PRic-100-E85 loaded samples show a more interesting behaviour. The 2wt% sample shows a lower O₂ permeability, the 4wt% the highest and the 6wt% is closer to the one of PLA. This shows a slight effect of the presence of the epoxide groups in favour of a more barrier behaviour regarding O₂, especially at low loadings at which the effect due to the increase of the free volume is lower. Overall, this set of additives is promising since the permeability values do not increase too much (less than 30%) and are stabilised around the one of neat PLA with the addition of epoxides.

Regarding the carbonated PRic-100 derivatives, the O₂ permeability are more interesting. When PLA was mixed with PRic-100-E25-Carbonate or PRic-100-E50-Carbonate, there was a noticeable decrease in O₂ permeability. More especially, the 6wt% PRic-100-E25-Carbonate sample displayed an O₂ permeability more than twice as low as the original O₂ permeability of PLA. Regarding the PRic-100-E50-Carbonate loaded samples, the same observations can be made; the sample containing the highest amount of additive displaying the lowest O₂ permeability. This pushes in favour of an effect of the cyclic carbonate groups on the O₂ permeability, showing that the presence of these chemical functions on the PRic backbone

Chapter 3

tend to lower the diffusion of O₂ in the matrix. However, in the case of PRic-100-E85-Carbonate, the permeability values were up again, slightly lower than the one of neat PLA. This is not expected considering the results obtained with the two other carbonated PRic-100 derivatives; indeed, more cyclic carbonate groups should have meant that the O₂ permeability would have been even more hampered. These results have therefore to be discussed with regard to the other analysis.

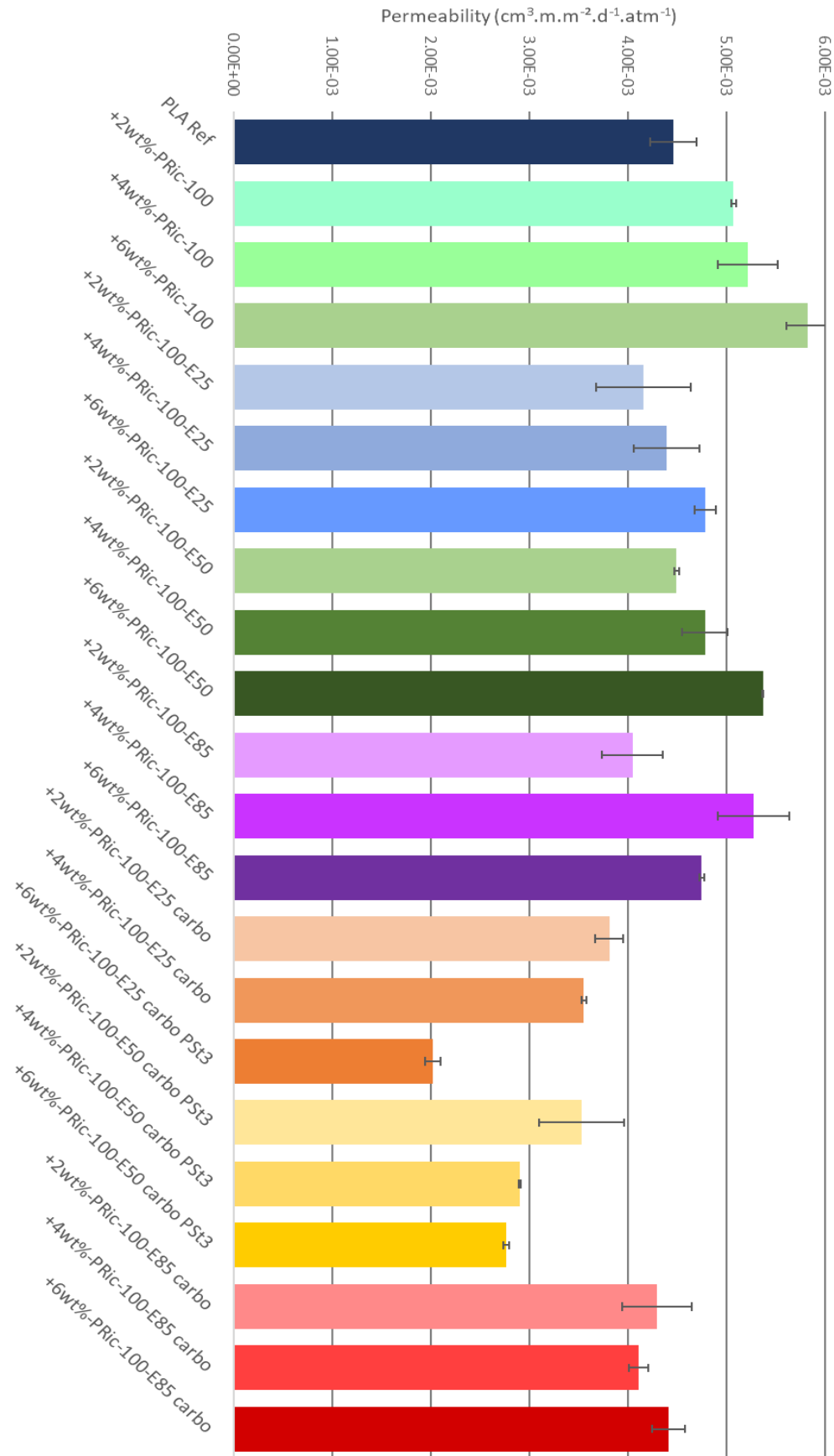


Fig III. 42: O_2 average permeability values (2 samples) of PLA samples with PRic-100 and its derivatives as additives - 23°C , 50% RH

Table III. 37: O₂ permeability results of PLA + PRic-100 and its derivatives

Samples	O₂ Permeability (10⁻³.cm³.m.m⁻².d⁻¹.atm⁻¹)
PLA ref	4.5 ± 0.2
+2wt%-PRic-100	5.1 ± 0.1
+4wt%-PRic-100	5.2 ± 0.3
+6wt%-PRic-100	5.8 ± 0.2
+2wt%-PRic-100-E25	4.2 ± 0.5
+4wt%-PRic-100-E25	4.4 ± 0.3
+6wt%-PRic-100-E25	4.8 ± 0.1
+2wt%-PRic-100-E50	4.5 ± 0.1
+4wt%-PRic-100-E50	4.8 ± 0.2
+6wt%-PRic-100-E50	5.4 ± 0.1
+2wt%-PRic-100-E85	4.1 ± 0.3
+4wt%-PRic-100-E85	5.3 ± 0.4
+6wt%-PRic-100-E85	4.8 ± 0.1
+2wt%-PRic-100-E25-carbo	3.8 ± 0.1
+4wt%-PRic-100-E25-carbo	3.6 ± 0.1
+6wt%-PRic-100-E25-carbo	2.0 ± 0.1
+2wt%-PRic-100-E50-carbo	3.5 ± 0.4
+4wt%-PRic-100-E50-carbo	2.9 ± 0.1
+6wt%-PRic-100-E50-carbo	2.8 ± 0.1
+2wt%-PRic-100-E85-carbo	4.3 ± 0.4
+4wt%-PRic-100-E85-carbo	4.1 ± 0.1
+6wt%-PRic-100-E85-carbo	4.4 ± 0.2

3. Discussion and conclusions

The use of PRic-100 and its epoxidized and carbonated derivatives has shown multiple results. First, the crystalline state of all the blends was similar whatever the considered additive, therefore eliminating of any bias on a particular property that could be due to a different crystallinity ratio. Second, for an unknown reason, the sets of samples made from PRic-100-E25-Carbonate and PRic-100-E50-Carbonate showed lower molar masses than their counterparts. This had serious consequences first from a mechanical point of view, since these samples showed very bad mechanical behaviours, having a lower mechanical resistance than neat PLA at room temperature. Moreover, as shown by the measured T_g values, such lower molar masses made the PLA matrix less stiff and therefore more prone to break. This probably also had consequences on the O₂ permeability of the samples. These samples actually displayed the best O₂ barrier properties, which can be explained by the fact that since the solubility of the additive was higher due to the lower mass of PLA, it was better mixed with PLA rather than being solely under the form of nodules, which are very localised. Therefore, the barrier effect of the additive was better displayed since it was better dispersed inside PLA and probably created more difficulty for O₂ to pass through the material. This also explains why the samples made with the third carbonated additive did not show such a decrease in terms of O₂ permeability. The observed SEM morphology confirms the presence of many more nodules therefore, *i.e.* a lower solubility and therefore an additive that is more localised in the PLA matrix and acts less as a barrier layer within PLA.

Regarding the other samples which have similar molar masses, the best mechanical behaviour is obtained when neat PRic-100 is used. At loadings as low as 2wt%, the mechanical properties of PLA are totally changed, going from a brittle polymer with no plastic deformation to a material that can withstand very high strains without breaking, while retaining a high modulus at low strains. The incorporation of epoxide groups on the PRic backbone caused the additive to be less efficient for the mechanical reinforcement of PLA. Two hypotheses can be made to explain this. First, the purification process through the precipitation in methanol eliminated a part of the oligomers that are present in PRic-100. These low molar mass oligomers can have a plasticising effect as well as acting as compatibilizers at the interface of PLA and PRic-100. Therefore, their absence fragilizes the interface between PLA and the additive and the mechanical reinforcement is not as good. The second hypothesis concerns

Chapter 3

the intrinsic properties of the epoxidized PRic-100. These additives showed a higher Tg which increased with the amount of epoxide groups. The additives having a higher Tg, their chain mobility is therefore not the same as neat PRic-100 and they are less prone to withstand a deformation or stop a fracture than neat PRic-100. The same considerations can be made regarding PRic-100-E85-Carbonate which displayed the highest Tg of all additives and showed only a very little improvement in terms of mechanical behaviour although the SEM morphology showed the presence of nodules dispersed in the PLA matrix with no defect at the interface.

Finally, these additives only had a very little effect on the O₂ permeability of PLA, which allowed to measure values close to the one of neat PLA. The main noticeable effect was attributed to the increase of free volume in the material due to the addition of an immiscible polymer. The presence of epoxide groups limited the O₂ permeability increase, however, this effect was overcome by the effect brought by the increase of the free volume in the matrix.

4. Experimental & SI

4.1. Synthesis and purification of PRic-100-EXX

PRic-100 was solubilised in THF (0.167g/ml) in a round-bottomed flask under a mechanical stirrer. Once the polymer was solubilised, the solution was cooled to 0°C using an ice-bath. A solution containing THF and *m*-CPBA (0.667g/ml) was prepared on the side. Once the polymer solution was cooled to 0°C, the THF solution containing *m*-CPBA was injected dropwise using a syringe and a needle with the polymer solution still kept in an ice-bath. After one hour, the ice-bath was removed to allow the reaction to proceed at room temperature for 20 hours. The epoxidized polymer was precipitated in cold methanol (-50°C) to eliminate the unreacted *m*-CPBA and eliminate the formed 3-chlorobenzoic acid. The volume of methanol used for precipitation was at least 10:1 compared to the THF solution containing the polymer. The process was repeated until the residual *m*-CPBA/3-chlorobenzoic acid was lower than 5mol%. The precipitated polymer was then collected and dried under vacuum at 50°C for 12 hours.

4.2. Synthesis of PRic-100-EXX-Carbonate

PRic-100-EXX and 3wt% of tetrabutylammonium bromide as a catalyst were put in a pressurised vessel equipped with a mechanical stirrer. At room temperature, the airtight vessel was loaded with 40bars of CO₂ and subsequently heated to 150°C. The stirring speed was set to 250RPM. Upon heating, the pressure inside the vessel increased to 80bars. Once the set temperature was reached, the reaction was left for 20h before cooling to room temperature. The obtained polymer had a sticky brownish aspect and was recuperated using diethyl ether and THF and subsequently dried under vacuum at 80°C.

4.3. SEM analysis

SEM samples were prepared by freeze-fracturing. The observed surfaces were taken on the side of the cups and perpendicularly to the injection flow. This was of outright importance since it was noticed that the observed morphology of surfaces taken on the same direction as the injection flow showed highly elongated ellipses. This proved that the injection moulding technique had a deep effect on the morphology of the samples. The SEM pictures were then analysed using the ImageJ software. Machine learning was used to recognise the nodules in the PLA matrix and isolate them. A macro was then developed by Quentin Jausaud to

measure the size of these elliptical shaped nodules. The perimeter, major axis and minor axis were measured along with the polydispersity index instead of the standard deviation.

4.4. Vertical compression testing

Vertical compression testing was conducted in an INSTRON apparatus using parallel plates. Tests were conducted at a -10mm/min speed using 10 replicas for each compound. Due to the complexity of the object, no definite section could be calculated, therefore values are reported as a force (N) vs displacement (mm). The values for the slope at origin, yield force, force plateau, strain at break were reported.

4.5. Oxygen permeability measurement

Two cups were used per formulation for this test. These were sealed off in a glove box using pure N₂ and a saturated solution of magnesium nitrate to compensate the global relative humidity to 53% RH at 23°C. The glass panels used to seal the cups were equipped with a Pst6 Presens sensor to measure the activity of O₂ inside the sealed atmosphere (Fig III. 43). The evolution of the amount of oxygen was monitored at least once a day until the increase followed a linear trend. The permeability was calculated using the following formula:

$$Perm = \frac{Slope \times volume \times thickness}{a \times \Delta P}$$

- Perm = the permeability in cm³ (O₂).m.m⁻².day.atm
- Volume in cm³, 49.2 cm³
- Thickness in m, 0.001225 m
- a = area in m², 0.000556 m²
- ΔP = O₂ pressure differential in atm, 0.21 atm

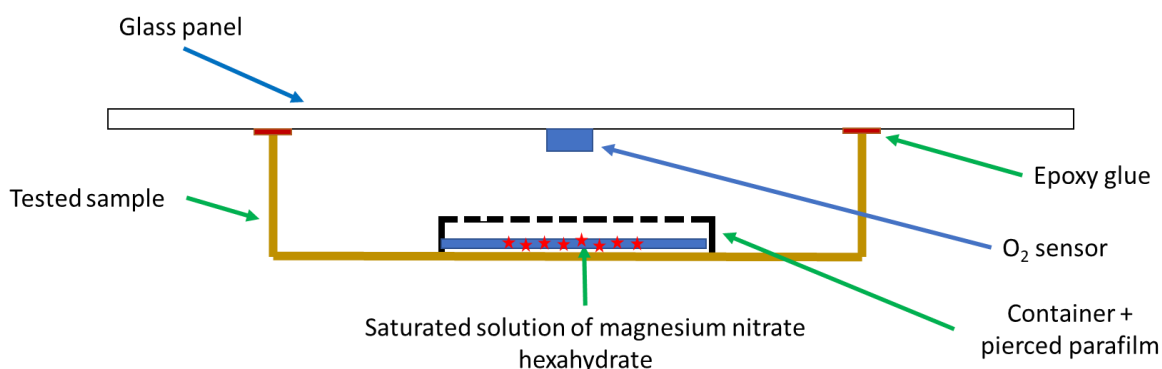


Fig III. 43: Schematic representation of the system used to measure the O₂ permeability of a sample

Comparison between both PRic grades

Table III. 38: Comparison of the performance between PRic-LCPO and PRic-100

	PRic-LCPO	PRic-100
Mn (g/mol)	5900	2500
Mw (g/mol)	24000	5200
Tg (°C)	-72	-81
Mechanical	No break from 6wt% Lesser performance than ITERG counterpart	Effective from 2wt% Best performance overall
O₂ permeability	Higher than neat PLA, increases with increasing amounts of additive	Higher than neat PLA, bigger increase than with PRic-LCPO
<u>Epoxidized</u>	E25 ; E50 ; E85	E25 ; E50 ; E85
Mn (g/mol)	7200 ; 8700 ; 12000	3100 ; 3800 ; 4100
Mw (g/mol)	27000 ; 29000 ; 28000	5800 ; 6000 ; 6700
Tg (°C)	-64 ; -54 ; -53	-70 ; -61 ; -52
Mechanical	Epoxidation improves mechanical properties	Epoxidation lowers toughening effect Higher loadings required
O₂ permeability	Reduces free volume effect Similar as neat PLA	Reduces free volume effect Higher than neat PLA
<u>Carbonated</u>	-	25% ; 50% ; 85%
Mn (g/mol)	-	3200 ; 3800 ; 4250
Mw (g/mol)	-	6600 ; 7500 ; 7800
Tg (°C)	-	-67 ; -52 ; -30
Mechanical	-	25% & 50% = poor mechanical properties (molar mass reduction) 85% = plastic behaviour but low performance compared to neat PRic
O₂ permeability	-	25% and 50% lowest permeability achieved 85% back to neat PLA level

Chapter 3

The study in this chapter covered the use of polyricinoleate as a bio-based additive for PLA. The scope of this study focussed both on the chemical modification of PRic by taking advantage of the alkene functions on the backbone and the effect of the molar mass by synthesising a homemade PRic with a higher molar mass than the commercially available grade. A comparison between the two grades is given through Table III. 38.

The PRic-LCPO showed higher M_n and M_w due to the purer grade of methyl ricinoleate used for the polymerisation with about a factor 4 difference. This gave a difference in the T_g of these two polymers, with one at -72°C and the other at -81°C . When the two were epoxidized, the T_g subsequently increased in both cases, although it remained lower in the case of PRic-100 derivatives than for the PRic-LCPO derivatives. The highest T_g increase was obtained with the carbonated PRic-100.

Regarding the mechanical behaviour, PRic-100 has a better toughening effect with PLA than PRic-LCPO does and was the best additive overall regarding that matter. At a loading of 2wt%, PRic-100 was already efficient enough to prevent a brittle fracture in the samples, thus allowing very high deformations to take place without decreasing the modulus value too much. When using PRic-LCPO, a loading of 6wt% was required to observe the same behaviour in terms of strain at break. However, at low loadings of PRic-LCPO, there was still a mechanical improvement since the sample would display a plastic behaviour, whereas neat PLA does not, and would break at strains around -20% with a relatively similar modulus.

The addition of an epoxide group on both grades led to different behaviours. In the case of PRic-LCPO; 25% of epoxide groups seemed to lower the toughening effect at 2wt% and 4wt% loadings, with lower strains at break, whereas at 50% of epoxide groups, the mechanical performance was improved at these loadings. A strain at break nearing -25% and measured forces being even higher than with neat PRic-LCPO were measured for the 2wt loaded sample. For either additive, the 6wt% loaded samples displayed no breaking and a higher measured force plateau. In the case of PRic-100, the epoxide derivatives were not as efficient as neat PRic-100 to enhance the mechanical properties of PLA. This was attributed to the elimination of the low mass oligomers during the precipitation and to the higher T_g of the epoxidized derivatives. Due to a change in molar mass of the samples during processing, the effect of the carbonation of PRic-100 could not be well assessed since only the most carbonated additive gave samples with comparable molar masses. In this particular case, the mechanical

properties would be better than neat PLA, however, they would remain much inferior compared to the ones obtained using the other additives.

Regarding the O₂ permeability, the addition of both PRic-LCPO or PRic-100 increased the measured values due to the increase of free volume in the sample. However, this increase is rather limited and does not exceed a 30% value compared to neat PLA, which is satisfactory. The epoxidized PRic-LCPO limited the effect of the free volume, therefore showing the effect of epoxide groups to limit the O₂ permeability and achieving similar permeability values than neat PLA. This effect was more limited with PRic-100 as the permeability values still increased with an increasing amount of additive, therefore showing the advantage of the higher molar mass polymer regarding this matter. Interestingly, the 25% and 50% carbonated PRic-100 additives showed the best O₂ barrier properties with permeability values halved compared to neat PLA. This trend was not observed for the samples made from PRic-LCPO-E85 which also suffered an important decrease in molar mass, therefore pushing for a real effect of the cyclic carbonate groups on the O₂ permeability. However, quite surprisingly, this effect was not seen with PRic-100-E85-Carbonate although the observed morphologies are similar through the SEM. This suggests that either there is an effect on the O₂ permeability specifically due to the lower molar mass of the samples, or that there is a sweet spot in terms of amount of cyclic carbonate groups borne by PRic-100 which could be between 25% and 50%. Experiments need to be redone to first verify whether there is still a decrease of molar mass and, if not, whether the mechanical properties are not as poor as first measured and, more importantly, if the O₂ permeability values are verified.

General conclusion and perspectives

This study showed that PRic-100, as produced by the ITERG, is the best toughening agent for PLA, only requiring very little amounts to greatly enhance its mechanical properties in terms of elongation at break without decreasing the modulus. The addition of epoxides to PRic was expected to create covalent bonds at the interface between PLA and PRic to have a better interfacial compatibility and to further increase this toughening effect. The use of epoxidized PRic-LCPO improved the toughening effect whereas this effect was limited for epoxidized PRic-100, mainly due to the loss of the low molar mass oligomers during the precipitation step,

which were acting as compatibilizers at the interface. More particularly, the dominant effect for PRic-100 was the increase of viscosity due to the increase of T_g . Unfortunately, due to a decrease in the molar mass of the PLA matrix, the study could not be conclusive regarding the mechanical reinforcement given by carbonated PRics.

Regarding the O_2 permeability values however, using PRic-100 only slightly increased the ability of O_2 to pass through the material due to free volume (a maximum of 30% increase), which was satisfactory. Looking at the other additives, the addition of epoxides partially limited the effect of free volume for PRic-LCPO, but this effect was less in the case of PRic-100. For both of these epoxidized grades, the permeability was stabilised near the value of neat PLA which was a very promising result. The carbonated PRic-100 gave the most promising results for the O_2 barrier properties, showing the biggest reduction of O_2 permeability. These were unfortunately coupled with poor mechanical properties due to a decrease in molar mass of the PLA matrix. Unfortunately, none of these evolutions represented a significant modification of the O_2 permeability of PLA either for a greater barrier behaviour or a greater permeable behaviour.

As for immediate perspectives, the study should be completed by trying to reproduce the obtained results and especially by replicating the samples which displayed a loss of molar mass. Eliminating such bias is necessary before forming a conclusion on the true effect of the carbonated additives both from a mechanical and an O_2 permeability point of view. Once this work is achieved, it would be of interest to explore the available chemical paths taking advantage of the epoxide or the cyclic carbonate groups. Thanks to these reactive moieties, further functionalisation or reactions can be reached. The epoxides can be opened to either self-react and crosslink the PRic chains, or they can also be hydrated to form a vicinal diol, or they can also react with amines to also crosslink PRic chains. Regarding the cyclic carbonates, they can be used to react with amines to yield hydroxyurethane groups which are of particular interest due to the hydrogen bond density they offer. It can therefore be imagined that novel materials based on PRic can be obtained through these media or PRic with novel properties that would be of further interest when used as additives for PLA.

References

- Oguz, O. *et al.* A Sustainable Approach to Produce Stiff, Super-Tough, and Heat-Resistant Poly(lactic acid)-Based Green Materials. *ACS Sustain. Chem. Eng.* **7**, 7869–7877 (2019).
- Al-Itry, R., Lamnawar, K. & Maazouz, A. Improvement of thermal stability, rheological and mechanical properties of PLA, PBAT and their blends by reactive extrusion with functionalized epoxy. *Polym. Degrad. Stab.* **97**, 1898–1914 (2012).
- Abt, T., Kamrani, M. R., Cailloux, J., Santana, O. & Sánchez-Soto, M. Modification of Poly (lactic) acid by reactive extrusion and its melt-blending with Acrylonitrile Butadiene Styrene. *Polym. Int.* **n/a**, (2020).
- Wu, B. *et al.* Design of Supertoughened and Heat-Resistant PLLA/Elastomer Blends by Controlling the Distribution of Stereocomplex Crystallites and the Morphology. *Macromolecules* **52**, 1092–1103 (2019).
- Lebarbé, T., Ibarboure, E., Gadenne, B., Alfos, C. & Cramail, H. Fully bio-based poly(l-lactide)-b-poly(ricinoleic acid)-b-poly(l-lactide) triblock copolyesters: investigation of solid-state morphology and thermo-mechanical properties. *Polym. Chem.* **4**, 3357 (2013).
- Zhang, P. *et al.* Full-biodegradable polylactide-based thermoresponsive copolymer with a wide temperature range: Synthesis, characterization and thermoresponsive properties. *React. Funct. Polym.* **142**, 128–133 (2019).
- Dworakowska, S., Coz, C. L., Chollet, G., Grau, E. & Cramail, H. Cross-Linking of Polyesters Based on Fatty Acids. *Eur. J. Lipid Sci. Technol.* **0**, (2019).
- Méheust, H., Le Meins, J.-F., Grau, E. & Cramail, H. Bio-Based Polyricinoleate and Polyhydroxystearate: Properties and Evaluation as Viscosity Modifiers for Lubricants. *ACS Appl. Polym. Mater.* **3**, 811–818 (2021).
- Cramail, H., Lebarbe, T., Gadenne, B. & Alfos, C. Use of polymers as additives in a polymer matrix. (2017).
- Vignolo, R. & Naughton, F. Castor: a new sense of direction. *Int. News Fats Oils Relat. Mater. USA* (1991).
- Kunduru, K. R., Basu, A., Haim Zada, M. & Domb, A. J. Castor Oil-Based Biodegradable Polyesters. *Biomacromolecules* **16**, 2572–2587 (2015).
- Mutlu, H. & Meier, M. A. R. Castor oil as a renewable resource for the chemical industry. *Eur. J. Lipid Sci. Technol.* **112**, 10–30 (2010).
- Park, J. Y. & Paul, D. R. Correlation and prediction of gas permeability in glassy polymer membrane materials via a modified free volume based group contribution method. *J. Membr. Sci.* **125**, 23–39 (1997).
- Ren, F.-Y. *et al.* Oligomeric ricinoleic acid synthesis with a recyclable catalyst and application to preparing non-isocyanate polyhydroxyurethane. *Eur. Polym. J.* 110501 (2021) doi:10.1016/j.eurpolymj.2021.110501.
- Carothers, W. H. Polymers and polyfunctionality. *Trans. Faraday Soc.* **32**, 39 (1936).
- Berto, P., Pointet, A., Le Coz, C., Grelier, S. & Peruch, F. Recyclable Telechelic Cross-Linked Polybutadiene Based on Reversible Diels–Alder Chemistry. *Macromolecules* **51**, 651–659 (2018).
- Roumanet, P.-J. *et al.* Novel aliphatic polyesters from an oleic acid based monomer. Synthesis, epoxidation, cross-linking and biodegradation. *Eur. Polym. J.* **49**, 813–822 (2013).
- Fox, T. G. Influence of Diluent and of Copolymer Composition on the Glass Temperature of a Polymer System. *Bull Am Phys Soc* **1**, 123 (1956).
- Van de Velde, K. & Kiekens, P. Biopolymers: overview of several properties and consequences on their applications. *Polym. Test.* **21**, 433–442 (2002).
- Södergård, A. & Stolt, M. Properties of lactic acid based polymers and their correlation with composition. *Prog. Polym. Sci.* **27**, 1123–1163 (2002).
- Alves, M. *et al.* Organocatalytic synthesis of bio-based cyclic carbonates from CO₂ and vegetable oils. *RSC Adv.* **5**, 53629–53636 (2015).
- Chaos, A. *et al.* Plasticization of poly(lactide) with poly(ethylene glycol): Low weight plasticizer vs triblock copolymers. Effect on free volume and barrier properties. *J. Appl. Polym. Sci.* **137**, 48868 (2020).

Conclusion and perspectives

This PhD work was dedicated to the synthesis and study of novel bio-based additives for PLA. A particular scope of this study was to consider food packaging as a specific application of these newly made materials. PLA is a bio-based and industrially compostable polymer which has been approved for food contact. Thanks to an ever-increasing production, its price now ranges between \$1.5 and \$2 per kilo¹, which makes it economically viable to replace commodity polymers such as PE, PP or PET. Although it is a well-known polymer, PLA still suffers from major drawbacks such as its brittleness, its low heat deflection temperature and in between O₂ gas barrier properties, which, as such, limit its use as food packaging². The strategy of this project was to mix additives in PLA to deal with these issues. The state-of-the-art regarding such matter is very rich thanks to years of intense research to promote PLA. Multiple strategies spanning from using plasticisers, oxides, fibres, polymers, organic or mineral nucleating agents have been contemplated to try to resolve these issues³.

Bio-based compounds derived from fatty acids were considered to synthesise such additives. These fatty compounds are annually renewable as they are extracted from plant oils and are of particular interest since their structure allows them to be involved in multiple chemical reactions. Chapter 2 deals with two challenges: enhancing the heat deflection temperature of PLA and reducing its gas permeability. The considered approach was to work on the crystallisation kinetics of PLA by using nucleating agents. Thanks to an already very rich literature regarding the subject, the choice was made to focus on bis-amide derivatives. More specifically, symmetrical bis-amides made from C18 fatty acids, and an aliphatic diamine were synthesised. The effect of the chain spacer and of the fatty derivative on the thermal properties was studied. Compounds with melting points above 130°C were obtained and were then used as nucleating agents for PLA. DMA samples were prepared by injection-moulding to assess the isothermal crystallisation performance of the additives. This revealed that it was possible to obtain PLA samples with crystallinity ratios above 50% using 0.5wt% of nucleating agents and for a total holding time of 25s in the mould, which was the shortest reproducible time that could be considered at the lab scale.

Conclusion and perspectives

Scale-up tests were run using a mini-industrial injection-moulding machine to try to replicate industrial injection-moulding conditions and assess the true potential of our nucleating agents. Extruding the PLA containing the nucleating agent was easier than with neat PLA since the obtained filament would crystallise and be simpler to recover and break into pellets. Unfortunately, during the injection-moulding process, the temperature of the mould could not be controlled well on the Babyplast machine which was used. This would not allow us to have the suitable temperature to make PLA crystallise. More experiments should be done using a different machine to assess the possibility to directly produce crystalline PLA objects at high speed. Would that processing step be successful, it will then be possible to measure the heat deflection temperature and the associated gas barrier and mechanical properties of the obtained material.

Chapter 3 focusses on the toughening of PLA using polyricinoleate, a bio-based low T_g polyester, as a polymeric additive. This polymer had already been reported to be a successful toughening agent when blended with PLA at very low loadings such as 3wt%. Two grades of polyricinoleate were used and studied: an industrially available polymer synthesised by the ITERG from an 85% pure monomer and a homemade polymer obtained from a 99% pure monomer. These polymers were then post-functionalised with epoxides by taking advantage of the available alkene groups in the repeat unit. Due to a higher availability, the industrial grade of polyricinoleate was also functionalised with cyclic carbonate groups. The addition of epoxide and cyclic carbonate groups increased the value of the glass transition temperature for both polyricinoleate grades, the more functionalised, the higher the value. The effect with cyclic carbonates was higher than with the epoxides, leading to the highest T_g values.

The aim was to evaluate the effect of the grade of polymer, which was used, along with the effect of the post-functionalisation on the mechanical properties of PLA and whether they would influence the gas barrier properties or not. When used as such, the industrial polyricinoleate was the best toughening agent for PLA and, surprisingly, higher loadings of homemade PRic were required to achieve the same mechanical performance. The epoxidation of the two grades of PRic led to different behaviours. The epoxidized industrial PRic was less efficient in enhancing the mechanical properties as the samples displayed a brittle breaking behaviour at low loadings which did not happen with the neat polymer. Also, the more epoxides, the less efficient the additive. In the case of the homemade PRic, the epoxidation

improved the toughening effect. Regarding the effect of the cyclic carbonate, the mechanical properties of the samples was not as good as with the epoxidized or neat PRic. Unfortunately, there was also a decrease of molar mass of the PLA matrix when two of the carbonated additives were used leading to very poor mechanical properties. However, the measured O₂ permeability values were halved with the presence 25% and 50% of cyclic carbonates, which leads to promising perspectives.

The key takeaways from this chapter are that the best toughening agent for PLA is the less pure industrial grade of PRic, which is efficient at just a 2wt% loading. Regarding the gas barrier properties, the carbonated additives obtained from the industrial PRic were the most promising however, they displayed the worst mechanical behaviour. They should be tested again so that the molar mass of the PLA matrix would not be so affected as in our case. The homemade PRic and its derivatives, with higher molar masses, showed lower mechanical properties and also a different evolution when post-functionalised.

From another perspective not discussed in this work, it is worth mentioning that the only drawback of the industrial PRic is its very low viscosity. When mixed with PLA, a twin-screw extruder had to be used since, in the case of a single-screw extruder, this PRic would lubricate the screw and therefore, the PLA pellets could not be fed into the extruder. The advantage of the epoxidation and the carbonation was that this industrial PRic became more viscous and could be blended more easily. More generally, this consideration is reinforced by the fact that unlike polyolefins, PLA has a low expansion coefficient when extruded, jointly with a low viscosity in the melted state, leading to difficulties to easily collect a filament after extruding.

As a general perspective, this work showed the potential of bio-based additives to solve major long-existing drawbacks of PLA. Fatty acids can be used to synthesise efficient nucleating agents that will render PLA able to crystallise from the melt at low cooling times and also polymer additives to toughen PLA at room temperature. This opens new opportunities for the use of PLA which were not considered yet. The immediate upcoming work should be to test the combination of these two types of additives to both evaluate the crystallisation kinetics of the resulting mix and the mechanical properties. Finer studies will then be required to tune the additives' loadings to optimise the properties of the final material. Moreover, more post-functionalisation can be conducted on the PRic derivatives to test new chemical architectures and their effect on PLA. Impact testing is also lacking from

Conclusion and perspectives

this study and would represent a more significant test regarding the assessment of the mechanical properties of PLA materials. The toxicity of the additives should be assessed to see whether they are compatible with food packaging requirements. Once this has been conducted, scale-up tests using the most promising materials should be run. Also, it would be interesting to run a life-cycle assessment of such materials to determine their energy impact and compare it to other available and widely used materials. Eventually, the biodegradability of the materials should also be assessed. Currently, PLA is only compostable in industrial conditions and should be directed towards an ability to biodegrade in home-compost conditions. Therefore, the influence of the additives on the biodegradation of PLA should be studied. This is also emphasised by the latest regulations regarding plastics which drive industrials and consumers to use more sustainable materials and rethink their well-established habits.

References

1. Polylactic Acid (PLA) Market | 2022 - 2026 | MarketsandMarkets.
<https://www.marketsandmarkets.com/Market-Reports/poly-lactic-acid-pla-market-29418964.html>.
2. Wu, F., Misra, M. & Mohanty, A. K. Challenges and new opportunities on barrier performance of biodegradable polymers for sustainable packaging. *Prog. Polym. Sci.* **117**, 101395 (2021).
3. Naser, A. Z., Deiab, I. & Darras, B. M. Poly(lactic acid) (PLA) and polyhydroxyalkanoates (PHAs), green alternatives to petroleum-based plastics: a review. *RSC Adv.* **11**, 17151–17196 (2021).

Materials and methods

1. Materials

A commercially available grade of poly(lactic acid) (PLA) was acquired from NaturePlast, (Caen, France) (PLI 005, D-lactide<0.5%, MFI=25-35g/10min at 190°C) and dried in a vacuum oven at 80°C for at least 12 hours before use.

Methyl ricinoleate was purchased from Nu-Chek-Prep (MN, USA) with a purity over 99% and were used without any further purification. Methyl ricinoleate (85%) and PRic-100 were kindly supplied by ITERG (Pessac, France). 1,6-diaminohexane, 3-metachloroperbenzoic acid (m-CPBA, 77%) and stearic acid were purchased from Sigma-Aldrich. 12-hydroxystearic acid and 1,4-diaminobutane were purchased from Alfa Aesar. 1,10-diaminodecane, 1,12-diaminododecane and oleyl chloride (70%) were purchased from TCI used without purification.

Titanium isopropoxide ($\text{Ti}(\text{O}i\text{Pr})_4$, 99.99%, Acros Organics) and triazabicyclodecene (TBD, 98%, Sigma-Aldrich) were used as catalysts as received.

2. Experimental methods

2.1. Dynamic Scanning Calorimetry (DSC)

A TA instruments liquid nitrogen DSC (Q100, LN2) was used for all DSC measurements. Samples were put through the following procedure:

- Dynamic measurements: 1st heating from 20°C to 190°C, isothermal at 190°C for 10 mins, cooling at -10°C/min from 190°C to 20°C, 2nd heating at 10°C/min from 20°C to 190°C. The crystallinity ratio of the sample was measured upon the 1st heating. Melt-crystallisation points and melt-crystallisation enthalpies were measured during the cooling run. Glass transition temperatures, melting points, cold crystallisation points, melting enthalpies, and cold crystallisation enthalpies were measured during the 2nd heating run.

2.2. Nuclear Magnetic Resonance (NMR)

The ^1H and ^1H - ^1H spectra (COrelated Spectroscopy, COSY) were recorded on a Bruker Advance 400 spectrometer (400 MHz for ^1H) by using CDCl_3 as a solvent at room temperature. In the case of bisamide compounds, a mixture of CDCl_3 with a few drops of hexafluoropropan-2-ol (HFIP) was used as a solvent instead. ^1H NMR analyses were performed with 16 scans unless mentioned otherwise and COSY experiments were performed with 16x16 scans.

2.3. Fourier Transformed Infrared Spectroscopy-Attenuated Total Reflection (FTIR-ATR)

Infrared spectra were obtained on a Bruker-Tensor 27 spectrometer using the attenuated total reflection (ATR) mode. The spectra were acquired using 16 scans at a resolution of 4 wavenumbers.

2.4. Dynamic Mechanical Analysis (DMA)

DMA measurements were performed on a TA instruments Q850 DMA apparatus. Samples were run using the single cantilever oscillation mode with a heating ramp of $3^\circ\text{C}/\text{min}$ from 25°C to 170°C , 1Hz, 0.1% strain with liquid nitrogen control. The T_g of the samples was measured using the onset of the storage modulus (E') curve and the T_α at the peak of the $\tan \delta$ plot.

2.5. Size exclusion Chromatography (SEC)

Polymer molar masses were determined by Size Exclusion Chromatography (SEC) using tetrahydrofuran (THF) as the eluent. Measurements in THF were performed on an Ultimate 3000 system from ThermoScientific equipped with a diode array UV detector. The system also includes a multi-angle light scattering detector (MALS) and a differential refractive index detector (dRI) from Wyatt technology. Polymers were separated on three G2000, G3000 and G4000 TOSOH HXL gel columns (300 x 7.8mm) (exclusion limits from 1000 Da to 400,000 Da) at a flowrate of 1mL/min. Columns were held at 40°C and low dispersity polystyrene (PS) was used as the standard to convert the elution times to molar mass.

2.6. Vertical compression test

Vertical compression testing was conducted in an INSTRON apparatus using parallel plates. Tests were conducted at a -10mm/min speed using 10 replicas for each compound. Due to the complexity of the object, no definite section could be calculated, therefore values are reported as a force (N) vs displacement (mm). The values for the slope at origin, yield force, force plateau, strain at break were reported.

2.7. Gas permeability measurements

Gas permeation measurements were conducted using Presens O₂ spot sensors at 23°C, 50% RH. PSt6 sensors were used unless specified otherwise. The spot sensors were glued to a glass panel and then the injection moulded samples were glued above them under a dry N₂ atmosphere in an airtight manner. Small containers holding a saturated hydrated magnesium nitrate salt solution were placed in the samples to adjust the relative humidity from 0 RH to 53% RH. The O₂ value was read using a Fibax 4 trace oxygen metre using temperature compensation. Two replicas were used and the mean O₂ permeability was calculated when the measured O₂ concentration values followed a linear trend according to the following formula:

$$Perm = \frac{Slope \times volume \times thickness}{a \times \Delta P}$$

- Perm = the permeability in cm³ (O₂).m.m⁻².day.atm
- Volume in cm³, 49.2 cm³
- Thickness in m, 0.001225 m
- a = area in m², 0.00556 m²
- ΔP = O₂ pressure differential in atm, 0.21 atm

2.8. Scanning electron microscopy (SEM)

SEM images were acquired using a Zeiss Gemini 300 microscope at the Bordeaux Imaging Centre (BIC). The acceleration tension was 1kV and the observation was conducted under high vacuum (4.8 10⁻⁵ Pa). Samples were cryo-fractured using liquid nitrogen so that the observed surface would be perpendicular to the injection flow and taken from the side of the injection

Materials and methods

moulded objects. Observations were made at a x500, x1000, x1500, x3000, x5000 and x10000 zoom using an in-lens detector and a secondary electron detector.

2.9. X-Ray Diffraction

X-Ray diffraction spectrograms were acquired using a RIGAKU HF-007 (8keV) machine at the CRPP (*Centre de Recherche Paul Pascal*). The X-Ray source was a copper lamp which produced an electromagnetic wave at $\lambda=1.5418\text{\AA}$. Samples were observed in diffracted transmission mode at room temperature in air using a flat image detector.

2.10. Polymer processing at the LCPO – DMA and tensile testing samples

Prior to melt-blending, PLA pellets were dried at least 12h at 80°C in a vacuum oven. A Thermoscientific Minilab II HAAKE Rheomex CTW5 twin screw mini compounder with a recirculating canal was used. The temperature was set to 190°C with a rotation speed of 100 RPM (corotation mode) and a mixing time of approximately 5 mins. About 7g of compound were loaded before being transferred to the injection moulding system. The injection moulding device is a Thermoscientific HAAKE MiniJet Pro apparatus which was heated at 183°C. A rectangular shaped mould was used to produce DMA specimens of approximately 60x10x1mm. These moulds were heated to either 63°C (cold conditions) or 110°C (hot conditions) to get either amorphous or crystallised PLA samples.

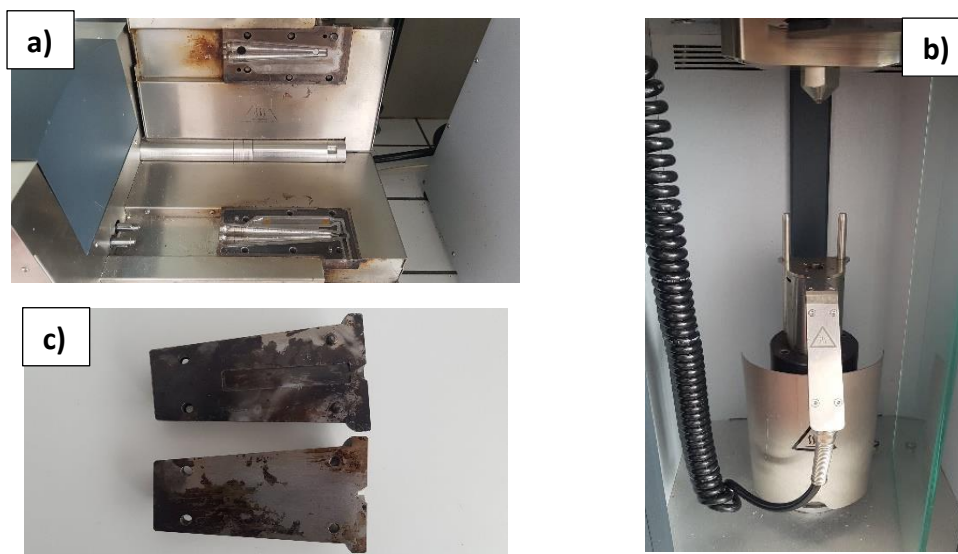


Fig VI.1: a) Opened twin screw compounder, b) Injection moulding apparatus, c) Mould for DMA samples

2.11. Polymer processing at the CTCPA

2.11.1. Melt-blending apparatus

PLA pellets were dried in an oven at 100°C for 4 hours prior to mixing and stored in an oven at 80°C if not used immediately. The additives were used as such. A Scamex Rheoscam twin screw micro extruder was used to prepare the different compounds. Specially profiled twin corotating screws with a diameter of 18mm were used with a circular die at the end of



Fig VI.2: a) Scamex extruder, b) Scamex pelletiser, c) Twin corotating screws

the barrel. Three successive heating zones were programmed respectively at 210°C, 180°C and 160°C. The obtained compound was directly cut into pellets using a Scamex pelletiser, both cut and drawing speeds were adjusted depending on the behaviour of the rod.

2.11.2. Melt-blending method

To produce the different compounds, a masterbatch was first made with a 6wt% loading of additive, regardless of it being a polymer or a nucleating agent. Neat PLLA pellets were used. The masterbatch was extruded twice to ensure the homogeneity of the batch, the first time at 13 RPM and the second time at 3 RPM. The processing time in the extruder was approximately 7 minutes. The obtained pellets were put in an oven at 100°C for 2 hours to make the pellets crystallise to help with the processing. Given the big difference in size between the neat PLLA pellets and the obtained compound pellets, neat PLLA was extruded

Materials and methods

to obtain pellets with a similar size. These small size PLLA pellets were then used to dilute the masterbatch to get the expected loading. Only one run at 3 RPM through the extruder was used this time, with a processing time of approximately 7 minutes. The obtained pellets were then put to crystallise in an oven at 100°C for 2 hours.

2.11.3. Injection moulding

Mini containers were produced using a Babyplast 6/12V injection moulding machine equipped with specifically a specifically designed mould. Objects of approximately 51mm of inside diameter, 25mm height and 1.23mm thickness were produced. The processing parameters were as such: the first heating chamber and the plasticisation chamber were heated to 200°C, the injection nozzle was heated to 220°C and the mould was set to 185°C. The injection pressure was 50 bar for 2.5 seconds and cooling time was set to 15 seconds. The total time cycle for 1 object was 22.5 seconds.



Fig VI.3: Babyplast 6/12V injection moulding machine

Additifs biosourcés dérivés d'acides gras pour l'amélioration des propriétés thermomécaniques et barrière du PLA

Résumé : Dans cette étude, plusieurs voies ont été considérées pour synthétiser des additifs biosourcés dans le but d'améliorer les propriétés mécaniques, thermiques et de perméabilité à l'O₂ du PLA. Dans un premier temps, des agents nucléants de type bisamides symétriques ont été synthétisés à partir d'acides gras et de diamines linéaires aliphatiques. Les relation structure-propriétés de ces agents a été établie. Leur utilisation a permis d'obtenir des taux de cristallinité supérieurs à 50% dans des conditions de moulage isotherme ainsi qu'une température de fléchissement sous charge proche de 120°C. Dans un second temps, des additifs polymères de type poly(ricinoléate de méthyle) ont été considérés ainsi que leurs dérivés époxydés et carbonatés. Leur utilisation a permis de grandement améliorer les propriétés mécaniques du PLA, le meilleur additif étant le poly(ricinoléate de méthyle) non-modifié, fourni par l'ITERG. Les perméabilités à l'O₂ ont été faiblement augmentées en présence de poly(ricinoléate de méthyle) non-modifié. Dans le cas des additifs époxydés et carbonatés, l'effet sur la perméabilité est bénéfique et permet d'obtenir des valeurs similaires à celles du PLA pur.

Mots clés : Poly(L-lactide), agents nucléants, biosourcé, cristallisation, poly(ricinoléate de méthyle), emballages alimentaires, renfort aux chocs, perméabilité O₂

Bio-based additives from fatty acid derivatives for PLA: enhancing its thermomechanical and gas barrier properties

Abstract : The aim of the PhD word is to promote the use of bio-based additives to enhance the mechanical, thermal and O₂ barrier properties of PLA. Firstly, novel symmetrical fatty bis-amides were synthesised as nucleating agents using fatty acids and linear aliphatic diamines. Their structure-property relationship has been established. Their use allowed to get PLA samples with a crystallinity ratio over 50% and a subsequent heat deflection temperature nearing 120°C. Secondly, polymeric additives based on poly(methyl ricinoleate) and its epoxidized and carbonated derivatives were considered. Their use allowed to enhance greatly the mechanical properties of PLA; the best results being obtained for neat poly(methyl ricinoleate) directly synthesised by the ITERG. Regarding the barrier properties, only a limited increase was reported with the use of such additives. More interestingly, the epoxidized and carbonated additives further limited the increase of permeability to the point where a similar value as for neat PLA was obtained.

Keywords : Poly(L-lactide), nucleating agents, bio-based, crystallisation, poly(methyl ricinoleate), food packaging, rubber-toughening,

Laboratoire de Chimie des Polymères Organiques

16 Avenue Pey-Berland
F-33607 Pessac

